VON KARMAN CENTER

SNAP-8 DIVISION

SNAP-8 ELECTRICAL GENERATING SYSTEM DEVELOPMENT PROGRAM (U)

CONTRACT NO. NAS 5-417

A REPORT TO

NATIONAL AERONAUTICS AND SPACE ADMINISTRATION

(NASA-CR-54030) SNAP-8 ELECTRICAL GENERATING SYSTEM DEVELOPMENT PROGRAM Quarterly Progress Report (Aerojet-General Corp., Azusa, Calif.) 323 p

N74-73955

Unclas
00/99 36737

FACILITY FORM 602

323 (PAGES)

27 (CODE)

CR54030 (NASA CR OR TMX OR AD NUMBER)

06 (CATEGORY)

CLASSIFICATION CHANGED TO - UNCLASSIFIED

By authority of E.O. 11652

Changed by L. Shirley Date 2-25-

"Available to U.S. Government Agencies and U.S. Government Contractors Only"

AEROJET GENERAL TIRE GENERAL

AEROJET-GENERAL CORPORATION

AZUSA, CALIFORNIA

NOTICE

This report was prepared as an account of Government-sponsored work. Neither the United States, nor the National Aeronautics and Space Administration (NASA), nor any person acting on behalf of NASA:

(A) Makes any warranty or representation, expressed or implied, with respect to the accuracy, completeness, or usefulness of the information contained in this report, or that the use of any information, apparatus, method, or process disclosed in this report may not infringe privately-owned rights; or

(B) Assumes any liabilities with respect to the use of, or for damages resulting from the use of any information, apparatus, method or process disclosed in this report.

As used above, "person acting on behalf of NASA" includes any employee or contractor of NASA, or employee of such contractor, to the extent that such employee or contractor of NASA, or employee of such contractor prepares, disseminates, or provides access to, any information pursuant to his employment or contract with NASA, or his employment with such contractor.

Requests for copies of this report should be referred to:

National Aeronautics and Space Administration
Office of Scientific and Technical Information
Washington 25, D.C.
Attn: AFSS-A

CASE FILE COPY

NASA CR-54030

AEROJET GENERAL TIRE GENERAL

SNAP-8 ELECTRICAL GENERATING SYSTEM DEVELOPMENT PROGRAM (U)

Contract No. NAS 5-417

a report to

NASA - LEWIS RESEARCH CENTER
SNAP-8 PROJECT OFFICE
H. O. SLONE, SNAP-8 PROJECT MANAGER

Report No. 0390-04-15 (Quarterly) March 1964

This document contains information affecting the national defense of the United States within the meaning of the espionage laws, Title 18, U.S.C., Section 793 and 794. Its transmission or the revelation of its contents in any manner to an unauthorized person is prohibited by law.

GROUP 4

Downgraded at 3-Year Intervals
Declassified After 12 Years

AEROJET-GENERAL CORPORATION
A SUBSIDIARY OF THE GENERAL TIRE & RUBBER COMPANY

"Available to U.S. Government Agencies and U. S. Government Contractors Only"

Report No. 0390-04-15

17266

ABSTRACT

The objective of the SNAP-8 Program is to design and develop a 35-kw electrical generating system for use in various space missions. This report covers the progress during the fifteenth quarter of contract performance by the Aerojet-General Corporation. The status of the various necessary systems analyses is presented. Design and fabrication of components - turbine alternator assembly, NaK and mercury pump-motor assemblies, bearings, seals-to-space, mercury boiler and condenser, mercury injection system, electrical insulation, and electrical components - are reported. Testing in the several component test loops is discussed. Materials evaluation of components exposed to mercury corrosion and erosion is presented.

CONTRACT FULFILLMENT STATEMENT

This is the fifteenth in a series of quarterly progress reports submitted in partial fulfillment of NASA Contract No. NAS 5-417. It covers the period December 1963 - February 1964.

CONTENTS

		Page
Glossary		xv
I.	INTRODUCTION	I-1
II.	SUMMARY	II-1
A.	System Engineering	II-1
B.	Reliability	II-1
C.	Rotating Machinery	II-2
D.	Nonrotating Components	II-3
E.	Test Engineering	II-4
F.	Materials	II-4
III.	SYSTEM ENGINEERING	III-1
A.	EGS Development Control and Coordination	III-1
B.	System Design	III-9
C.	System Analysis	III-11
D.	SL-1 Project Coordination	III-21
E.	SL-2 Project Coordination	III-22
IV.	RELIABILITY	IV-1
A.	Management and Planning	IV-1
B.	System Statistical Analysis	IV-2
C.	Reliability Design Engineering	IV-2
D.	Test Planning/Failure Analysis	IV-4
E.	Reliability Control and Liaison	IV-5
V.	ROTATING MACHINERY	V-1
A.	Turbine Alternator Assembly Design and Analysis	V-1
B.	Turbine Assembly (TA)	V-2

CONTENTS (cont.)

		Page
C.	Alternator	V-5
D.	Ball Bearings and Bearing Lubrication System	V-6
E.	Seals	V-12
F.	Pump Projects	V-15
VI.	NONROTATING COMPONENTS	VI-1
A.	Heat Exchanger Components	VI-1
B.	Expansion Reservoirs	VI-9
C.	Valves	VI-10
D.	Mercury Injection Systems (MIS)	VI-12
E.	Electrical Insulation Development Program	VI-12
F.	Electrical Controls and Components	VI-19
G.	NaK Traps	VI-32
H.	Mercury Filter-Separator	VI-32
VII.	TEST ENGINEERING	VII-1
A.	Non-Nuclear Test Loops and Stands	VII-1
B.	Test Facilities and Equipment Design	VII-3
C.	Nuclear Systems Testing	VII-5
D.	Test Support Services	VII-5
VIII.	MATERIALS	VIII-1
A.	Staff Support	VIII-1
B.	Mercury Corrosion Study	VIII-4
C.	Heat Exchanger Materials - Fabrication Development	VIII-18
D.	TAA Materials Evaluation	VIII-28
References		R-1

CONTENTS (cont.)

	Table
Anticipated Maximum Transients of System Parameters	1
Current Schedule - PCS-2/SL-2	2
Lubrication Rig No. 1 - Buildup Summary	3
Summary of the SNAP-8 Ball Bearing Test Programs	4
Model A Seal Simulator Leakage Rates	5
NaK PMA Bearing Test Summary - 99 Hours at 600°F	6
Summary of Heat Rejection Loop Losses	7
SNAP-8 -1 Boiler Stress Analysis Schedule	8
SNAP-8 -1 Condenser Stress Tabulation	9
Insulation Resistance, Inorganic Insulated Motor	10
Organic Resin Weight Loss - 168 Hours at 392°F in Air	11
Statorette Insulation Systems	12
Insulation Resistance, Statorette HML-1	13
Insulation Resistance, Statorette HML-2	14
Insulation Resistance, Statorette ML/997-1	15
Insulation Resistance, Statorette ML/997-2	16
Insulation Resistance, Statorette ML-3	17
Insulation Resistance, Statorette ML-4	18
Insulation Resistance, Statorette ML-5	19
Insulation Resistance, Statorette ML-6	20
Transducer Pressure and Temperature Data from Run 11	21
Temperature Data from Runs 10 and 11	22
Hot-Start Data	23

CONTENTS (cont.)

Table

Weights and Semiquantitative Spectrographic Analyses of Deposits and Residues from Thermal Convection Loop 1 ____ 24

Weights and Semiquantitative Spectrographic Analyses of Mercury Residues from Thermal Convection Loop 2 ____ 25

Analysis of Deposits and Residues from Thermal Convection Loop 3 ____ 26

Analysis of Deposits and Residues from Thermal Convection Loop 4 ____ 27

Weight and Distribution of Corrosion Products Collected from 9Cr-1Mo Thermal Convection Loops ____ 28

Hydrogen Cleanup and Brazing Cycles ____ 29

Nominal Chemical Composition of Materials Exposed to Erosion Test Environment ____ 30

Heat Treatment of Erosion Specimen Materials ____ 31

Test Condition and Results of Materials Specimens Exposure to Erosive Environment ____ 32

Figure

Cross Section of Mercury Chamber for PVT (Pressure, Volume, Temperature) Apparatus ____ 1

PVT Apparatus - Test Results, Run 1, Log psia vs Log ^{o}K ____ 2

Mollier Diagram for Mercury ____ 3

Schematic Diagram PCS-1 - Phase I ____ 4

Schematic Diagram PCS-1 - Phase II ____ 5

Schematic Diagram PCS-1 - Phase III ____ 6

Schematic Diagram PCS-2 - Phase I ____ 7

Schematic Diagram PCS-2 - Phases II and III ____ 8

SNAP-8 PCS Start-up Runs, Reference System B, Complete System Simulation - Maximum Rate of Temperature Change vs Internal Reactor Power ____ 9

CONTENTS (cont.)

Figure

SNAP-8 PCS Start-up Runs, Reference System B, Complete System Simulation - Maximum Reactor Outlet Temperature vs Initial Reactor Power ____ 10

SNAP-8 PCS Start-up Runs, Reference System B, Complete System Simulation - Effect of Parameter Variations on Maximum Rate of Temperature Change ____ 11

SNAP-8 PCS Start-up Runs, Reference System B, Complete System Simulation - Effect of Parameter Variations on Maximum Reactor Outlet Temperature ____ 12

SNAP-8 PCS Start-up Runs, Reference System B, Complete System Simulation - Effect of TAA Acceleration on Maximum Rate of Temperature Change ____ 13

Cylindrical Radiator - Shade Conditions ____ 14

Cylindrical Radiator Performance - Sun Conditions ____ 15

Radiator Transfer Function Parameter ____ 16

Frequency Response for Cylindrical SNAP-8 Radiator in Sun ____ 17

In-Sun and In-Shade Transfer Function Simulation of the Space Radiator to be Simulated in SL-2 ____ 18

Power Conversion System 2, Phase I ____ 19

Discharge Coefficients for the Plate Orifice ____ 20

Turbine Assembly Components - SNAP-8 Turbine Alternator Assembly ____ 21

Turbine-Nozzle-Assembly Flow Tests - TAA Buildup No. 1 ____ 22

No-Load Saturation - EME Alternator ____ 23

Load Saturation - EME Alternator ____ 24

Fault Saturation - EME Alternator ____ 25

Three-Phase Short-Circuit Saturation - EME Alternator ____ 26

Efficiency - EME Alternator ____ 27

Windage and Friction Losses - EME Alternator ____ 28

CONTENTS (cont.)

	Figure
Open-Circuit Core Loss - EME Alternator	29
Pre-prototype Alternator	30
Lubrication Rig No. 1 - Build-up No. 4 and No. 5	31
Bearing Outer Race Average Steady-State Temperature vs Inlet Flow Rate	32
Lubricant Temperature Rise vs Inlet Flow Rate	33
Lubricant Inlet Pressure vs Inlet Flow Rate	34
Slinger Scavenging Characteristic - Model A Seal and Lubrication System Simulator	35
Mercury Visco Pump Interface - Housing Grooves - 11,700 rpm	36
Mercury Visco Pump Interface - Shaft Grooves - 11,980 rpm	37
Mercury Visco Pump Interface - Shaft Grooves - 6220 rpm	38
Mercury Visco Pump Interface - Shaft Grooves - 12,000 rpm (ΔP = 40 psi)	39
Mercury Visco Pump Interface - Shaft Grooves - 5980 rpm	40
Mercury Visco Pump Interface - Housing and Shaft Grooves - 12,000 rpm (ΔP = 80 psi)	41
Mercury Visco Pump Interface - Housing and Shaft Grooves - 6000 rpm (ΔP = 80 psi)	42
Mercury Visco Pump Interface - Housing Grooves - 12,000 rpm (ΔP = 110 psi)	43
Mercury Visco Pump Interface - Housing and Shaft Grooves - 12,000 rpm (ΔP = 120 psi; T = 310°F)	44
Mercury Visco Pump Interface - Housing and Shaft Grooves - 6000 rpm (ΔP = 70 psi)	45
Mercury Visco Pump Interface - Shaft Grooves - 12,000 rpm (ΔP = 120 psi; T = 330°F)	46
Pressure Differential vs Axial Engagement - Build-up 1-8	47

CONTENTS (cont.)

	Figure
Pressure Differential vs Axial Engagement - Build-up 1-9	48
Pressure Differential vs Axial Engagement - Build-up 1-10	49
Pressure Differential vs Axial Engagement - Build-up 1-11	50
Pressure Differential vs Axial Engagement - Build-up 1-12	51
Pressure Differential vs Axial Engagement - Build-up 1-13	52
Pressure Differential vs Axial Engagement - Build-up 1-14	53
Pressure Differential vs Axial Engagement - Build-up 1-15	54
Seal Assembly, Integrated	55
Integrated Seal Assembly - Type B Model X	56
Motor Load Test - Heat Rejection Loop NaK PMA	57
Motor Load Test - Primary Loop NaK PMA	58
Prototype HRL Motor Stator Assembly	59
Prototype HRL Motor Stator Assembly - Close-up of Slot Portion	60
End View and Section View of Canned Stator	61
Pivot Fretting Test Apparatus	62
Schematic - Pivot Fretting Test Apparatus	63
M2-T1-M2 Bearing Test Specimens Following 99 Hours in 600°F NaK	64
Component Losses, NaK PMA Recirculation System - Capacity vs Component Losses	65
NaK PMA Recirculation Loop Losses - Capacity vs ΔP	66
NaK PMA Mounting Arrangement	67
Mercury Jet Pump - Test Set-up	68
Mercury Jet Pump - Performance Curves for Water and Mercury Tests	69

CONTENTS (cont.)

	Figure
Mercury Jet Pump, -X Model, Water Test Setup	70
Boiler Hot-Start Test No. 1	71A
Thermocouple Location, Mercury Boiler Outlet	71B
Local Temperature Difference Between NaK and Mercury at Liquid Interface vs Mercury Outlet Pressure Fluctuation - TS-2B Test Section with 0.135-in.-dia Wire in Plub Section	72
Boiler Pressure Drop with Varied Plug Exit Quality	73
Boiler Thermal Profile, Boiler Test Section - Data Point 42	74
Boiler Thermal Profile, Boiler Test Section - Data Point 44	75
Boiler Thermal Profile, Boiler Test Section - Data Point 43	76
Mercury Outlet Tube Header, -1 Boiler	77
Plug Assembly, -1 Boiler Inlet	78
SNAP-8 -1 Boiler Assembly, No. A-1. Mercury Outlet End Shown Near Completion of Final Hand Welding and Assembly	79
SNAP-8 -1 Boiler Assembly, No. A-2. Side View Showing Partially Assembled Boiler with Tubes Mounted on Inner Shell	80
SNAP-8 -1 Boiler Assembly, No. A-1. Mercury Inlet at Lower Center. Boiler Shown Near Completion of Final Hand Welding and Assembly	81
SNAP-8 -1 Boiler Assembly, No. A-1. Close-up of Mercury Inlet Header (Center) and NaK Outler (Tube at Left) in Process of Final Assembly	82
Wood Mockup of SNAP-8 -1 Boiler Assembly	83
SNAP-8 -1 Boiler, Major Stress Areas	84
SNAP-8 -1 Condenser	85
SNAP-8 -1 Condenser. Tube-to-Tube Sheet Weld. Sample Development No. 2	86
SNAP-8 -1 Condenser. Tube-to-Tube Sheet Weld. Sample Development No. 6	87

CONTENTS (cont.)

Figure

SNAP-8 -1 Condenser Structural Analysis. Numbered Points Show Parts Analyzed ____ 88

SNAP-8 -1 Auxiliary Start Loop Heat Exchanger ____ 89

SNAP-8 Turbine Simulator ____ 90

SNAP-8 PCS-1A Schematic Showing Location of Valves ____ 91

Preliminary Design - SNAP-8 Heat-Rejection-Loop Temperature Control Valve ____ 92

Preliminary Design - SNAP-8 Lubricant-Coolant and Auxiliary Shutoff Valves ____ 93

SNAP-8 Mercury Injection System ____ 94

Mercury Flow Control Valve for the SNAP-8 Mercury Injection System ____ 95

Isolation Valve for SNAP-8 Mercury Injection System (PCS-1 and PCS-2 Use) ____ 96

Organic Encapsulant Samples Ready for Weight-Loss Study ____ 97

Encapsulation Trials - HTM Series Using LM-1625 Cement ____ 98

Encapsulant Study Trial - LM-1625 Pressed at 250 psi After Final Cure ____ 99

HRL Trial Stator in Dummy Housing ____ 100

HRL Trial Stator in Dummy Housing - Following Test ____ 101

Organic Statorettes for Radiation Effects Program ____ 102

Inorganic Statorettes for Radiation Effects Program ____ 103

Twisted Wire Insulation Test Samples for Radiation Effects Program ____ 104

Organic and Inorganic Encapsulants in Electrical Sample Cube for Radiation Effects Program ____ 105

Ceramic Terminal Trial Assembly Ready for Long-Term Vacuum Aging at 1000°F ____ 106

Speed Control, Serial No. 3 - Frequency vs Magnetic Amplifier Output (Current vs Maximum Gain) ____ 107

CONTENTS (cont.)

	Figure
Speed Control, Serial No. 3 - Frequency vs Magnetic Amplifier Output (Current vs Minimum Gain)	108
Transfer Curves for the -X Saturable Reactor - Gate Voltage vs Gate Current	109
Electrical Schematic - Start Programer	110
Electrical Components for Radiation Tests, Prior to Shipment	111
Materials for Radiation Effects Test Program	112
Schematic - Three-Transistor Inverter Frequency Control	113
Transformer-Reactor Assembly	114
Schematic Diagram of Component Test Loop 2, Showing Location of Pressure Transducers	115
Corrosion Product Cyclone Separator, As Installed in Component Test Loop 2 for Run 11	116
Thermocouple Well as Modified for Run 12	117
Mercury Boiler	118
Adjustable Choked Nozzle for Expanding Mercury Vapor	119
Turbine Simulator Heat Exchanger	120
Turbine Simulator Blade Mockup	121
Mercury Condenser	122
Corrosion Loop Assembly - Cell A (Front View)	123
Corrosion Loop Assembly - Cell A (Side View)	124
Corrosion Loop Assembly - Cell B	125
Impingement Separator	126
Component Test Loop 2 Modification, Including Details of Thermocouple Assembly	127
As-Fabricated 9Cr-1Mo/316SS Transition Joint Evaluation (Reduced 1/3 in reproduction)	128

CONTENTS (cont.)

Figure

A. Thirteen-Tube 9Cr-1Mo Sample, Welded and Back Brazed with AMS 4778 Alloy, Illustrating Braze Alloy Flow and Filleting ____ 129

B. Section Through Welded and Back-Brazed Joints of Sample Shown in A, Illustrating Alloy Flow to Root of Welds, Erosion Diffusion of Tube Wall, and Porosity in Fillets ____ 129

Thirty-Seven-Tube Welded and Back-Brazed Sample Illustrating Flow and Filleting at the Upper Tube Sheet Joints ____ 130

Thirty-Seven-Tube Welded and Back-Brazed Sample Illustrating Poor Flow and Filleting at Lower Tube Sheet Joints ____ 131

Section Through Welded and Back-Brazed 37-Tube Sample, Illustrating Gaps in Brazed Joints ____ 132

Full-Scale -1 Condenser Suspended from Small Header in Brazing Fixture ____ 133

Full-Scale -1 Condenser Suspended in Brazing Fixture, with Radiation Shield in Position ____ 134

Volume Loss of Specimens - Accelerated Mercury Erosion Test ____ 135

APPENDIX - CALCULATIONS FOR SNAP-8 EXPANSION RESERVOIRS

Distribution List

GLOSSARY

Abbreviations commonly used in the SNAP-8 Program are defined below.

AA	Alternator
AEC	Atomic Energy Commission
AGC	Aerojet-General Corporation
AGN	Aerojet-General Nucleonics
AI	Atomics International
AOC	Award of Contract
ATL	Acceptance Test Loop
AZFO	NASA - Azusa Field Office
BOD	Beneficial Occupancy Date
CGEST	Cold Gas Electrical System Test
CL	Corrosion Loop (AGN)
CPC	Ceramic Potting Compounds
CTL	Component Test Loop (AGN)
DDAS	Digital Data Acquisition System
DWG	Drawing
EGS	Electrical Generating System
EM	Electromagnetic
EME	Electromagnetic Equivalent
FPS	Flight Prototype System
FPTF	Flight Prototype Test Facility
FRA	Flight Radiator Assembly
GE	General Electric
GN_2S-1	Gaseous Nitrogen Test Stand No. 1
GPS	Ground Prototype System
GPTF	Ground Prototype Test Facility
HR	Heat Rejection
HRF	Heat Rejection Fluid
HRL	Heat Rejection Loop
HRS	Heat Rejection System
HTL	Heat Transfer Loop
L/C	Lubricant-Coolant
L/CL	Lubricant-Coolant Loop
LeRC	Lewis Research Center
LML	Liquid Mercury Loop
LMS	Liquid Mercury Stand
LNL	Liquid NaK Loop
LOL	Liquid Organic Loop
LOS	Liquid Organic Stand
LPL	Low Power Loop
MIS	Mercury Injection System
MLA	Mercury Loop Assembly
MN_2S	Mercury-Nitrogen System
MPMA	Mercury Pump Motor Assembly
NaK	Sodium-Potassium

GLOSSARY (cont.)

NASA	National Aeronautics and Space Administration
NF	Nuclear Facility
NHRA	NaK Heat Rejection Assembly
NPA	NaK Pump Assembly
NPMA	NaK Pump Motor Assembly
NPS	Nuclear Power System
NPSH	Net Positive Suction Head
NS	Nuclear System
ORNL	Oak Ridge National Laboratory
PBRF	Plum Brook Reactor Facility
PCS-1	Power Conversion System No. 1
PCS-2	Power Conversion System No. 2
PCS-3	Power Conversion System No. 3
PCS-4	Power Conversion System No. 4
PLR	Parasitic Load Resistor
PMA	Pump Motor Assembly
PNLA	Primary NaK Loop Assembly
PO	Purchase Order
PTAT	Preliminary Type Approval Test
RPL	Rated Power Loop
SC	Speed Control
S8DS	SNAP-8 Development System
S8ER	SNAP-8 Experimental Reactor
SL-1	System Loop Test Facility No. 1
SL-2	System Loop Test Facility No. 2
SL-3	System Loop Test Facility No. 3
SL-4	System Loop Test Facility No. 4
SMU	Structural Mockup
SNAP	Systems for Nuclear Auxiliary Power
TA	Turbine Assembly
TAA	Turbine Alternator Assembly
TAT	Type Approval Test
TCL	Thermal Convection Loop (AGN)
TRW	Thompson Ramo Wooldridge
TSE	Test Support Equipment
VLB	Vehicle Load Breaker
VR	Voltage Regulator
WOO	Western Operations Office

I. INTRODUCTION

The Aerojet-General Corporation is proceeding with the design and development of the SNAP-8 Power Conversion System, as authorized by National Aeronautics and Space Administration (NASA) Contract No. NAS 5-417. The effective starting date of the contract was 9 May 1960 and this report covers the technical progress, the work accomplished, and the program status for the fifteenth quarterly period, from December 1963 through February 1964.

The ultimate objective of the SNAP-8 program is to design and develop a 35-kw electrical generating system for use in various space missions. The power source for this system will be a nuclear reactor furnished by the Atomic Energy Commission (AEC). The SNAP-8 system will use a eutectic mixture of sodium and potassium (NaK) as the reactor coolant and will operate on a Rankine cycle, with mercury as the working fluid for the turbogenerator. The SNAP-8 system will be launched from a ground base and will be capable of unattended full-power operation for a minimum of 10,000 hours. After the system is placed into orbit, activation and shutdown may be accomplished by ground command.

The nomenclature defined below is used in this series of reports.

Electrical generating system (EGS) - the complete SNAP-8 power plant, including all nuclear-system and power-conversion components, and the flight radiator assembly (FRA)

Power-conversion system (PCS) - all components of the SNAP-8 system being developed by Aerojet-General

Nuclear system (NS) - all parts of the SNAP-8 system being developed by Atomics International.

Other pertinent abbreviations for the SNAP-8 program are listed in the Glossary. These abbreviations were established to aid in communications between the NASA Lewis Research Center and Aerojet-General.

II. SUMMARY

A. SYSTEM ENGINEERING

The general test plan for PCS-1 was prepared and issued. The PCS will be tested in three major phases. Preliminary requirements for the GPS test support equipment - including instrumentation - were established. Coordination between Aerojet and Atomics International on integration of the nuclear system with the power conversion system continued.

Fabrication of the mercury loop assembly for PCS-1 is essentially complete. Fabrication of PCS-2 components was initiated.

A start-up analysis program was initiated to determine the effects of a large number of system parameter variations on start-up transients. Several computer runs were made, and an evaluation of these runs was started. Analyses were also made to define the operating characteristics of components during start-up, and to determine certain system conditions during the various start-up phases that cannot be readily determined with the aid of the computer. The thermal analyzer simulation of the cylindrical tube-and-fin radiator was completed. This radiator is considered the reference system model for use between an earth orbit and Mars.

In other systems analyses, investigations were made to determine requirements for the lubricant-coolant loop and to evaluate its performance.

B. RELIABILITY

The revised reliability program plan, incorporating specific NASA requirements and definitions, was submitted to NASA-LeRC for review and approval. The reliability micrometeorite trade-off analysis and the methodology for allocating reliability goals to the EGS were submitted to NASA-LeRC. Analytical studies were conducted at all SNAP-8 system design levels using reliability criteria, predictions, and apportionments. A general test plan for the reliability start-up test program was developed including test levels, test duration and sequence, functional test fluids, schedules, PERT, manpower requirements, and costs. Reliability monitoring of test activities continued.

C. ROTATING MACHINERY

The final TAA design review was held. The turbine assembly, seals, and alternator were reviewed in detail with respect to the analyses, materials, fabrication and assembly methods, and the test program. The TAA mockup was completed. Review of the turbine assembly was included as part of the TAA final design review.

The SNAP-8 alternator contract was signed with General Electric. The electromagnetic-equivalent (EME) alternator was completed and tested; results are reported herein. The pre-prototype alternator, Serial No. 1, was assembled and tested three times at General Electric.

Design modifications to the TA lubrication test rig No. 1 were completed. Results of tests made prior to modification are discussed in this report.

Tests of the visco pump and of the Model A and Model B seal simulators were completed. The seal-to-space program will be essentially finished with the completion of one additional test of the Model B simulator. A topical report is being prepared.

NaK pump motor development and fabrication included (1) completion of the uncanned in-air design verification testing, (2) winding and connecting several inorganic-insulated stators, (3) fabrication of interim ML-insulated stator assemblies, (4) fabrication and inspection of rotor assemblies, and (5) establishment of a stator canning procedure. The design verification testing for both the primary-loop and the HRL NaK pump motors was completed.

All detail drawings for the mercury pump-motor assembly were completed. Orders of all parts for six complete units were placed. Much of the hardware has been received, including shafts, dynamic sealing elements, face seals, and locknuts.

Re-evaluation of the lubricant-coolant PMA program led to a reduction in work scope. The details of the new program are being worked out with the subcontractor.

D. NONROTATING COMPONENTS

Tests of single-tube coiler test section (TS-2B, a 60-ft-long counter flow tube-in-tube boiler) were made to investigate boiling heat-transfer characteristics, pressure drop, stability, and overall performance at varied conditions. Results are discussed. The -1 boiler design was improved following a more detailed stress analysis, further study and incorporation of TS-2B test results, and greater economy and simplicity of design.

Fabrication was completed of the first two units of the -1 condenser. A program was initiated to develop a tube-to-tube header connection not requiring a back braze. Planning was started for fabrication of the third condenser which will be sent to NASA LeRC.

The final design review for the -1 auxiliary start loop heat exchanger, which couples the primary and heat-rejection loops during start-up, was completed. Fabrication of the first three units for RPL-2, SL-1, and SL-2 was completed. The turbine simulator program is essentially complete, with units delivered to both RPL-2 and SL-1 test loops.

Calculations for the conceptual design of all three SNAP-8 system expansion reservoirs (primary loop, heat rejection loop, and lubricant-coolant loop) were completed.

In the electrical insulation development program, testing was continued of an inorganic insulated motor for the determination of the long-term electric strength of the insulation system. This 1000-cps motor has operated satisfactorily for 4311 hours with a winding hot-spot temperature of 450°F. Evaluation of organic resins continued, and tests of promising organic insulation systems applied to stator-core sections is in progress. Electrical monitoring of the stator-core sections (statorettes) will continue until the units have accumulated 10,000 hours aging at 392°F. Fabrication of electrical insulating material specimens, to be evaluated in the SNAP-8 radiation effects program, is complete.

A preprototype voltage regulator design was completed by General Electric and approved by Aerojet, after which fabrication was started. In speed-control design, failure of the large Mo-Permalloy tuned inductor cores necessitated

a redirection of design effort to include the small Mo-Permalloy cores and the gapped C core inductors. The design for both types of inductor was completed. Fabrication of three uncut C core saturable reactors was completed, and testing was initiated. Test results are discussed herein. A revised electrical schematic of the start programer was completed which incorporates all presently available information. The specification for the parasitic load resistor was released, and four units were ordered. Negotiations for a contract between Aerojet and Lockheed-Georgia for conduct of the radiation effects program was completed.

E. TEST ENGINEERING

Design of liquid mercury loop No. 3 was completed, and fabrication is in process. All hardware for gaseous nitrogen stand No. 1 has been installed and connected. The final design for SL-1 is nearly complete, and fabrication was initiated. Design and procurement of parts and equipment for SL-2 is in progress.

The digital data acquisition system for the integrated non-nuclear test complex was re-installed and checked out. Instrumentation design for Building 187 is about 60% complete.

Preliminary design of the test support equipment for the GPTF was initiated, and a preliminary estimate of TSE power requirements was completed. Review and evaluation of FPTF design criteria continued with coordination between Aerojet and AI.

Modification of the control room in Building 156 (to accommodate an advanced data processing center) was approved. Final design is near completion.

F. MATERIALS

In support of the boiler design program, materials analyses of both the TS-1E-1 and TS-2B boiler test sections were made.

Welding techniques for SNAP-8 component fabrication were evaluated, and recommendations were made.

Operation of mercury corrosion loops at AGN continued, and test findings are discussed herein. Design and fabrication of component test loops for mercury corrosion evaluation is in process.

The program to evaluate the resistance to mercury erosion of candidate turbine rotor and nozzle materials was completed, and findings are reported herein.

III. SYSTEM ENGINEERING

A. EGS DEVELOPMENT CONTROL AND COORDINATION

1. SNAP-8 Reference System

A revision of the reference system diagram was initiated. The system changes will be reflected in Revision "D" of the SNAP-8 Reference System Schematic Diagram, Drawing No. AGC 090122. The major changes which are in effect in the program are as follows:

a. Elimination of the NaK to lubricant-coolant (L/C) heat exchanger, piping, and control (L/C system heating scheme)

b. Elimination of the 3-way L/C valve at the mercury pump-motor assembly (PMA) bearing inlet in favor of a 2-way valve

c. Rerouting the L/C piping to eliminate the 3-way L/C valve and increase system efficiency

d. Change of the mercury injection system from a pump-driven device to a pneumatic injection system.

2. System Working Fluids

a. Purification and Sampling

The preliminary requirements for purification and sampling of the working fluids for power conversion systems 1 and 2 (PCS-1), (PCS-2), and for the ground prototype system (GPS) have been determined. These requirements are discussed below.

(1) Primary NaK Loop

Prior to loading with NaK, the primary loop will be evacuated to 1.0 mm of mercury measured at the interface of the vacuum system and the NaK loop. The NaK will be purified prior to loading to an Na_2O concentration of 20 ppm. The NaK and the primary loop will be purified by cold trapping and hot trapping until the oxygen concentration in the NaK is less than 10 ppm with the loop at 1000°F. If the loop is opened, the purification procedure will be repeated.

Samples will be taken at reasonable intervals to determine the NaK purity.

Following completion of primary loop NaK purification and initiation of tests, NaK samples will be taken in accordance with the following sampling table:

Interval	Amount	Location
First week of operation, daily	Two samples of 5 g each	Hot leg
Next month of operation, weekly	Two samples of 5 g each	Hot leg
Remainder of operation to be determined	Two samples of 5 g each	Hot leg

(2) Heat Rejection Loop (HRL)

The purification and sampling requirements for the HRL are similar to those for the primary loop except that the HRL will be heated to a maximum of 600°F.

(3) Mercury Loop

The mercury will be completely purified prior to loading into the mercury loop. The mercury loop will be evacuated to 0.1 mm of mercury measured at the interface of the vacuum system and the mercury loop. Sampling of the mercury in the operating loop is not required.

(4) Lubricant-Coolant (L/C) Loop

Purification of the ET-378 (the lubricant-coolant fluid) will be accomplished prior to loading into the L/C loop. Purification requirements will be provided at a later date. Sampling of the L/C during test operations will be in accordance with the following schedule:

Interval	Amount	Location
Weekly	Two samples of 25 cu cm each	Downstream of the main filter

The working fluids procurement requirements were established and are currently being integrated into procurement specifications.

b. Investigation of Superheated Mercury

The objective of this program conducted by the Chemical Division was to determine whether superheated mercury vapor behaves as an ideal

gas or deviates significantly from the ideal. The original intent was to measure the Joule-Thompson coefficient by diffusion through a porous plug; experimental difficulties and a shift of emphasis caused this approach to be dropped in favor of directly measuring the pressure, volume, and temperature (PVT) of superheated mercury vapor.

While the mercury-vapor PVT apparatus (Figure 1) was being completed, testing showed that the diaphragm-probe system for indicating balanced pressures failed at high temperatures. A replacement system was developed in the form of an indicating U-tube manometer using molten lead as the manometer fluid. With this system, construction of the PVT apparatus was completed and a successful run was made.

During this run, mercury vapor was superheated from 784°F at 40.2 psia to 1076°F at 49.5 psia. The data obtained (Figure 2) show that the compressibility factor, Z, was a constant value of 0.874 and varied by less than 1%. However, this value represents a 13% deviation from ideal gas behavior. The 13% deviation could be accountable by assuming a 13% loss of mercury vapor into the lead filled tube. The data obtained from this run are not sufficient to establish conclusively one value or the other as correct. For SNAP-8 purposes, the information given in the Mollier diagram for mercury (Figure 3) is assumed to be adequate.

3. Development Systems

a. PCS-1

The General Test Plan for PCS-1 was prepared and issued. The plan calls for testing the PCS in three major phases with the following objectives:

(1) Phase I

(a) Evaluate performance of development components.

(b) Demonstrate stable operation of mercury Rankine cycle at rated electrical output.

(c) Verify cooling and lubricating requirements for turbine alternator assembly (TAA) and mercury pump-motor assembly (MPMA).

(2) Phase II

(a) Explore steady-state limits of system parameters for stable operation.

(b) Determine transient effects due to variation in simulated radiator heat load (sun-shade) rates and magnitudes.

(c) Verify L/C requirements for primary and heat rejection loop (HRL) PMA.

(d) During the above test, the system will be operated to demonstrate a capability for continuous operation.

(3) Phase III

Demonstrate 10,000 hours of continuous operation with steady-state system parameters selected to give the highest assurance of generating 35 kwe minimum for the 10,000-hour operation. During the endurance test, simulated radiator heat loads (sun-shade) and simulated vehicle electrical loads will be applied periodically.

Essentially all test support equipment requirements have been established, including instrumentation.

System schematic diagrams for each of Phases I, II, and III were prepared and issued. They are included as Figures 4, 5, and 6.

A preliminary PCS-1 Test Requirements Specification, which incorporates all of the above information in addition to detailing the tests which are to be performed, has been prepared and is being reviewed.

b. PCS-2

The conceptual design and test requirements for PCS-2 were completed during the report period. Figures 7 and 8 are the latest system schematics. The test plan for PCS-2 was completed and requires the testing of the PCS in three major phases with the following objective:

(1) Phase I

(a) Evaluate performance of the development components as integrated in the PCS-2.

(b) Demonstrate stable operation of the mercury Rankine cycle at rated electrical output.

(c) Explore reference system startup techniques.

(2) Phase II

(a) Explore steady-state limits of system parameters for stable operation.

(b) Determine transient effects due to variation in simulated radiator heat load (sun-shade) rates and magnitudes.

(c) Develop PCS reference system startup techniques.

(d) Demonstrate 18 out of 20 successful PCS starts without system adjustment.

(3) Phase III

Demonstrate 10,000 hours of continuous operation with steady-state system parameters selected to give the highest assurance of generating 35 kwe minimum for a 10,000-hour operation. During the endurance test, simulated radiator heat loads (sun-shade) and simulated vehicle electrical loads will be varied periodically.

c. Ground Prototype System (GPS)

Preliminary requirements for the GPS test support equipment, including instrumentation, were established. The reference system arrangement, pressures, temperatures, and flow rates were specified for use in GPS test planning.

4. EGS and PCS Model Specifications

Drafts of the PCS model specification and SNAP-8 EGS model specification were submitted to NASA for review and comment during this report period.

5. Nuclear System Coordination

a. Aerojet-Atomics International (AI) Project Coordination Meetings

The Aerojet-AI SNAP-8 project coordination meetings were held on 17 December 1963 and 6 February 1964. The actions described below were taken as a result of this meeting and associated working group meetings.

AI provided a detailed table of calculated values of the pressure drops associated with NaK flow through each region of the NS from flange to flange with the following results:

	600 kwt	450 kwt
Nuclear System	6.05 psi	3.21 psi
Core	4.28 psi	2.23 psi

Aerojet and AI defined design problem areas arising from the variation of the reactor outlet NaK temperature. The steady-state operating range is presently conceived to be 1300 $\pm 40^{\circ}$F. This value is considered incompatible with PCS operating requirements. In addition, temperature drop-out due to parasitic load resistor action increases this ΔT from a nominal 80°F to about 94°F. Approaches considered for design improvement included the following:

Increase primary loop flow rate
Remove PLR from primary loop
Decrease drum worth per step
Improve temperature sensor tolerance
Increase heat capacity of PLR.

Aerojet provided AI with the SNAP-8 conceptual layout for the PCS, and calculated results of NaK pipe deflections for the NS to PCS configuration.

A draft copy of the Aerojet EGS model specification was furnished to AI for consideration in updating the NS model specification.

A review of the GPS General Test Plan of Aerojet was attended by AI. Comments by AI are being considered in the revision of the test plan.

Aerojet incorporated AI comments and pertinent logic of the AI management network into the Aerojet NS/PCS integration PERT network.

b. Nuclear System (NS) Model Specification

Aerojet and NASA comments on the NS model specification were informally transmitted to AI for consideration in the next revision of this specification.

Changes in the NS model specification that were agreed upon during the SNAP-8 program specifications review (NASA/AEC/AGC/AI) will appear in the next revision. (See paragraph III,A,5,f below.)

c. NS/PCS Integration Plan

Informal Aerojet and NASA comments on the NS/PCS Integration Plan were received for consideration in the preparation of the next draft of the plan.

d. NS Design Review Plan

The requirements and procedures for Aerojet review of the SNAP-8 nuclear systems of AI were agreed upon and formulated in the NS Design Review Plan by NASA/AEC/AGC/AI.

e. SNAP-8 Development System (S8DS) Design Review

AI furnished Aerojet with drawings, specifications, and design data sheets on their development system (i.e., the S8DS). Aerojet formulated questions, based on this data, which were answered at a conference at AI. Aerojet is preparing comments and recommendations on the S8DS design and development from the conference presentations and information received.

f. NASA 417 Series Specifications

A SNAP-8 joint agency-contractor meeting was held 4 and 5 December 1963 at AEC, Canoga Park. The NASA 417 series specifications were

discussed in order to resolve differences among the participating organizations in preparation for incorporation of the NASA specifications into the NS development program.

g. EGS Shock Requirement During Space Operation

AI was informed that the shock requirement of NASA SNAP-8 Environmental Specification No. 417-2 was reduced from 7 to 3 g on the EGS during space operation.

h. SNAP-8 Interface Control Drawing and Document Agreement

The subject agreement was approved and signed by Aerojet and AI SNAP-8 management. This agreement provides a mutually acceptable method of controlling the physical interfaces between the NS, PCS, and the test facilities.

i. Aerojet Resident Engineer at AI

The Aerojet resident engineer was assigned at AI during the report period.

j. SNAP-8 NS/PCS Flight Reference System Simulation Data

System parameters simulation data were provided to AI from Aerojet on the PCS; similarly, NS data was transmitted to Aerojet from AI.

k. FPS-FPTF Spares Provisioning

A joint agency-contractor ad hoc committee meeting was held at AEC in Canoga Park to study the influence on the SNAP-8 program schedule of possible FPS malfunction during testing in the FPTF.

l. SNAP-8 Nuclear Power System (NPS) Review Plan

The requirements and procedures for AI review of the SNAP-8 nuclear power systems for nuclear safety and facility compatibility were agreed upon and formulated in a NPS review plan by NASA/AEC/AGC/AI.

m. SNAP-8 Joint Agency-Contractor Meeting

Aerojet prepared and issued rough draft minutes of the joint agency-contractor meeting of 4 and 5 December 1963. These minutes covered

the NASA 417 series specifications review, the NS model specification review, the ad hoc committee meeting on FPS-FPTF spares provisioning, and the NS and NPS design review plans discussion.

n. NS Quality Assurance and Reliability Program Plan

The NS quality assurance and reliability program plan was received from AI for informal comment and review by Aerojet.

B. SYSTEM DESIGN

Fabrication was essentially completed for the MLA. Fabrication for the PCS-2 components was initiated.

Coordination has been maintained in the areas of fabrication, system requirements, materials, component design, and testing.

1. Mercury Loop Assembly (MLA)

The following design review has been presented:

Final Design Review - SL-1/PCS-1, 16 January 1964.

The following technical memoranda have been issued:

TM 340:63-1-165, A Method for Analysis of Insulated Cylindrical Shapes on MLA, 26 November 1963.

TM 340:63-1-166, Insulation Survey for MLA-1A, SL-1, 26 November 1963.

TM 518:63-13-776, Final Report on the SL-1 Mercury Loop Heat Transfer and Insulation Analyses, 6 December 1963.

TM 340:64-1-187, Component Piping Connection Loads - MLA, SL-1, 5 February 1964.

TM 340:64-2-189, Mercury Loop Assembly, Fluid - Circuit Pressure Drop, 20 February 1964.

TM 340:64-1-185, Piping Load and Stress Analysis - MLA, SL-1, 24 February 1964.

a. Design and Drawings

The assembly drawings have been updated as necessary to the current design status.

b. Analyses

Analyses have been completed. Results of these analyses are given in the technical memoranda.

c. Materials

The materials requirements were reviewed with the Materials Department.

d. Assembly

Preliminary work on the turbine simulator assembly was initiated. To assure that the TAA will mate when upgraded, a fixture will be used to simulate the interfaces.

e. Procurement and Fabrication

All parts have been completed with the exception of the bellow assemblies. The later delivery of the bellows is not expected to delay the MLA assembly.

2. PCS-2

The following design reviews have been presented:

Conceptual Design Review - PCS-2, January 1964

PCS-2 Preliminary Design Review and Final Structural Design Review, 19 February 1964

a. Design and Drawings

The PCS-2 assembly consists of the mercury loop assembly with the addition of the -1 NaK components, L/C components, -1 mercury injection system, and -1 or -x electrical components. The design for the structure has been completed. Additional work is being performed for design of the NaK and L/C piping.

b. Analyses

Thermal, stress, and pressure-drop analyses have been conducted for the NaK and L/C loops. Min-K F-182 insulation is being used.

c. Materials

Type 316 stainless steel is being used for the NaK loops and 304 SS is being used for the L/C loop.

Structural steel is being used for the mountings and structure.

d. Procurement and Fabrication

The materials for piping, flanges, structure, and insulation was ordered and has been received with the exception of the insulation. The flanges and mounts of the mercury loop have been fabricated.

3. Conceptual PCS Flight Assembly

The piping interface loads were analyzed. A preliminary coordination meeting with Atomics International was held. Gyrodynamic forces from the rotating components are being studied.

C. SYSTEMS ANALYSIS

1. Startup Analysis

A startup analysis program was begun with the aid of the analog computer to determine the effects on startup transients of a large number of system parameter variations. A considerable number of computer runs were made and an evaluation of these runs was started.

The operating characteristics of components during startup were defined. Certain system conditions during the various startup phases, which cannot be readily determined with the aid of the analog computer, were described.

a. Analog Computer Investigations

An analog computer investigation of reference-system startup conditions was initiated following the programing and checkout of the complete reference system simulation on the analog computer. The primary purpose of this investigation was to determine whether or not conclusions reached and conditions chosen as a result of previous computer startup investigations were

still valid. The previous computer startup investigations were conducted with the aid of a simulation which represented only the primary loop portion of the system, whereas the present computer simulation includes all three liquid-metal loops.

A computer program plan similar to that used for the previous startup investigation was outlined. The study was divided into two main series of computer runs. During the first series of runs, the effects of variations to the initial primary-loop flow rate and the initial reactor power were to be investigated. From this series of runs, a set of reference values for these two variables would be chosen and a second series of computer runs would be made with the two main variables held constant. The effects of the following additional variables would then be investigated:

Initial mercury-flow-rate ramp
Time at nominal 40% rated mercury flow
Time to ramp mercury flow from nominal 40% to rated
Time for TAA to accelerate to rated speed
Initial reactor outlet temperature
Reactor control sampling time
Reactor control reactivity per step
Initial radiator outlet temperature
Radiator thermal capacity.

The first series of computer runs was completed and evaluated to determine the effect of initial primary-loop flow rate and reactor power on the maximum rate of change of reactor temperatures and the maximum temperature at the reactor outlet. The results of this series of runs are shown in Figures 9 and 10. The results of this series of runs were also compared with the results of similar runs made previously with only the primary-loop portion of the system simulation. The trends established were generally the same for both investigations; however, absolute values were different. The values for the maximum rate of change of reactor temperature are generally greater in the latest series of runs for the same system conditions. This is primarily due to the increase in primary-loop flow rate associated with the TAA and pump

acceleration. The primary-loop flow-rate increase is faster than the programed ramp rates used in the previous investigation. The values for the maximum reactor outlet temperature are generally lower in the latest series of runs for the same system conditions. This can be attributed to the fact that temperature transients at the reactor outlet are less severe than for similar runs made during the previous investigation. The general conclusion reached from the first series of computer startup runs was that differences in results, when compared with similar runs made during the previous investigation, were not significant enough to require a change in reference values for the initial primary loop flow rate and the initial reactor power level.

The next series of analog computer runs was therefore made with the initial primary-loop flow rate and the initial reactor power level kept constant at the reference values of 50% rated flow and 56 kw, respectively. This series of runs included variations in initial mercury flow rate ramp, time at nominal 40% rated mercury flow, time to increase mercury flow from nominal 40% to rated flow, and initial reactor outlet temperature. The runs were evaluated to determine the effect on the maximum rate of change of reactor temperature and the maximum reactor outlet temperature.

The results are shown in Figures 11 and 12. From Figure 11 it can be seen that the initial primary-loop flow rate and the initial reactor power level have the greatest influence on the maximum rate of change of reactor temperature. From Figure 12 it can be seen that the initial reactor outlet temperature and the initial reactor power level have the greatest influence on the maximum reactor coolant outlet temperature. The influence of initial reactor outlet temperature on the maximum reactor outlet temperature indicates that the initial reactor outlet temperature should be set at 1320°F when computer runs are made for evaluation of other variables.

Additional computer runs were made in which the reactor control sampling time and the reactor control reactivity per step were investigated. The results of these runs are not reported herein because of security classification.

A series of computer runs was also made to determine the effect of TAA acceleration on the maximum rate of change of reactor temperature

and on the maximum reactor outlet temperature. The TAA acceleration directly influences the rate of change of primary-loop flow which, in turn, directly influences reactor temperatures. The results of this series of runs are shown in Figure 13. The maximum reactor outlet temperature was not noticeably affected. The computer simulation and the assumptions used for defining startup conditions tend to result in a minimum TAA acceleration time. Therefore, this series of runs is believed to show conservative values for the maximum rate of change of reactor temperature at any particular set of conditions.

Further computer runs were made to evaluate the effect of the initial radiator outlet temperature and the radiator thermal capacity. These variables have no noticeable influence on primary-loop parameters, but can significantly affect conditions in the secondary loop. Therefore, this series of runs is presently being evaluated to determine the effect on mercury pump NPSH during startup.

b. Startup Component Investigations

Off-design operating conditions were checked for the coiled tube-in-shell type of auxiliary heat exchanger. The results showed that the heat-exchanger outlet temperature would exceed the radiator inlet temperature limitation during portions of the startup cycle. To satisfy the radiator inlet temperature limitation with this type of heat exchanger design, it was necessary to bypass a portion of the start loop flow rate around the heat exchanger, thereby mixing cold NaK from the radiator with hot NaK from the heat exchanger outlet. Therefore, the NaK flow rate in the heat rejection loop was increased slightly during the startup period.

The changes in heat-rejection-loop flow rates and temperatures during startup which result from the use of a coiled tube-in-shell type of auxiliary heat exchanger affect the operation of the thermal control valve in the heat rejection loop. Therefore, new operating characteristics were determined for the thermal control valve and these characteristics were used to describe the valve operation for the analog computer simulation.

A qualitative study was made of several mercury injection systems which could be used for injecting mercury at the inlet of the pump. A comparison was made between these systems and the system presently planned for development which will inject mercury at the mercury pump discharge. The conclusion reached from the study was that the system which will inject mercury at the pump discharge is more advantageous and is preferable to any of the systems which will inject mercury at the pump inlet. In addition, analyses conducted to date, based on the use of a system which injects mercury at the pump discharge, have resulted in the definition of straightforward component requirements and characteristics. Also, preliminary analyses of system perturbations resulting from the use of this type of system in conjunction with the reference startup procedure have not indicated the existence of any significant problem areas.

The analysis of the TAA acceleration during startup was completed for the reference system (Revision B). The results of the analysis, the assumptions, and the analytical methods employed are described in a recently issued technical memorandum (SNAP-8 TAA Acceleration During Startup for the Reference System, TM 340:64-1-195).

c. Startup Condition Investigations for PCS-1 and PCS-2

Investigations were conducted to determine mercury-flow conditions during specific phases of startup for PCS-1 and PCS-2.

One investigation was made to determine the minimum mercury flow rate required to operate the TAA at rated speed during early tests of PCS-1. The minimum flow rate was determined to be approximately 15% of rated mercury flow, and was based on system operation with no vehicle load and with all system pumps operating on test facility power.

A brief investigation was conducted to evaluate the possible mercury-flow-rate variation during the transition period which occurs at the end of mercury injection (when the mercury pump must provide the circulation of mercury in the secondary loop). The mercury injection system pressure was assumed to be slightly higher than the mercury pump shutoff pressure, and the head-capacity for the -1 mercury pump was used. The results of the investigation show that the flow rate will change from 40% rated flow during mercury

injection to approximately 38% rated flow after the mercury provides the circulation. The magnitude of the change depends, to some extent, on the specific hardware in the circuit and on the difference between the injection-system discharge pressure and the mercury-pump shutoff pressure.

An investigation was conducted to determine the minimum mercury flow rate for PCS-2 during the intermediate startup period. (The intermediate startup period occurs in the time between the end of the first mercury flow rate ramp and the start of the second mercury flow rate ramp.) The required mercury injection rate was determined to be between 43 and 45% of rated mercury flow. When secondary loop operation is switched to mercury pump output at the end of the injection period, the mercury flow rate will be reduced to a value between 42 and 44% of rated mercury flow – which is sufficient to maintain the TAA at rated speed.

2. System Studies

a. Space Radiator Simulations

The thermal analyzer simulation of the cylindrical tube-and-fin radiator was completed. This radiator is considered to be the reference system model for use between an earth orbit and Mars. Special circuits were devised and implemented to simulate the radiation of heat to space with varying external heat flux from solar and planetary sources, and to simulate heat transfer from the coolant fluid with variable flow and radiator inlet temperature.

The thermal analyzer simulation has been used to develop performance criteria on which the radiator simulation in the system test loop SL-2 will be based. The SL-2 simulation must approximate the dynamic response of a space radiator under startup conditions and under transients at nominal rated conditions. The data developed from the thermal analyzer consisted of steady-state off-design performance under sun and earth-shade conditions, and transient performance data under conditions anticipated during reference-system startup. The steady-state off-design performance data are depicted in Figures 14 and 15; these figures show the radiator fluid exit temperature as a function of inlet temperature and coolant flow rate, under sun and shade conditions.

Steady-state data were reduced to two equations which are accurate to approximately 1% of the absolute temperature levels, within the ranges of temperatures anticipated during startup. The equations are as follows:

For operation in the sun

$$T_{out} = K_{sun} (T_{in} - 325) + 572$$

For operation in the shade

$$T_{out} = K_{shade} (T_{in} - 200) + 485$$

where all temperatures are in degrees Rankine. The coefficients K_{sun} and K_{shade} are a function of the flow rate and are shown in Figure 16.

The transient radiator data were obtained by making frequency response runs at flow rates and temperature levels expected during reference system startup. In each run the flow rate was held constant and the inlet temperature was varied sinusoidally about a nominal temperature level at various frequencies. The frequency response data were plotted on Bode' plots. Figure 17 is a typical Bode' plot showing the variation in amplitude ratio and phase shift as a function of frequency of radiator inlet temperature. Similar runs and Bode' plots were made at other flow rates. The Bode' plots were used to develop a transfer function which would approximate the dynamic response of the space radiator.

The transfer function is of the form

$$G(S) = \frac{1}{\left(1 + \frac{S}{\omega}\right)^3}$$

where

$$\frac{1}{\omega} = \frac{204}{W_{NaK}}$$

W_{NaK} = third loop NaK flow rate

S = Laplace operator

These data were used to develop an analog computer simulation of the space radiator. An information diagram of this simulation is depicted in Figure 18. The analog simulation was checked out against the thermal analyzer simulation under typical startup transients. The agreement between the two simulations was within 1% of the absolute temperature levels under steady-state conditions and within approximately 2% during transient conditions. The radiator analog simulation has been subsequently incorporated into the analog simulation of the reference system.

This analog simulation of the radiator has also been recommended for inclusion into the HRS simulator in system test loop SL-2.

b. Lubricant-Coolant (L/C) Loop Investigations

Additional investigations were made to determine requirements and to evaluate performance of the L/C loop.

(1) Sun-Shade Operation of L/C Loop

The variation of L/C loop temperature levels and flow rates due to the variation of external heat flux on the L/C radiator during sun-shade operation was re-evaluated with two assumptions made. The first assumption was that the Sieder-Tate heat-transfer correlation, reported in the last quarterly report (Reference 1), was applicable for describing heat transfer with ET-378 in the radiator. The second assumption was that the net heat rejected from the loop remained essentially constant.

The mean temperature in the radiator was found to vary from 228°F in the sun to 207°F in the shade. The corresponding variation in the radiator outlet temperature was 210 to 186°F. The nominal overall flow rate variation was approximately 5360 to 4310 lb/hour for the sun-shade perturbation. The variations in temperature levels and flow rates were lower than anticipated. This phenomenon is explained by the fact that the radiator is, to a degree, self compensating. The radiator model used in this analysis operates with flow in the transition regime, between laminar flow and fully developed turbulent flow, under sun conditions. When operating in the shade, the flow is

in the laminar regime which results in a considerable reduction in the heat-transfer coefficient. There is a corresponding increase in temperature drop between the fluid bulk temperature and the radiating surface. Therefore, even though the external absorbed flux is considerably reduced in the shade and the radiator rejects heat at a lower temperature, the total radiated flux is reduced and there is only a small reduction in the fluid bulk temperature.

Component designers were asked if the aforementioned temperature variation would permit satisfactory operation of components. In general the reply was that on a theoretical basis, component performance would not be significantly affected. This will have to be verified during system tests.

It was concluded, therefore, that temperature controls are not required in the L/C loop considering the present knowledge about component performance.

(2) Report on L/C Loop Investigations

A technical memorandum report (Reference 2) was prepared summarizing the investigations of the L/C loop. The material covered in this report includes the evaluation of the following items:

(a) Lubricant-Coolant Loop Operating Parameters and Heat Loads

(b) Heat Transfer Criteria

(c) Flow-Pressure Drop Characteristics of the L/C Loop

(d) L/C Radiator Weight Trade-Off

(e) L/C Loop Startup Investigations

(f) Effects of Sun-Shade Operation on the L/C Loop

c. Review of NASA Digital Computer Simulation of SNAP-8 System

A review was made of the digital computer simulation of the SNAP-8 system which is being prepared at NASA-LeRC. A critique was prepared

and a list of recommended changes was submitted to H. O. Slone in a letter dated 4 February 1964.

d. Instrumentation Transient Response Requirements

An investigation was made to evaluate the transient-response requirements for the instrumentation to be provided in the system test loops. The results of many system analog computer runs were reviewed. This included startup and shutdown runs as well as system load change runs. Table 1 shows the estimated maximum rates of change of significant system parameters.

e. Study of Certain System Tolerances

An investigation was initiated to determine the tolerances on certain system operating parameters and to evaluate their effect on alternator output power and controls. The following parameter tolerances are being investigated:

Turbine inlet temperature
Turbine inlet pressure
Turbine exit temperature
Turbine speed
TAA efficiency
Alternator voltage.

In addition, the effects of vehicle acceleration during system operation are being investigated.

3. Additional Investigations

a. Constants for NASA Computer

System and component constants for the reference system, revision C, were compiled and forwarded to NASA for use in the digital computer simulation.

b. Preliminary Simulation of GPS

Coordination with SNAP-8 Test Operations has begun in order to determine GPS characteristics which will be used as a basis for a preliminary GPS transient study on the analog computer.

c. Study of Increased Thermal Capacitance of the Parasitic Load Resistor

An investigation was initiated to determine possible methods for increasing the thermal capacity of the parasitic load resistor. This investigation was undertaken as the result of an effort to determine means by which the reactor temperature transients could be reduced so that the reactor-control temperature dead band could be reduced. Initial results of the investigation showed that significant changes in thermal capacity of the parasitic load resistor would be difficult to achieve and would result in large weight penalties.

A further appraisal was made of the methods by which the reactor temperature transients might be reduced and it was determined that significant improvements could not be achieved by changing any of the parasitic-load parameters. Therefore, no further work will be conducted on this investigation.

D. SL-1 PROJECT COORDINATION

SL-1 is the first SNAP-8 power conversion system (PCS) to be tested at a system level. Testing will be non-nuclear and will be performed in Building 187 at Aerojet's Von Karman Center.

Phase I will consist of a mercury loop assembly (MLA) containing -1 model turbine alternator assembly, boiler, condenser, flow control valve, and mercury pump-motor assembly. The primary, heat rejection and lubricant-coolant loops will be constructed of nondevelopment (work horse) equipment. This phase will evaluate the performance of development components and system integrity.

Phase II will consist of the same mercury loop assembly and support loops with the exception that the work-horse primary-loop and heat-rejection-loop NaK pumps will be replaced with -1 model pump-motor assemblies. This phase will test the system's ability to perform with simulated sun/shade variations. Lubrication and cooling requirements for the -1 model NaK pumps will be verified, and the capability for continuous operation will be demonstrated.

Phase III will upgrade the Phase II system to include -1 model heat-rejection-loop temperature control valve and shutoff valve, parasitic load

resistor, L/C pump-motor assembly, and the reference system arrangement of lubrication and cooling piping. This phase of testing will consist of 10,000 hours of endurance operation.

During this report period the SL-1/PCS-1 final design review package 340-2500 was prepared and the final design review meeting was held on 16 January 1964. The review package contains the general test plan, -1 model and test support equipment component data sheet lists, Schematic Diagram Phase I (Drawing Number 092824). Schematic Diagram Phase II (Drawing Number 092486), Schematic Diagram Phase III (Drawing Number 093460), instrumentation lists for all phases, mercury loop assembly design information and assembly instructions, and schedules including a PERT network.

Project coordination meetings are held at 2- to 3-week intervals to discuss and resolve action items and coordination items that exist between SNAP-8 groups and/or NASA. The status and results of these meetings are summarized and published on a SL-1 Action Item Status List (340-64-3016) following each coordination meeting.

A list of dates for availability of SL-1 major components is published at 2-week intervals or at the time of major changes. The major component availability dates are used on the SL-1 PERT network that is distributed at 4-week intervals.

The MLA mounting structure was completed and is ready for assembly with components and piping. A condenser, turbine simulator, mercury pump-motor assembly and piping were delivered to the assembly area in Building 187 for assembly. Construction of the test loop mounting structure has started in the test cell in Building 187. All test loop components and piping were ordered and are scheduled for delivery and installation during the next report period.

E. SL-2 PROJECT COORDINATION

SL-2 is the second SNAP-8 power conversion system loop being developed for non-nuclear testing at the Aerojet Von Karman Center. It will comprise the PCS-2 undergoing test, the SL-2 test facility in Building 187, and the associated test support equipment. The PCS-2 test objectives and configuration

are generally similar to those for PCS-1. (PCS-2 involves tests to develop and demonstrate performance of a PCS using -1 model components, followed by endurance testing with the objective of 10,000 hours of continuous unattended operation.) The major difference in PCS-2 is the emphasis on the development and demonstration of a -1 model automatic PCS startup system and associated techniques.

The project engineer has the responsibility for the development and testing of PCS-2 in the SL-2 test facility. This task involves coordination of the efforts of Systems Engineering and other departments (particularly Test Engineering) in establishing requirements for the PCS-2 system and components, monitoring the ensuing procurement and assembly, planning the test program, and defining the required SL-2 support equipment.

A PCS-2 conceptual design review meeting was held at Azusa on 20 December 1963 to review progress. Among the topics discussed at this meeting were preliminary versions of the PCS-2 test plan, schematics, design approach, layout drawings, schedule, and PERT network. This review led to recommendations for (1) correcting and completing various documentation, (2) establishing a procedure to define PCS-2 component interfaces, (3) considering installation of an emergency mercury-vapor bypass, (4) reviewing mercury conditioning plans, and (5) continuing to evaluate certain system reliability-performance tradeoffs.

A series of PCS-2/SL-2 internal coordination meetings was initiated on 30 December 1963 to identify and assign responsibility for action on questions arising in the PCS-2 system and SL-2 test support equipment design. Further coordination meetings were held on 31 December 1963, and on 21 January and 17 February 1964. These meetings were aimed primarily at resolving differences between system engineering (PCS-2) and test engineering (SL-2 test support equipment) prior to the SL-2 conceptual and PCS-2 preliminary design reviews on 28 January and 19 February 1964.

Progress in the design and procurement of SL-2 support equipment for testing PCS-2 is discussed in the Test Engineering section of this report. The status of PCS-2 development at the end of the reporting period is described in the data package prepared and distributed for the PCS-2 design review

scheduled for 19 February 1964. This material was considered appropriate for a preliminary design review of the PCS-2 as a complete system, and for final design review of the PCS-2 structure, bracketry, piping, and insulation. The progress in the primary areas involved in PCS-2/SL-2 project coordination may be summarized as indicated below.

1. Test Requirements (See Section III,A)

The final draft of the general test plan for PCS-2 was completed on 7 February 1964. This plan calls for (a) Phase I for testing-shakedown, performance, and exploratory reference startups, (b) Phase II for reference startup development and demonstration of 18 out of 20 successful startups, and (c) Phase III for endurance testing to 10,000 hours. Additional information on the test plans and milepost schedule is given in Table 2.

2. Component Requirements (See Section III,A)

Data sheets giving system engineering requirements for the PCS-2 and -1 model components and related TSE were essentially completed by early February 1964. Most of these requirements are the same or slightly modified versions of the requirements for PCS-1. Major additions and changes for PCS-2 startups include the -1 model electrical startup programer-inverter and the mercury injection system.

3. System Schematics (See Section III,A)

Figure 8 is a schematic illustrating the PCS-2 test equipment for Phase II and III testing. A similar schematic was completed for the Phase I test configuration, which uses experimental and workhorse (rather than the -1 model) electrical controls and expansion reservoirs.

4. Instrumentation (See Section III,A)

Preliminary lists of instrument sensors desired for measurement of PCS-2 system and component performance were prepared. The total sensors requested came to 275 for the Phase I tests (149 of these for temperature) and 323 for Phase II and III tests (179 for temperature). In general, the requested instrumentation is similar to that for PCS-1, with adjustments to monitor the added -1 model startup components and system performance.

5. Structure Design and Assembly (See Section III,B)

Figure 19 is a two-view drawing of the PCS-2 assembly. The structure and configuration designs are similar to PCS-1. However, frame height has been increased about 6 in. to allow installation of a mercury injection system near the mercury-loop low point, and the lower portion of the frame has been extended out at the side, to accommodate the -1 model NaK pump-motor assemblies and the associated piping required to limit thermal stresses. A detailed parts list with material callouts was completed for the PCS-2 assembly shown in Figure 19.

6. Schedules and PERT

PCS-2 and SL-2 PERT networks have been formulated and cross-checked for logic and for expected milepost dates. These networks are scheduled to go operational in March 1964.

IV. RELIABILITY

A. MANAGEMENT AND PLANNING

The Reliability Program Plan (Aerojet Report No. 2406) was submitted to NASA-LeRC for review and approval. The revised plan reflected specific NASA requirements and definitions, resulting in:

1. Reduction in report size through simplification and elimination of redundancies.

2. Tailoring of the plan to SNAP-8 Program orientation.

3. Use of the SNAP-8 Quality Assurance Program Plan (Aerojet Report No. 2405) to support the Reliability effort.

In subsequent coordination meetings with NASA-LeRC personnel, further clarification of the interface between reliability and quality assurance was requested and will be submitted to NASA-LeRC for review and approval.

Informal reliability indoctrination was continued, on a person-to-person basis, regarding failure analysis, failure reporting, reliability criteria, reliability data requirements (equipment and buildup logs) and reliability procurement requirements.

A series of meetings was held which determined the scope of the reliability startup testing program and implementation of the program was initiated.

In association with Mr. M. E. Langston (NASA-LeRC), a coordination meeting was held with AI and AEC personnel at Atomics International regarding implementation of the AI Reliability Program, establishment of a Working Group for Reliability and Quality Assurance revision of NASA Specification 417-4, and preliminary evaluation of the AI Reliability Program Plan.

Coordination meetings were held with AI personnel regarding reliability requirements for the NPS.

In conjunction with NASA personnel, NASA Specification 417-4 was reviewed; problem areas were defined, and revision recommendations were submitted.

Definition of nuclear-system reliability requirements and reliability test monitoring of RPL-2 were submitted for SNAP-8 management coordination.

Coordination meetings were held with NASA personnel regarding the status of the SNAP-8 Reliability Program and its implementation.

B. SYSTEM STATISTICAL ANALYSIS

The reliability micrometeorite tradeoff analysis and the methodology for allocating the reliability goals to the EGS was submitted to NASA-LeRC. A reliability assessment of alternate configurations for the mercury injection system was completed and formally submitted to NASA-LeRC.

In accordance with verbal direction from NASA-LeRC (M. E. Langston) that the NPS reliability is to equal 0.90 (including meteorite hazard), a reliability allotment was initiated; the verbally approved techniques defined in the SNAP-8 Reliability Methodology Report were used to evaluate redefinition of reliability goals.

A detailed evaluation of failure modes and effects analysis techniques was made. System simplification studies, including simplification of startup procedures, consideration of multiple startup requirements vs single startup mission, meteoroid analysis, and shutdown criteria were conducted. Reliability assessments of the proposed L/C shutoff valve configuration and the HRS/auxiliary start loop thermally controlled valve were initiated.

C. RELIABILITY DESIGN ENGINEERING

Reliability Design Engineering personnel participated in 15 formal design reviews at all system levels; reliability problems, considerations, and/or evaluations were defined and submitted. (For example, Reliability recommended further study of the coolant system to permit use of a single valve configuration of simpler design, and also recommended that the HRL temperature-control requirements be reviewed to possibly permit simplification of the temperature control valve.) The AI design review on the S8DS was attended by Reliability personnel. The Design Review Checklist was revised to differentiate between systems loops and components.

Analytical studies were conducted at all SNAP-8 system design levels using reliability criteria, predictions, and apportionments. Analysis of potential shutdown problems was completed showing that definitive design/test considerations must be given to unscheduled shutdown to prevent significant PCS component degradation. Based on two alternative reliability goals, reliability requirements for PCS components were analyzed and detailed analyses were made on the mercury PMA bearings and the speed controller. Analysis of the L/C shutoff valves was conducted, including system function, means of actuation, timing, failure modes, environmental test program, relationship to face seals, and cost. Evaluation of reliability trade-offs and system performance by relocating the parasitic load resistor from the NaK primary loop to the heat rejection loop was completed and submitted to the SL-2 project engineer. Pursuant to a reliability analysis recommending the elimination of L/C shut-off valves, the valves were removed from the flight system design, and may be eliminated in designs that are established following SL-2 testing.

The comparative reliability of reference pneumatic and hydraulic mercury injection systems was developed and submitted to the MIS designer. A detailed analysis of NaK PMA shafts and associated balancing methods was conducted. A reliability analysis, regarding reduced power density of the parasitic load resistor, revealed that failure modes associated with shorts, welds, and other characteristics (which were directly proportional to the number of elements) became dominant and that no net reliability improvement was achieved.

Problems arising from the inability of the voltage regulator to meet the conducted audio-interference requirements of MIL-I-26600 were discussed and analyzed with responsible design personnel. It was determined that introduction of a 3-v, 15 to 15,000 cps signal would affect the voltage regulator operation and corrective design modifications were initiated. Other areas of reliability-design coordination included turbine balancing, start programer logic circuit, mercury injection system, integrated seal assembly, auxiliary start loop shut-off valve, and bearing launch dynamics.

A planning meeting was conducted with responsible personnel regarding the Reliability Startup Testing Program. A listing of components, tentative schedules, and the need to conduct separate studies for each component was

developed which included the following considerations: failure definition, degree of repairability, overstress test levels, and significance of failure.

A general test plan for the Reliability Startup Test Program was developed; the plan included test levels, test duration and sequence, functional test fluids, schedules, PERT, manpower requirements, and costs. An evaluation of various methods to reduce test costs with minimum loss of confidence in test results is currently being conducted.

The mercury injection system reliability test plan was initiated; including test objectives, scope, test equipment requirements, test sequence, and failure criteria.

Reliability data relating to boiler and condenser reliability and potential reliability growth was submitted to Component Design Engineering and was presented to NASA-LeRC. Relative reliabilities of diodes and relays were given to the responsible personnel. The properties of ET-378 were reviewed in relationship to the desired lubricant-coolant fluid properties with the cognizant engineers. Failure rates and applicable data on silicon-controlled rectifiers were supplied.

Six hundred and twenty-five engineering design drawings/design changes were reviewed and corrective action (RAR) was requested on 53 items. To date, corrective action on 18 RARs has not been completed; standard closed-loop follow-up is being maintained. Twenty component specifications were reviewed and the corrective action requested on four specifications has been implemented.

D. TEST PLANNING/FAILURE ANALYSIS

Test and buildup activities on -X, -1, RPL-2, LML-3, SL-1 and the gaseous nitrogen loop were monitored during this report period; waivers 1 through 54 were in effect.

Reliability personnel participated in seven design reviews: MLA structure and piping, LML-2 and -3, RPL-2, SL-1, SL-2, PCS-1, and PCS-2.

A list of PCS hardware requiring equipment logs was issued to all responsible personnel. Equipment logs were issued for the listed PCS hardware which has been delivered to the test area.

Nine Reliability Failure Reports were received and investigated. All failures were classified as incidental and corrective action was implemented for detailed data.

The -1 Boiler Test Request was reviewed and a statistical test design was developed to assist performance mappings. A brief statistical analysis of anticipated error in boiler ΔT was made at the request of the design engineer. It was verified statistically that the error in the difference was the square root of the sum of the squares of the individual errors, $\left\{ \sigma_T = \sqrt{\sigma_1^2 + \sigma_2^2} \right\}$.

Specific hardware test plans were reviewed prior to inclusion in the SNAP-8 Integrated Test Plan, and applicable reliability recommendations were made to the cognizant engineer.

Seventy-six Inspection Reports were reviewed for adequacy of the corrective action implemented and potential degradation of inherent reliability. Seven -X hardware equipment logs were audited and supplemental instruction together with closer communication was initiated to upgrade equipment log data on the next generation of hardware.

Thirty-nine E drawings and 17 preliminary environmental test procedures were reviewed and reliability recommendations were submitted to the cognizant design personnel.

E. RELIABILITY CONTROL AND LIAISON

1. Supplier and Subcontractor Reliability Control

A coordination meeting was held with AGN personnel defining the reliability requirements for the Corrosion Loop Program. AGN will submit a Reliability Program Plan implementing the reliability requirements.

The mercury PMA motor (Westinghouse) Reliability Program Plan was approved. The Westinghouse Factory Inspection Test Plan was reviewed and reliability recommendations were coordinated with Aerojet Quality Assurance. Drawings, specifications, and progress reports were reviewed and reliability recommendations were coordinated with Quality Assurance and cognizant engineers.

Alternator (GE) design and data reviews and progress reports were reviewed. Three failures were reported on the pre-prototype No. 2 alternator, and the corrective action taken was coordinated with Aerojet. The alternator apportionment and prediction was not submitted on schedule by GE; the report was requested.

GE design and data reviews, and progress reports on the regulator were reviewed. GE has been requested to submit the past-due reliability apportionment and prediction.

The L/C PMA (TAPCO) work statement was renegotiated and the reliability requirements remained as defined in the original work statement. Progress reports and design data were reviewed.

Specific reliability program requirements applicable to the following potential subcontracts were prepared:

Load breaker, hermetically-sealed (Type I)
Contactor, transfer, hermetically-sealed (Type II)
Contactor, transfer, open (Type III)
Parasitic load resistor
Inverter, rotary, hermetically-sealed.

Six-hundred and forty-one stores and purchase requisitions were reviewed and applicable reliability requirements included.

AGC SNAP-8 Reliability personnel participated in the review of the AI S8DS nuclear system design data package. Preliminary reliability requirements applicable to the nuclear system were developed and reviewed with NASA.

All waiver requests generated during the report period were investigated prior to reliability action (approval/rejection).

Variables data requirements for the NaK PMA shaft were directed to QA and implemented as a subcontract requirement.

Direct coordination was maintained with QA regarding the reliability/QA interface; i.e., Program Plan implementation and revision, procurement, corrective action, process control, and test monitoring.

V. ROTATING MACHINERY

A. TURBINE ALTERNATOR ASSEMBLY DESIGN AND ANALYSIS

The final TAA design review was held on 19 December 1963. The turbine assembly, seals, and alternator were reviewed in detail including the analyses, materials, fabrication and assembly methods, and the test program.

The TAA mockup was completed, instrumented, and piped. An analysis of the L/C system showed that wide variations in system flow balance could result from expected tolerances in the system. This is due to the fact that the Reynolds number of ET-378 changes rapidly at the operating temperatures of the L/C system coupled with the fact that system Reynolds numbers (at constant temperature) range from 130 to 3300. As can be seen from Figure 20, large changes in the orifice coefficient occur within the expected operating band of the L/C system. Because of this, the decision was made to flow check the major flow restrictors that make up the L/C circuit. This testing will be done in conjunction with the checkout of the L/C stand. The test request for this work has been prepared. Ninety percent of the drawings for the L/C system (development instrumented unit) for TAA Number 1 have been completed. Fifty percent of the drawings for the subsequent TAAs have been completed. All valves, filters and flowmeters are in-house, and fittings, piping and miscellaneous small hardware are in process or on order.

Each TAA will be mounted on its own mounting stand at assembly. This stand will be used for supporting the TAA from then on (i.e., from assembly through test and storage). The same mounting stand will be used for all initial testing including GN_2S-1, RPL-2, PCS-1, and PCS-2.

Two of these mounting stands have been ordered and are in fabrication. In addition, fabrication of two more stands, which will be used for TAAs going into PCS tests, was completed.

The test plans for GN_2S-1 and RPL-2 were prepared, reviewed, corrected, and are being readied for release. The TAA installation drawing and the assembly drawing are 90% complete.

The critical speed of the turbine alternator assembly and the critical resonances of the components have been reviewed. No problems arose during this review.

B. TURBINE ASSEMBLY (TA)

Review of the TA was included as part of TAA final design review, held on 19 December. This review included detailed technical summaries of the analyses, materials, and design parameters of each major component of the TA.

The turbine assembly drawing was sent out without a released inspection plan for the assembly. A waiver was issued permitting the first turbine to be assembled without Inspection Review Board release. This action was taken to permit experience gained in the first TA buildup to be incorporated in the buildup logs and released QC plan. Full assembly buildup logs and the preliminary quality control assembly plan were used with the first assembly. No waiver is planned for unit No. 2. The first TA was assembled in the new SNAP-8 clean room under conditions outlined in AGC-10336 (Figure 21).

The integrated sand-cast turbine exhaust seal housing was dropped. Satisfactory patterns had been received, but no casting work had been accomplished. Weld assembly and final machining drawings have not been released. Also, the preload spring calibration fixtures and lubricant injection ring test fixture have been discontinued. High-temperature yield and failure tests for the turbine wheel holding bolt were postponed.

1. Inlet Housing

The balance piston bleed tube was increased from 1/2 to 1 in. on Serial No. 2 and succeeding inlet housings. This will eliminate the possibility of choking the dummy piston labyrinth leakage under extreme dimensional and fluid conditions.

2. Seals

Seal rig test results indicated necessary design changes in the turbine assembly, and these changes were initiated. Formal test reports are currently being prepared.

The TA mercury visco pump seal design was changed from a 13-lead helical screw to a 13-lead herringbone to obtain more stable performance. As a result of this design revision, nominal operating radial clearance of the visco pump was increased from 0.003 to 0.006 in. The molecular pump radial seal clearances were increased from 0.003 to 0.005 in. These increased clearances will improve mechanical reliability and yet keep leakage losses within allowable design limits.

Antiwetting Teflon stationary walls have been investigated for use on the outboard faces of the outboard slingers. Lubricant leakage will be reduced, and the possible difference in ground test and zero-gravity leakage lessened, thus improving the validity of leakage performance tests. The Teflon film walls will be incorporated into either the Serial 2 or the Serial 3 turbine assembly as fabrication details are worked out.

No. 3 turbine assembly and succeeding units will include a lift-off device enabling the carbon seals to retract from contact when the turbine is at operating speed. Seal face wear will be reduced and multiple starts will be possible at any point in the working life of the unit. However, retrofitting of Serial 1 and Serial 2 turbine assembly components is not practical for the first buildups. This is because the bearing housings were fabricated with a physical interference with the lift-off components. Reworking is impracticable.

3. Bearings

The first six turbine assemblies will employ bearings of M-50 single-vacuum-melt steel in lieu of consumable electrode triple-vacuum-melt M-50 steel. This deviation from original design was necessitated by schedule. The triple-melt material delivery would have delayed fabrication. Any additional bearing purchases will be fabricated with the triple-melt steel to obtain the best possible reliability for life requirement. These bearings will be available for all endurance testing.

4. Nozzle Flow Checkout Tests

The effective flow areas of the nozzle assemblies in each stage were measured by flow testing with gaseous nitrogen. The procedure

consisted of installing the nozzle diaphragm assembly in a specially designed holding fixture and flowing the nitrogen through the nozzle row at pressure ratios above and below the critical. The nozzle exhausted to atmosphere.

The flow rate at any particular pressure ratio was measured by a calibrated orifice upstream of the nozzle. The temperature and pressure of the gas were measured in the plenum of the holding fixture which is immediately upstream of the nozzle inlet.

From a graphical plot of the parameters $\dot{W}_{N_2} T_{in}/P_{in}$ against nozzle pressure ratio, the effective flow area of the nozzle assembly can be calculated.

Accuracy in the measured effective flow areas can be $\pm 3.5\%$ based upon accuracy of measured parameters such as temperature, pressure, and flow rate. In addition, drawing dimensional tolerances could allow $\pm 7\%$ area variation from the nominal designed values. Thus, combination of dimensional tolerance and the accuracy of the measured test parameters could result in a $\pm 11\%$ area variation and remain within the design tolerance.

To date the following nozzle assemblies have been flow tested:

One first-stage nozzle
One second-stage nozzle
Six third-stage nozzles
Six fourth-stage nozzles

The first available set of nozzles was assigned to the first TA unit.

The effective flow areas of these nozzles were 0.372, 0.489, 0.962, and 1.850 sq in. for the first-, second-, third-, and fourth-stage nozzle assemblies. These flow areas were smaller than the nominal design for effective flow areas by 1% for the first stage and approximately 10% for the second-, third-, and fourth-stage nozzles (see Figure 22).

The remaining five third-stage and fourth-stage nozzle assemblies showed effective flow areas ranging from 4 to 10% smaller than the design nominal areas.

Dimensional checks of nozzle passages in the first TA (excepting the first stage) indicated physical areas only 2 to 5% smaller than nominal. Undetermined factors must be present to account for the effective flow areas 10% smaller than nominal.

C. ALTERNATOR

The alternator specification (AGC 10175) was revised and released (revision dated 10 December 1963). The contract with General Electric Company was negotiated and signed in January.

The EME (electro-magnetic-equivalent) alternator was completed and tested. Results are shown in Figures 23 through 29. In general, the alternator meets the design requirements except that field current is 20% above design, indicating saturation in the magnetic circuit. Because of design conditions, EME alternator tests to determine compliance with the thermal requirements of the specification are not practicable. Whether or not the alternator will comply with the thermal limitations as set forth in the specification is, as yet, undetermined.

Serial No. 1 (alternator pre-prototype) was completed (Figure 30), and has been assembled and tested three times, with failures occurring shortly after startup on each test. There were three immediate causes of these failures: (1) undersized injector holes in the bearing lubricator injection ring, (2) rubbing of the screw seals due to inadequate clearances, and (3) chips in the lubrication system which restricted oil flow causing overheating of the drive end bearing.

Formal failure determination has not been conducted.

General Electric is taking action to alter its mode of operation; engineering is providing manufacturing with detailed buildup procedures, assembly instructions, and improved inspection procedures. GE has undertaken to improve its cleaning facilities and to install interim clean areas which will meet the immediate needs of the program. As a result of these problems, the delivery of the first alternator has slipped approximately 2 months from the contract schedule.

The prototype design review was held and the prototype design was approved except in the areas of the trunnions and lift-off seals. The electromagnetic design is identical to that in the pre-prototype alternator. The mechanical configuration is generally the same except that lift-off seals, molecular pumps, and Teflon coating on the stationary walls in the slinger area have been added and the trunnions and terminal mountings will be revised.

A review of the trunnion mounts indicated that stresses under shock-loading conditions specified in NASA Specification 417-2 could be excessive and that the trunnion design should be revised to reduce these stresses. This is presently being done. To eliminate the lubricant-coolant valves in the TAA, lift-off seals similar to those used in the turbine assembly will be installed in the alternator. Envelope requirements and exact performance requirements are presently being worked out jointly by GE and Aerojet. Incorporation of these changes plus the problems associated with the pre-prototype alternator presently indicate a slippage of 2 months in the delivery of the first prototype alternator.

D. BALL BEARINGS AND BEARING LUBRICATION SYSTEM

1. TA Bearings

The last four of the total of 16 size 208, 52100 steel angular-contact bearings ordered from the Barden Corporation were shipped to Aerojet during the week ending 1 December 1963.

Four of the 14 TA bearings made of single-vacuum-remelt M-50 material ordered from Industrial Tectonics, Inc. were delivered during the week ending 13 December 1963.

Because of the timely delivery of the M-50 bearings, a decision was made to use these parts in the first TA buildup in place of the 52100 bearings.

The remaining ten M-50 bearings of the 14 TA bearings were delivered to Aerojet during the week ending 29 December 1963. Dimensionally, they were acceptable by the Aerojet Inspection Department; however, the accompanying bearing documentation was insufficient. Disposition has been made to return to the vendor only the bearing documentation. Action was not completed by the end of this report period.

Quotations were received from six vendors for the TAA bearings made of triple-remelt M-50 material. Preliminary review of the six vendor quotations resulted in a tentative selection of two bearing suppliers. Further action has been postponed due to budget review.

2. TA Lubrication System

a. Test Equipment

Certain design modifications of Lubrication Rig No. 1 have been completed. These modifications were made to obtain visual and instrumented data regarding the extent to which the bearing inlet cavity is flooded during operation with jet lubrication and with the cavity at low pressure. Additional testing of Lubrication Rig No. 1 has been postponed indefinitely.

b. Test Results – Lubrication Rig No. 1

Final data sheets and plots were issued for the tests performed on Lubrication Rig No. 1 during the previous quarterly period. The most significant data obtained were with buildup No. 5 of the test rig, which contained a bearing and slinger assembly closely simulating the TAA design. Table 3 gives a summary of the Lubrication Rig No. 1 buildups. Figure 31 shows the test head, buildup Nos. 4 and 5. The bearing is a size 207 angular-contact type, with a low shoulder on the inner race and with a vaneless slinger on each side of the bearing. Three equally spaced jet nozzles, 0.040-in. dia, inject lubricant onto the inner race of the bearing. The bearing is spring preloaded to approximately 50 lb.

During most of the test operations with this assembly, the average temperature of the lubricant (degassed ET-378) in the inlet manifold was 220°F. The bearing outer race temperature was allowed to stabilize at each test flow rate prior to recording of operating data. Bearing cavity pressure averaged about 0.90 psia, while the pressure in the front cavity outboard of the exit slinger was maintained at 0.25 psia or less.

Figure 32 shows the steady-state bearing outer race temperature plotted against inlet flow rate. The data points represent the

average temperature of three thermocouples equally spaced around the bearing. The maximum temperature differential around the race circumference was 5°F at a flow rate of 1.9 lb/min. Over the entire test flow range of 1.9 to 5.8 lb/min, the average circumferential differential was 2°F. The figure shows that at the design flow rate of 3.33 lb/min (200 lb/hour) the outer race temperature is about 251°.

The temperature rise of the lubricant through the bearing and the exit slinger is plotted against total inlet flow rate in Figure 33. At 200 lb/hour, the temperature rise is 35°F.

Inlet pressure to the jet-nozzle manifold vs total inlet flow rate is shown in Figure 34. The curve indicates that a pressure of approximately 18 psia is required for a total flow rate of 200 lb/hour through three 0.040-in.-dia nozzles and with a bearing cavity pressure of 0.90 psia.

Accurate measurement of discharge flow from the slinger on the bearing inlet side was not obtained during these tests because of instrumentation difficulties. Data for the proportion of flow transmitted through the bearing is therefore not yet available.

Deceleration rate data were obtained for the purpose of estimating bearing power loss. Analysis and interpretation of these data were not performed during this report period.

c. Test Results — Seal and Lubrication System Simulator

As a result of integration of the seal and the lubrication system development into the seal and lube system development effective the week ending 1 November 1963, there were brief lubrication test runs on the Model A Seal and Lubrication System Simulator in December 1963, and on the Model B System in January 1964.

The Model A Seal and Lubrication System Simulator contains 207 bearings. The slinger and bearing cavity configuration is identical to that of the TAA and the Model B Seal and Lubrication System Simulator except for the size of the bearings, which is 208 for the latter two machines.

The Model A Seal and Lubrication System Simulator was instrumented to permit simultaneous measurement of slinger discharge pressure and bearing cavity pressure. For the normal scavenged running condition, the bearing cavity contains a spray of oil droplets within an oil-vapor atmosphere. As long as the bearing cavity is scavenged, the pressure within the cavity is close to zero. A finite pressure reading within the bearing cavity indicates a flooded or near-flooded condition. Slinger discharge pressure was increased, during the Model A Seal and Lubrication System Simulator test, until further increase in discharge pressure caused an increase in bearing cavity pressure, thus indicating some flooding of the bearing cavity. The results of the tests, shown in Figure 35, indicate that flooding occurred for slinger discharge pressures of 10 to 15 psia. The results show that further increases in slinger discharge pressure caused additional pressure increase in the bearing cavity. At no point, however, did the pressure rise in the bearing cavity equal the pressure rise applied at the slinger discharge. An equal pressure rise is what should be expected if a complete liquid continuum had filled the bearing cavity. Therefore, the data appear to indicate the existence of a flooded condition above slinger discharge pressure of 15 psia (but occurring under conditions such that some cavitation within the bearing cavity could exist). The scatter in the data leaves the point not well illustrated with the limited number of tests, although the general trend is clear enough. It is quite evident that well-scavenged operation occurs for slinger discharge pressures below 10 psia.

A similar test series was conducted on the Model B Seal and Lubrication System Simulator. In this case the machine contained size 208 bearings and, due to its prototype configuration, no measurement of bearing cavity pressure was possible.

An attempt was made to measure bearing and slinger power consumption for some of the investigated range of slinger discharge pressures of 5 to 25 psia in the Model A Seal and Lubrication System Seal Simulator tests. Power was measured by the inertia method. This method requires measurement of the inertia of the rotating parts. It also requires accurate measurement of the deceleration transient. These measurements were recorded for a range of slinger

discharge pressures. It is anticipated that the test results will provide a measure of the difference in power consumption between scavenged and flooded bearings.

3. Ball Bearing Test Programs

Three programs were proposed covering endurance and wear bearing life as functions of M-50 bearing material, bearing material fiber, and vacuum and nuclear radiation. Technical improvements as well as possible cost savings which could result from the proposed tests justified the programs. Technical data resulting from these programs would give assurance that the 10,000-hour bearing life requirement could be met. A summary of these programs is shown in Table 4.

An order was placed with the SKF Industries for the endurance ball bearing test program as a function of M-50 bearing material during the week ending 31 January 1964. An outline of this program is shown below.

a. Test Bearings

SKF Industries, Inc., will manufacture the following two groups of deep-groove ball bearings:

Twenty bearings made of M-50 tool steel twice consumable-vacuum remelted

Twenty bearings made of M-50 tool steel five times consumable-vacuum remelted.

These ball bearings will be size 309, both made from the same air melt heat of material.

The bearings will be ABEC Class 1 tolerance and of customary SKF design and construction for endurance test purposes. They will be 100% inspected.

b. Testing Outline

SKF Industries, Inc. will test bearings in accordance with the plan outlined on the following page.

No. of Bearings	Material M-50	Lubricant	Outer Race Temperature, °F
10	2nd remelt	Mineral oil	210
10	5th remelt	Mineral oil	210
10	2nd remelt	Dow Chemical ET-378	200-240*
10	5th remelt	Dow Chemical ET-378	200-240*

*Exact temperature to be established at the time of test.

c. Lubricants

Mineral oil will be the Socony Mobil DTE Extra Heavy or equivalent.

Polyphenyl ether oil will be the Dow Chemical ET-378.

d. Test Parameters and Procedure

The test will consist of endurance runs, under 4240 lb radial load applied to the stationary outer ring, at approximately 9700 rpm constant speed. The test will be continued until a fatigue failure on one of the rolling elements in the bearing is indicated by a vibration sensor on the machine and verified by visual inspection. The test load corresponds to a maximum compressive Hertz stress of 380,000 psi at the inner-ring-to-ball contact in the position of the maximum load.

Load and speed will be adjusted at the beginning of the test and will not vary as a consequence of tester design. Test bearing outer ring temperatures, oil "in" and oil "out" temperatures, and oil flow will be monitored throughout the test. Bearing outer ring and oil "out" temperatures will be sensed at intervals not exceeding 10 min by a digital system which provides alarms when temperatures exceed preset limits. The other variables will be monitored manually at intervals of 8 hours. Load to the test bearings will be applied by a dead-weight lever arm system.

The duration of the above tests will be sufficient to cause fatigue bearing failures in at least 20% of the bearings tested, or 200 million revolutions, whichever occurs first.

E. SEALS

The primary accomplishments of the past quarter were completion of the visco pump tests and testing of the Model A and Model B Seal Simulators. The Seal-to-Space Program will be essentially finished with (1) the completion of one additional test of the Model B Seal Simulator, and (2) the writing of the seal test rig reports and final seal design documents. All of this work, currently in progress, will be completed during the next quarter.

1. Visco Pump Test Rig

During the previous quarter a visco pump configuration with helical grooves in the housing and with an 0.003-in. radial clearance was judged to provide a satisfactory liquid-vapor interface for the SNAP-8 seals-to-space. During the past quarter, many additional visco pump configurations were tested with favorable results. Configurations were tested with grooves in the housing, with grooves on the shaft, and with grooves on both the housing and shaft. Tests were run at radial clearances of 0.003, 0.005, and 0.007 in.

No signs of incipient breakdown were observed for any of the conditions tested. Therefore a radial clearance of greater than 0.007 in. is required to cause breakdown of the visco seal operating at SNAP-8 conditions. As a result of this finding, it has been possible to open up the radial clearance in the TAA visco seal from 0.004 to 0.006 in.

Micro-flash photographs of the visco pump liquid-vapor interfaces are shown in Figures 36 to 46. These pictures show stable interfaces for all conditions tested. Tests conducted at the smaller radial clearance values show a pronounced cavitation at the leading edge of the helical lands. This cavitation occurs within 1/8 to 1/4 in. of the zero psia interface, but is suppressed in the rest of the visco pump where higher pressures prevail. This tendency to cavitate diminishes as the radial clearance is increased. It is significant that during the entire test series no cavitation damage occurred within the working section of the quartz visco pump.

The most intense cavitation occurred with grooves in both the shaft and housing, and with a radial clearance of only 0.003 in. In general,

it was found that for a given clearance the pumping is doubled by placing grooves in both the shaft and housing. If the effective clearance with grooves on the shaft and housing is half the actual clearance, it is quite understandable that this configuration should produce the greater turbulence and a more pronounced cavitation pattern. But even in this case, as the clearance was increased, the cavitation pattern diminished to only a trace observable near the interface (Figure 45).

Pumping characteristics of the visco pump configurations are shown in Figures 47 to 54. Where possible, data were taken at three speeds: 6000, 9000, and 12,000 rpm. Since pumps with short axial length are of primary interest in turbo machinery applications, it was of particular interest to know whether or not the pumping rate for very small axial engagement between the pump and fluid was the same as that for large engagements. The results revealed that at low shaft speeds there is no appreciable edge effect, but at higher speeds there is a noticeable short section of pump which is apparently ineffective. Furthermore, the length of the ineffective entrance section is noticeably greater for the configuration having grooves located only in the shaft than it is for the other two configurations. Thus, for short pumping lengths, grooves in the housing are preferable to grooves on the shaft. This confirms the choice of housing grooves for the TAA seal-to-space.

On the other hand, once sufficient axial length has been allowed to permit the grooved shaft configuration to become effective, its pumping rate is superior to that of the grooved housing configuration. Such an arrangement is probably preferable for axial engagements over 0.5 in. This shows that our previous selection of shaft grooves for the 0.7-in.-long mercury PMA seal-to-space is a sound choice and need not be changed.

Figure 43 represents quite closely the visco pump operating condition for the current TAA seal design. Figure 38 represents most closely the visco pump operating condition for the current mercury PMA seal design. Figure 45 represents the visco pump operating condition recommended for future use in the mercury PMA seal should it prove desirable to double the radial clearance.

2. Model A Seal Simulator

During the week of 16 to 20 December, tests of the Model A Seal Simulator were conducted. This test rig simulates the TAA seal configuration completely with the exception that it possesses no start seals and that it uses a recirculating mercury flow instead of an oil heat exchanger to cool the mercury seal liquid-vapor interface. Most importantly, it includes the 700°F, 20 psia mercury vapor environment of the actual seal. A drawing of the simulator is shown in Figure 55; the results of the 20-hour run are presented in Table 5. For the representative SNAP-8 operating conditions with recirculating mercury entering the interface at 210°F and leaving at 300°F, the leakage rates are 1 to 3 lb/year of oil and 15 to 20 lb/year of mercury.

Although the mercury leakage is a reasonable value, it is essentially an order of magnitude greater than that which theory and previous component testing would indicate for an interface temperature of 210°F. The measured mercury leakage rates are more representative of what would be expected for interface temperatures 100°F higher. Since the recirculating mercury experiences a 100°F temperature rise in passing through the slinger interface, it is conceivable that the effective interface temperature is considerably higher than that of the inlet flow. The results seem to support such a contention. If this is true, then introduction of 210°F mercury at the interface is not as effective a cooling method as was previously supposed. And such an approach would not appear to be superior to cooling the interface with the oil-cooled housing heat exchanger used in the current TAA and the Model B Seal Simulator.

The main conclusion of the Model A Seal Simulator test is that the integrated seal has been shown to perform essentially as intended and that a satisfactory TAA seal-to-space does indeed exist.

The main contribution of the Model B Seal Simulator tests will be to illustrate the effectiveness of the start seals and the mercury seal oil-cooled heat exchanger.

3. Model B Seal Simulator

The seal configuration of the Model B Seal Simulator is identical to that of the TAA. Since the test includes the introduction of 700°F

mercury vapor into a dummy turbine cavity, actual functioning of the TAA seal is simulated both mechanically and thermally. Figure 56 is a drawing of the Model B Seal Simulator.

During the week of 27 to 31 January, a 71-hour test of the Model B Seal Simulator was conducted. Two problems occurred during the test that, to a large extent, prevented achievement of all the test objectives.

First there was an excessive amount of dissolved gas in the oil. This caused foaming at the oil seal interface and large amounts of oil were carried across the seal (100 to 1000 lb/year). Although this was regrettable, it was not significant since proper functioning of the oil seal-to-space — already well demonstrated in the Model A Seal Simulator tests — was not a point in question. The main result of this experience is that greatly improved measures have been adopted for the prevention of such an occurrence in the future.

The second and more important problem encountered was the unintentional rubbing of the start seal during normal operation of the simulator. As a result the mercury leakage rate was considerably lower than would have been measured with the start seals in the lifted-off condition. Mercury leakage values were only a pound per year, and the evaluation of the effectiveness of the mercury seal oil-cooled heat exchanger was not conclusive.

The possibility of conducting an additional test of the Model B Seal Simulator is currently being examined. If such a test is run, it will be conducted only after a modified start seal lift-off device is installed in the test vehicle and an improved de-gassing oil circuit is incorporated into the test console.

F. PUMP PROJECTS

1. NaK Pump-Motor Assemblies

a. Motor

The motor development and fabrication, for this report period, basically covers: (1) the completion of the uncanned in-air design verification testing, (2) the winding and connecting of several inorganic-

insulated stators, (3) the complete fabrication of interim ML-insulated stator assemblies, (4) the fabrication and inspection of rotor assemblies, and (5) the empirical establishment of a stator canning procedure. These activities, with the exception of No. (2), apply to both the 2.12-hp primary NaK PMA motor and the 4.45-hp heat rejection NaK PMA motor, and will be described in the following paragraphs.

The design verification testing for both designs was completed on 24 December 1963. This series of tests was run on motor components simulating the final motor assemblies, but modified to the extent necessary for expedient adaptation to an existing standard housing and bearing assembly fixtures. The test motors differed only in the following respects: (1) conductor conductivity was 100% – not 92%; (2) the rotor and stator were not canned; and (3) the insulation system was ML – not ceramic (inorganic).

The load tests were run coupled to a dynamometer with precision metering under controlled temperature conditions. Identical tests, except for hp loading, were run on both the HRL and primary motors. The general test procedures and results are described below.

(1) Rated Load – Rated Conditions

To ensure that the actual performance of the motor was in agreement with the calculated data, motor performance at various loads – including rated load – was established under rated conditions.

The motor was loaded to approximately full-load on the dynamometer, until the winding temperature stabilized near 200°C. Readings of watts, amps, speed, and torque were recorded as the load torque was varied from zero to approximately 130% of full-load torque. The actual stator in-coil and rotor end-ring temperatures were determined at the conclusion of the above tests by the resistance vs time method.

The results of these tests were analyzed, with electrical efficiency and power factor being computed; the experimentally determined values were found to agree with the initial calculated values within 2%. See Figure 57 for the HRL motor performance and Figure 58 for the primary-loop NaK motor performance.

(2) Rated Load – Variable Conditions

Steps were taken to provide data for future motor design optimization in the event of a major change in the pump brake horsepower requirements, and to assist in determining system parameters under startup conditions. To obtain such data, the reduced frequency startup cycle tests and a re-run of the rated load tests were performed at the specified voltage and at ±10% of the specified voltage.

These tests were run with the dynamometer, and readings of watts, amps, speed, and torque were recorded as the load torque was varied from zero to approximately 130% of full-load torque. The actual voltages were as follows: 208, 187, and 229 v at 400 cps; 79, 88, and 97 v at 220 cps; and 17, 19, and 21 v at 95 cps.

The results of these tests cannot be fully analyzed until the system performance parameters from the Phase I testing of SL-1 and SL-2 are known. However, a preliminary evaluation of the motor losses at the present rated loads indicates that maximum efficiency will occur within the prescribed ±10% voltage band (i.e., the levels of air gap and iron flux densities determined by design are near optimum).

(3) Maximum Torque

To ensure that the motors develop the minimum specified maximum torque (130% of full-load torque), the speed-torque characteristic was obtained in the area of maximum torque. This test was run on the dynamometer and a series of speed-torque points was taken at (a) 400 cps and 208 v, (b) 220 cps and 88 v, and (c) 95 cps and 19 v.

At rated temperature conditions, the HRL motor developed 150%, while the primary motor developed 146% of full-load torque. At the 130% overload condition, the speed was in excess of the 5610 rpm minimum requirement for both motors. The results of these tests have shown that not only have the motors met specified conditions, but also that a minor overload condition is tolerable.

(4) Locked Torque

The minimum starting torque was determined to establish that no stalling would be encountered during motor startup regardless of rotor position or input frequency. This test was run on a dynamometer in two parts. Part 1 was a locked torque vs rotor position test to determine the minimum starting torque. Part 2 was a locked torque test under the worst conditions (that is, the minimum condition established in Part 1, and with the rotor cold). Part 2 of the test was run at (a) 208 v and 400 cps, (b) 88 v and 220 cps, and (c) 19 v and 95 cps.

The test results are as follows:

Test Condition	HRL Motor	Primary Motor
208 v and 400 cps	19.4 lb-in.	8.6 lb-in.
88 v and 220 cps	11.7 lb-in.	4.0 lb-in.
19 v and 95 cps	3.7 lb-in.	2.9 lb-in.

These tests indicate that no starting problems should be encountered as the torques are in excess of the previously specified 30% of full-load torque.

(5) Segregation of Losses

This test was run to separate the no-load motor losses and thereby determine the full-load loss segregation. The no-load losses consist of core loss, copper loss due to magnetizing current, and the friction-windage losses of the test shaft assembly.

The test was run with the motor removed from the dynamometer, the minimum load being the shaft friction and windage losses only. The motor temperature was allowed to stabilize, and the voltage was varied in discreet steps from about 10% to about 125% of rated voltage. The watts input and current vs applied voltage was plotted. The plot was extended to zero volt to determine the friction-windage loss, which in turn enabled the core loss and stator copper loss to be segregated. The tests were run at 208 v and 400 cps, 88 v and 220 cps, and 19 v and 95 cps.

The net results of these tests cannot be evaluated now, but these tests of uncanned motors will enable accurate calibrations to be made for the later non-dynamometer testing using the can configuration in a non-conducting fluid and in NaK. The tabulation below is an illustration of this extrapolation, showing the actual loss breakdown for the motors operating in air and the projected loss breakdown for the motors operating in NaK. The motors are shown at the same operating temperature and hp loading.

SUMMARY OF NaK PMA MOTOR LOSSES

	HRL		Primary	
	In Air (watts)	In NaK (watts)	In Air (watts)	In NaK (watts)
Core loss	153	153	86	86
Stator copper loss	284	340	188	254
Rotor copper loss	98	104	48	51
Stray load loss	78	78	55	55
NaK and can loss	0	576	0	319
Total Losses	613	1251	377	765

The winding and connecting of the first inorganic-insulated prototype stator assembly is complete and the second HRL and first primary prototypes are in process. The winding and insulating techniques employed in the present 3-week cycle per stator assembly fabrication (not including encapsulation) were developed through the study of a trial unit and the rejection of the first prototype winding attempt.

The new winding techniques in terms of material preparation and accompanying fixtures are described in the Electrical Insulation Materials Development section of this report. These modifications in winding techniques have no effect on motor characteristics and can be summarized as follows:

(a) The first six coils (rather than the four) placed in the slots are left with the opposite coil side open until completion of the remaining coil throws around the stator bore.

(b) Additional Mylar wrapping is added to the first six coil sides for increased flexibility at this pivot point in accordance with Step (a).

(c) The use of a superior impregnated wire with an improved nonraveling tendency greatly simplifies the working of wires into the slots.

(d) End-turn retaining fixtures and intercoil Teflon inserts are added to absorb winding stresses previously imposed on the slot cell insulation and stator core.

Steps (a) and (b), above, are shown in the photographs taken at the time of initial winding of the prototype HRL stator assembly (see Figures 59 and 60). The initial "hold-back" of the first six coils prior to final coil insertion is illustrated in Figure 59 and a close-up of the slot portion is shown in Figure 60. This enlargement of the "coil throw" area shows the slot cell protection ring in the lower edge of the photo and the unruffled coil geometry before and after slot entry.

An investigation was also made to determine the capabilities of alternate motor winding facilities to expedite delivery of later motors. However, this investigation led to the conclusion that neither schedule nor technical improvements could be accomplished by such an effort — mainly because of the material procurement problems, cleanliness requirements, and lack of applicable experience. Furthermore, the remedial measures previously described in streamlining the Aerojet insulation laboratory efforts were ultimately successful in minimizing previously pending schedule slippage.

The fabrication of motor rotors, including the mounting sleeves and end cans for later welding to the final rotor OD can, was completed by 27 December 1963. Final acceptance-testing and inspection revealed that

several primary rotors had cracked sleeves at the OD. The metallographic study of these material failures revealed the presence of significant nonmetallic inclusions in the Inconel 600 sleeves; this imperfection could be traced to the entire material lot from which the sleeves were made. Therefore, it became imperative to impose additional inspection (ultrasonic) to those rotors which had passed the helium leak and dye-penetrant checks, and to re-order new sleeve material for the rework of the faulty rotors. This defective material problem, coupled with the necessary quality assurance requirements, delayed the delivery of the four motors for ultrasonic inspection. Five primary and nine HRL rotors are presently being reworked with the new material.

The four ML-insulated stators (two primary and two HRL) were delivered to the motor housing supplier on 6 February 1964. These stators will be employed in the fabrication of interim NaK PMAs for testing in water as well as for providing the backup spares for the inorganic stator fabrication and test.

Experimentation was conducted on expanding the stator can against the stator bore and into the stator tooth slots. The purpose of the expansion against the bore is to provide high-pressure contact between the can OD and bore ID for heat-transfer purposes (this is because most of the motor losses are transmitted through the can to the coolant NaK). Also, expansion into the tooth slots is being provided for can stability as the resulting ribs produce both axial stiffening and relief for the differential expansion rates of the can and stator iron. Additional expansion into the end-turn area is designed to provide additional rotor clearance and to reduce hydraulic losses (entrance and exit) of the NaK coolant across the rotor. A clearance between the stator can and stator encapsulant is introduced during canning to accommodate any differential expansion rates between the Inconel and encapsulant.

The final required can configuration shown in Figure 61 is accomplished by pressurizing the inside of the can, which is 0.002 to 0.006 in. loose in the stator bore, until yielding occurs.

Pressures ranging from 1500 to 7500 psi were imposed with slot deformation and can tightness evaluated in increments of about

1000 psi. At 7500 psi, a nominal can depression into the slots of 0.007 in. was assured with the minimum being 0.004 in. As a result of this experiment, a detailed can expanding procedure was generated for use on all NaK PMAs.

b. Bearings

A series of tests of pivot fretting and wear damage was conducted duplicating the configurations and material combinations selected for the thrust and journal bearing assemblies. These included extensive measurements of the motions induced in the tests to ensure no gross deviations from actual motions expected in the actual bearing assemblies. The last part of the test series consisted of a 99-hour continuous run, conducted with the pivot assemblies submerged in 600°F, high-purity NaK 78. A photograph of the pivot fretting test rig is shown in Figure 62.

The test fixture consisted of positions to test simultaneously 6-pivot configurations. The fixture was driven by a single shake table as shown schematically in Figure 63.

A summary of the 99-hour test at 600°F is shown in Table 6.

The initial loads indicated are the maximum bearing pivot loads under 3-1/2 g (radial) and 1 g (thrust) conditions. During the course of the test, the load springs relaxed as a result of high-temperature creep. Coincidentally, the final loads simulate the maximum 1-g (radial) and zero-g (thrust) loads expected for the SNAP-8 10,000-hour life. The imposed motion simulated the maximum unloaded pad motion expected in the bearing assembly (in the actual bearing, amplitude will decrease with increased load).

The most severely damaged specimens were the M2-T1-M2 combinations. Photographs of this specimen are shown in Figure 64 where it can be seen that only minor evidence of a reaction product (or surface oxidation) existed (see Figure 64b). There was, however, an almost insignificant amount of fretting damage as the grinding marks are still visible in the contact area of the race (see Figure 64d).

From these fretting tests, the following conclusions can be made:

(1) The pivots as presently designed, and with present material combinations, are not subject to any significant damage. They will function satisfactorily for long periods.

(2) The 44A combinations are superior to the tool steel combinations. There was no macroscopic damage with the 44A specimens and virtually no microscopic damage. The tool steel specimen also had no macroscopic damage but there was some microscopic damage.

Design verification testing of both the journal and thrust bearings was conducted during this report period. In these tests, which were run in room-temperature, silicon oil to simulate NaK viscosity, the pad film thickness was measured under varying speeds and loads. Preliminary evaluation of the test results showed excellent correlation with theoretical calculations and performance exceeding SNAP-8 specification requirements.

c. Recirculation System

To verify performance, a pressure-loss and cold-trapping test was performed on the cold trap, filter, and economizer using NaK at 350°F and ET-378 coolant at 210°F. Pressure-loss tests were also performed on six sets of the above-mentioned components using methanol at room temperature. The use of room-temperature methanol (viscosity and density similar to NaK at 350°F) permits a convenient means of acceptance-testing these components.

The first two sets of recirculation system components tested had inlet and exit tubing with wall thicknesses of 0.063 in. The pressure losses that occurred during these tests indicated that the available pumping pressures would be insufficient to supply the required heat rejection loop flow rate of 1.6 gpm at the extremes of the estimated recirculation pump performance. Test results along with calculated losses for these thick-walled recirculation system components are shown as Curve A in Figure 65. Only the filter, economizer, and cold-trap pressure losses are shown in Figure 65.

Because of these excessive pressure losses, the remaining four sets of recirculation components were fabricated using 0.035-in. wall tubing. The resulting reduced pressure losses are listed in Table 7 and are also shown as Curve B in Figure 65.

The cold trap and economizer now have higher losses than previously reported. In addition, a valve and a flowmeter were added to the system for test purposes. In order not to exceed the estimated pump performance, the excessive pressure loss was reduced by revising the motor housing entrance losses and by establishing the maximum filter pressure loss. The motor housing loss reduction was accomplished by increasing the single inlet passage and the distributing holes. The filter loss was established from the pressure loss results.

All revised system losses are listed in Table 7 and are shown as Curves A and B in Figure 66. The HRL and primary system flow rates, 1.6 and 1.2 gpm, respectively, are also indicated. From Figure 66 it can be seen that the components with the thick-wall tubing are satisfactory for use on the primary loop PMA.

The thin-wall tubing components will be used on the HRL PMA. For early SNAP-8 system tests, the pressure excesses will be taken up across the valve in the recirculation system.

The trapping-rate test was performed by introducing a known oxide content into the system and measuring the contamination level of the effluence. A single pass of this contaminated NaK through the system fluid, at rated flow and design temperature, resulted in a reduction of sodium oxide from 75 parts per million (ppm) to less than 25 ppm. Based on these results, it is estimated that less than 15 min will be required to clean up the PMA system NaK to less than the design objective of 10 ppm.

d. Mounting Structure

The design of the NaK PMA mounting structure was completed. The mounting arrangement, shown schematically in Figure 67, solves the following problem areas:

(1) The mounting had to be flexible enough to fit into the undefined system structures and the component test loops. This was provided by a simple four-bolted foot mounting to the base. Horizontal mounting in any plane is possible by securing the base to a cell floor or to any structure consisting of plates, and/or angles, etc.

(2) PMA thermal distortions are eliminated by isolating the PMA from the base assembly through low-thermal-conductivity, high-compressive-strength pads.

(3) The hold-down strap, providing reaction against pipe forces, is secured by four springs which allow for uniform loading and compensation for manufacturing tolerances (the PMA, itself, is designed to accommodate all rigid structure pipe loads).

(4) All torque about the axis, along with axial pipe forces, is taken by a pin connecting one of the base pads to the PMA.

2. Mercury Pump-Motor Assembly

All detail drawings were completed by 15 January 1964. Assembly drawings and parts lists are complete and presently in the release cycle.

Orders for all parts were placed by the end of January; a total of six complete units was involved. Two units will be fully instrumented and will include pressure pickups located in the pump housing and seal housing to gather pressure data. From these data, pressure profiles will be plotted to determine pump thrust and radial load characteristics. The balance of four units will be without the pressure pickups. The latter units will be used for PCS-1, PCS-2, NASA-LeRC, and a spare. One of the two former units will be installed in LML-3, with the other maintained as a standby spare.

A considerable quantity of hardware has been received, including shafts, dynamic sealing elements, face seals, and locknuts, etc.

A PERT network, with activity descriptions, was released on 10 January 1964. This includes the first four assemblies for LML-3, PCS-1, PCS-2, and NASA-LeRC.

All of these units will include the space seal liftoff device and carbon-face bellows-type startup seals. Pull-off groove bearings will also be included.

An insulation container is being built for LML-3 testing. The mercury PMA will be mounted inside the container, and the voids will then be filled with an insulating material.

a. Motor

All mercury PMA detail drawings were completed by Westinghouse on 19 November 1963 and submitted to Aerojet for approval. Design verification testing is about 80% complete for this report period. Verbal communications revealed that all data obtained to date conform to the Aerojet specification control requirements. Completely documented data will be presented with the next report.

b. Jet-Centrifugal Pump

(1) Jet Pump

The mercury jet pump testing of the P/N 093061, 0.093-in.-dia nozzle, 0.404-in.-dia mixing section was tentatively completed on 4 February 1964. The mercury test setup, shown in Figure 68, accomplished the following objectives: (a) established the noncavitating jet pump performance, (b) satisfied most system NPSH requirements, and (c) confirmed the water jet pump results in axial location of the jet pump nozzle and the mixing section length.

(a) Noncavitating Jet Pump Performance

The performance curve of head vs capacity, as shown in Figure 69, varied from 0 to 10% below the water test values. After rechecking of the instrumentation, free gas or vapor logged in the system is the only apparent explanation for the head reduction. This jet pump head variation is not important since the jet pump head is less than 10% of the combination jet and centrifugal pump's total head.

(b) System NPSH Requirements

The jet pump test NPSH results of less than 1 ft at 1.625 gpm for a 5% jet pump head drop satisfied the 10,000-hour system operating requirement of 1.4 ft NPSH at the same capacity. Likewise, the system's startup NPSH valve of 1 ft NPSH at 1.775 gpm was more than met by the tested value of less than 0.7 ft NPSH. At 0.404 gpm the test results approximately matched the system required NPSH of 0.063 ft, indicating but not assuring that this objective had been met. Further work to clarify the test data will result in preparation of an NPSH vs capacity curve or call for retest in necessary areas.

(c) Water Jet Pump Results

The mercury test setup confirmed the water jet pump results in axial location of the jet pump nozzle and the mixing section length. The water jet pump test setup is shown in Figure 70.

(2) Centrifugal Pump

The first pump housing casting was approved on 21 January 1964. This item is being machined and is scheduled for delivery in March. A second casting is scheduled for completion in March.

The single-vane 3-to-1 enlarged panagraph master for the mercury impeller was approved on 7 January 1964, with delivery scheduled for March. Jet-pump nozzles are also scheduled for delivery in March 1964.

c. Bearings

The size 207 angular-contact ball bearings are now scheduled for delivery in mid-March of 1964. These bearings are of single-vacuum-melt M-50 steel and include a pulling-off groove on the inner ring. The anticipated delivery will allow these bearings to be included in the assembly of the first mercury PMA for LML-3. An additional 12 bearings have been ordered for delivery in mid-May of 1964.

d. Seals

The step between molecular and viscous pump mercury space seal has been modified to include purging vanes on the stationary member. Seal tests have shown this to be advantageous on startup in transmitting the mercury contained in the molecular pump seal through to the viscous pump seal.

If this feature is not provided, the mercury thus trapped in the molecular pump will remain there until vaporization takes place.

Bellows-type carbon-face seals were delivered on 17 January 1964. Delivery of the space seal mercury-pressure-actuated bellows liftoff device has been rescheduled for mid-March of 1964. This will still allow for inclusion in the first PMA. The liftoff device at the motor-end bearing seal has been eliminated from the design for the present. Improved reliability may be achieved by allowing the motor to be flooded or by including a slinger pump which would provide for purging the flooded motor. At present, however, a carbon-face seal is included at this position for startup sealing.

e. Lubricant-Coolant System

Bearing lubricant filters were delivered on 16 January 1964. These are 5-micron filters and will be included in the LML-3 installation.

f. Analysis

The thermal analysis for the mercury PMA was released (Reference 3). As discussed in the previous quarterly report (Reference 1), however, the space seal heat exchanger design was changed subsequent to the thermal analysis being completed. The design now used includes 36 slots 0.01 in. deep by 0.10 in. wide. The analysis referenced in the previous quarterly report shows this design can maintain a mercury temperature at the space seal of 300°F by using 2600 lb/hour of 210°F ET-378. The design used in Reference 3 can only cool to 320°F for the same coolant conditions.

An analysis has also been made for the flooded motor condition. Stagnant flooded conditions were assumed. A stator winding hot-spot temperature of 476°F is calculated for this condition. This value is considered to be too high for a 10,000-hour operation.

g. Assembly Procedure

An assembly procedure has been written and this, together with the buildup log, will be available for the first assembly. During the first assembly, the assembly procedure will be modified, if necessary, and then issued as a released document to be used in conjunction with the assembly drawing on subsequent assemblies. All detail parts including bearings will be ultrasonically cleaned prior to assembly in accordance with cleaning specification AGC 10319.

Assembly tools have been designed and detailed, and are scheduled for completion in March. Also included is a special pulling tool for gripping the bearing pull-off groove.

h. Testing

A complete test plan (No. 395/64/0001) was released on 2 January 1964. This covers the complete development and life testing in LML-3 as well as detail subassembly and assembly checkouts and prerotational checks.

A test request for LML-3 is in rough-draft form and is scheduled for issue early in March. This request provides for: (1) nonrotational testing, (2) rotation without mercury, (3) rotation with cold mercury, and (4) hot mercury performance testing.

3. Lubrication and Cooling Pump Motor Assembly

a. Subcontract Status

Pursuant to a re-evaluation of the L/C PMA program requirements, Aerojet notified Thompson-Ramo Wooldridge (a subcontractor) of an intended reduction in scope of work with an interim funding limitation for FY 1964. The major reductions were as follows:

(1) Reduce all machining, assembly, engineering coordination, and testing activity to six units in place of eleven.

(2) Reduce all supplier procurement requirements consistent with six units.

(3) Delete two special development test units and employ one standard unit with a later retrofit for delivery as part of the six.

(4) Eliminate instruction manuals.

(5) Eliminate TRW PERT reporting activities.

(6) Eliminate environmental testing.

A revised work statement, dated 22 January 1964, was sent to TRW for review and comment. Based on the TRW acceptance of the work statement on 30 January 1964, Aerojet issued a purchase requisition to incorporate the changes. Aerojet and TRW met on 17 and 18 February 1964 and negotiated a basis for a new L/C PMA subcontract. A new revised contract will be written in the immediate future.

b. Design and Fabrication

All detail drawings for the PMA critical components were released by 2 December 1963. The remaining detail drawings were completed on 1 January 1964. The layout drawing, assembly drawing, and installation drawing were completed on 16 February 1964. The L/C PMA interface drawing was prepared by Aerojet in accordance with the TRW layout and became a part of the contract requirement.

Westinghouse (a TRW sub-vendor) has delivered two windings to TRW and plans to deliver the remaining motors the first week in March. Westinghouse has encountered problems in the manufacturing of the rotor shaft assembly and has slipped their rotor delivery date to 6 March 1964.

The TRW casting supplier has experienced problems in casting the volute housings and has scrapped the first three housings because of excessive shrinkage. After some pattern alterations were made, two additional castings were poured and were lost due to cracking of the molds. Additional volute housings are being poured. The present projected delivery of the first L/C PMA based on completion of the volute housings is 23 March 1964. Minor casting deviations were noted on the bearing housings, motor housings, and mounting brackets. These parts were found to be acceptable and the drawings were revised accordingly.

c. Test Planning

Aerojet and TRW engineering personnel met at TRW on 18 and 19 December 1963 to review and coordinate the L/C PMA test program, and to make a tour of the plant. The tour of the test facilities showed the test loop to be 85% complete. This test loop is now complete and has the capacity for conducting the development and acceptance testing simultaneously.

All deliverable units will be acceptance-tested in the following areas:

Performance calibration
NPSH cavitation testing
Hydrostatic proof testing
Helium leak testing
Heat stabilization testing
Dielectric strength testing.

The development test unit will be subjected to a 1000-hour abbreviated life test at design conditions. Then will come (1) cavitation testing, (2) calibration testing, (3) complete disassembly and inspection, and (4) retrofitting and acceptance testing.

The Aerojet immersion test of an ML-insulated motor in polyphenyl ether (ET 378) has been running for 7200 hours at 250°F. The successful continuous operation of the motor substantiates the compatibility of the organic fluid with the insulation system. There has been no significant change in either the 1-min megger or the polarization index in the last 4000 hours. A plot of resistance and polar index vs chronological time is shown in Figure 71. Evaluation of the chemical analysis indicates no change in fluid properties beyond the acceptable test control margin, thus precluding any unacceptable degradation of the ET 378 fluid.

VI. NONROTATING COMPONENTS

A. HEAT EXCHANGER COMPONENTS

1. Boiler

a. TS-2B Single-Tube Boiler Test Sections

Test Section TS-2B, a 60-ft-long counterflow tube-in-tube (9Cr-1Mo) boiler was composed of (1) 0.902-in.-ID mercury flow passage with a twisted ribbon turbulator (pitch = 7.2 in.), and (2) outer NaK passage of 2.5 in. OD.

Two interchangeable 10-ft-long plug inserts, supported by a coiled wire (0.105 in. and 0.135 in. dia), were installed in the inlet portion of the mercury passage.

The primary purpose of this series of tests was to verify the -1 mercury boiler tube configuration. The tests investigated overall boiling heat-transfer characteristics, pressure drop, outlet pressure stability, and general operating behavior. Parameters of importance included (1) startup conditioning time period requirements, (2) hot-start performance, (3) production of superheated vapor, (4) boiler outlet pressure stability, (5) boiler response to NaK temperature variations, (6) effect of gravity on the boiler performance, and (7) effect of exposure to air after use.

Analysis of the data is discussed below and on the next few pages.

(1) Boiler Start-up

The data showed that immediate start-up of the boiler can be obtained using a hot vacuum out-gassing pre-conditioning of the boiler (Test Procedure RPL-2-001). This is important in the simplification of the programing of the SNAP-8 system start-up.

(2) Hot Starts

The boiler outlet pressure increases with the mercury flow rate, and superheated vapor is generated continuously as illustrated

in Figure 71A. In addition, the same boiler performance was obtained whether the mercury was injected into a boiler heated to the full temperature, or into a relatively cool boiler with a subsequent program of temperature increase. The ability of the boiler to receive the mercury injection while at full temperature simplifies the SNAP-8 start-up programing. A technical memorandum is being prepared concerning this phase of testing.

(3) Superheated Vapor

The 60-ft boiler tube length and plug and turbulator configurations are adequate to produce superheated vapor in the absence of suppressed boiling. Superheated vapor was generated with either of the two plug insert configurations (0.105-in. and 0.135-in. dia wire support) at conditions above and below system conditions. The primary indications of superheat were the group of vapor temperature sensors and the NaK temperature profiles. The group of temperature sensors was arranged as illustrated in Figure 71B, to be sensitive to entrained liquid and to indicate a nonsymmetrical temperature distribution in the vapor pipe. When these temperature sensors indicated no liquid entrainment and were all well above the saturation temperature, superheat was considered to be indicated. When this indication was combined with a NaK temperature profile that showed no significant heat transfer from the NaK for 10 ft or more of pipe length, superheat was considered to be verified.

(4) Stability Performance

The mercury outlet pressure of the boiler was monitored during testing to determine the extent of outlet pressure oscillations. The majority of test points showed outlet pressure fluctuations of less than $\pm$10 psi (see Figure 72) which is considered tolerable for the SNAP-8 system. An attempt was made to correlate outlet pressure fluctuations with the temperature difference between the NaK and mercury at the liquid-vapor interface (pinch-point temperature difference). However, an unexpected flow stratification of the NaK at the boiler outlet prevented an accurate determination of this pinch-point temperature difference and thus a quantitative relationship was not obtained.

Pressure oscillations in the boiler may be significantly affected by the interactions between the four parallel tubes as well as other system characteristics. Therefore, final evaluation of pressure stability can not be accomplished until time of PCS-2 testing (when the system geometry and components will first be available). However, preliminary data on the -1 design will be obtained in the RPL-2 and PCS-1 tests.

(5) Boiler Response to NaK Temperature Vibration

The boiler has several types of response to a variation of NaK inlet temperatures, including changes in mercury inventory and in mercury pressure drop.

The mercury inventory can be significantly increased with a reduction in NaK inlet temperature. In operation of the fixed-inventory mercury loop, the boiler inventory is established by the NaK inlet conditions for constant mercury flow rate, the condenser receiving the remaining mercury inventory. The condenser must absorb the changes in boiler inventory and still provide the required net positive suction head (NPSH) to the mercury pump, and a back-pressure on the turbine which is not excessive. An inventory variation of $\pm$20 lb is tentatively considered acceptable for the -1 condenser design.

The inventory in the boiler is primarily determined by the length required for the addition of the sensible heat. A decrease in NaK inlet temperature decreases the pinch-point temperature difference, thereby increasing the liquid inventory. Estimates for the TS-2B boiler tests showed that the inventory in the boiler increased by 20 lb with a decrease in NaK inlet temperature from 1330 to 1300°F. With additional decreases in NaK inlet temperature to 1270°F, the inventory increase was excessive as the pinch-point temperature difference approached zero and suppressed boiling occurred. On the basis of experience at TRW and the TS-2B boiler tests, a 10°F temperature difference at the pinch-point is considered the minimum allowable. The reactor NaK temperature control spread is a major concern. Large temperature cycles or low-temperature transients can

cause problems in the system operation. Final temperature control specifications must be balanced with the needed turbine inlet pressure defined by turbine performance tests and the boiler pressure drop to establish the minimum NaK temperature required at the pinch-point. This temperature, when combined with the final reactor performance characteristics, will determine the NaK flow rate necessary for satisfactory boiler operation.

The mercury pressure drop responses to changes in NaK inlet temperature are coupled to the changes in interface position. A higher NaK temperature to the boiler results in a higher boiler pressure drop. With the higher NaK temperature, more mercury vapor (higher quality) is generated in the plug flow annulus as the sensible heat is transferred in less length. Figure 73 qualitatively shows the effect this has on the pressure drop in the mercury flow through the plug. As an example, the boiler pressure drop varied from 62 to 46 psi with NaK inlet temperatures of 1320 and 1280°F, respectively (data points 42 and 44, Figures 74 and 75).

Increased pressure drop commensurate with higher NaK temperatures is not considered detrimental to system operation if kept within bounds. The increased pressure drop in the boiler decreases the mercury flow rate slightly, but this decrease is compensated for by the increased temperature (higher enthalpy) to the turbine with the higher NaK inlet temperature.

(6) Gravitational Effects

An indication of gravitational effects on the boiler performance was obtained in the TS-2B tests. The 3.5-g requirement appears to have more effect than zero-g, but neither will significantly affect the boiler performance. The effect is centered around the physical necessity for keeping the liquid mercury against the heat-transferring walls of the tube. Throughout most of the boiler, the forced spin of the turbulator produces more than 3.5-g radially outward acceleration. In this case, neither 0 nor 3.5-g will cause any change in the flow and heat-transfer pattern. However, just after the mercury saturation point is reached, and until a sufficient amount of vapor is generated, there is insufficient spin to produce 3.5-g radial acceleration.

At test conditions with low mercury flow rates (0.2% rated flow), significant temperature differences were noted between the top and bottom temperature profiles along the sloping plug inlet section. This is shown in Figure 76. An explanation for this is that the liquid mercury was staying in the bottom of the annulus passage while the vapor was in the top part. With higher heat-transfer rates to the liquid than to the vapor, a larger NaK temperature drop along the bottom is expected. The length of this condition would be, in part, a function of the amount of clearance between the helical wire and the tube wall and plug surface; it would be expected to be worse for relatively large radial clearances such as the 0.020 to 0.035 in. present in the latter portion of these tests. Under these conditions, the separation persisted for only a foot or two at the 0.2% rated flow rate. When the flow rate was increased to full rated flow, any significant difference in the NaK temperature disappeared. From this it can be concluded that the effect of acceleration on the boiler is primarily centered at the saturation point and that there was no significant effect in the boiler performance at rated flow.

(7) Effect of Air Exposure on 9Cr-1Mo Alloy Boiler Tube

The 9Cr-1Mo alloy boiler tube shows no major sensitivity to air exposure after use. Experience with 316 SS boiler tubes showed a sensitivity to air exposure after use. The effect was a serious degradation of the heat-transfer performance, to the extent that a boiler tube would no longer produce superheated vapor. In these cases, sectioning of the boiler tube showed an inside surface leaching of some 0.002 in. or more in depth, wherein the nickel and chromium had been preferentially dissolved, leaving a porous surface.

The SNAP-8 Project belief is that, after the mercury had been driven from the porous material and an exposure to air, the liquid mercury would no longer penetrate into these small pores; this resulted in their being filled with mercury vapor, which has a much lower thermal conductance. The 9Cr-1Mo alloy does not become porous on exposure to mercury leaching and no change in heat-transfer path conductance was expected. The 9Cr-1Mo alloy

mercury boiler tube was operated for a total of 269 hours. At the end of this time, air was drawn through the boiler while the boiler was at 1300°F for 1 hour. This was followed by the hot outgassing procedure (Test Procedure RPL-2-001); immediately upon subsequent injection of the mercury, the original performance was obtained. No problems are foreseen in the -1 boiler operation if air exposure occurs during the boiler use.

b. Isothermal Two-Phase Flow Tests

A technical memorandum covering the isothermal two-phase flow tests is in process.

c. -1 Boiler

(1) Design

The boiler design was improved as a result of more detailed stress analysis, further study and incorporation of TS-2B test results, and greater economy and simplicity of design. In the development of the boiler design, a number of changes have been made; three of the most significant changes involved the mercury outlet, plug design, and mercury inlet.

(a) Mercury Outlet

Detailed stress investigations revealed a need for changing the original mercury outlet design. Accordingly, design studies and the attendant stress analyses have been made, and certain tests conducted to determine an acceptable redesign for this mercury outlet for RPL-2 and SL-1. The design selected used the original 9Cr-1Mo tube sheet, with the flange removed and replaced with one of 316 SS. A representative test specimen was made up and tested by thermal cycling. The welds on the test specimen showed no deterioration. This design (Figure 77) was therefore selected for use on boiler No. 1, S/N A-1 and A-2. A technical memorandum covering full details on these studies with this new mercury outlet design, will be published.

(b) Plug Design

The boiler tube mercury passage plug design was modified after consideration of the various factors involved. Such factors

include effects of wire, tube, and plug surface erosion; a double helix pattern to give a discharge compatible with the two-passage twisted tape turbulator; pressure drop, etc. A 0.135-in.-dia wire was selected, and the plug center was changed from tubing to rod material to improve reliability by eliminating the possibility of mercury entering the center of the tube through cracks or erosion holes. The single helix wire design was changed to a double helix. The diametral clearance between the wire and the plug and tube wall was controlled at 0.015 in. ±0.010 in. To improve the intertube flow stability, an inlet restriction of approximately 30 psi pressure drop at a mercury flow rate of 9,500 lb/hour total was added to each boiler tube. The new plug design is presented in Figure 78. The throat diameter varies from 0.095 in. to 0.096 in. ID.

(c) Mercury Inlet

The mercury inlet was changed to an elliptical-head design with an off-center inlet pipe connection. This design was selected to permit draining of the mercury passages.

(2) Fabrication

Assembly of the -1 boiler No. A-1 was completed except for X-ray of final closure welds, the welding of the 2-in.-length 316 SS mercury inlet tubing, connections, and the final helium leak check. Figures 79 through 83 show this boiler nearing the stages of final assembly at the Western Way Manufacturing Corp., Van Nuys, California.

The assembly of the -1 boiler No. A-2 at the Western Way Manufacturing Corp. included mounting of the tubing on the inner shell (Figure 80). The boiler is now ready to start the automatic internal tube-to-tube sheet welding process as soon as welding certification is complete.

The assembly of the -1 boilers A-3 and A-4 at the Western Way Manufacturing Corp. is awaiting a review and decision on the design of the plug. The boilers are otherwise to be identical with the A-1 and A-2 boilers.

Fabrication of a wooden mockup of the -1 boiler assembly was completed at Aerojet-General Corporation, Azusa, on 7 January 1964. Figure 83 shows a picture of this model which was used to assist in piping installations of RPL-2 and SL-1 before delivery of the actual -1 boiler assemblies.

(3) Stress Analysis

Stress analysis has been continued. Figure 84 shows the areas of concern. Table 8 shows the extent of the completion of the stress analysis for the conditions of steady state, thermal transients, and environmental. The critical areas have been given extensive stress analysis attention.

2. Condenser

Fabrication of the first two units of the -1 condenser was completed. Figure 85 shows the second unit scheduled for use in SL-1.

The MECA Program (Mercury Evaporating-Condensing Analysis) data have indicated that the heat-transfer design of this condenser is very conservative. The single-tube MECA experiments have shown condensing lengths of less than 20 in. under SNAP-8 operating conditions. It is expected that tapered tube geometries to be tested in the MECA program will permit fewer and shorter tubes than in the current design.

A program has been initiated for the development of a tube-to-tube header connection not requiring a backbraze. This program is aimed at reducing the fabrication cost and the number of thermal cycles to which the tube bundle must be subjected prior to final assembly of the unit.

An all-welded joint is being considered that can make use of the tube sheets already fabricated. Such a joint is shown in Figure 86. Another concept is shown in Figure 87.

Planning has begun for fabrication of the third condenser which will be sent to NASA-LeRC. It has been requested that this unit be sent as a group of specific subassemblies to be assembled later at LeRC. A design review is planned for the incorporation into this unit of a revised tube-to-tube sheet joint.

The stress analysis is progressing toward completion. The areas of concern are shown in Figure 88. The status of the stress analysis with regard to steady-state conditions, thermal transients, and environmental conditions are shown in Table 9.

3. Auxiliary Start Loop Heat Exchanger

The final design review was completed of the -1 model component which couples the primary and heat rejection loops during start-up.

Detail drawings were completed and fabrication was initiated. Fabrication was completed on the first three units for RPL-2, SL-1, and SL-2 (see Figure 89).

4. Turbine Simulator

The turbine simulator program has been essentially completed with units delivered to the RPL-2 and SL-1 test loops. As the tube-to-tube sheet joint used only the weld for mechanical strength and sealing between the two fluids, an americium gammagraph inspection was performed on all the tube-to-tube header welds. The bimetallic (316 SS tube with 9Cr-1Mo internal coating) mercury-vapor tube which was originally scheduled to be incorporated into the SL-1 unit has been replaced by a 316 SS tube until such time as the bimetallic tube becomes available. Figure 90 shows the completed unit to be installed in SL-1.

B. EXPANSION RESERVOIRS

Calculations for a conceptual design lubricant-coolant (L/C) expansion reservoir were prepared. These calculations were established for a system having an 80-lb ET-378 inventory with 60 cu in. losses assumed for each of three periods: start-up, evaporation during run, and restart.

L/C expansion reservoirs meeting these conditions and having cylindrical tanks with elliptical heads would be 14.75 in. in dia by 22.5 in. long.

Calculations for a preliminary design heat-rejection-loop (HRL) expansion reservoir were prepared. These calculations were established for a closed system having a 153-lb NaK inventory with temperatures increased from 50 to 665°F and pressure increased from 17 to 44 psia. The capacity provides a 10% safety margin for unknown contingencies.

HRL expansion reservoirs meeting these conditions and having cylindrical tanks with elliptical heads would be 14.0 in. in dia by 14.6 in. long.

Calculations for a preliminary design primary-loop expansion reservoir were prepared. These calculations were established for a closed system having a 250-lb NaK inventory with a 1680-cu-in. displacement for temperatures increased from 50 to 1375°F and pressure increased from 15.4 to 50.0 psia. The system inventory includes extra volume for expansion loops, so little safety margin is included. This design established the necessity of thermal management of pressurizing gas temperature for control of reactor pressures.

Primary expansion reservoirs meeting these conditions and having cylindrical tanks with elliptical heads would be 20.0 in. in dia by 35.1 in. long.

Electrical position transducers are included in expansion reservoirs of the NaK systems to identify the reservoir liquid inventory. This expansion reservoir inventory transducer will be used to establish the pressure of the auxiliary test system expansion reservoir.

C. VALVES

A preliminary design review was held this quarter on the temperature control valve, the lubricant-coolant shutoff valve, and the auxiliary loop shutoff valve.

The review showed the type and configuration of valves to be used on the PCS-1A (Figure 91).

The heat rejection loop temperature control valve marked No. 2 on Figure 91 controls the NaK flow in the third loop during PCS startup to produce the required condenser outlet temperature.

The lubricant-coolant valve marked No. 1 on Figure 91 isolates the ET-378 lubricant from the bearing cavities of the turbine alternator assembly and mercury pump-motor assembly.

The auxiliary loop shutoff valve marked No. 3 on Figure 91 isolates this loop from the third loop after startup.

The heat-rejection-loop temperature-control valve preliminary design chosen is shown in Figure 92. This valve will establish the NaK flow range

characteristics. To meet the requirement in adjustment of operating ranges, a small screw-adjusted bellows for adjustment of the expansion volume has been provided for test use to determine operating parameters. Flight valves may not need this feature.

The valve butterfly circumferential design will be of the type that will not cause either butterfly or valve wall-wear.

The temperature control valve has 2-in. OD tubing ports to match HRL line sizes. The flow rate is 37,600 lb/hour of NaK. The valve will operate at a temperature of 700°F, which is more than the highest temperature of the current HRL loop design.

Power for actuating this butterfly valve is derived from the expansion of the NaK contained in the annulus surrounding the valve housing. If a bellows failure occurs, a spring is provided to hold the valve in the normal diversion position.

The working pressure environment of this valve is 45 psi at 100°F through 700°F.

The lubricant-coolant and auxiliary shutoff valves preliminary design chosen is shown in Figure 93 and will meet the requirements of isolating the working fluids as required. The valve is a 2-way gate type solenoid valve. Dual (Ceroc insulated) solenoids actuated by 28 v,dc will move the gate into the two positions - open and closed. Two spring-loaded ball latches (shown in detail on Figure 93) are provided to hold the gate in either position. Note all-welded closure construction of the fluid passage areas.

The lubricant-coolant loop design flow rate of 600 lb/hour at 30 psi inlet pressure, 250°F, and a ΔP of 5 psi maximum, will be provided.

Since the fluid handled is ET-378, material selection is simplified. Type 316 SS will be the material chosen, with Stellite 6B as the "floating seal" closure elements.

Leakage to space will be zero, and assured by the all-welded construction of this Valcor Engineering Corp. valve. Internal leakage will be no more than specified - 0.5 cu-cm/hour.

A 10,000-cycle test life is being specified.

The auxiliary start system shutoff valve is the same dual solenoid-operated 2-way (one-and-off) valve shown in Figure 93. This valve handles NaK at 100 to 700°F, and has a flow rate to 2010 lb/hour at 44-psi line pressure, with a ΔP of 2.5 psi. This valve will have a body of 316 SS and magnetic parts of 410 SS.

Start-up reliability program progress is discussed in Section IV of this report.

D. MERCURY INJECTION SYSTEM (MIS)

The preliminary design review was held this quarter on the mercury injection system. The review showed the type and schematic of the MIS to be used in PCS-1 and PCS-2. The system presented was discussed as one of the conceptual designs. This design is shown in Figure 94; it was also discussed in the preceding quarterly report (Reference 1).

Evaluation has been completed of a mercury flow control valve design submitted by vendors for use in PCS-1 and PCS-2. The metering flow control valve shown in Figure 95 was the design chosen.

An isolation valve design for use in PCS-1 and PCS-2 has been submitted by vendors. Figure 96 shows the valve proposed for selection in the preliminary design review.

E. ELECTRICAL INSULATION DEVELOPMENT PROGRAM

1. High-Temperature Motor Test

Testing continued on an inorganic-insulated motor to determine the long-term electric strength of the insulation system. The motor stator was fabricated previously for the original 2-loop SNAP-8 system, and the insulation system used in the stator is essentially the same as now being employed in the new HRL and primary loop NaK motors. This 1000-cps motor has external bearings and operates on a reduced 60-cps voltage to eliminate the need for a special power supply.

To date the unit has operated satisfactorily for 4311 hours with a winding hot-spot temperature of 450°F. As shown in Table 10, winding insulation

resistance has not changed significantly through 3324 hours aging at 450°F. These results indicate that the inorganic insulation system is stable and is thus promising for long-term operation at 450°F - a level anticipated for the new NaK motors.

2. Evaluation of Organic Resins

Efforts continued to determine the most promising organic resins to use in impregnating and encapsulating the alternator electronic controls components. Previously, 15 resins had been selected for evaluation. During this quarterly period, one of these resins was eliminated from further consideration because of its bad handling characteristics. Two additional resins selected by General Electric for use in the SNAP-8 alternator and voltage regulator-exciter were included in the program, bringing to 16 the total number of resins undergoing screening.

A weight-loss test was selected for initial screening of the 16 resins. This test, which is based on the MIL-I-16923D specification, provides indications of thermal stability of resins. Samples of the various resins were cast in glass petri dishes about 2 in. in diameter and 1/2 in. in height (Figure 97). Following curing in accordance with recommendations of the resin manufacturer, the samples were removed from the dishes. The samples were then subjected to the following procedure:

a. Dried at 220°F for 24 hours to remove moisture and low-temperature volatiles.

b. Cooled to room temperature in a dessicator and then weighed to the nearest 0.1 mg on an analytical balance.

c. Thermally aged for 168 hours at 392°F in a furnace with forced air ventilation.

d. Subjected again to Step b.

Table 11 summarizes the weight-loss data obtained for the 16 resins following 168 hours at 392°F. Testing of the samples was resumed, but a furnace control failure during the second 168-hour run destroyed the samples. Another test has been initiated using smaller samples that were cast at the same time as the original samples.

3. Organic Insulated Statorettes

Testing of promising organic insulation systems applied in stator core sections was continued. The test consists of exposing test units (statorettes) either to air or to organic fluids (Dow ET-378 and Monsanto OS-124) in a furnace at 392°F. Eight statorettes using four candidate organic insulation systems are presently undergoing evaluation. Four of the units were aged in air, and serve as controls. Of the remaining four statorettes, two were immersed in ET-378 fluid and two units were immersed in OS-124 fluid. Throughout the test, statorette winding insulation resistance (hereafter referred to "IR") was measured to establish trends in the condition of the electrical insulation. Table 12 provides a description of the insulation systems used in the eight statorettes.

Tables 13 through 20 summarize the test results obtained to date for the units. The most significant results and tentative conclusions reached thus far are summarized below.

a. Statorettes HML-1 and HML-2

Statorettes HML-1 and HML-2 have each accumulated 9709 hours aging at 392°F. Following 9709 hours aging at 392°F, the control unit (HML-2) operating in air had an IR of 6.7×10^{11} ohms as compared with a value of 8.9×10^{9} ohms for unit HML-1 that was immersed in OS-124 fluid. Since the corresponding IR values for these units following only 240 hours aging at 392°F are approximately the same as for the 9709-hour aging point, it appears that OS-124 fluid is compatible with ML polymer materials. However, it should be noted that the resistivity of OS-124 fluid is less than the resistivity of air at 392°F, based on a comparison of IR obtained for the two units.

b. Statorettes ML/997-1 and ML/997-2

Statorettes ML/997-1 and ML/997-2 have each accumulated 9892 hours aging at 392°F. Throughout this period, the control unit (ML/997-1) in air has shown an IR of about 5.0×10^{11} ohms. A similar statorette (ML/997-2) immersed in OS-124 fluid throughout the same period has exhibited an IR range of 2.2×10^{9} to 1.3×10^{10} ohms. This variation is attributed to changes in the level of OS-124 fluid in the statorette container that have occurred as a result of

evaporation of the fluid. For example, when completely immersed in OS-124 fluid, IR was found to be about 10^9 ohms. When a portion of the statorette winding was exposed to air following evaporation of some of the fluid, IR increased to the 10^{10}-ohm level. Based on the above, it appears that the insulating materials used in these statorettes are compatible with OS-124 fluid; however, as was the case for statorette HML-1, OS-124 fluid reduces the winding IR significantly.

c. Statorettes ML-3 and ML-5

Statorettes ML-3 and ML-5 have each accumulated 4356 hours aging at 392°F. The control unit (ML-5) aged in air has maintained an IR of between 7.0×10^{11} ohms and infinity (10^{12} ohms or higher). A similar unit (ML-3) immersed in ET-378 exhibited an IR of 6.6×10^7 ohms following 45 hours aging. Then as evaporation of ET-378 occurred, winding IR increased. Following 2732 hours aging, no fluid remained in the statorette container and IR had increased to 9.0×10^{10} ohms. After 4356 hours, additional fluid originally absorbed in the winding apparently had evaporated since IR increased to 3.7×10^{11} ohms. The above shows that ET-378 fluid reduces the IR of the insulation system; however, there is no evidence as yet that the fluid is chemically incompatible with the insulating materials used in the statorettes.

d. Statorettes ML-4 and ML-6

Statorettes ML-4 and ML-6 have each accumulated 4356 hours aging at 392°F. The control statorette (ML-6) aged in air has maintained a winding IR of from 1.7×10^{10} ohms to infinity (10^{12} ohms or higher) throughout the test. A similar unit (ML-4) immersed in ET-378 fluid showed an IR of 4.4×10^7 ohms after 45 hours aging. Evaporation of ET-378 fluid occurred so rapidly that no fluid remained in the test container after 2732 hours aging. Winding IR at this point in the test had increased slightly to a level of 3.2×10^8 ohms. Inspections following 2732 hours aging (Reference 1) showed that ET-378 had chemically attacked the varnish (Westinghouse Doryl) used to impregnate the winding. Subsequent measurements through 4356 hours aging have revealed continuing improved IR (maximum of 1.7×10^{10} ohms) although the varnish is apparently badly deteriorated. The latter finding suggests that visual and electrical measurements following 10,000 hours aging at 392°F are required to establish the full extent of degradation of the insulation system.

Electrical monitoring of the statorettes will continue until the units have accumulated 10,000 hours aging at 392°F. Following 10,000 hours aging, each statorette will be inspected and electrically tested to destruction to determine the final condition of the insulation.

4. HRL and Primary Loop NaK Motor Insulation Development

Efforts were continued to improve the techniques in handling, applying, and processing inorganic electrical insulating materials used in the -1 HRL and primary loop NaK motors. The following techniques and procedures were developed and incorporated in winding procedure AGC-10284 for the NaK motors:

a. Aluminum rings were fabricated for use in supporting the ends of the stator slot liner insulation during winding operations. These rings permit the coil end turns to be flexed without developing excessive mechanical forces on the slot liners, thus preventing damage to the liners.

b. Teflon inserts were constructed for use in supporting the sides of the slot liners that extend beyond the end of the stator slots. These inserts protect the slot liners from bending forces encountered during installation of the coils in the stator core.

c. The tops of the slot liners in the stator slots were taped to the core by means of Mylar pressure-sensitive tape. This prevented shifting of the slot liners during coil installation.

d. Burrs were removed from the stator core end laminations by manually filing the lamination edges, followed by vapor honing of the edges with a ceramic slurry.

Additional work was done in the areas of ceramic impregnation, encapsulation, and diamond grinding. To completely define the process of impregnating and encapsulating the HRL and primary loop NaK motors with inorganic cements, a series of trials of insulation system models was made.

Two wound stators (HTM-5 and HTM-6) available from the previous SNAP-8 2-loop system program were installed in housings and conditioned as described below.

Unit HTM-5 was impregnated with a low-viscosity slurry of calcium aluminate cement and encapsulated with Norton LM-1625 cement. Immediately after the winding end turns were filled with the cement, vibration was applied to the housing in an attempt to fill all voids in the winding end turn areas.

Unit HTM-6 was impregnated with a low-viscosity calcium aluminate slurry, then encapsulated with LM-1625 cement. The encapsulant was pressed in place at 500-psi pressure.

Following curing of the ceramic cements, the trial stators were sectioned and inspected. Sections of each unit are shown in Figure 98, along with unit HTM-4 that had previously been encapsulated with LM-1625 cement under 500-psi pressure. Results of the inspections are as follows:

HTM-4 - There were some voids in the winding end turns, but the ceramic encapsulant appeared very dense and was without cracks.

HTM-5 - The end turns were well filled with encapsulant, but the encapsulant was cracked in several areas.

HTM-6 - Good fill of ceramic was achieved throughout the end turn area, and no cracks were observed in the encapsulant.

It was felt that 500-psi pressure might distort the stator end winding and cause electrical failure at a later time, so an additional housing with a blank stator in place was potted using a combination of vibration and 250-psi placement pressure (Figure 99). This sample was in excellent condition following both curing and thermal aging for 168 hours at 1000°F; consequently, the process pressure for all future units will be reduced to 250 psi.

A final processing test was run to check all steps in the impregnation and encapsulation procedure. A trial HRL motor stator was installed in a dummy housing (Figure 100), heat conditioned to remove organics, impregnated, encapsulated, cured, and finally conditioned at 1000°F for 406 hours. The unit was then cycled ten times from room temperature to 1000°F.

Figure 101 shows the unit following the test. No cracks were observed in the ceramic, and the material appeared to be dense and well bonded.

Based on the above work, process specification AGC 12085 was prepared in final form and published.

Concurrent with the latter unit, a second housing was filled with a blank stator, encapsulated, cured, and sent to the NaK motor assembling vendor for bore sizing and can expansion trials. The vendor tried to machine the core cement with a single point diamond, but this was found to be unsatisfactory. Dry diamond grinding was then tried and found to be successful. A change in Specification AGC 10285 will be initiated to incorporate this change.

5. Radiation Effects Program Support Work

Fabrication was essentially completed of electrical insulating material specimens that are to be evaluated in the SNAP-8 radiation effects program. Four insulation system models (statorettes) were fabricated. Two statorettes use ML polymer organic insulation systems (Figure 102) while the remaining units use inorganic insulation systems identical to those now being used in the HRL and primary loop motors (Figure 103). Also fabricated were magnet wire twist specimens (Figure 104) and organic encapsulant cubes with embedded electrodes. Some of the latter specimens are shown in Figure 105. A total of 72 encapsulant cubes were fabricated of which 75% were organic types and the remaining 25% were inorganic materials. Other materials used in the program include various tapes, sheets, laminates, ceramic through-type terminals, sleevings, cloths, organic fluids (Dow ET-378 and Monsanto OS-124) and flexible lead wires. Following fabrication, the statorettes, encapsulant cubes, and wire twist specimens were measured for key electrical properties to provide Aerojet with reference data.

Packaging of the materials for shipment to the reactor vendor was in progress at the end of the quarter.

6. Ceramic Terminals

Ceramic through-type terminals designed by Aerojet for the main leads of the HRL and primary loop motors have been received and helium-leak tested. All terminals passed the leak test satisfactorily. A torque value of 15 in.-lb has been established for assembling the terminal to the motor housing mounts. It is anticipated that the new terminal will be more reliable than standard commercial

types, since the terminal transmits mechanical forces applied to it to the motor housing directly and does not rely on the strength of the ceramic-metal joint to resist structural strain.

Efforts were resumed on a test which was previously developed to determine the vacuum reliability of ceramic terminals at elevated temperature. Figure 106 shows a trial assembly in which a ceramic terminal is welded to a metal mount, which in turn is welded to a metal tube. The metal tube is joined to a glass tube by a glass-to-metal seal. The procedure planned to evaluate a ceramic terminal at elevated temperature is as follows:

a. A vacuum is developed on the assembly and all joints are helium-leak checked.

b. While the vacuum is established inside the tube, the glass tube is flame-sealed.

c. The assembly is placed in a furnace with the terminal inside and the glass tube extended through the modified furnace door.

d. Prior to and throughout the test at elevated temperature, the pressure inside the glass tube is monitored by means of an electric field applied by a Tesla coil. A vacuum of about 5×10^{-4} mm mercury will exhibit a very light blue color, 1×10^{-3} mm mercury pressure is indicated by a light purple color, 5×10^{-2} mm mercury is indicated by a dark purple, and atmospheric pressure is indicated by no color.

F. ELECTRICAL CONTROLS AND COMPONENTS

1. Voltage Regulator-Exciter (VR)

A preprototype voltage regulator design has been completed by General Electric. Aerojet has approved this design, and fabrication has been started. The original General Electric design of the -1 modules did not include hermetic sealing. General Electric was advised that the -1 modules must be hermetically sealed. This will require the use of ceramic terminals to make the electrical connections. Attaching the ceramic terminal nickel flanges to the aluminum housing is a major problem in the -1 module design. General Electric proposed a process for welding the nickel flange to aluminum. General Electric

sent to Aerojet a ceramic terminal with the nickel flange welded to an aluminum structure using the General Electric process. This terminal was evaluated by the Aerojet Materials Department. The fusion of the aluminum to the nickel appeared to be good, but after thermal cycling between room temperature and 700°F, a crack appeared along the fusion joint between the aluminum and the nickel. Aerojet feels that use of this type of hermetic seal is questionable for the PCS. Aerojet is investigating a system which would use a TIG weld and a cold weld to produce the ceramic-hermetic seal.

General Electric sent Acceptance Test Procedure 44A257630 to Aerojet for approval. After some changes, the test procedure was approved by Aerojet.

The first breadboard tests of the General Electric voltage regulator were not completely successful. The amount of excitation current supplied by the saturating current potential transformer (SCPT) was not adequate. The SCPT was redesigned to provide higher power output. The following development tests were successful except that the system did not meet the dip-and-rise requirements of the Aerojet specification. General Electric will ship the first two preprototype regulators without the larger SCPT, but will be required to install the larger SCPT in the third preprototype unit.

Copies of the General Electric preliminary design review manual were distributed by Aerojet in January. A preliminary design review meeting was held on 4 February 1964 to discuss the information as presented in the design review. The thermal design as presented was considered satisfactory by Aerojet. The stress analysis of the low-temperature module indicated that the design was not marginal, but no stress analysis was given on the SCPT module. General Electric has been requested to submit the stress analysis on the SCPT assembly.

2. Speed Control

Failure of the large Mo-Permalloy tuned inductor cores redirected effort to the small Mo-Permalloy cores and the gapped "C" core inductors. The design of both types of inductors was completed during the last report period. Fabrication

of the "C" core inductor and a small Mo-Permalloy inductor was completed. The "C" core inductor is considered the primary design, but due to the higher Q of the Mo-Permalloy small inductors, it was decided to test both types.

The -1 sensing circuit of the -1 design will require that the inductors be potted. Test plans and instructions have been written for the impregnation and potting process for the "C" core and the small Mo-Permalloy cores. The "C" core inductors were impregnated and potted with no problem. The small toroidal Mo-Permalloy cores could not be successfully impregnated and potted. During the impregnation process of the 20 small toroidal tuned inductors, all of the cores broke. These were not failures due to handling techniques or isolated conditions. Further analysis of the failures indicated excessive copper on the inner diameter of the small cores. With the total failure of the small Mo-Permalloy inductor cores, it was decided to stop all work on the Mo-Permalloy inductors.

The impregnation and potting tests were continued on the silicon iron gapped inductors. After the impregnation, the silicon iron inductors were stabilized by cycling the inductors from ambient to 150°F. After the stabilization process, the maximum change in inductance was 0.1%. Additional temperature tests on the silicon iron inductors showed the same 0.1% change in all cases.

The inductors were assembled with their respective capacitors for the long-term temperature tests. These tests were designed to determine what the long-term drift of the sensing circuit might be under the 150°F temperature conditions. The long-term drift tests were started on 22 January 1964; since that time, no measurable drift has been noted. The drift is being measured at the d-c output of the sensing circuit at 208 v,ac and a frequency of 400 cycles. The temperature is being held constant at 150°F. These tests are scheduled to last for 10,000 hours.

Fabrication of Serial No. 3 speed-control amplifier assembly has been completed and acceptance-tested. The gain curves are shown in Figures 107 and 108. Fabrication of Serial No. 4 assembly has been completed, but this unit has not been acceptance-tested.

A preliminary draft of the acceptance-test procedure of the -X speed control amplifier, the speed control tuning procedure, and the time-response

procedure have been completed and reviewed. To eliminate additional tuning of the sensing circuit after assembly, the inductor and capacitor were tuned with their respective magnetic amplifier. The tuning procedure has been modified requiring that the sensing circuit be tuned with its respective magnetic amplifier and that these components remain together in all systems.

The specification control drawings for the -1 resistors, capacitors, and diodes were completed. An analysis of the -1 magnetic characteristics was also made to ensure that the -1 design incorporated all of the information available from the -X units.

After the analysis had been completed, drawings for the -1 magnetics were completed.

Layout drawings of the speed control low-temperature module have been started. This module will contain all of the rectifiers, the sensing circuit, the magnetic amplifier, and the associated resistors. These components will be contained in an aluminum housing with ceramic terminals for making the electrical connections. Here again the problem arises of connecting the nickel flanges on the ceramic terminals to the aluminum housing. As a result of investigations of cold weld processes, it was decided to use a copper transition piece between the nickel flange of the ceramic terminal and the aluminum housing. This copper transition piece will be TIG welded to the nickel flange, after which it will be cold welded to the aluminum housing. This will then allow the cold weld joint to be made from copper and aluminum. Details of this design are being worked out. The vendor has been contacted regarding the tooling for making the cold weld. This method of attachment can be used not only on the speed control module but on all of the other modules - regardless of whether they are located in the high-temperature assembly or the low-temperature assembly.

The drawings of the ceramic terminals have been submitted to the vendor to show how Aerojet would like to modify the terminal design to increase the reliability of the commercial design. The vendor has indicated that some points of the Aerojet design need some rework in order to maintain the proper configuration of the ceramic terminals. Terminal design in accordance with vendor's recommendations have been started.

a. Electrical Laboratory Facilities

To provide for the experimental, development, and the acceptance-testing of the electrical components of the PCS supplied by the Electrical Controls group, it was necessary to install the required special test equipment to provide for all of the different types of testing.

Four major items of STE are required for testing: a 400-cycle 100-hp motor, a 400-cycle motor-generator set, a simulated parasitic load, and a simulated vehicle load. The 1000-cycle load banks were reworked to the proper rating for the 400-cycle simulated parasitic load resistor. This unit is now installed and ready for use. The motor-generator set is a 400-cycle, 3-phase, volts-per-cycle, 133 kva system. This motor-generator set will be used for two purposes. First, it will be used to provide a 400-cycle (volts-per-cycle) system for the electrical laboratory for testing the electrical components, subassemblies, and main assemblies of the PCS. Secondly, it will be used in conjunction with the 100-hp motor for providing the power for driving the SNAP-8 alternator for making the alternator-voltage regulator tests in the electrical laboratory. The motor-generator set has been received from the vendor and installed in the electrical laboratory. The simulated vehicle load banks have also been received from the vendor and have been installed in the electrical laboratory.

With the motor-generator set, the simulated parasitic load resistor, the simulated vehicle load bank, and the 400-cycle 100-hp motor installed in the electrical laboratory, all of the basic power equipment is now available for testing the SNAP-8 electrical components.

Final acceptance tests were successfully completed on all of the special test equipment. The high-current bus system has been installed in the electrical laboratory. A block diagram has been started which will show the complete electrical laboratory SNAP-8 test facilities. Provisions are being made for the testing of all components, subassemblies, and main assemblies.

b. Cold Gas Electrical Systems Tests (CGEST)

The Electrical Controls Department has prepared and forwarded a CGEST test request to Test Engineering. The test request provides for the following specific tests to be made in the cold gas system:

(1) Voltage and speed regulation for varying loads.

(2) Voltage and speed transient response for varying loads and gain settings.

(3) Start-up stability performance.

(4) Waveform and harmonic analysis.

(5) Radio-frequency interference (RFI).

(6) Short circuit tests.

The test request includes a written description of the aforementioned tests, an electrical block diagram, and an instrumentation wiring diagram for the visual instrumentation. It also includes an inter-connecting wiring diagram for the electrical components.

The speed control amplifier and the saturable reactors for the cold gas electrical systems tests have been fabricated. The amplifier has been acceptance-tested and is ready for installation into the loop. The saturable reactors will be acceptance-tested in March. The preprototype voltage regulator-exciter will be supplied by General Electric. The additional equipment will be supplied by the responsible Aerojet department.

3. Saturable Reactors (SR)

Fabrication of three uncut "C" core saturable reactors was completed. Testing of these assemblies after the control winding was installed was not successful on two assemblies due to shorts in the gate windings. Efforts to clear those shorts without removing the control windings were not successful. The remaining uncut "C" core saturable reactor was successfully load-tested on the 400-cycle motor-generator set.

Because of fabrication problems resulting from the use of uncut cores, the decision was made to change the design to a standard "C" core configuration. Further examination of the problem of assembly showed questionable reliability because splicing of wire in the control winding was necessary when using the uncut cores. The new design will use the cut "C" cores with emphasis placed on the reduction of the effective air gap to minimize excitation current.

The design of the cut "C" core saturable reactor has been completed, and fabrication of the first three units has been completed. Quotations from three vendors for the fabrication of one set of -X saturable reactors were received. The engineering evaluation of these quotes has been completed and a vendor was recommended to the Aerojet Purchasing Department.

Response-time tests of the -X three-phase saturable reactor were conducted to verify the calculated time constant of this particular saturable reactor assembly. The first series of tests showed the "off-to-on" time constant was 32% shorter than calculated; the "on-to-off" time constant was 6.4% longer than calculated. Additional time-response tests were conducted on this saturable reactor because the aforementioned tests showed a large time difference between the "on" and "off" condition. The new test series which more nearly duplicated actual operating conditions produced approximately equal "on" and "off" times. These times were 35% less than the calculated time constant, but the calculated time constant was based on a cooler operating temperature than actually existed in the saturable reactor. As the temperature rises in the saturable reactor, the resistance of the control winding will increase, thereby resulting in a lower time constant. The second series of tests verified as accurate the method used for calculating the time constant of the saturable reactor.

Transfer curves on the -X saturable reactor have been plotted. Examination of the family of curves shows that the voltage drop across the saturable reactor will not exceed the calculated 10%. This particular saturable reactor had a voltage drop of 7%. Gate current vs gate voltage can be seen in Figure 109.

Temperature rise tests were also conducted on the -X saturable reactor. At no load and no heat sink, the temperature rise was 135°F. At no load and with a heat sink, the temperature rise was 110°F. At approximately 50% load, the temperature rise was 155°F. These tests were conducted to gather information for the -1 design. To obtain a picture of the saturable reactor temperature profile, 20 thermocouples were installed on the assembly. The hot-spot temperature occurred between the gate and the control winding. It appears that the -1 design will require heat shunts for reducing the hot-spot temperature.

The -X saturable reactor assembly consists of three separate reactors. The design for the -1 will bring the three gates and cores together in one package with one control winding. The electrical and magnetic design of the -1 saturable reactor has been completed. The mechanical layout drawing has been completed. The detail drawings for the saturable reactor have been started. A thermal analysis is being conducted. The results of this thermal analysis may require some modifications in the mechanical design.

The -1 assembly will be potted in an aluminum housing, then located on the heat sink in the transformer reactor assembly. The power and control leads will be brought through the housing using ceramic terminals.

4. Harness Assembly

A design review of the harness assembly was held during the last report period. In this design review, a cold-weld technique was recommended for connecting the copper to the aluminum bus bar. As pointed out in this design review, more information was needed to ensure the reliability of an aluminum-to-copper cold-weld joint. To pursue this investigation, samples of nickel, copper, and aluminum were sent to the vendor. The vendor indicated complete success in the cold-weld between the copper and the aluminum. The nickel-to-aluminum cold-weld was not considered successful by the vendor because of the difference in hardness of the aluminum and the nickel, and the lack of a properly designed die. The vendor felt that the technique of the cold-weld between the nickel and the aluminum could be developed with few problems if these two matters could be resolved.

The cold-welded samples were returned from the vendor and forwarded to the SNAP-8 Materials Department for evaluation. An evaluation test program was completed for the copper-to-aluminum cold-weld transition pieces. Based on the vendor's opinion of the nickel-to-aluminum cold-weld, it was decided not to evaluate these transition pieces. The SNAP-8 Materials Department evaluation of the copper-to-aluminum cold-weld established that the joint was very good. The technique of this process appears to be highly reliable. Results of the evaluation of the cold-weld butt joint transition piece between the copper and the aluminum were issued as a technical memorandum (Reference 4).

The least understood factor related to the cold-weld joint is the effect of temperature in the diffusion layer of cold-weld. The vendor stated that at 500°F the cold weld may begin to deteriorate; the actual rate of this deterioration was not known.

In order to investigate the effect of temperature, a cold-weld sample of the copper and aluminum was placed in the oven at 500°F. Three samples will be cut from the cold-weld; the first sample will be cut at 500 hours, the second at 1000 hours, and the third at 1500 hours. At the end of 1500 hours at 500°F, the SNAP-8 Materials Department will perform a thorough investigation to see what effect the 500°F temperature had on the cold-weld joint. It appears that if the harness temperature rises above the 500°F level at any point, the cold-weld technique cannot be used in that area. Copper will be used throughout areas where the temperature might reduce the reliability of a cold-welded copper-to-aluminum transition piece.

The basic concept for all of the external harness has been developed. During this report period, a conceptual design of the high-current bus inside the transformer/reactor assembly was started. This harness assembly will use braided copper wire with G7 laminate and mica as the insulation system. The G7 laminate will be used as the standoff for the braided harness, and the mica will be used as a wrapping to cover the braided copper wire. These components have been ordered from the vendors to investigate the use of G7 laminate and mica for the installation system.

The commercial standoff ceramic terminal design does not have the required mechanical strength to withstand the environmental requirements of the PCS. A slight modification has been made in the commercial ceramic standoff to increase its strength. This design will be submitted to the ceramic terminal vendors for quotations and subsequent fabrication.

5. Start Programer

A revised electrical schematic diagram of the start programer has been completed which incorporates all of the information that is available at the present time (Figure 110). In addition to the electrical schematic diagram,

an electrical sequence of operation has been written. This report describes the operation of the start programer as related to the electrical schematic diagram, and includes a bar chart showing the functions performed vs time. This report has been sent to the required division personnel for review.

A development timer specification (AGC No. 10209) was completed and forwarded to possible timer manufacturers. Five vendors submitted bids on the start programer timers. The bids were evaluated and the vendor best qualified to meet the timer specification was recommended. A resistor-capacitor type timer was selected in view of the simplicity of the design. One of the bidders proposed a mechanical timer, but the device was much too complicated for the PCS start programer. The vendor-promised delivery date for the timer is the middle of March. This delivery schedule will not adversely affect the fabrication of the first -X breadboard inasmuch as experimental timers will be used. The breadboard will be so designed that, upon receipt of the new timers, the experimental timers can be easily replaced by the development timers.

The experimental timers have been fabricated and mounted on the -X start programer breadboard. The wiring diagram for this breadboard has been started.

6. Load Breaker

Specification AGC 10264 has been completed and approved. It includes the requirements for the inverter contactors as well as the vehicle load breaker.

Stores and Purchase Requisitions have been prepared for the procurement of development test samples for each of the contactors specified. Requests for Quotation have been sent to five potential vendors.

7. Parasitic Load Resistor

The specification for the parasitic load resistor (AGC-10270) has been approved and released. A Stores and Purchase Requisition has been prepared for the procurement of four units. A Request for Quotation has been sent to four potential vendors.

Additional substantiating data and justification for the selection of the design power density presented in the conceptual design review was prepared. Part of this data was presented in answer to NASA Technical Direction No. 15.

Testing of the three sample resistor elements at approximately 1100°F sheath temperature is continuing. Accumulated operating time is approximately 2400 hours.

8. Protective System

The conceptual design review for the protective system was held on 17 December 1963. A method of under-voltage sensing of each phase was presented. This system will provide protection for single- and multiple-phase faults and for overloads in the vehicle load.

An extensive review of vendor's data on voltage-sensitive relays has been started. The available data indicate that the few types of a-c-voltage-sensitive relays available are also frequency-sensitive and would not be suitable for use with a frequency-dependent voltage regulator of the type used in the SNAP-8 system. Other types of "so-called" a-c-voltage-sensitive relays are actually d-c relays with semiconductor rectifiers and solid-state voltage-sensing circuits contained within the same enclosure. The use of components of this type is not desirable in the absence of extensive detailed evaluation of the circuit and individual components based on the SNAP-8 environmental requirements, including nuclear radiation and the high-reliability requirements.

The preliminary test unit will be based on the use of d-c-voltage-sensitive relays with the required semiconductor components selected separately. Rectifier selection will be based on components picked for use in other parts of the SNAP-8 system included in the Radiation Effects Program. The use of Zener diodes to reduce the relay sensitivity requirements and improve circuit performance is still being considered. The effect of nuclear radiation on the operation of Zener diodes of the required rating is reported to be slight, but further review of available data is necessary before a decision can be reached.

A laboratory test of a resistor-capacitor timing circuit for use in the protective system has demonstrated the feasibility of this circuit for the time ranges anticipated.

9. Radiation Effects Program

Negotiation of a final contract between Aerojet and Lockheed-Georgia for the conduct of these tests was completed. Work was started by Lockheed-Georgia on 27 January for design and procurement. Assembly and preliminary tests were completed on all test specimens fabricated by Aerojet. All items to be included in these tests, except two General Electric alternator statorettes, were shipped to the reactor site. General Electric has indicated a delivery for these items which would not delay the Lockheed test schedule. Photographs of the test items prior to shipment are shown in Figures 111 and 112. The picture of the electronic component and subassembly panels in Figure 111 also includes one of ten test-load inductors which will be used to simulate the reactive load which some of the circuits will experience in the SNAP-8 system.

Engineering liaison has been established with Lockheed-Georgia to provide technical coordination on this program.

10. NaK and Coolant Startup Pumping System

a. Inverter

An Advance Quotation Request and preliminary specification were sent to potential inverter vendors during the first week of December. Response from the AQR indicated three companies are interested in proposing.

A Request for Quotation and the final specification (AGC 10281) were submitted on 7 February 1964.

A revision of the estimated start-up time for the nuclear system has required a change in the specified operating time for the inverter. It has been requested that the inverter proposals be based on 5 hours of operation at low speed and 8-1/2 min at high speed, instead of the 4-hour and 5-min intervals previously specified.

b. Inverter Contactors

Requirements for the voltage tap changing contactor and the contactor used for transferring the pump motors from the inverter to the alternator have been included in Specification AGC 10264 with the vehicle load contactor.

c. Inverter Frequency Control

The inverter frequency control is used to control the speed of the inverter d-c motor by maintaining constant field current at the two operating frequencies and varying the field current at a fixed rate during the transition period. The frequency control is located in the start programer. It consists basically of a transistor circuit acting as a current regulator when supplied with a fixed-input voltage from a voltage divider. The ramp control allows the frequency of the inverter to increase from 95 cps to 220 cps in approximately 120 sec. The maximum rate of frequency change is not to exceed 2.1 cps/sec. At the end of the speed change ramp, the circuit is again supplied with a new value of fixed-input voltage from a voltage divider and acts as a current regulator to maintain field current and frequency approximately constant.

Three types of inverter frequency controls have been built and tested. They have been designated as the 1-, 2-, and 3- transistor circuits. Each unit was designed to control the inverter field current over the range of 3 amp (95 cps) to 1 amp (220 cps) with a ramp time of 120 sec and a range of inverter field coil resistance change with temperature of 2 to 1.

The 3-transistor unit, shown schematically in Figure 113, in preliminary tests shows excellent stability and drift characteristics with changes in control system temperature and field resistance change. The 1-transistor unit indicated unacceptable characteristics and required impracticable component values to obtain the required ramp time. New -X versions of the 2- and 3-transistor units have been built for further testing.

11. Transformer-Reactor Assembly (TR)

The second conceptual design of the TR assembly has been completed (Figure 114). This conceptual design employs the same basic design as proposed in the original conceptual design.

The heat sink design will consist of an aluminum casting which surrounds a nickel tube. To investigate the bonding between the nickel tube and the aluminum casting, an experimental heat sink was fabricated. Three types of nickel tubes were cast into the aluminum; copper-plated nickel, gold-plated nickel, and elemental nickel. These three tube types were cast into the aluminum casting by the vendor and returned to Aerojet for evaluation.

The SNAP-8 Materials Department sectioned the casting and made an investigation into the bondings between the three types of tubes. The first results showed the nickel and gold-plated nickel tubes to be well bonded to the aluminum. The copper-plated nickel tube bond did not hold very well. Additional investigations showed holes in the aluminum casting. These holes were probably formed from moisture that was not removed before the casting was made. If moisture was actually present - and this appears to be the case - then a copper oxide would form on the copper-plated nickel tube. The oxide on the copper would prevent a good bond from existing between the nickel and aluminum.

Because of the problem of copper oxide in the first casting, it was decided to fabricate an additional test heat sink assembly - this time with effort made to prevent the presence of moisture during the casting procedure. The SNAP-8 Materials Department is currently conducting a survey to find vendors capable of making these aluminum castings over the nickel tubes in the absence of moisture. When this has been done, the second sample heat sink will be returned to the SNAP-8 Materials Department for sectioning and evaluation.

G. NaK TRAPS

Detailed design of -1 hardware was held in abeyance pending completion and evaluation of system loop NaK conductance problems, experimental hot-trap performance, and Oakridge National Laboratory NaK-loop tests.

H. MERCURY FILTER-SEPARATOR

There was no further work on the design of a flight-type filter for the SNAP-8 system. All design effort has been held in abeyance until FY 1965 pending evaluation of initial system's tests.

VII. TEST ENGINEERING

A. NON-NUCLEAR TEST LOOPS AND STANDS

1. Liquid NaK Loop No. 3 (LNL-3)

LNL-3 will have the capabilities of testing NaK pump-motor assemblies (both primary and HRL), the parasitic load resistor, and NaK valves. The loop will be located in Building 180, Cell 2. Rated Power Loop No. 1 (RPL-1) which formerly occupied that location has been dismantled. RPL-1 equipment will be used in LNL-3 as applicable.

LNL-3 is presently in the final design phase. Mechanical design is essentially complete, and electrical control and instrumentation design is nearing completion. The majority of material procurement has been initiated.

2. Liquid Mercury Loop No. 3 (LML-3)

LML-3 will have the capability of testing mercury pump-motor assemblies. The loop will be located in Building 180, Cell 3. Low Power Loop No. 1 (LPL-1) which formerly occupied that location has been dismantled. Some of the LPL-1 equipment will be used in LML-3.

LML-3 is now in the fabrication phase. All design has been completed, as has fabrication of the mercury and lubricating coolant supporting structures. Fabrication of the mercury loop is approximately 50% complete. Fabrication of the lubricating-coolant loop is approximately 25% complete.

3. Rated Power Loop No. 2 (RPL-2)

Design effort for RPL-2 upgrading is nearing completion and is reduced now mainly to fabrication support. Test requests and/or test plans have been received for TAA testing, boiler testing, and condenser testing. Tests of the auxiliary start loop heat exchanger and the lubricant-coolant pump-motor assembly are also planned for this facility. NASA has requested that boiler and condenser tests be added to the program for RPL-2. The test sequence and procedure are presently under study. Fabrication of RPL-2 is 45% completed; work is progressing in all areas of fabrication, including piping, controls, instrumentation, and structures.

4. Gaseous Nitrogen Stand No. 1 (GN_2S-1)

Activity on this facility centers around functional testing prior to start of checkout. All hardware has been installed and connected. Final fit-up of a turbine alternator assembly (TAA) will be made when a unit is available. Planning is in progress to use this facility to accomplish a series of lubricant-coolant flow checks of sample hardware in conjunction with TAA development prior to rotating tests of a TAA.

5. System Loop Test Facility No. 1 (SL-1)

The conceptual and preliminary designs are complete, and the final design is nearly complete. Fabrication of the system has been initiated.

SL-1 Test Facility Design Specifications were distributed. These cover the general system requirements, the alternator electrical controls circuitry requirements, and the mercury loop fill and dump requirements. Specifications were initiated which define the operator controls and instrumentation requirements.

Analytical mechanical design is essentially complete and includes hydraulic, thermal, and stress analyses. Layout design of piping and components is approximately 50% complete. A 1/12 scale model was built showing component placement with interconnecting piping for equipment located within the test cell and the outside equipment pad. Procurement of all mechanical hardware was initiated and the majority of raw materials has been delivered.

Instrumentation and controls designs were initiated, and required hardware is being procured.

Fabrication of test stands and small vessels was initiated. A concentrated fabrication effort was not started owing to insufficient drawings and materials.

Preparation of preliminary system shakedown and checkout procedures was initiated.

6. System Loop Test Facility No. 2 (SL-2)

Significant progress was made in the design and procurement of SL-2. Designs of the pressure-vent and vacuum system for all five basic loops were completed. Design of the seal vacuum system for the turbine alternator assembly and for the mercury pump-motor assembly is nearly complete. Mechanical design for the SL-2 is about 40% complete, and 60% of mechanical procurement (100% on long-lead items) is complete. Most of the instrumentation sensors have been ordered, and many have been received.

The conceptual design review for SL-2 was presented on 4 February 1964.

B. TEST FACILITIES AND EQUIPMENT DESIGN

1. Integrated Non-Nuclear Test Complex

a. Digital Data Acquisition System (DDAS)

The DDAS which was returned to the vendor for warrantee rework and modification has been reinstalled and checked out by the vendor to his satisfaction. Aerojet acceptance-test programing is now in preparation.

All intrabuilding DDAS control and instrumentation transmission lines have been installed.

b. Mechanical

The passageway between Buildings 180 and 187 has been raised to the level of the Building 187 pad.

The air compressor installation and piping distribution system in Building 187 has been completed and checked out. Connection of the 2-in. supply line from the air receiver to the present distribution system in Building 180 is all that is required to make the new air supply system operational in both buildings.

Installation of the 4-in. gaseous nitrogen and 2-in. gaseous argon supply lines from the gas storage pad at Building 75 to Buildings 180 and 187 has been completed and checked out. The high-pressure manifolding

of the cascade nitrogen and argon receiver tubes has been completed except for the nitrogen regulator and remote-control equipment. Both systems have been charged with gas and are ready for operation with the RPL-2 and GN_2S-1 loops in Building 180.

2. Building 180

a. Instrumentation

Instrumentation design is 100% complete. Installation of instrumentation signal conditioning and recording equipment is 95% complete and checked out. The grounding system is 90% complete.

b. Mechanical

Support equipment for the RPL-2 and GN_2S-1 loops, which has been installed on the Building 180 pad, includes the NaK electric heater, NaK cooler, electromagnetic pump blowers, nitrogen heater, and TAA exhaust stack.

3. Building 187

a. Instrumentation

Instrumentation design is 60% complete and the documentation is approximately 50% complete. Installation of instrumentation in all cells is approximately 20% complete.

Installation of the grounding system is underway.

b. Controls

Control transmission wires to all cell boxes have been installed. The control-main distribution frame wiring connections are nearing completion. All gutters have been installed.

c. Mechanical

Foundations for the four gas-fired NaK heaters are completed and ready to receive the heaters.

Pneumatic louvre actuators have been installed on the air inlets to all cells.

Design of the heavy support structure for Cell 3B (SL-1) has been completed. Since this same basic structure will be erected in Cell 4A (SL-2), enough material was ordered for two assemblies.

C. NUCLEAR SYSTEMS TESTING

1. Ground Prototype Test Facility (GPTF)

Review of GPTF test support equipment (TSE) requirements, PERT, and specifications continued.

Preliminary design of TSE was initiated and continues. A conceptual P&I diagram and an instrumentation schematic were initiated and are being reviewed.

Discussions were held with AI on the installation drawings, manuals, and AI subcontract work scope for Aerojet equipment installation in the GPTF. A date of 15 April 1964 was established for the Request for Proposal (RFP) submittal to AI.

A copy of a review of GPTF component and system operating characteristics was sent to NASA. A DDAS technical description was released and has been discussed with prospective vendors. A preliminary estimate of the TSE power requirements was completed and is being reviewed.

2. Flight Prototype Test Facility (FPTF)

Review and evaluation of the FPTF design criteria continued with coordination between AI and Aerojet. FPTF control-room layouts were discussed on a continuing basis with AI. AI and Aerojet control room equipment was defined. Estimates of the outgassing loads for the PCS and TSE were prepared and sent to AI.

D. TEST SUPPORT SERVICES

1. Data Reduction Services

The modification of the control-room of Building 156 to accommodate an Advanced Data Processing Center has been approved. Final design of this area is nearing completion.

Coordination with the Aerojet Computer Sciences Division has continued to develop means of producing complete programs for the DDAS by use of the IBM 7094 computer.

2. Chemical Support Services

a. Lubricant-Coolant Fluid

An evaluation of the lubricant-coolant fluid has progressed sufficiently to establish a purchase specification, AGC-10320. This specification incorporates the requirements of high purity (99% minimum) and a specified boiling range. The fluid (Dow Chemical Co. ET-378) previously used will not meet the new specification without additional purification Other sources of mix-4P3E (chemical nomenclature for the SNAP-8 lubricating-cooling polyphenyl ether) have been sought, resulting in bids received from Monsanto Chemical Co. and Shell Oil Co. Evaluation has continued for the development of methods of purification of the lubricant-coolant after test use. The current method adopted is distillation. The investigation is continuing in an effort to improve this technique and reduce the cost of the operation.

b. NaK

Coordination with SNAP-8 Materials and System Engineering Departments is in process to establish a purchase specification for NaK. The current specification, AGN-60207A, must be updated in order for the vendor to be able to meet the requirements.

Compatibility of NaK with ET-378 at test-operation temperatures has been investigated. Tests have recently been completed and a report of the evaluation of these results is in process. These tests were performed to establish safety requirements for facilities design and test operation.

c. Mercury

Coordination with SNAP-8 Materials and System Engineering Departments has continued in an effort to establish the purity requirements of mercury to be incorporated into a purchase specification.

VIII. MATERIALS

A. STAFF SUPPORT

1. Component Design and Development Support (Task A.1)

a. Post-Test Analysis of TS-1E-1 Boiler

The TS-1E-1 boiler was fabricated of 316 SS. Tests were made to determine an optimum diameter for the mercury-tube-inlet flow-restriction plug. The plug, whose purpose it is to restrict the flow of mercury to the surface area of the inner diameter of the tube, is located in the straight inlet portion of the boiler tube. The boiler initially performed within design expectations, but performance degradation occurred as testing continued. Degradation appeared to have started following a second plug change. Replacement with the initial plug failed to restore the proper performance. The poor performance of the boiler was manifested by its failure to raise the mercury to the required superheat temperature, regardless of the time the boiler operated.

Analysis of the mercury-containment coils from the TS-1E-1 boiler after 238 hours of operation revealed a porous layer indicative of general leaching-type corrosion on the inner diameter of all mercury-containment coils. A technical memorandum reporting the results of this investigation is being prepared.

b. Post-Test Analysis of TS-2B Boiler

The mercury-containment coil of the TS-2B boiler was analyzed after 269 hours of mercury service in RPL-2 test loop. This boiler was fabricated of 9Cr-1Mo alloy steel (i.e., the reference alloy for the SNAP-8 boiler and condenser). Examination of the mercury-containment tube disclosed deposits of mass transfer products; the heaviest buildup - a maximum of 0.008 in. at one point - occurred in the middle four turns of the eight-turn boiler tube bundle. It is estimated that the vapor quality in this region is approximately 90 to 95%. The inlet and outlet sections (liquid mercury and superheated mercury vapor, respectively) had only a few small localized areas of buildup approximately 0.0002-in. thick.

2. Component Fabrication Support (Task A.2)

a. Specifications

During the quarter, the following specifications were issued, modified or initiated:

AGC 10319 - SNAP-8 Components, Cleaning of

AGC 10320 - Polyphenyl Ether, MIX-4P-3E

AGC 10327 - Mercury, Heat Transfer Grade

Technical data for a specification covering welding of electrical connections were submitted to the Specifications Group.

b. Elevated-Temperature Components Identification Procedure

A survey of procedures usable for identification of elevated-temperature components resulted in selection of the electrolytic technique as being superior. The adherence of high-temperature paints was found to be inconsistent. The electrolytic method has numerous advantages and seems capable of providing satisfactory identification after service at elevated temperatures. Among these advantages are: (1) the marking is permanent (not removed unless the surrounding metal is removed), (2) any type of metal can be marked, and (3) the marking is made without stress, strain, or deformation, and is not a source of stress raisers.

c. Fusion Welding

The Palmer Company, Whittier, California, incurred difficulties in fusion welding of 0.020-in.-thick 9Cr-1Mo sheet for use in the turbine exhsust bellows. A review of the problem was made. Visual weld defects

occurred in the form of small modules on both the face and the root side of the weld. Radiographic and metallographic examination showed the welds to be of excellent quality despite the visual defects. As the base material surface condition was poor, mechanical or electropolishing was recommended to correct the condition. Subsequent welded samples prepared with the use of abrasive belt sanded material exhibited much improved weld surface contour, but the problem is not yet completely solved.

d. Tube-to-Tube Weld Penetration

Weld samples were prepared at the Aerojet Von Karman Center to determine weld penetration of turbine simulator tube-to-tube sheet joints as a function of welder current setting. Sections welded at 40 amp showed 0.025 to 0.032 in. penetration along the faying surfaces. Sections welded at 70 amp showed 0.085 to 0.093 in. weld joint penetration. The weld penetration of the second sample exceeded 1-1/2 times the tube wall thickness (0.050 in.). The latter welds should perform satisfactorily, and thus 70 amp was recommended as a proper current setting for completion of these welds.

e. Tube Joint Welds

Internally welded tube joints simulating the -1 boiler configuration were submitted by the Kynex Corporation, Rome, New York, for evaluation. Visual examination of these welds indicated excellent weld contour; however, the welds did not meet the radiographic standards of AGC-13860, Class 15.

Similar samples were submitted by Western Way (the fabricator of the -1 boiler). These welds did meet radiographic requirements of AGC-13860, Class 15, but were rejected for other reasons. Causes of rejection were that visual examination revealed excessive weld "suck-back" on the OD surface, and that metallographic examination (100X) revealed surface pitting and tears. The latter defects were located at the edge of the weld fusion zone on the tube ID.

Western Way was asked for further qualification samples.

B. MERCURY CORROSION STUDY

1. Corrosion Loop Program (Task C.1)

The dynamic corrosion loops (1/16th scale) are designed to determine corrosion and mass-transfer patterns in the mercury and NaK loops of the SNAP-8 system. Corrosion Loops 1 and 2 were constructed of Haynes-25 alloy. Operation of the first loop has been completed, and the second loop has been converted into Component Test Loop 2 (CTL-2), which is being operated to check the performance of certain components to be used in subsequent loops (3, 4, and 5). Corrosion Loops 3, 4, and 5 (CL-3,-4, and-5) are being constructed with 9Cr-1Mo as the mercury-containment material. The NaK primary loop will be constructed of 316 SS and, in the high-temperature area, of chromized Hastelloy N, with a section of Hastelloy C in the low-temperature area.

During the report period, CTL-2 was operated to test pressure transducers, a cyclone corrosion product separator (Run 11), and a hot-start procedure (Run 12).

A mercury Chempump to be used in CL-3 completed a 1000-hour endurance test at 500°F in an all-liquid pump-test loop.

Assembly of CL-3 continued throughout the quarter, and the loop is ready for installation in the test cells. Assembly of CL-4 was deferred until such time as a corrosion product separator could be tested successfully in CTL-2.

a. Component Testing

Some components to be used in CL-3,-4, and-5 - including the mercury pump, adjustable choked nozzle, pressure transducers, and corrosion product separator developed under Task C.2 - are being tested in CTL-2 to determine their operating characteristics. An all-liquid pump test loop (described in Reference 5) is also being operated for checkout and endurance runs of the mercury Chempumps to be used in CL-3,-4, and-5.

(1) Mercury Chempumps

The 405 SS mercury Chempump was installed in the pump test loop after the repairs were completed, as described in the last

quarterly report (Reference 1). The pump operated continuously for 1073 hours, under the following typical conditions:

Pump outlet pressure, psig	670
Pump inlet pressure, psig	35
Pump inlet temperature, °F	435
Pump outlet temperature, °F	595

Upon completion of the test, the pump was removed from the test loop and installed in CL-3.

One of the mercury Chempumps, with the impeller and impeller case fabricated from 9Cr-1Mo, was installed in the pump test loop. After it had operated satisfactorily for 8 hours, it was removed and installed in CL-3.

(2) Pressure Transducers

Seven electronic pressure transducers with two types of cooling leg were installed in CTL-2 during the last quarter to obtain dynamic data on loop operation, and to evaluate the cooling legs. Two test runs were completed.

The pressure instrumentation for CTL-2 Run 10 consisted of five Statham pressure transducers (0 to 500 psia) and two Consolidated Electrodynamic Corporation (CEC) pressure transducers (0 to 100 psia and 0 to 700 psia) that were excited by two bridge balance units.

The outputs of the pressure transducers were fed through amplifiers and recorded on a Visicorder oscillograph. Interaction between channels in this system resulted from using the bridge balance units, which prevented valid pressure data from being obtained.

The run was repeated after the problems were corrected. The 100-psia CEC transducer was not used and the bridge balance units were replaced by a Microdot unit for each transducer, as will be used in CL-3.

Transducer pressure and temperature data from Run 11 are listed in Table 21 and summarized below.

(a) The frequency on the CEC transducer at the pump outlet was approximately 480 cps, with a maximum peak-to-peak magnitude of 45 psi.

(b) A frequency of approximately 160 cps and 10 psi peak-to-peak was noted on the Statham transducer at the inlet to the boiler. All other Statham transducers registered this frequency periodically, but at a decreased amplitude.

(c) A variance in the boiler outlet pressure with a peak-to-peak amplitude of about 20 psi was noted on the three Statham transducers located between the boiler and the adjustable choked nozzle. The period of the fluctuation varied between 5 and 25 sec.

(d) Rated pressure can be established in approximately 1/2 sec after the pump is turned on.

(e) Pressure drops to zero in about 1 sec when the pump is shut off.

(f) The adjustable choked nozzle smooths out most of the boiler fluctuations and maintains a reasonably steady outlet pressure.

Horizontal and vertical pressure taps were installed in CTL-2 during the previous report period to determine the pressure differences and cooling capacities of the two types of tap (Figure 115). Temperature profiles of the pressure taps and transducers are shown in Table 21. No great temperature or pressure difference was noted between the two types of tap; however, the vertical attachment eliminated the possibility of mercury vapor being condensed and returned to the loop as liquid.

As a result of this test, vertical attachment of transducers was selected for use in CL 3.

(3) Corrosion Product Cyclone Separator

The corrosion product separator described in the preceding quarterly report was installed in CTL-2, as shown in Figure 116.

According to the test plan, the loop was brought to operating conditions similar to those for a test without a separator. The boiler output pressure was set at 265 psig by means of the adjustable nozzle, and the loop was to be operated for 100 hours, or until the boiler output pressure reached 300 psig. Neither the nozzle, the mercury flow rates, nor any other controls were adjusted during the run. It was expected that if the boiler outlet pressure remained constant for 100 hours, this would indicate that the cyclone separator was effective in reducing buildup in the nozzle; if the boiler output pressure increased to 300 psig, it would mean that the separator was not trapping the corrosion products effectively.

The loop operated for approximately 13 hours after the boiler output pressure was set at 265 psi, at which time the boiler outlet pressure reached 300 psig and the loop was shut down.

The fact that about the same amount of time was required to raise the nozzle inlet pressure from 270 to 310 psig with and without the cyclone separator (see Table 22) indicates that this device, as installed, was not effective in preventing deposition in the nozzle. System operating conditions were comparable, if not exactly equal, throughout the test period.

The separator was removed from the loop and sectioned. No deposit was found in the cyclone section as was postulated would occur if liquid droplets were thrown against the wall and dried out. The weight of the columbium wool from the collector increased by 1-1/3 g during testing; however, there was evidence that a pool of liquid mercury remained in the collector pot and that some refluxing took place in the sides of the pot. The presence of liquid in the collector pot is evidence that the experimental conditions did not provide a satisfactory test for the cyclone. The start-up procedure, stipulating that the separator be full of liquid mercury which then had to be boiled out after start-up, also proved detrimental to testing. The cyclone separator test will be repeated after a hot-start procedure for CTL 2 is proven. Improvements in test conditions will also be incorporated so that the device can be fairly evaluated.

(4) Component Test Loop 2 Condenser

During reassembly of CTL-2 prior to Run 12, leaks (caused by cracks) were found in the Haynes 25 radiator condensing tubes. Copper-finned 304 SS condensing tubes were substituted for the defective Haynes 25 tubing. The copper fins were affixed with a thin layer of Thermon heat-transfer cement applied between the tube and fin. This method of attaching the copper fins to the tubing replaces the brazed joint used in the previous radiator.

(5) Hot Start of Component Test Loop 2

The start-up technique used through Run 11 involved filling the entire loop with liquid mercury. To provide a better test for future separators, a hot-start procedure was established. This consists of (a) evacuating the loop, (b) heating the boiler to approximately 1300°F, and (c) starting the mercury flow into the boiler without filling the loop, so that the nozzle will be exposed only to mercury vapor. To accomplish this hot start, the following minor modifications were made to CTL-2:

Addition of twisted tape in tubing from the boiler outlet to nozzle inlet

Modification of thermocouple wells in the superheated section shown in Figure 117

Removal of the fill valve at the top of the loop between the boiler outlet and nozzle inlet.

The twisted tape was added to help dry the vapor from the boiler. The thermocouple wells were changed to prevent condensation on them. The fill valve was removed to prevent vapor from condensing in the tube leading to the valve and mercury dripping back into the vapor stream. Also, since the hot-start technique was to be used, the fill valve was not needed.

Run 12 consisted of the following steps:

(a) Component Test Loop 2 was successfully hot-started.

(b) The loop was allowed to settle out, and the boiler outlet pressure was set at 265 psia by adjusting the nozzle.

(c) The loop operated for 9 hours until the boiler outlet pressure reached 300 psia, indicating that corrosion products had accumulated at the nozzle.

(d) The loop was shut down by turning off the mercury pump and the heat to the boiler, and by valving off the mercury system so that mercury could not fill the loop.

This test demonstrated that circulating hot mercury through the loop prior to start-up was not the cause of corrosion product build-up at the nozzle, and that the build-up on the nozzle as indicated by increased boiler outlet pressure would be a desirable method of evaluating the effectiveness of corrosion product separation devices (see Table 23).

b. Corrosion Loops 3, 4, and 5

(1) Design

The purpose of this task is to establish the mechanical and thermal design of the corrosion loop, including the preparation of engineering drawings and procedures, and the evaluation of test data as they apply to heat-transfer, fluid-flow, and corrosion phenomena.

The following procedures for CL-3 have been completed and reviewed: (a) mechanical calibration and checkout, (b) instrument pre-checkout, (c) NaK filling, (d) instruments and controls operation, (e) NaK purification, (f) mercury filling and cleaning, (g) loop start-up and operation, and (h) periodic operation checkout.

(2) Fabrication

The purposes of this task are to fabricate the individual components for Corrosion Loops 3, 4, and 5 (described in Reference 6), to assemble the loops, and to install the instrumentation and facilities necessary to operate them.

(a) Facility

The electrical and mechanical modifications to the test facility were completed.

(b) Components

All components for Corrosion Loops 3, 4, and 5 scheduled for fabrication at AGN were completed this quarter, except for the mercury condenser and the turbine simulator heat exchanger, both of which were fabricated for Corrosion Loops 3 and 4 only, and the NaK purification system, fabricated for CL 3 only. Photographs of the mercury boiler, the adjustable choked nozzle, the turbine simulator heat exchanger, the turbine simulator blades, and the mercury condenser, appear as Figures 118 through 122, respectively. All components purchased from outside vendors have been received.

Difficulties with the construction of the turbine simulator heat exchangers occurred because the 9Cr-1Mo bar stock from which the end adapters were machined contained inclusions. Leak checks after post-heat treatment of the welds for 30 min at 1350°F revealed porosity. A weld bead, using 9Cr-1Mo weld wire approximately 0.060-in. thick was then applied over the entire surfaces of the adapters. The weld was heat treated. Leak-check of the turbine simulator heat exchanger was completed successfully after the weld bead was placed on the adapters.

(c) Instrumentation

The control console previously fabricated and installed in the test area was completely checked out. The thermocouples and pressure transducers were installed in the loop and the system interconnection was started.

(d) Assembly

Assembly of CL-3 in Cells A and B continued throughout the report period (Figures 123, 124 and 125). After all subassemblies have been installed in the test cells, the final connections will be made in the mercury system between the mercury boiler outlet and the adjustable choked nozzle inlet, and the pump outlet to the flow control valve inlet.

All welds made during assembly have been X-ray inspected, and the primary and condensing NaK systems were satisfactorily

helium leak-checked. While those parts of the mercury system which were completed on each assembly were helium leak-checked, the entire mercury loop will be tested after the final Fe-9Cr-1Mo welds have been heat-treated.

Insulation of the primary and condensing NaK loops was completed, and insulation of the mercury loop was begun.

c. Corrosion Product Separators

A task was established toward the end of the quarter to develop a corrosion product separator for CL-4. This is a continuation of the former Corrosion Product Control Task (C.2) which was concluded. Work performed during this quarter included the design of an impingement separator and modifications to Component Test Loop 2 for separator testing.

(1) Separator Design Considerations

Theoretically, to design a corrosion product separator, the size and composition of the undesirable particles must be known. Actually they are not known, and it has been postulated that mercury droplets entrained in vapor containing dissolved corrosion products cause corrosion product build-up on the nozzle. Since the vapor is superheated, the mercury droplets will evaporate continuously until equilibrium is reached. Equilibrium may be characterized by liquid mercury containing corrosion products or dry corrosion product powder. But since a limited time is required for the droplet to travel from the boiler section to the nozzle, equilibrium may never be reached. Therefore either dry corrosion products, or corrosion products in the mercury droplets, or both, may accumulate on the nozzle. Even less is known about the size of the particles; for the design of the prototype separators, particle diameter will be assumed to be in the micron range. Tests of the separation will then yield some information on particle size.

(2) Impingement Type

An impingement separator (Figure 126) was designed for CTL-2 and will be tested next quarter. It consists, basically, of a pipe with 115 impingement screens at right angles to the mercury vapor flow. The separator, being fabricated by Mectron Industries, is intended to remove entrained mercury droplets containing corrosion products. The design of the

impingement separator is based on available data in the literature and is described below.

(a) Design Requirements

The design requirements for the impingement separator are tabulated as follows:

Mercury flow rate	1000 lb/hr
System pressure	270 psia
Mercury vapor temperature	1250°F
Mercury droplet temperature	1075°F
Maximum pressure drop	10 psi
99% removal of 0.5-micron mercury droplets	

The impingement screens are made of woven 0.0014-in. 304 SS wire mesh, having 325 wires/in., and approximately 0.01 in./layer.

(b) Design Calculations

The impingement separator was designed using the experimental data given in Reference 7 and the procedure from Reference 8, described below:

The allowable approach velocity to the wire screens, as determined by re-entrainment considerations, was calculated from Equation 18-126 in Reference 8.

$$V_o = K \left(\frac{\rho_L - \rho_V}{\rho_V} \right)^{0.5} \qquad (1)$$

For V_o* in ft/sec, the value of K varies from 0.35 to 0.4 at atmospheric pressure. It was noted in Reference 8 that the value of K is higher at greater than atmospheric pressures. In the absence of specific data, K was taken to be 0.4. Therefore,

$$V_o = 0.4 \left(\frac{762 - 3.1}{3.088} \right)^{0.5} = 6.27 \text{ ft/sec}$$

*Nomenclature is listed on the final page of Section VIII.

The target efficiency is defined in Perry's Handbook to be the sum of the interception and impact (inertial) efficiencies.* The interception efficiency is given by Equation 18-128 in Reference 8.

$$\eta_i = \frac{D_p}{D_c}\left(\frac{2 + \frac{D_p}{D_c}}{1 + \frac{D_p}{D_c}}\right) \qquad (2)$$

Substituting the appropriate values in Equation (2), the interception efficiency was calculated to be 2.8%. The impact efficiency has been determined experimentally by Ranz and Wong (Reference 7) and the results correlated, using a dimensionless parameter, $\psi^{1/2}$, defined by

$$\psi^{1/2} = D_p\left(\frac{C\rho_L V_o}{18\,\mu\, D_c}\right)^{1/2} \qquad (3)$$

The parameter C is a function of the mean free path of mercury and the droplet size

$$C = 1 + \frac{2.5\,L}{D_p} \qquad (4)$$

Using Equation 17-26 in Reference 8, the mean free path of Hg was calculated as shown below.

$$L = \frac{1}{1.414\,\pi\, N_m\, \sigma^2} \qquad (5)$$

N_m, the number of molecules per unit volume, was calculated by temperature and pressure ratioing of Avogadro's number and the volume of a gram-mole at STP. The value of L was calculated to be 0.0168 μ. The values of C and $\psi^{1/2}$ were calculated to be

*Overall target efficiency is also defined as that fraction of the particles swept by the body which will impinge on the body.

$$C = 1.084$$

$$\psi^{1/2} = 0.34$$

With the use of Figure 10 in Reference 7, the impact efficiency is determined to be 3.0%. Note that the area of the curve used to determine this efficiency was beyond the range of the experimental data. However, analytical data presented in Reference 9 substantiate the extrapolation.

The number of wire screens required is related to the overall target efficiency by Equation (6)*.

$$N = \frac{\ln \frac{1}{1 - F}}{\frac{a_o}{A_o} \eta_T} \qquad (6)$$

The number of screens required was calculated to be 115.

With the allowable upstream velocity and the required flow rate known, the upstream vessel inside diameter was calculated to be 1.62 in.

The pressure drop of the vapor through the wire screens was calculated using the friction factor data in Reference 9, Figure 108. The following parameters were calculated:

$P' = 0.9$

$G_{av} = 77{,}400$ lb/hr-ft^2

Deq = 0.0126 in.

Re = 300

f = 0.72

$\Delta P_{dry} = 4.24$ psi

*This equation is derived from the definition of the overall target efficiency of the screen.

During separator operation, the lower layers of wire screen should be wet with mercury. The additional pressure drop caused by the decrease in flow area, in the presence of liquid mercury, is estimated (from Figure 18-148, Reference 8) to be 2 to 5 psf per layer; therefore, the maximum increased pressure drop caused by wetting should be approximately 4 psi. The total pressure drop through the 115 screens is about 8 psi.

The areas of greatest uncertainty in the design calculations are the prediction of impact efficiency and the calculation of pressure drop. Short of an experimental program to determine the relationship between η_{im} and $\psi^{1/2}$, there seems to be no way of substantiating the extrapolation. Pressure measurements along the CTL-2 loop should indicate the accuracy of the pressure drop calculations.

(3) Component Test Loop 2 Modifications

Experience with Run 11 with CTL-2 indicated that improved temperature- and pressure-determination of the mercury vapor is needed for reliable separator testing. It is also desirable that the piping geometry be the same for the testing of each separator.

CTL-2 was modified as shown in Figure 127 to accomplish these objectives. Beyond the obvious change in tubing geometry, the twisted tape section will be lengthened and the instrumentation changed.

(a) Piping Configuration

The piping configuration was modified to facilitate the testing of various separators in CTL-2. The subassembly of the impingement separator and its location in the loop are shown in Figure 127. Subsequent corrosion product separators will be identically located.

(b) Twisted Tape Section

The heated, twisted tape length extending from the boiler outlet was increased. This was done to compensate for the increased heat loss due to the lengthening of the tubing from the boiler outlet to the adjustable nozzle inlet.

(c) Instrumentation

Although the immersion thermocouples were designed to measure vapor temperature, their performance during Run 12 indicated possible deficiencies. The boiler outlet temperature, as compared to the adjustable nozzle inlet temperature (Table 23), showed as much as a 150°F temperature drop although the line between them was both insulated and heated. The modified thermocouple assembly is shown in Figure 127. A skin thermocouple was located at each probe assembly (Type A and B) to indicate both heat loss and probable thermocouple error during loop operation.

(d) Performance

The pressure drop of the mercury vapor as it flows through CTL-2 has been calculated for the following conditions:

Flow Rate	1000 lb/hr
Vapor Temperature	1250°F
System Pressure	270 psia

The results are as follows:

Straight Tubing, 5/8-in. OD	
0.065-in. wall	0.87 psi/ft
5/8-in. 90° elbow	0.89 psi/elbow
5/8-in. twisted tape	2.16 psi/ft

Data obtained from Reference 10 were used to calculate the friction factor. It was assumed that 35 velocity heads will be lost by the mercury vapor when it flows through a 90° elbow.

2. Corrosion Product Control (Task C.2)

The objectives of this task were (a) to determine the chemical composition of corrosion products formed in the SNAP-8 mercury loop with 9Cr-1Mo alloy, and (b) to develop and test methods of removing or restricting the circulation of corrosion products in the mercury loop.

Four thermal convection loops were operated and all results have been reported, except for residue analyses for Thermal Convection Loop 4.

A cyclone separator test in CTL-2 was completed and is reported in Section VIII,B,1,a(3). The task was ended when thermal convection loop work was completed. Further work with vapor separators was transferred to the corrosion loop task (C.1) and is covered in Section VIII,B,1,c. The residues from TCL-4 were analyzed during this quarter and corrections made to previously reported data. Final conclusions from the thermal convection loops were drawn.

a. Analysis of Residues from Thermal Convection Loops

The validity of the residue analysis was suspected because of the small amount of Cr found. Examination of the procedure showed that data had been handled inconsistently. Data from some samples had been normalized because large fractions of some residues were not accounted for. The data were recalculated to be shown as analyzed. Iron was previously reported only as the principal constituent. Its actual level was re-estimated and is now reported.

Corrected analyses of deposits and residues from Thermal Convection Loops 1, 2, and 3, are given in Tables 24, 25, and 26. Residues from TCL-4 were collected and analyzed as shown in Table 27. (The magnetic fraction was not analyzed.) The weights of residues obtained from all loops are listed in Table 28 for comparison.

b. Observations from Thermal-Convection-Loop Tests

(1) The presence of even a small cold spot in the vapor region produces a significant amount of corrosion.

(2) Of the four loop boilers, measurable corrosion-product deposition was found only in the boiler of Loop No. 1. This loop operated at 1075°F without corrosion-product separators.

(3) Corrosion patterns in Loop No. 2 (700°F boiling temperature) were similar to those found in Loop No. 1 (1075°F boiling temperature). The amount of corrosion was, of course, greater in Loop No. 1 with the higher boiling temperature.

(4) Loops 3 and 4 contained the greatest total corrosion products. (These are the loops that contained corrosion-product separators.)

Corrosion products did not preferentially deposit on any of the experimental surfaces (9Cr-1Mo walls, columbium, or iron wools).

The magnet was relatively ineffective in trapping corrosion products, but cannot be eliminated from further consideration because (a) it was located at the end of the trapping region (where the trappable load was very small), and (b) it collected some relatively large iron crystals.

C. HEAT EXCHANGER MATERIALS - FABRICATION DEVELOPMENT

1. Boiler Materials Fabrication Development (Task D.1)

a. 9Cr-1Mo Weld Evaluation (Task D.1.a)

The object of this task is to establish the gross weld efficiency of 9Cr-1Mo alloy steel by short-time tensile and creep-rupture tests at the maximum boiler operating temperature, 1325°F.

Material for test specimens (in accordance with FED-STD-151a, Method 211.1, Type F-2) were out from the as-received 1/8-in.-thick 9Cr-1Mo alloy sheet. The material was purchased, inspected, and found to conform to Aerojet Specification AGC-10197.

One section of the sheet was machined into 20 base-material test specimens for short-time tensile-strength and creep tests. A second section was machined into six panels for specimen preparation. The weld edges were prepared for a 90° V groove with a 1/32-in. land. The base material test specimens and the weld panels were heat treated in argon by normalizing at 1700 ±25°F for 45 min, and air cooling. The panels were then welded in accordance with Specification AGC 10227. A preheat temperature of 400°F was used. A full penetration filter root pass was first made, followed by subsequent filler passes to build up a full bead. The welded assemblies were allowed to cool slowly on the fixture to room temperature. The welded assemblies were placed in a holding furnace at 400°F over a weekend since it was not possible to stress relieve within 12 hours after welding. The base material test specimens and the welded panels were stress relieved in argon at 1350 ±25°F for 1 hour and cooled to room temperature.

The welds were inspected by X-ray and dye penetrant methods. They conformed to class 15 of AGC 13860. Fourteen test specimens were machined from the welded panels.

AGN, San Ramon, was contacted to perform the creep tests on available Arcweld creep frames.

b. 9Cr-1Mo Environmental Cyclic Creep Evaluation (Task D.1.b)

The purpose of this program is to determine the creep properties of 9Cr-1Mo alloy exposed to NaK under temperature, time, and stress conditions that simulate those of the SNAP-8 system.

Requests for quotation were sent to nine establishments for cyclic creep tests to be performed in NaK. Two proposals have been received to date.

c. 9Cr-1Mo/316 Transition Joint Development (Task D.1.e)

The object of this task is to evaluate welded transition joints connecting 9Cr-1Mo alloy steel and 316 SS. Such a joint is required at the mercury-superheated-vapor manifold of the boiler. It must withstand extended service at up to 1325°F.

Four test capsules containing a transition joint were fabricated. The edges to be welded were prepared for a 90° V groove with a 1/32-in. land (Figure 128 shows a welded capsule). The welds were made in accordance with Specification AGC 10227. Dye penetrant and X-ray inspection was performed. Class 15 of radiographic standard specification AGC 13860 was met. The welds were stress relieved at 1350 ±25°F in argon for one hour and air cooled. One as-prepared capsule was sectioned for metallographic examination and bend tests.

Two capsules were roll-formed at 1700°F to a wall reduction of 25% to break up the weld microstructure. They were subsequently heat treated by normalizing in argon at 1700 ±10°F for one hour and tempered at 1500 ±25°F for 30 minutes. The tempering temperature was selected to achieve full-grain refinement of the hot-worked weld structure. The two capsules were

X-rayed. One capsule showed shear cracks in the heat affected zone of the weld. The other capsule conformed to Class 15 of AGC 13860.

d. Refractory Bimetal Tube Material Development (Task D.1.f)

The object of this task is to establish the availability of refractory bimetal tubing. If direct-bonded tubing (refractory to 316 SS) cannot be fabricated or proves to be unusable because of elevated temperature diffusion effects, a source is to be developed for refractory-bimetal tubing fabricated using interface materials between the refractory and the 316 SS.

The evaluation of three prototype refractory bimetal tubes furnished by Nuclear Metals, Incorporated, was completed. No bond defects were found in a pure columbium/316 SS tube before or after coiling to an 8 in. dia. Two tubes of columbium-1% zirconium/316 SS were found to contain gross unbonded areas in the as-received condition and to be completely unbonded in the outer fiber after coiling. The inspection methods employed were metallography and ultrasound.

2. Condenser Fabrication Development (Task D.2)

a. Tube-to-Tube Sheet Back Brazing Development (Task D.2.a)

The object of this task is to select a satisfactory alloy and develop an adequate procedure for back-brazing the 73-tapered-tube -1 SNAP-8 condenser.

(1) Braze Alloy Selection

Lap shear specimens of the 9Cr-1Mo alloy, which were brazed with GE braze alloys J8100 and J8400 during a previous report period (Reference 5), were tested. The results are listed on the following page.

Braze Alloy	Gap Width in.	Brazed Area sq in.	Ultimate Load, lb	Ultimate Load/ Brazed Area, psi
J8100	Surface contact	0.0930	1,300	13,970
J8100	0.003	0.1010	1,440	14,250
J8100	0.006	0.1050	1,645	15,660
J8400	Surface contact	0.0940	2,170	23,080
J8400	0.001	0.1033	2,180	21,100
J8400	0.006	0.1050	2,360	22,470
J8400	0.010	0.1053	2,310	21,930

A comparative evaluation of these braze alloys and another braze alloy, AMS-4778, was completed. Tests of the latter alloy were completed during a previous report period (Reference 5). As a result of this evaluation, AMS-4778 alloy (Nicrobraz 130-3.5%B, 4.5%Si, 0.20% Max. C, bal. Ni) was selected for use as the reference brazing alloy. The selection was based on the lower melting point of this alloy when compared to the J8100 and J8400 alloy and its ability to wet and flow as adequately as the J8100 alloy and better than the J8400 alloy and its compatibility with NaK. The following tabulation compares the properties of these alloys:

	J8400	J8100	AMS-4778
Liquidus, ^{o}F	2100	2075	1875
Solidus, ^{o}F	2025	1975	1800
Recommended Brazing Temperature Range, ^{o}F	2150 to 2200	2125 to 2175	1875 to 1950
Flow on 9Cr-1Mo	Poor	Good	Good

(2) Brazing of Tube-to-Tube Sheet Simulated Joints

A 3-in.-long, thirteen-tube sample simulating the condenser tube assembly configuration (tube-to-tube sheet joint at each end) was

welded and back brazed. A prebrazing cleanup cycle was performed at 1800°F in a -65°F-dewpoint hydrogen atmosphere. The reference braze alloy, AMS-4778, was applied as a slurry composed of powdered alloy and acrylic cement, and as precast washers held in place in one of two ways; either acrylic cement or a braze alloy - acrylic slurry. The brazing operation was accomplished with the configuration in the vertical position. The part was held at 1925°F for five minutes in a -65°F dewpoint hydrogen atmosphere.

Visual examination, after brazing, of both top and bottom brazed joints revealed adequate flow and filling by the braze alloy except where the precast washers were held in place with only the acrylic cement. Washers held in this manner had fallen away from the top joint area and did not produce adequate joints. The sample containing the unsatisfactory joints was rebrazed using a slurry of the braze alloy in acrylic cement. After rebrazing, the joints visually appeared filled and filleted.

The samples were dye-penetrant inspected. The joints contained porosity but no propagating type defects were detected. The samples were subjected to 20 thermal cycles of heating to 800°F (by placing in a furnace at 800°F) followed by air cooling to room temperature, and were again dye-penetrant inspected; no change was indicated by the dye-penetrant test. Subsequent sectioning of the sample revealed that the joints had been filled with braze alloy to the root of the tube-to-tube sheet weld, but that porosity existed in the braze alloy. Erosion-diffusion of the braze alloy had occurred to a depth of 8 mils in the tube wall at the location of braze alloy placement (Figure 129A and B).

(3) Brazing of 37-Tube Simulated Condenser

A 37-tube simulated condenser sample was prepared, using 0.5-in.-OD by 4-in. long tubes. The tube sheets were 0.300-in. thick by 5 in. dia. The tube sheets were trepanned around the tube holes. Automatic welding was used for completing the tube-to-tube sheet joints.

The part was precleaned by heating in a -80°F dewpoint hydrogen atmosphere to 1800°F, holding for 1 hour, cooling to 1400°F, and holding at 1400°F for 5 hours to accomplish elevated temperature isothermal

transformation of the 9Cr-1Mo steel microstructure to ferrite and carbides; furnace cooling to 300°F followed before removal from the furnace. The cleaning operation required 17 hours furnace time. The material exhibited a bright metallic, clean surface appearance. The hardness of the tube sheet was Rockwell C 38, indicating that the isothermal transformation to ferrite and carbides had not been accomplished. Metallographic examination of the tube and the tube sheet material revealed a totally martensitic structure in the tube sheet and about 50% ferrite in the tube (the other 50% was a bainite-type structure). A section of the tube-sheet material was re-heat treated by heating to 1900°F and cooling to and holding at 1300°F for 6 hours, rather than at 1400°F for 5 hours. This treatment resulted in a hardness of Rockwell B 83. The resultant microstructure was a ferrite matrix containing a uniform distribution of carbides, indicating full isothermal transformation had occurred. Dry AMS-4778 braze alloy powder was applied to the joint area of the tube sheets with a hypodermic syringe and held in place by subsequently wetting it with acrylic cement. The sample was placed on a ceramic plate in the furnace in the vertical position. The ceramic plate contained thermocouple wires on the top surface. This made an air gap, the thickness of the shielded-thermocouple wires, that separated the sample from the plate. Brazing was accomplished at 1925°F in a -80°F dewpoint hydrogen atmosphere, followed by furnace cooling to 300°F. The sample was immediately tempered at 1400°F for one hour before removal from the furnace. This cooling cycle, different from the optimum, produced tempered martensitic rather than the ferritic structure resulting from complete isothermal transformation. However, it was judged to be satisfactory for braze evaluation and expedited completion of the sample.

Visual examination of the sample revealed adequate filling and filleting of the joints at the upper end of the sample (flow against gravity) but very poor flow and filleting at the lower end (Figures 130, 131, and 132). It was decided that a contributing factor to the unsatisfactory brazing result at the lower end was the sample support pedestal, which probably was too close to the tube sheet and acted as an excessively large heat sink. The lower tube sheet apparently never reached proper brazing temperature.

A sectioned sample revealed that the upper tube sheet joint had filleted well but that some gaps in the joints existed. Poor filling of the lower gaps was apparent. The sample was rebrazed. The lower joints were improved in appearance, and filleting was complete; however, sectioning revealed that some gaps still existed in the joint area.

Physical distortion of the tubes in this simulated condenser did not occur during the brazing procedure. Initial rough calculations had indicated the maximum temperature differentials of 100°F below 1400°F and 50°F above 1400°F between the inner and the outer tubes of the full-scale condenser 73-tube bundle would be permissible without causing distortion. Average furnace heating rates during brazing of 475°F/hr to 1400°F and 655°F/hr from 1400°F to 1925°F resulted in maximum temperature differentials of 71°F and 30°F respectively. The cooling rate, averaging approximately 300°F/hr from 1900°F to 1350°F, was too rapid to measure temperature differentials with the slow readout time of the instrumentation being used.

(4) Brazing of Experimental Full-Size Condenser Tube Bundle

An experimental full-size condenser tube bundle with 73 tapered tubes was welded for back-brazing evaluation. The assembly was suspended from the large header containing the larger diameter of the tapered tubes during the hydrogen precleaning and the brazing cycles. Thermocouples were inserted into the tubes to measure temperatures of tubes at the center and outer periphery of the tube bundle. As with the previous 37-tube sample, this mockup was precleaned in hydrogen at 1800°F. During the hydrogen cleaning cycle, average heating rates of 900°F/hr from 200°F to 1100°F, 425°F/hr from 1100°F to 1525°F and 275°F/hr from 1525°F to 1800°F resulted in indicated maximum temperature differentials of 60°F below 1300°F and 20°F above 1300°F. Cooling of the assembly was performed at an average rate of 240°F to 1325°F. The part was held at 1325°F for 5 hours to effect isothermal transformation. Proper transformation was effected as evidenced by a hardness measurement of Rockwell B 85. Distortion of the tubes occurred. The outer row of tubes, not supported by the spacer assembly, was warped the most. Some of these tubes were bowed as much as one inch. To

complete the brazing cycle evaluation with this assembly, the tubes were bound in three places along their length to maintain the required alignment as closely as possible. More refined calculations of allowable temperature differentials indicated that a 20°F maximum was necessary to avoid tube distortion. It was also deemed necessary to use a more rapid printing multipoint recorder to obtain more accurate time-temperature data.

Braze alloy was applied to each header as a powder; it was held in place by saturating it with acrylic cement. The assembly was brazed at 1925°F with AMS-4778 alloy, in a hydrogen atmosphere with a -80°F dewpoint. During the cooling cycle, the assembly was isothermally transformed to a ferritic structure by holding at 1325°F for 5 hours. The brazed joints were filled and well-filleted at the end of the tube sheet containing the smaller tapered tube diameter. This end was at the bottom of the suspended assembly during brazing. The tube sheet at the top end, containing the larger tapered tube diameter, exhibited some gaps in the joints where adequate flow and filleting had not occurred. In addition, braze alloy had run down three of the tubes. The hardness of the 9Cr-1Mo steel tube sheets was Rockwell B 85 after brazing, indicating that proper isothermal transformation was achieved.

An attempt was made to straighten the distorted tubes by heating the entire bundle to 1800°F in a -80°F-dewpoint argon atmosphere, while the bundle was dead-weight loaded to produce a stress of 100 psi on each tube wall. This attempt was not successful.

(5) Brazing of -1 Condenser Tube Bundle Assembly

Two full-scale -1 condensers were back-brazed with AMS-4778 alloy. To overcome the problems previously encountered during the brazing of the experimental condenser (distortion and inadequate filling and filleting of the joints), a fixture was fabricated to free-hang the condenser from the small header under a dead load of 100 psi on each tube wall (Figure 133). In addition, a radiation shield was positioned around the tube bundle during hydrogen cleaning and brazing to minimize the temperature differential within the tube bundle (Figure 134).

The hydrogen cleanup cycle of the first -1 condenser resulted in a minor distortion of the tube bundle. Cleaning was not completely adequate. This was attributed to inadequate hydrogen-transfer rates within the radiation shield. A temperature differential maximum of 35°F at 1300°F occurred during the cleanup cycle, and of 25°F at 1360°F during the brazing cycle. Forty-two hours of furnace time were required for the cleanup operation. Increased experience with the furnace operation and with the anticipated temperature differentials permitted the brazing cycle to be completed in 38 hours while maintaining the low temperature differential. The hydrogen cleanup and brazing cycles used to fabricate the first -1 model condenser are described in Table 29.

After the first cleanup cycle was completed, hydrogen distribution within the retort was altered to provide direct flow of part of the hydrogen inside the radiation shield by the insertion of a tube into the base of the inlet line passing to a Y and into the bottom inside of the shield 180° apart. After brazing, the first condenser exhibited areas of poor joint filling, poor filleting, poor wetting, and the appearance of incomplete melting at the outer edge of the braze alloy on the large header end. These difficulties were attributed to an insufficiently low hydrogen dewpoint at the joint areas, caused by inadequate movement of hydrogen inside the radiation shield. The hydrogen transfer rate was increased by partially blocking the main hydrogen inlet tube to force more hydrogen through the Y tube into the shield. The shield was also vented by drilling 1/4-in.-dia holes 3 in. on centers, every 60° around the shield for its full length. Additional braze filler alloy was applied to the areas which exhibited poor wetting and the part was rebrazed. After the second brazing cycle, the joints were adequately filleted, but excess braze alloy was present resulting in running of braze alloy down several of the tubes.

The second -1 condenser was back brazed using the same procedure as that for the first -1 model condenser. Minor bowing of the tubes occurred. A few unfilleted gaps existed at the large header at the bottom and gap filling and filleting were poor at the small header at the top. The assembly was reversed with the large header at the top, a small amount

of additional braze alloy was added, and the assembly was rebrazed at 1950°F. Visually satisfactory brazed joints resulted. Helium leak checking of the units indicated no leakage through the welded and back brazed joints.

b. Refractory Brazing Program (Task D.2.b)

The objective of the task will be to develop techniques of joining refractory bimetal tube-to-tube sheet for boiler application using back brazing procedures. The bimetal alloy system is pure columbium and 316 SS.

Discussions were held among NASA, Pyromet, and Aerojet personnel to redirect this program. The redirected effort will be performed under the limitation of the remaining funds of the existing subcontract. Pyromet is to develop a proposal meeting the new objective of this task. An outline of the work scope is as follows:

(1) Pyromet will develop a refractory bimetal tube-sheet fabricated using the Horton-clad process. The tube sheet shall consist of 40-60 mils of unalloyed columbium clad on 240 mils of 316 SS.

(2) Aerojet-General Corporation will supply pure columbium/316 SS bimetal tubing samples.

(3) Pyromet will perform machining of tube and tube sheet samples.

(4) Aerojet will perform welding of columbium to columbium on samples.

(5) Pyromet will perform brazing development tests on samples.

(6) The specific approach will be outlined by Pyromet and subsequently discussed with, and approved by, the SNAP-8 Materials Department.

(7) Analysis will include (a) microanalysis, (b) microhardness, and (c) possible thermal cycle testing with subsequent micro-analysis.

D. TAA MATERIALS EVALUATION (TURBINE ROTOR AND NOZZLE MATERIAL EVALUATION (TASK E.1)

The objective of this task is to evaluate the resistance of candidate turbine blade and nozzle materials to erosion by elevated temperature wet mercury vapor. Material samples were exposed to accelerated erosion testing in the SNAP-8 Low Power Loop to provide a basis for the recommendation of a material for use in the SNAP-8 Turbine Assembly.

The program for the evaluation of the erosion resistance of candidate turbine rotor and nozzle materials was completed. A full description of the test procedure is included in Reference 5. During the current report period, eleven additional materials samples were exposed to the accelerated erosion environment in the Low Power Loop. The samples were exposed to 85%-quality mercury vapor flowing at a velocity of 1000 ft/sec. A total of 21 samples, comprising 11 different materials, were exposed during the full test program. Tables 30, 31, and 32 and Figure 135 carry a description of the materials evaluated and the test results.

The results indicated that the cobalt-base alloy, Stellite 6B, provided the greatest resistance to wet mercury vapor erosion and was recommended as the material to be used for -3 SNAP-8 turbine rotors and nozzles.

Preparation of a technical memorandum covering all details of the test program was started.

NOMENCLATURE

Symbol	Definition	Units
a_o	Frontal area of the wires in the screen	sq in.
A_o	Flow area in the trap vessel	sq in.
C	Correction factor defined by Equation 4	-
D_c	Screen wire diameter	in.
Deq	Equivalent diameter of the wire screens	in.
D_p	Droplet diameter	in.
f	Fanning friction factor	-
F	Fraction of the droplets removed by the trap	-
G_{av}	Average mass flow rate in the screens	lb/hr-sq in.
K	Constant in Equation E-1	ft/sec
L	Mean free path of Hg	in.
N	Number of layers of screen	-
N_m	Number of molecules per unit volume	molecules/cu in.
p'	Average void in the screen	-
ΔP_{dry}	Pressure drop of the Hg vapor under dry screen conditions	psi
Re	Reynold's number	-
T	Temperature	^oF
V_o	Allowable upstream gas velocity	ft/sec
W	Flow rate	lb/hr
Ψ	Correlation factor target efficiency defined by Equation E-3	-
η_i	Interception target efficiency	-
η_{im}	Impact target efficiency	-

NOMENCLATURE (cont.)

Symbol	Definition	Units
μ	Hg vapor viscosity	lb/in.-sec
ρ_L	Hg liquid density	lb/cu in.
ρ_v	Hg vapor density	lb/cu in.
σ	Molecular diameter of Hg	in.
η_T	Overall target efficiency	-

REFERENCES

1. SNAP-8 Electrical Generating System Development Program, Aerojet-General Corporation, Quarterly Report No. 0390-04-14, December, 1963.

2. E. F. Perez and W. W. Tingle, Investigations of the SNAP-8 Lube and Coolant Loop, Aerojet-General Corporation, Technical Memorandum No. TM 340:64-1-209, 20 Feb. 1964.

3. E. B. Bridges, SNAP-8 Mercury Pump Motor Assembly Thermal Analysis, Aerojet-General Corporation, Technical Memorandum No. TM 395:64-1-208, 20 February 1964.

4. R. A. Mendelson, Evaluation of Koldwelded Butt Joint Transition Piece, Aerojet-General Corporation, Technical Memorandum No. TM 390:64-4-183, 21 January 1964.

5. SNAP-8 Electrical Generating System Development Program, Aerojet-General Corporation, Quarterly Report No. 0390-04-13, October 1963.

6. Design Report on Dynamic Corrosion Loops for the SNAP-8 System, Aerojet-General Corporation, Report No. 2596, June 1963.

7. W. E. Ranz, and J. G. Wong, "Impaction of Dust and Smoke Particles on Surfaces and Body Collectors," Ind. and Engr. Chem., 44, p. 1379 (June 1952).

8. R. H. Perry, et al., Chemical Engineers' Handbook, 4th ed., New York, McGraw-Hill, 1963.

9. W. M. Kays, and A. L. London, Compact Heat Exchangers, New York, McGraw-Hill, p. 121, 1958.

10. W. R. Gambill, et al., Heat Transfer, Burnout, and Pressure Drop for Water in Swirl Flow Through Tubes with Internal Twist Tapes, ORNL-2911, 11 April 1960.

TABLE 1

ANTICIPATED MAXIMUM TRANSIENTS OF SYSTEM PARAMETERS

Parameter	Maximum Rate of Change
Temperatures	
Reactor Inlet Nak	5.0°F/sec
Reactor Outlet Nak	5.0
Boiler Inlet Nak	1.0
Preheater Inlet Nak	1.4
Auxiliary Heat Exchanger Inlet NaK	1.8
Parasitic Load Resister Inlet NaK	4.0
Condenser Inlet Hg	9.9
Boiler Inlet Hg	6.2
Superheater Inlet Hg	6.5
Turbine Inlet Hg	2.9
Radiator Inlet NaK	7.5
Radiator Outlet NaK	5.0
Subcooler Inlet NaK	5.0
Condenser Outlet NaK	11.1
Auxiliary Heat Exchanger Outlet NaK	6.6
L/C Radiator Inlet L/C	3.0
L/C Radiator Outlet L/C	2.0
TAA Outlet L/C	4.0
Hg PMA Bearing Outlet L/C	4.0°F/sec
Flow Rates	
Primary Loop NaK	0.36 lb/sec^2
Hg Loop	1.6
HRL NaK	0.3
L/C Loop	0.2 lb/sec^2
Turbine Speed	24 rev/sec^2
Pressures	2 psi/sec

TABLE 2

CURRENT SCHEDULE - PCS-2/SL-2

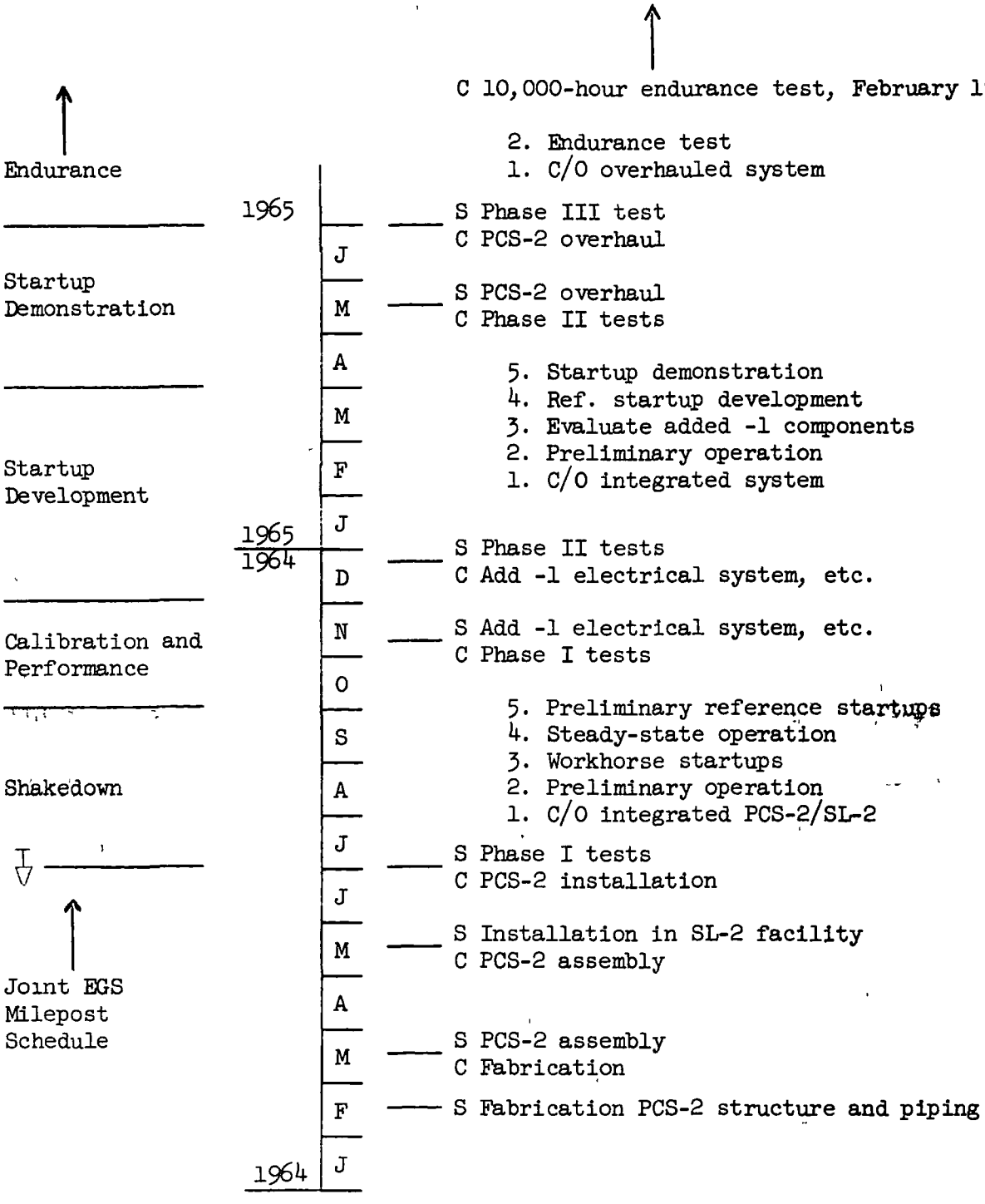

Table 2

TABLE 3

LUBRICATION RIG NO. 1 - BUILDUP SUMMARY

Buildup No.	Test Bearing	Test Slinger	Assembly	Test Run No.	Data Status	Remarks
1	Barden 207HJB[a]	One-vane type (inlet only)	Six 0 028-in. dia jets, plastic front housing	D-1-B-1[d] through D-1B-5	Issued raw and preliminary	·First test series ·Useful data at atmospheric pressure ·Rig and loop leakage problems
2	Barden 207HJB[a]	Two-vane type (inlet and exit)	Three 0.040-in. dia jets, metal front housing with quartz window	None	None	·Drive motor burn-out on first check-out run
3	Barden 207HJB[a]	Two-vane type (inlet and exit)	Same assembly as B/U No. 2, new drive motor	D-1-B-1[b] through D-1-B-7	Issued final	·Second test series ·Insufficient flow via inlet slinger ·Motor bearing failed on last run
4	MRC 207SJ-1[b]	Two vaneless (inlet and exit)	Replaced drive motor bearing	None	None	·Motor bearing failure, unit returned for repairs
5	MRC 207SJ-1[b]	Two vaneless (inlet and exit)	Installed new drive motor	D-1-B-8 through D-1-B-14	Issued final	·Most significant test data ·Inaccurate measurement of slinger exit flow
6	Barden 207BX1[c]	Two vaneless (inlet and exit)	Added Brg. cavity vent tube and new flow meter	None	None	·Updated unit and instrumentation ·Testing postponed indefinitely

[a] Low shoulder on outer race, light cage.

[b] Low shoulder on inner race, heavy cage.

[c] Low shoulder on inner race, light cage.

[d] Numbering system repeated in second test series.

TABLE 4

SUMMARY OF THE SNAP-8 BALL BEARING TEST PROGRAMS

	Program Description	Objectives	Expected Results
I	Endurance Ball Bearing Test Program as function of M-50 bearing material 1 2nd remelt and mineral oil 2 5th remelt and mineral oil 3 2nd remelt and ET-378 4 5th remelt and ET-378	Find endurance life of M-20 2nd and 5th remelt material	Increase bearing life on order of 1.5 to 3.0 times.
II	Endurance and Wear Ball Bearing Test Program as function of bearing material fiber 1 Solid and hollow controlled fiber balls and mineral oil 2 Solid and hollow controlled fiber balls and ET-378 3. R ce controlled fiber and mineral oil 4 Race controlled fiber and ET-378 5 Cage controlled fiber and mineral oil 6. Cage controlled fiber and ET-378	(a) Find endurance life of controlled fiber bearing material (b) Control infant mortality of bearing failures (c) Find wear life of bearing cage	(a) Increase bearing life on order of 1.2 to 2.0 times (b) Practically eliminate early bearing failures.
III	Endurance and Wear Ball Bearing Test Program as function of vacuum and radiation A. Rolling Contact Fatigue Tests (Four ball) (1) Room temperature, air and mineral oil (2) 210°F, air and ET-378 (3) 210°F, degassed ET-378 and vacuum (4) 210°F, degassed ET-378 vacuum and radiation B Sliding Wear Tests (1) Room temperature, air and mineral oil (2) 210°F, air and ET-378 (3) 210°F, degassed ET-378 and vacuum (4) 210°F, degassed ET-378 vacuum and radiation C. Full-Scale Bearing Tests (1) 210°F, degassed ET-378 vacuum and radiation	(a) Find effect of vacuum and radiation on lubrication and on bearing life	(a) Find decrease in endurance bearing life, order of magnitude unknown (b) Find decrease in wear bearing life; order of magnitude unknown
IV	Analytical support of the above test programs	(a) Predict results (b) Optimize tests (c) Optimize number of tests	Optimize programs.

TABLE 5

MODEL A SEAL SIMULATOR LEAKAGE RATES

Duration of Measurement, hours	Mercury Leakage, lb/10^4 hours	Recirculating Mercury Inlet Temperature, ^oF	Oil Leakage, lb/10^4 hours	Bearing Outer Race Temperature ^oF
1	14.9	200	1.8	300
2-1/3	34	250	0.9	315
1	30.4	335	-	-
1	46.7	350	12.6	310
2/3	19.6	210	-	-
2	16.3	250	2.6	320
2	2.9	245	2.9	310

TABLE 6

NaK PMA BEARING TEST SUMMARY - 99 HOURS AT 600°F

Materials			Loads (lb)			Damage		
Socket	Ball	Race	Initial	Final	Simulating	Sliding	Fretting	Description
M-2	T-1	M-2	50	11	Journal Pad Pivot	Yes*	Yes	Welding and Plowing Surface Oxidation
M-2	T-1	M-2	50	13	Journal Pad Pivot	No	Yes	Surface Oxidation
WC44A	WC44A	WC44A	25	7	Thrust Pad Pivot	Yes	Some	Surface Oxidation
WC44A	WC44A	WC44A	25	9	Thrust Pad Pivot	No	Some	Surface Oxidation
T1	WC44A	T1	50	16	No. 2 Thrust Gimble Rate	Yes	--	Metal transfer, Surface Oxidation
WC44A	WC44A	T1	50	12	No. 1 Thrust Gimble Rate	Yes	--	Metal Transfer

*Sliding in this test producing welding and plowing was rig-induced, and has been discounted.

TABLE 7

SUMMARY OF HEAT REJECTION LOOP LOSSES

System Component		Calculated Losses 1.6 gpm NaK at 350°F Thick Walled (psi)	Thin Walled (psi)
Filter		1.24	0.66
Cold Trap		1.56	0.66
Economizer		5.09	2.60
	Subtotals	7.89	3.92
Motor Housing Entrance		0.75	0.75
Motor Air Gap		3.80	3.80
Flow Meter		2.00	2.00
Valve (Full open)		0.24	0.24
System Piping		0.48	0.48
	Totals	15.16 psi	11.19 psi

TABLE 8

SNAP-8 -1 BOILER

STRESS ANALYSIS SCHEDULE

No.	Major Stress Areas (See Figure 84)	Reference Document - Stress Analysis		
		Steady State	Transient*	Environmental*
1	Maximum heat flux zone 9 Cr-1 Mo	*OK	(Note 5) OK 1/15/64	OK/Inspection
2	Tube butt weld 9 Cr-1 Mo	*OK	OK/Inspection	OK/Inspection
3	Outer shell - 316 SS	(Note 1) OK	OK/Inspection	OK/Inspection
4	Tube bend - 9 Cr-1 Mo	*OK Preliminary analysis by SNAP-8 Stress Group	OK/Inspection	OK/Inspection
5	Inner shell - 316 SS	(Note 1) OK	OK/Inspection	OK/Inspection
6	Torus to shell connection 316 SS	(Note 1) OK	OK/Inspection	OK/Inspection
7	316 SS to 9 Cr-1 Mo transition weld	OK	OK/Inspection	**OK
8				
9	Mercury outlet - 316 SS	(Note 2) OK	OK/Inspection	OK/Inspection
10	Tube-to-tube sheet connection (outlet) 9 Cr-1 Mo	OK	OK/Inspection	OK/Inspection
11	Mercury inlet - 9 Cr-1 Mo	(Note 3) OK	OK/Inspection	OK/Inspection
12	Mounting ring assembly - 316 SS	(Note 4) OK	OK/Inspection	**OK

*Now being reviewed and completed by SNAP-8 Stress Group (estimated completion, 2 to 4 weeks).
**Preliminary analysis by E. M. Corbin indicates safe stresses. Final analysis now being conducted by H. D. Tabakman.
Note 1: Memorandum dated 10/4/63, subject: Structural Analysis of the SNAP-8 Boiler -1 Pressure Vessel
Note 2: Memorandum dated 11/12/63, subject: Structural Analysis of the Mercury Outlet of the SNAP-8, -1 Boiler
Note 3: Memorandum dated 2/6/64, subject: Structural Analysis of Boiler Mercury Inlet Housing, No. 092, 703 and 092, 708
Note 4: Memorandum dated 10/16/63, subject: Structural Analysis of the SNAP-8 Mounting Ring Assembly
Note 5: Memorandum dated 1/15/64, subject: Transient Stress Values in the Boiler Tubes

TABLE 9

SNAP-8 -1 CONDENSER STRESS TABULATION

Identification		Documentation or Disposition		
Location (Reference Figure 88)	Part Name	Steady State	Thermal Transient	Environmental Conditions
1.	Mercury exit plenum	350:0156		OK (by inspection)
2.	Transition	350:0156		OK (by inspection)
3.	Tube sheet	350:0161		OK (by inspection)
4.	NaK shell	350:0157		350:0160, 350:0158
5.	Mercury tubes	OK (by inspection)		350:0160, 350:0159
6.	Mercury tubes	OK (by inspection)		350:0160, 350:0159
7.	Mercury tubes	OK (by inspection)		350:0160, 350:0159
8.	NaK shell	350:0157		OK (by inspection)
9.	NaK shell	In process		In process
10.	NaK outlet	In process		In process

OK (by inspection)

TABLE 10

INSULATION RESISTANCE, INORGANIC INSULATED MOTOR

Hours of Aging at 450°F	Winding Temperature, °F	Insulation Resistance* Winding to Ground ohms
504	434	1.2×10^7
504	380	1.9×10^7
504	71	1.5×10^{10}
1344	430	1.4×10^6
↓	290	5.0×10^8
↓	265	9.0×10^8
↓	240	1.9×10^9
↓	220	2.8×10^9
↓	195	4.0×10^9
↓	175	5.3×10^9
1344	165	6.1×10^9
2268	445	7.0×10^6
2268	295	4.0×10^8
↓	215	4.6×10^9
↓	160	1.5×10^{10}
↓	135	2.2×10^{10}
2268	120	2.6×10^{10}
3324	440	7.0×10^6
↓	305	2.1×10^8
↓	205	1.4×10^9
↓	172	2.3×10^9
3324	125	5.3×10^9

*Measured with General Radio 544B megohm bridge, 500v, dc; 1-min reading.

TABLE 11

ORGANIC RESIN WEIGHT LOSS - 168 HOURS AT 392°F in Air

	Material	Type	% Change*
1.	3M Scotchcast 292	Epoxy Impregnant	6.97
2.	3M Scotchcast 241	Epoxy Encapsulant	3.26
3.	3M Scotchcast 235	↓	6.60
4.	Epoxylite 813-9	↓	0.96
5.	Epoxylite 8793	↓	0.45
6.	Epoxylite 8794	↓	0.61
7.	Epoxylite 2154	↓	3.41
8.	Furane Epocast 17-B	Epoxy Encapsulant	0.94
9.	Furane Epocast 17-A	Epoxy Impregnant	0.31
10.	Furane Epocast 3	Epoxy Impregnant	0.69
11.	Hysol 7-4252	Epoxy Encapsulant	2.70
12.	GE Novalak Epoxy	Epoxy Encapsulant	0.30
13.	GE Bisphenyl A Epoxy	Epoxy Encapsulant	0.57
14.	Dow Corning Sylgard 182	Silicone Elastomer Encapsulant	2.01
15.	Dow Corning Sylgard 183	Silicone Elastomer Encapsulant	1.60
16.	Dow Corning Sylgard 7521	Silicone Impregnating Resin	3.79

*All percentages are referred to the organic base.

TABLE 12

STATORETTE INSULATION SYSTEMS*

Unit	Slot Liners and Phase Insulation	Varnish
HML-1 and HML-2	Pyre-ML polyimide-coated glass fabric, Du Pont Quality Code 6508	Pyre-ML polyimide varnish, Du Pont Type RK-692
ML/997-1 and ML/997-2	Macallen 806P mica paper composite	Dow Corning 997 silicone varnish
ML-3 and ML-5	Pyre-ML polyimide-coated glass fabric, Du Pont Quality Code 6508	Pyre-ML polyimide varnish, Du Pont Type RK-692
ML-4 and ML-6	Pyre-ML-coated glass fabric, Type 6508	Westinghouse Doryl Type B-109-4 (diphenyl oxide)

*Throughout, magnet-wire is Anaconda heavy ML polyimide film over copper.

TABLE 13

INSULATION RESISTANCE, STATORETTE HML-1*

Hours of Aging	D-C Insulation Resistance** Winding to Ground (at 392°F), ohms
240	3.0×10^9
480	2.8
792	3.3
1152	3.4
1508	5.0
1751	5.3
1991	5.8
2231	6.4
2687	6.6
3137	7.7
3461	6.5
3629	6.4
3965	7.7
4133	8.6
4301	8.6
4517	8.6
4661	8.6
5069	7.0
5285	8.8
5466	6.73
5562	6.7
5852	7.75
6023	7.0
6167	6.8
6983	6.5
7487	6.5
8085	8.0
8253	8.0×10^9
9307	1.0×10^{10}
9709	8.9×10^9

*Insulation system: magnet wire - heavy ML over copper; slot liners and phase insulation - ML-coated glass-fiber cloth; varnish - ML. Statorette immersed in OS-124 fluid; system held at 392°F.

**Measured with General Radio 544B megohm bridge; 500v, dc; 1-min reading. Values given are averages of readings for three coil groups.

TABLE 14

INSULATION RESISTANCE, STATORETTE HML-2*

Hours of Aging	D-C Insulation Resistance** Winding to Ground (at 392°F), ohms
240	5.0×10^{11}
480	
792	
1152	
1508	
1751	
1991	
2231	
2687	
3137	
3461	
3629	
3965	
4133	
4301	
4517	
4661	
5069	5.0×10^{11}
5285	1.25×10^{11}
5466	∞
5562	7.0×10^{9}
5852	4.9×10^{10}
6023	∞
6167	
6983	
7487	
8085	
8253	
9307	∞
9709	6.7×10^{11}

*Insulation system: magnet wire - heavy ML over copper; slot liners and phase insulation - ML-coated glass-fiber cloth; varnish - ML. Statorette aged in air at 392°F.

**Measured with General Radio 544B megohm bridge; 500v, dc; 1-min reading. Values given are averages of readings for three coil groups.

TABLE 15

INSULATION RESISTANCE, STATORETTE ML/997-1*

Hours of Aging	D-C Insulation Resistance** Winding to Ground (at 392°F), ohms
408	5.0×10^{11}
648	
816	
1056	
1320	
1608	
1800	
2020	
2279	
2423	
2687	
2879	
3089	
3353	
3645	
3813	
4149	
4317	
4485	
4701	
4845	
5253	5.0×10^{11}
5469	1.25×10^{11}
5673	5.1×10^{9}

*Insulation system: magnet wire - heavy ML over copper; slot liners and phase insulation - mica-paper composite; varnish - Dow Corning 997. Statorette aged at 392°F in air.

**Measured with General Radio 544B megohm bridge; 500v, dc; 1-min reading. Values given are averages of readings for three coil groups.

TABLE 15 (cont.)

Hours of Aging	D-C Insulation Resistance Winding to Ground (at 392°F), ohms
5724	∞
5841	↓
6159	↓
6206	↓
6350	↓
7166	↓
7670	↓
8268	↓
8436	∞
9490	5.0×10^{11}
9892	5.8×10^{11}

TABLE 16

INSULATION RESISTANCE, STATORETTE ML/997-2*

Hours of Aging	D-C Insulation Resistance** Winding to Ground (at 392°F), ohms
576	5.6×10^9
648	5.6
1056	5.9
1320	6.8
1608	8.1
1800	9.1
2020	9.5
2279	7.7×10^9
2423	1.05×10^{10}
2687	1.23
2879	1.21
3089	1.4
3353	1.73
3645	1.23
3813	1.23
4149	1.73
4317	1.7
4485	1.7
4701	1.8
4845	1.8
5253	1.9
5469	2.1
5673	1.3×10^{10}

*Insulation system: magnet wire - heavy ML over copper; slot liners and phase insulation - mica-paper composite; varnish - Dow Corning 997. Statorette immersed in OS-124 fluid; system held at 392°F.

**Measured with General Radio 544B megohm bridge; 500v, dc; 1-min reading. Values given are averages of readings for three coil groups.

TABLE 16 (cont.)

Hours of Aging	D-C Insulation Resistance Winding to Ground (at 392°F), ohms
5724	2.17×10^{9}
5841	2.9
6159	8.0
6206	8.2
6350	7.78
7166	7.6
7670	8.3×10^{9}
8268	1.1×10^{10}
8436	1.1
9490	1.2
9892	1.2×10^{10}

TABLE 17

INSULATION RESISTANCE, STATORETTE ML-3*

Hours of Aging	D-C Insulation Resistance** Winding to Ground (at 392°F), ohms
45	6.6×10^{7}
137	1.27×10^{8}
213	1.72
305	2.2
499	2.13
623	2.0
814	8.4×10^{8}
1630	5.3×10^{9}
2134	9.1×10^{9}
2732	9.0×10^{10}
2900	9.3×10^{11}
3954	3.5×10^{11}
4356	3.7×10^{11}

*Insulation system: magnet wire - heavy ML over copper; slot liners and phase insulation - ML-coated glass-fiber cloth; varnish - ML. Statorette immersed in ET-378 fluid; system held at 392°F.

**Measured with General Radio 544B megohm bridge; 500v, dc; 1-min reading. Values given are averages of readings for three coil groups.

TABLE 18

INSULATION RESISTANCE, STATORETTE ML-4*

Hours of Aging	D-C Insulation Resistance** Winding to Ground (at 392°F), ohms
45	4.4×10^{7}
137	1.0×10^{8}
213	1.2×10^{8}
305	1.3×10^{8}
499	1.37×10^{8}
623	1.18×10^{8}
814	1.28×10^{8}
1630	1.3×10^{8}
2134	1.7×10^{8}
2732	3.4×10^{8}
2900	5.7×10^{8}
3954	2.0×10^{9}
4356	1.7×10^{10}

*Insulation system: magnet wire - heavy ML over copper; slot liners and phase insulation - ML-coated glass-fiber cloth; varnish - Westinghouse Doryl. Statorette immersed in ET-378 fluid; system held at 392°F.

**Measured with General Radio 544B megohm bridge; 500 vdc; 1-min reading. Values given are averages of readings for three coil groups.

TABLE 19

INSULATION RESISTANCE, STATORETTE ML-5*

Hours of Aging	D-C Insulation Resistance** Winding to Ground (at 392°F), ohms
45	∞
137	
213	
305	
499	
623	
814	
1630	
2134	
2732	
2900	
3954	∞
4356	7.0×10^{11}

*Insulation system: magnet wire - heavy ML over copper; slot liners and phase insulation - ML-coated glass-fiber cloth; varnish - ML. Statorette aged in air at 392°F.

**Measured with General Radio 544B megohm bridge; 500 vdc; 1-min reading. Values given are averages of readings for three coil groups.

TABLE 20

INSULATION RESISTANCE, STATORETTE ML-6*

Hours of Aging	D-C Insulation Resistance** Winding to Ground (at 392°F), ohms
45	1.69×10^{10}
137	5.25×10^{10}
213	1.19×10^{11}
305	5.32×10^{11}
499	8.0×10^{10}
623	1.75×10^{11} to 1.0×10^{12}
814	3.5×10^{11} to 1.0×10^{12}
1630	6.5×10^{11}
2134	6.5×10^{11}
2732	∞
2900	∞
3954	5.0×10^{11}
4356	8.7×10^{11}

*Insulation system: magnet wire - heavy ML over copper; slot liners and phase insulation - ML-coated glass-fiber cloth; varnish - Westinghouse Doryl. Statorette aged in air at 392°F.

**Measured with General Radio 544B megohm bridge; 500 vdc; 1-min reading. Values given are average of readings for two coil groups.

TABLE 21

TRANSDUCER PRESSURE AND TEMPERATURE DATA FROM RUN 11

Time From Start of Test hours	Horizontal Leg: Transducer Number	Temperature at Thermocouple Location, °F: A	B	C	Corrected Pressure psia	Vertical Leg: Transducer Number	Temperature at Thermocouple Location, °F: A	B	C	Corrected Pressure psia
	A_1					B_1				
0	Boiler Outlet	100	100	230	18	Boiler Outlet	110	110	340	17
1	↓	185	210	575	137	↓	180	285	390	140
3		205	225	560	170		*No Reading*			160
23		200	230	540	275		-	230	-	275
28	↓	200	230	540	295	↓	-	252	-	308
36	Boiler Outlet	205	240	540	335	Boiler Outlet	-	245	-	335
	A_2					B_2				
0	Nozzle Outlet	100	110	240	25	Nozzle Outlet	100	115	150	20
1	↓	195	210	545	47	↓	180	280	380	45
3		215	215	550	47		180	285	390	47
23		230	240	670	55		210	290	440	55
28	↓	250	240	700	55	↓	222	298	458	55
36	Nozzle Outlet	255	270	650	55	Nozzle Outlet	210	270	430	56
	A_4									
0	Separator Inlet	100	120	220	20					
1	↓	180	210	575	145					
3		200	225	550	275					
23		205	230	560	295					
28	↓	205	230	565	305					
36	Separator Inlet	205	235	560	355					
	A_5									
0	Boiler Inlet	100	110	340	51					
1	↓	120	135	470	190					
3		130	140	475	220					
23		130	160	485	330					
28	↓	135	165	490	390					
36	Boiler Inlet	140	170	495	410					

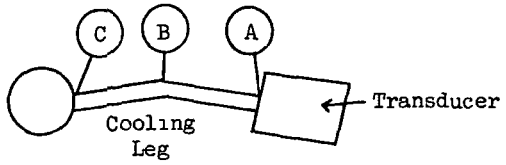

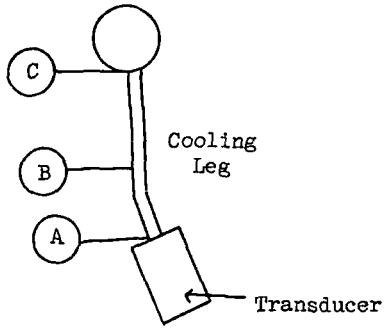

TABLE 22

TEMPERATURE DATA FROM RUNS 10 AND 11

Duration hours	Flow Rate lb/hour	Boiler Inlet Pressure psig	Boiler Outlet Pressure psig	Boiler Coil 2/3 Down Temp, °F	Boiler Outlet Temp, °F	Nozzle Inlet Temp, °F	Separator Inlet Temp, °F	Separator Outlet Temp, °F	Separator Collection Pot Inlet Temp, °F	Separator Collection Pot Bottom Temp, °F
				Run 10 (Without Separator)						
0 - 40	During this period, adjustments to flow temperature and adjustable nozzles were made. The last 11 hours of this run were used to compare boiler outlet pressure increase vs time.									
41	1000	330	270	1140	1210	1130	-	-	-	-
45	1000	350	275	1140	1210	1135	-	-	-	-
47	1000	360	280	1140	1210	1135	-	-	-	-
50	1000	370	300	1140	1210	1135	-	-	-	-
51	1000	375	305	1140	1210	1135	-	-	-	-
				Run 11 (With Separator)						
0										
1	1200	68	40	460	520	190	500	400	170	100
3	1100	190	125	670	795	290	690	640	415	205
6	1000	230	135	830	970	660	850	720	590	395
10	1000	260	175	1080	1160	940	1055	930	615	445
14	1000	275	200	1090	1168	1050	1090	1030	900	750
18	1000	295	225	1085	1170	1100	1090	1080	1080	1010
24	1000	330	265	1095	1190	1130	1090	1080	1250	1200
26	1000	360	270	1095	1190	1140	1100	1080	1240	1250
27	1000	360	270	1095	1195	1150	1100	1085	1230	1260
28	1000	360	270	1095	1195	1145	1140	1100	1210	1240
29	1000	360	275	1095	1190	1140	1130	1100	1200	1230
30	1000	355	280	1095	1190	1160	1130	1100	1180	1195
31	1000	370	285	1080	1185	1150	1120	1095	1170	1190
32	1000	370	300	1080	1190	1150	1110	1095	1160	1190
37	1000	380	325	1080	1185	1140	1090	1080	1160	1185

TABLE 23

HOT-START DATA

Duration hours	Flow Rate lb/hour	Boiler Inlet Pressure psig	Boiler Outlet Pressure psig	Boiler Coil 2/3 Down Temp, °F	Boiler Outlet Temp, °F	Nozzle Inlet Temp, °F	Preheater Temp, °F		Chempump Temp, °F	
							In	Out	In	Out
0	1200	270	190	1200	1250	1100	500	800	200	385
1	900	250	200	1150	1200	1090	530	820	200	390
2	900	275	260	1220	1290	1240	530	830	210	390
3	1000	310	250	1180	1270	1200	540	830	210	390
4	1000	330	270	1200	1250	1210	540	820	210	390
5	1100	340	275	1200	1250	1200	540	820	210	390
6	1100	345	280	1200	1250	1210	540	820	210	390
7	1000	350	285	1200	1240	1200	540	820	210	390
8	1000	350	290	1200	1240	1200	540	820	210	390
9	1000	350	300	1200	1240	1210	540	820	210	390
9.5	1000	350	300	1200	1240	1210	540	820	210	390

TABLE 24

WEIGHTS AND SEMIQUANTITATIVE SPECTROGRAPHIC ANALYSES OF DEPOSITS AND RESIDUES FROM THERMAL CONVECTION LOOP 1

	Analysis, Wt%*				
	Deposits from Walls of Loop			Mercury Residues	
Element	Boiler Liquid-Vapor Interface (0.0176 g)	Superheater (0.0262 g)	Cold Leg (0.0546 g)	Magnetic Fraction (0.1059 g)	Nonmagnetic Fraction (0.0618 g**)
Fe	18	70	105	70	1
Si	0.27	2	1	0.1	0.1
Mg	0.007	0.04	0.04	0.006	0.002
Pb	-	-	0.02	0.02	-
Sn	-	0.008	0.003	-	-
Cr	1.3	4	0.10	0.9	1
Mn	0.1	0.8	0.2	0.1	0.04
Al	0.003	0.12	0.1	0.02	0.01
Ni	0.35	0.6	0.2	2	31
Mo	0.01	2	1	0.2	0.02
Cu	0.02	0.1	0.06	0.1	0.2
Zn	-	0.4	0.2	-	-
Ti	-	0.012	0.006	0.006	-
Ag	0.01	0.008	0.003	-	14
Co	-	0.014	0.005	0.01	0.03

*±50% accuracy, analyzed by American Spectrographic Laboratories, San Francisco.

**Separated from the liquid mercury by molecular distillation at about 120°F after the magnetic fraction was separated; approximately 50% of this residue was not accounted for by the spectrographic analysis. Because all residue was consumed, no further analysis was possible.

TABLE 25

WEIGHTS AND SEMIQUANTITATIVE SPECTROGRAPHIC ANALYSES OF MERCURY RESIDUES FROM THERMAL CONVECTION LOOP 2

Element	Analysis, Wt%* Magnetic Residue (0.0312 g)	Nonmagnetic Residue** (0.0085 g)
Fe	70	28
Cr	4	3
Mo	0.8	1
Ni	0.2	0.3
Cu	0.06	16
Si	0.5	4
Mn	0.5	0.5
Ag	-	2
Al	0.04	0.7
Zn	0.1	2

*±50% accuracy, analyzed by American Spectrographic Laboratories, San Francisco.

**Separated from the liquid mercury by molecular distillation after the magnetic fraction was separated.

TABLE 26

ANALYSIS OF DEPOSITS AND RESIDUES FROM THERMAL CONVECTION LOOP 3

	Analysis, Wt%*				
	Separator Deposits				
Element	Columbium Wool	Iron Wool**	Magnet Pole	Post-Condenser-Deposit	Mercury Residue
Fe	50	84	14	35	***
Cr	0.1	1.0	2.3	2.4	0.2
Ni	0.05	0.03	0.5	0.05	0.8
Na	0.1	-	-	0.1	0.5
Mg	0.006	0.01	0.002	0.003	0.07
Al	0.04	0.1	0.03	0.05	0.8
Si	0.2	0.2	0.3	0.6	4.8
Ca	0.007	0.03	0.06	0.03	0.09
Ti	-	0.01	0.006	0.008	-
V	0.002	0.002	0.002	0.002	-
Mn	0.01	0.1	0.16	0.1	0.3
Co	0.01	0.02	0.003	0.05	0.1
Cu	0.05	0.02	0.01	0.04	8.5
Zr	0.01	-	0.01	-	-
Mo	0.002	0.2	0.2	0.1	0.2
Pb	0.009	-	-	-	7
Ag	-	-	-	-	0.9
Zn	-	-	-	-	15

* ±50%, semiquantitative spectrographic analysis by American Spectrographic Laboratories, San Francisco. Values shown are percentage of element in the sample of residue submitted.

** X-ray diffraction analysis indicated that this separated material was alpha iron.

*** Principal constituent.

TABLE 27

ANALYSIS OF DEPOSITS AND RESIDUES FROM THERMAL CONVECTION LOOP 4

	Analysis, Wt%*				
	Separator Deposits			Post-Condenser-Deposit	Mercury Residue
Element	Columbium Wool	Iron Wool	Magnet Pole		
Fe	50	56		50	30
Cr	0.5	2		3.4	5
Ni	0.05	0.02		0.09	0.6
B	-	-		-	1
Na	0.1	0.2	not	-	-
Mg	0.02	0.03		0.4	0.03
Al	0.3	0.8	analyzed	6.5	0.4
Si	0.4	0.5		0.9	6
Ca	0.1	0.5		0.9	0.04
Ti	0.003	0.05		0.2	0.05
V	-	0.004		0.008	-
Mn	0.04	0.2		0.3	0.02
Co	0.007	0.02		0.2	0.02
Cu	0.04	0.03		0.08	20
Zn	-	0.06		-	5
Zr	-	-		-	0.02
Mo	0.2	0.3		0.1	0.03
Ag	0.002	-		-	1
Sn	-	0.009		0.02	0.03
Ba	0.0009	-		0.0009	0.0009
Pb	0.005	-		0.005	1
Cb	2	-		-	-

*±50%, semiquantitative spectrographic analysis by American Spectrographic Laboratories, San Francisco. Values shown are percentage of element in the sample of residue submitted.

UNCLASSIFIED

TABLE 28

WEIGHT AND DISTRIBUTION OF CORROSION PRODUCTS COLLECTED FROM 9Cr-1Mo THERMAL CONVECTION LOOPS

Location	Loop 1		Loop 2		Loop 3		Loop 4	
	Weight, g	Distribution, %	Weight, g	Distribution, %	Weight, g	Distribution, %	Weight, g	Distribution, %
Boiler Wall	0.0176	6.6	-	-	-	-	-	-
Superheater	0.0262	9.9	-	-	-	-	-	-
Cold Leg	0.0546	20.5	-	-	0.1962	41.0	0.3340	56.0
Iron Wool	-	-	-	-	0.1227*	25.6	0.1530*	25.6
Columbium Wool	-	-	-	-	0.1315	27.4	0.0657	11.0
Magnet Pole	-	-	-	-	0.0177	3.7	0.0376	6.3
Trap Totals	-	-	-	-	0.2719	56.7	0.2563	42.9
Mercury Residue Magnetic	0.1059	39.8	0.0312	79	0.0109	2.3	0.0068	1.1
Mercury Residue Nonmagnetic	0.0618	23.2	0.0085	21	-	-	-	-
Loop Totals	0.2661	100.0	0.0397	100.0	0.4796	100.0	0.5971	99.9

*Determined by difference between weights of wool before and after test; includes 0.1016 g (Loop 3) and 0.1220 g (Loop 4) of corrosion products actually collected and analyzed.

Note: Boiling temperatures were: Loop No. 1 - 1075°F, Loop No. 2 - 700°F, Loop No. 3 - 1075°F, Loop No. 4 - 1075°F.

UNCLASSIFIED

TABLE 29

HYDROGEN CLEANUP AND BRAZING CYCLES

Step	Observed Heating or Cooling Rate	
CLEANUP CYCLE		
Heat to 1800°F in -80°F dewpoint hydrogen atmosphere	RT to 700°F 700 to 1300°F 1300 to 1400°F 1400 to 1800°F	48-276°F/hr 270-180°F/hr 50-250°F/hr 250-100°F/hr
Hold 1 hr at 1800°F in -80°F dewpoint hydrogen atmosphere		
Furnace-cool to 1325°F in -80°F dewpoint hydrogen atmosphere	156°F/hr at 1800°F and 28°F/hr at 1325°F	
Hold 5 hr at 1325°F in -80°F dewpoint hydrogen atmosphere		
Furnace-cool to 700°F in -80°F dewpoint hydrogen atmosphere	70°F/hr at 1325 to 1200°F 25°F/hr below 1200°F	
Purge hydrogen from retort with exothermic atmosphere		
Air-cool retort to room temperature		
BRAZING CYCLE		
Heat to 1700°F in -80°F dewpoint hydrogen atmosphere	RT to 700°F 700-1300°F 1300-1700°F	112-234°F/hr 234-162°F/hr 143-288°F
Stabilize at 1700°F in -80°F dewpoint hydrogen atmosphere		
Heat to 1925°F in -80°F dewpoint hydrogen atmosphere	465°F/hr	
Hold at 1925°F for 5 min in -80°F dewpoint hydrogen atmosphere		
Furnace-cool to 1325°F in -80°F dewpoint hydrogen atmosphere	225°F/hr to 1750°F 156°F/hr at 1750°F 28°F/hr at 1325°F	
Hold 5 hr at 1325°F in -80°F dewpoint hydrogen atmosphere		
Furnace cool to 700°F in -80°F dewpoint hydrogen atmosphere	70°F/hr at 1325 to 1200°F 28°F/hr below 1200°F	
Purge hydrogen from retort with exothermic atmosphere		
Air-cool retort to room temperature		

TABLE 30

NOMINAL CHEMICAL COMPOSITION OF MATERIALS
EXPOSED TO EROSION TEST ENVIRONMENT

Material	Major Elements*													
	C	Cr	Ni	Mo	Ti	Zr	Cb	Fe	W	Co	V	Cu	Cb+ Ta	Al
Mo Alloy-TZM	0.02	-	-	Bal	0.5	0.08	-	-	-	-	-	-	-	-
Mo-1/2Ti	0.02	-	-	Bal	0.5	-	-	-	-	-	-	-	-	-
Cb-752	40 ppm**	-	-	-	-	2.5	Bal	-	10	-	-	-	-	-
17-4PH	0.07**	16.5	4.0	-	-	-	-	Bal	-	-	-	4.0	0.30	-
Lapelloy	0.30	11.8	-	2.8	-	-	-	Bal	-	-	0.25	-	-	-
AISI 347	0.08**	18	10.5	-	-	-	***	Bal	-	-	-	-	-	-
AISI 410	0.15**	12.5	-	-	-	-	-	Bal	-	-	-	-	-	-
PH15-7 Mo	0.09**	15.0	7.0	2.5	-	-	-	Bal	-	-	-	-	-	1.0
18-4-1 Tool Steel	0.75	4.0	-	-	-	-	-	Bal	18	-	1.0	-	-	-
Dynacut Tool Steel	1.23	3.75	-	8.7	-	-	-	Bal	1.8	8.2	2.0	-	-	-
Stellite 6B	1.15	30	1.2	1.5	-	-	-	0.8	4.5	Bal	-	-	-	-

*Wt% except where otherwise indicated
**Maximum
***Ten times the carbon content

TABLE 31

HEAT TREATMENT OF EROSION SPECIMEN MATERIALS

Material	Heat Treatment	Room-Temperature Hardness
TZM	Stress relieved, 2250°F for 1/2 hr	$28R_C$
MO-1/2Ti	Stress relieved, 2100°F for 3/4 hr	$29R_C$
Cb-752	Stress relieved, 2200°F for 1 hr	$84R_B$
17-4Ph	900°F for 1 hr, air cooled	$44R_C$
Lapelloy	2000°F for 1 hr, oil quench, 1200°F for 2 hr	$34R_C$
AISI 347	1950°F, water quench	$71R_B$
AISI 410	1550°F, furnace cool 50°F/hr to 1100°F	$95R_B$
PH15-7Mo	1750°F for 10 min, air cool, -100°F for 8 hr, 950°F for 1 hr	$48R_C$
18-4-1 Tool Steel	2250°F oil quench, 1200°F for 1 hr, air cool, 1200°F for 1 hr	$55R_C$
Dynacut Tool Steel	2200°F, oil quench, 1100°F for 2 hr, air cool, 1100°F for 2 hr	$66R_C$
	2200°F, oil quench, 1200°F for 2 hr, air cool, 1200°F for 2 hr	$62R_C$
	2200°F, air cool, 1200°F for 2 hr, air cool, 1200°F for 2 hr	$54R_C$
Stellite 6B	2250°F rapid air cool, 1650°F for 4 hr, furnace cool to 700°F, air cool	$39R_C$

TABLE 32

TEST CONDITION AND RESULTS OF MATERIALS
SPECIMENS EXPOSURE TO EROSIVE ENVIRONMENT

Material	Density $lb/in.^3$	Original Weight g	Test Temp ^oF	Exposure Time hr	Weight Loss g	Calculated Volume Loss $in.^3 \times 10^5$
Mo-TZM	0.369	9.8613	637	5	0.8023	479.0
Mo-1/2Ti	0.369	10.6385	653	5	0.7061	421.6
Mo-1/2Ti	0.369	9.7699	627	5	0.6707	400.1
Cb-752	0.326	7.1344	620	3.5	0.5867	396.4
17-4PH	0.281	7.9403	620	5	0.1448	113.5
Lapelloy	0.281	7.9118	620	5	0.1483	116.3
Lapelloy	0.281	7.9022	620	5	0.1403	110.0
Lapelloy	0.281	8.0322	620	4	0.1329	104.2
AISI 347	0.286	7.7620	628	5	0.1145	88.3
AISI 410	0.280	7.7548	629	5	0.0749	58.9
PH15-7Mo	0.271	7.5480	615	5	0.0393	31.25
18-4-1 Tool Steel	0.290	8.8753	620	5	0.0173	13.14
Dynacut Tool Steel	0.284	7.8966	620	5	0.0369	28.62
Dynacut Tool Steel	0.284	8.0063	620	5	0.0216	16.75
Dynacut Tool Steel	0.284	8.2336	639	14	0.0070	5.42
Dynacut Tool Steel	0.284	8.2336	655	5	0.0045	3.49
Stellite 6B	0.303	8.4745	636	15	0.0091	6.61
Stellite 6B	0.303	8.4770	625	15	0.0088	6.40
Stellite 6B	0.303	8.4745	650	5	0.0059	4.29
Stellite 6B	0.303	8.6966	620	5	0.0055	4.00
Stellite 6B	0.303	8.4770	637	5	0.0046	3.34

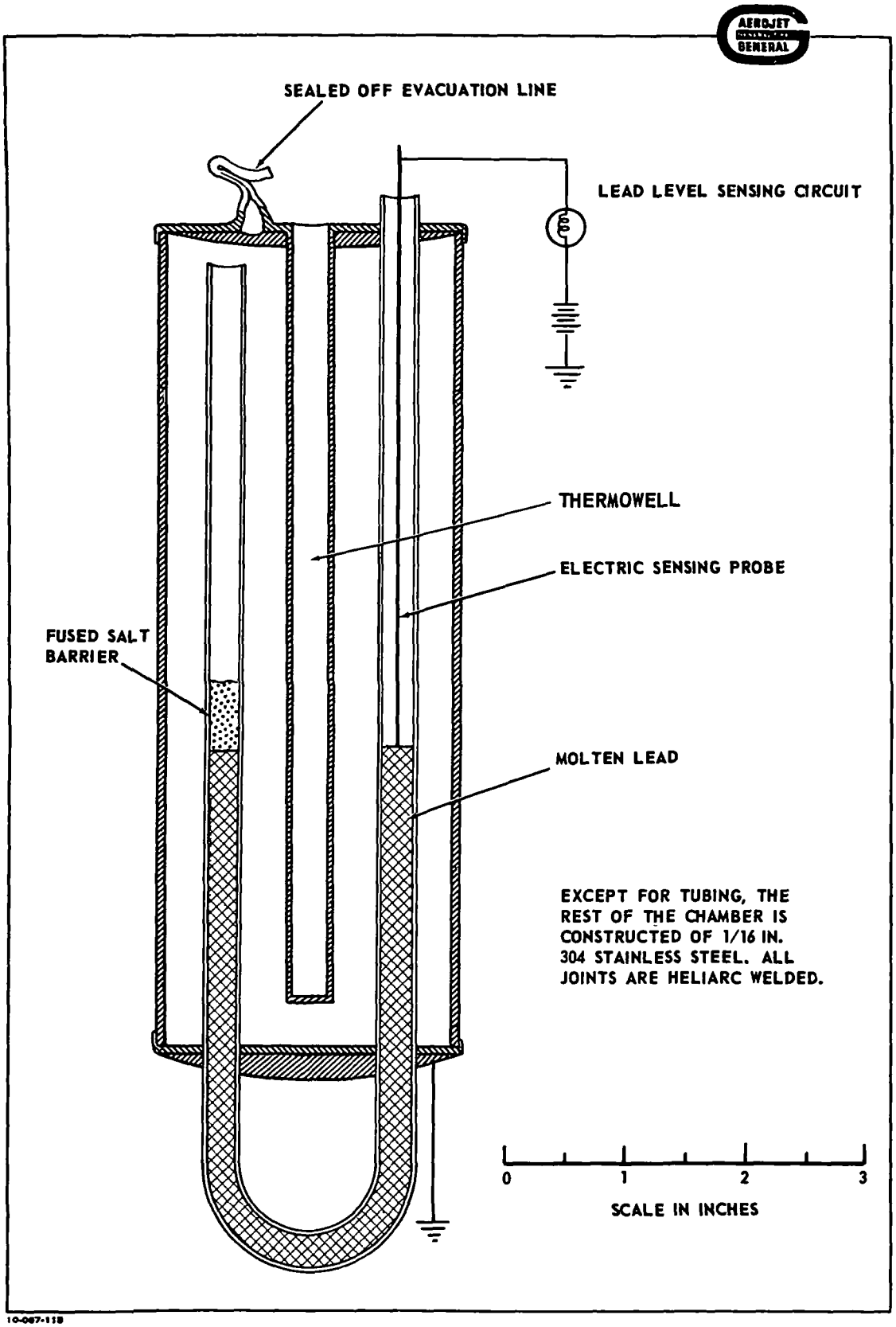

Cross Section of Mercury Chamber for PVT (Pressure, Volume, Temperature) Apparatus

Figure 1

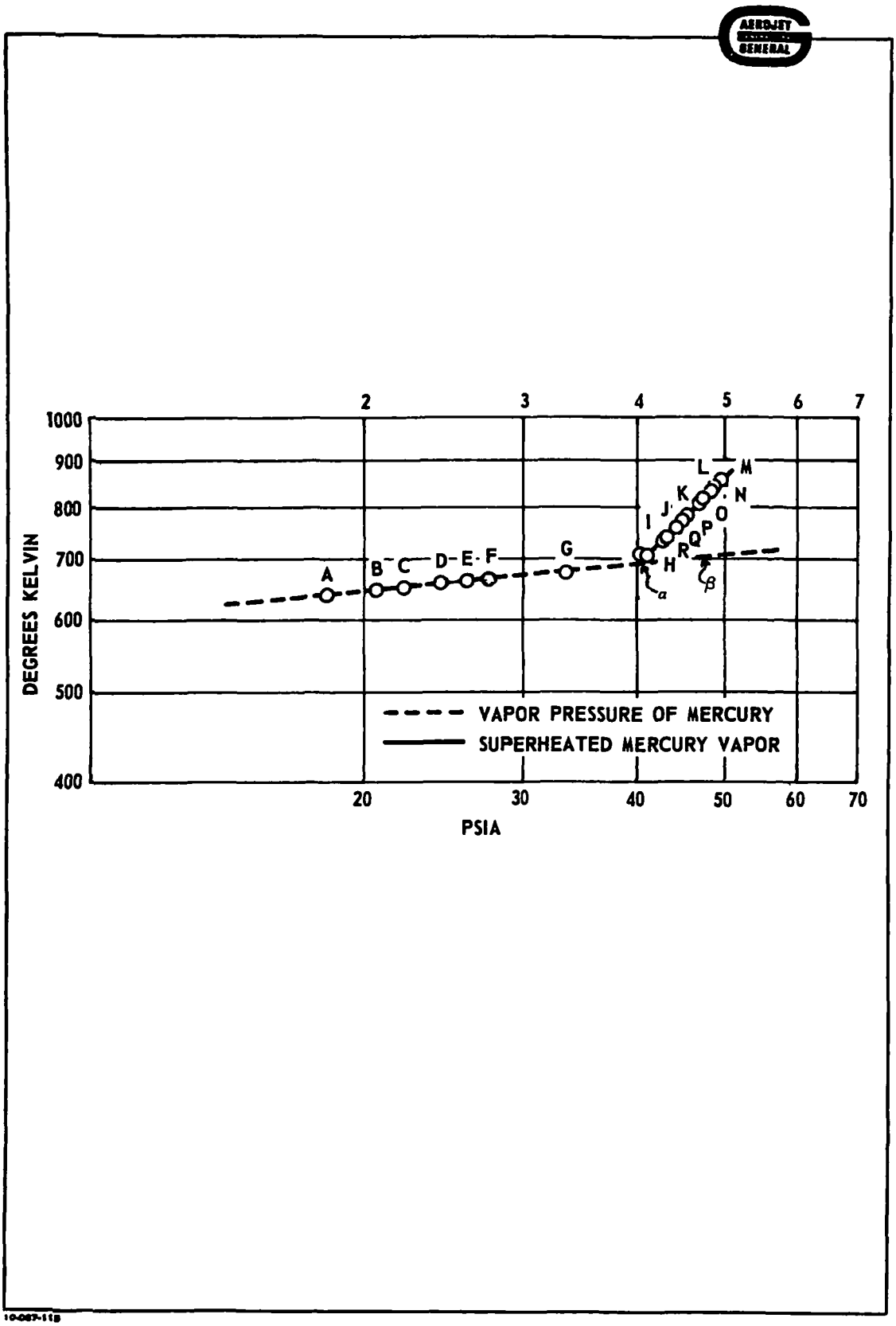

PVT Apparatus - Test Results, Run 1, Log psia vs Log ^{o}K

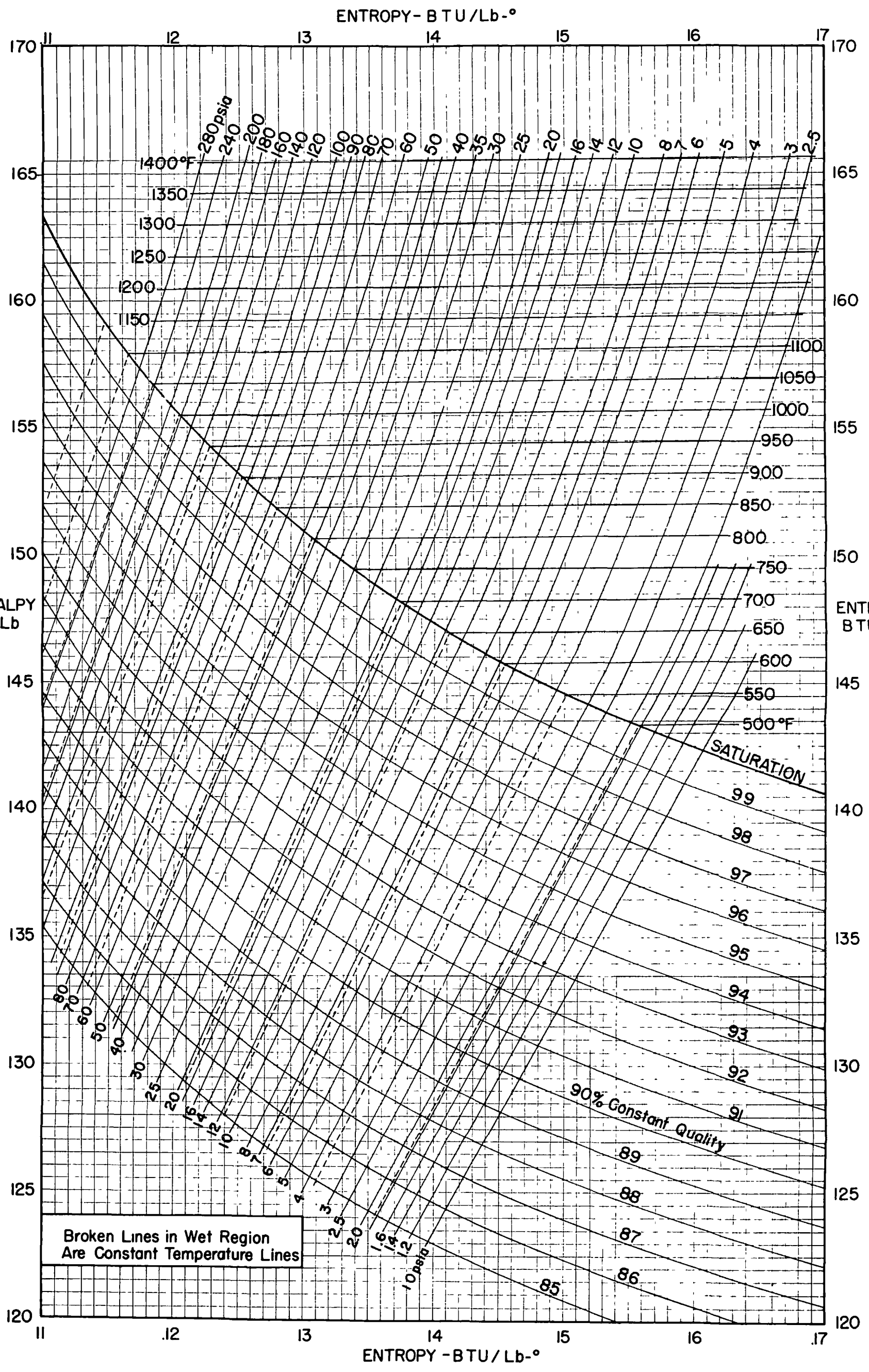
ENTROPY - B T U / Lb - °
11
12
13
14
15
16
17
170
165
160
155
150
145
140
135
130
125
120
ENTHALPY BTU/Lb
280psia
240
200
180
160
140
120
100
90
80
70
60
50
40
35
30
25
20
16
14
12
10
8
7
6
5
4
3
2.5
1400°F
1350
1300
1250
1200
1150
1100
1050
1000
950
900
850
800
750
700
650
600
550
500°F
SATURATION
99
98
97
96
95
94
93
92
91
90% Constant Quality
89
88
87
86
85
80
70
60
50
40
30
25
20
16
14
12
10
8
7
6
5
4
3
2.5
2.0
1.6
1.4
1.2
1.0psia
Broken Lines in Wet Region
Are Constant Temperature Lines
ENTROPY - BTU / Lb - °

Figure 3

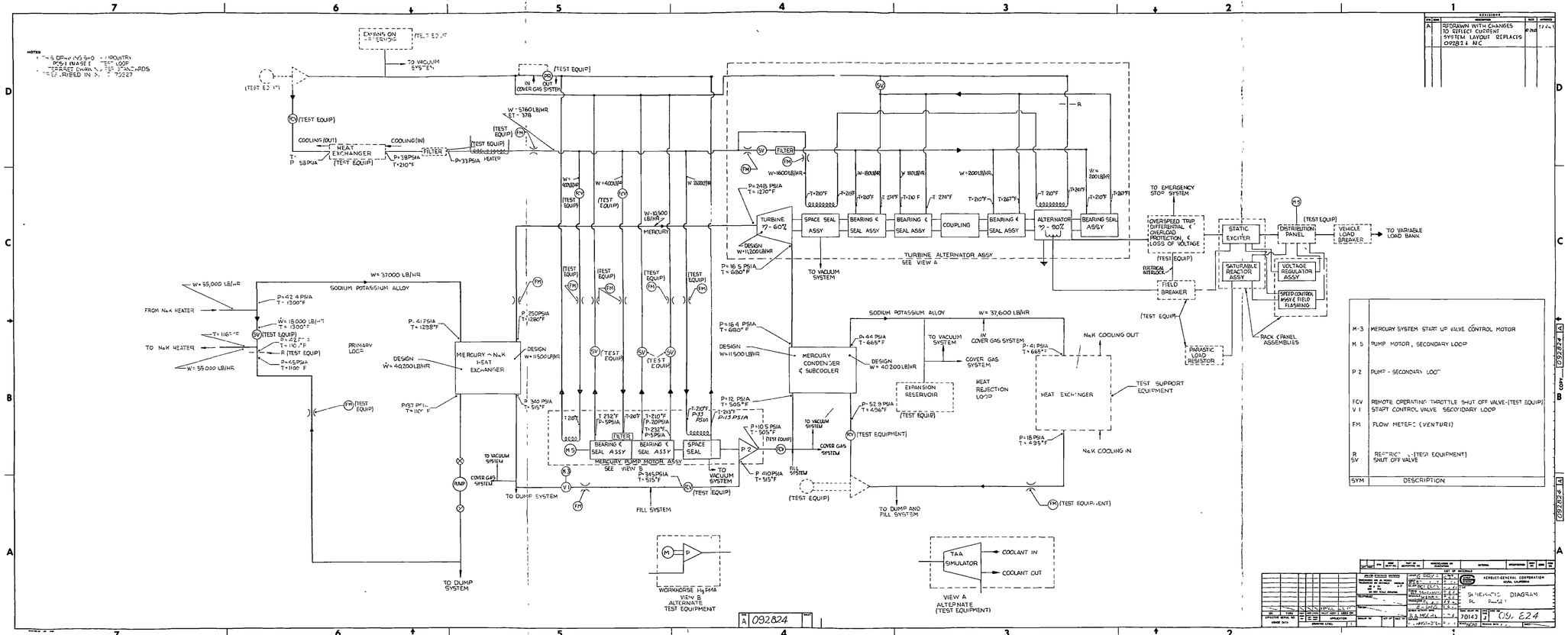

Schematic Diagram PCS-1 - Phase I

Figure 4

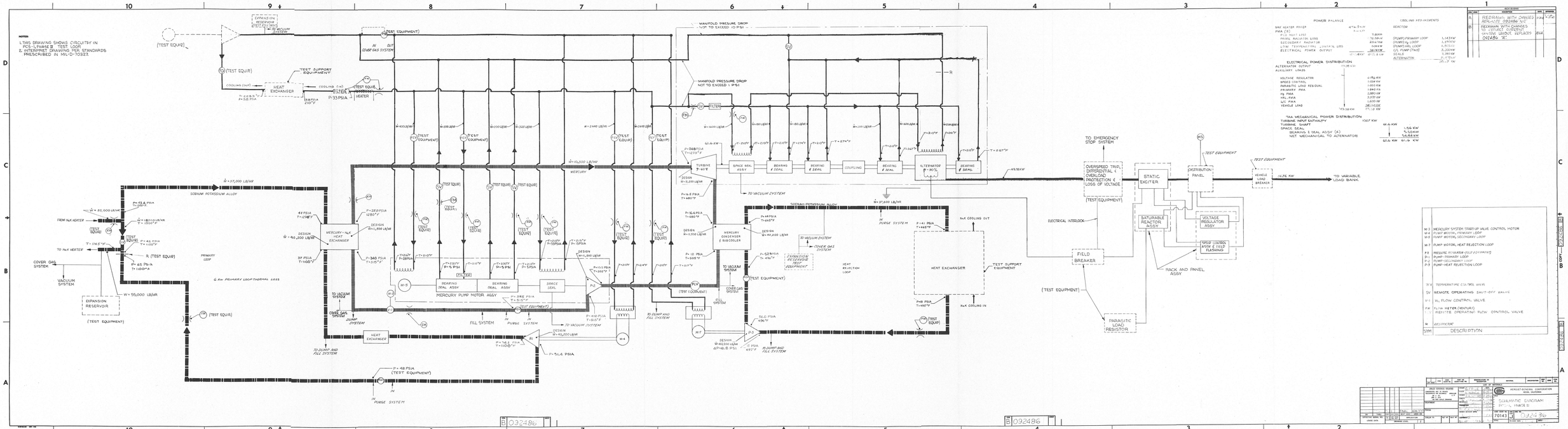

Schematic Diagram PCS-1 - Phase II

Figure 5

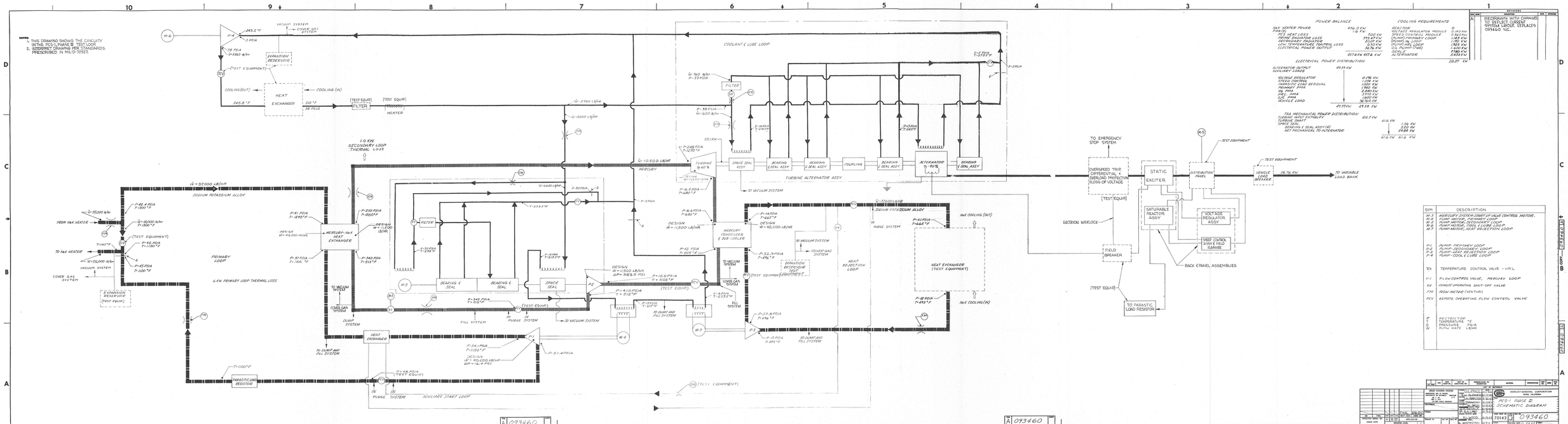

Schematic Diagram PCS-1 - Phase III

UNCLASSIFIED

Figure 6

NOTES: 1. REMOVE ALL BURRS AND SHARP EDGES

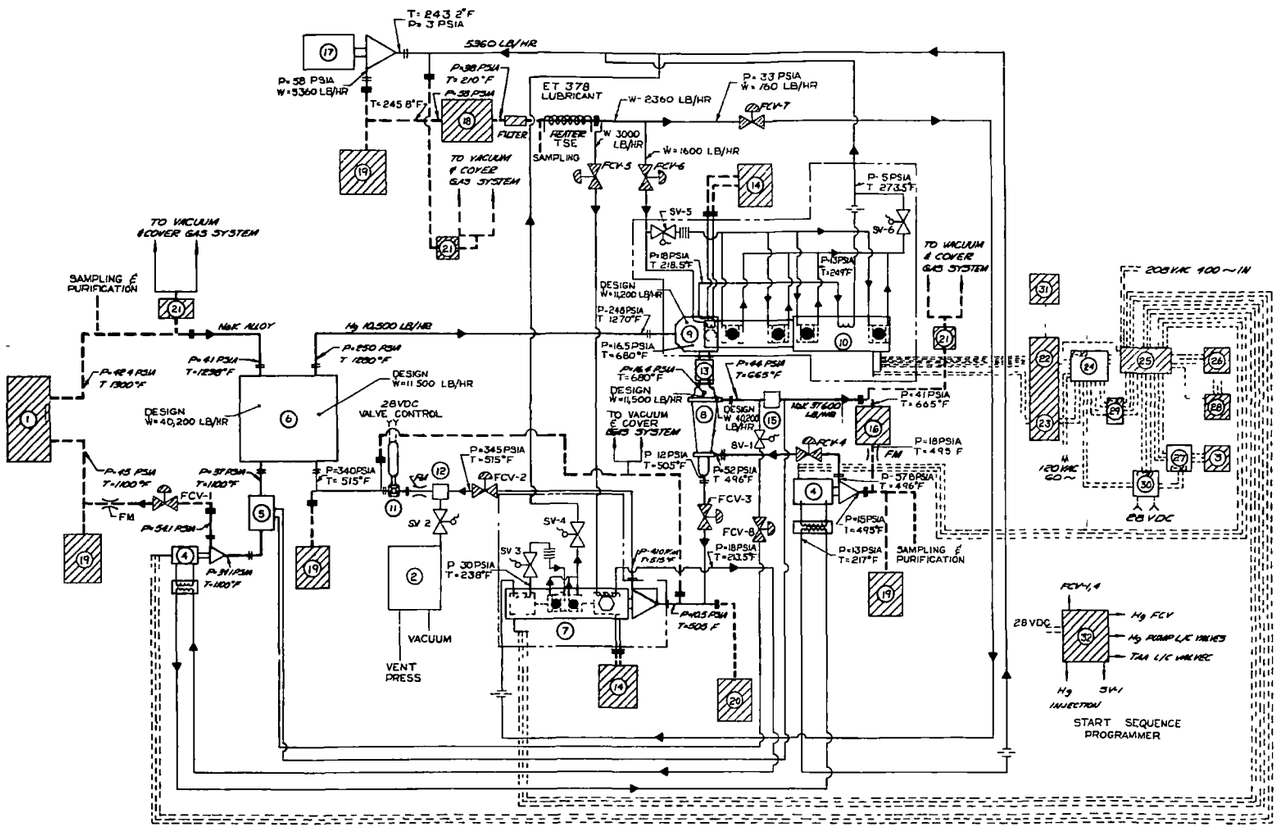

ELECTRICAL WIRING	
SPACE SEAL	
FLANGED JOINT	
BEARING	
FILTER	
SOLENOID SHUTOFF VALVE	
FLOW CONTROL OR TRIM VALVE	
TEST SUPPORT EQUIPMENT	
ORIFICE	
TEST SUPPORT/PCS-2 INTERFACE	
SYMBOL	DESCRIPTION

	35
	34
	33
START SEQUENCE PROGRAMMER	32
EMERGENCY SHUTDOWN PANEL	31
SPEED CONTROL	30
VOLTAGE REGULATOR	29
VEHICLE LOAD SIMULATOR	28
SATURABLE REACTOR	27
VEHICLE LOAD BREAKER	26
DISTRIBUTION PANEL	25
STATIC EXCITER	24
FIELD BREAKER	23
PROTECTIVE SYSTEM	22
NAK EXPANSION TANK RESERVOIR	21
Hg INVENTORY CONTROL SYSTEM	20
DUMP TANK	19
HEAT EXCHANGER	18
LUBRICATION AND COOLANT PUMP	17
RADIATOR SIMULATOR HEAT EXCHANGER	16
TEMPERATURE CONTROL VALVE	15
SPACE SEAL VACUUM SYSTEM	14
TURBINE EXHAUST BELLOWS	13
INJECTION VALVE	12
FLOW CONTROL VALVE	11
ALTERNATOR	10
TURBINE	9
CONDENSER	8
MERCURY PUMP	7
BOILER	6
AUXILIARY START HEAT EXCHANGER	5
NaK PUMP	4
PARASITIC LOAD SIMULATOR	3
Hg INJECTION TANK ASSEMBLY	2
NaK HEATER	1

ITEM	QTY PER UNIT	CODE IDENT NO.	PART OR IDENTIFYING NO.	NOMENCLATURE OR DESCRIPTION	MATERIAL	SPECIFICATION	UNIT SYM.	ZONE	ITEM NO.

LIST OF MATERIALS

UNLESS OTHERWISE SPECIFIED DIMENSIONS ARE IN INCHES TOLERANCES ON DECIMALS ANGULAR ± FRACTIONS ± DO NOT SCALE DRAWING	DRAWN	I.A. BECKER	DATE
	CHECKED		
	ENGINEER		
	STRUCTURES/PIPING		
	EQUIPMENT		
	MATERIALS		
	PRODUCTION		
	PURCHASING		
	QUALITY ASSURANCE		
	RELIABILITY		

AEROJET-GENERAL CORPORATION
AZUSA, CALIFORNIA

SCHEMATIC
PCS-2 PHASE I

SIZE E | CAGE CODE NO. 70143 | DRAWING NO. 094144 | REV. LTR

SCALE | RELEASE DATE | SHEET

Schematic Diagram PCS-2 - Phase I

Figure 7

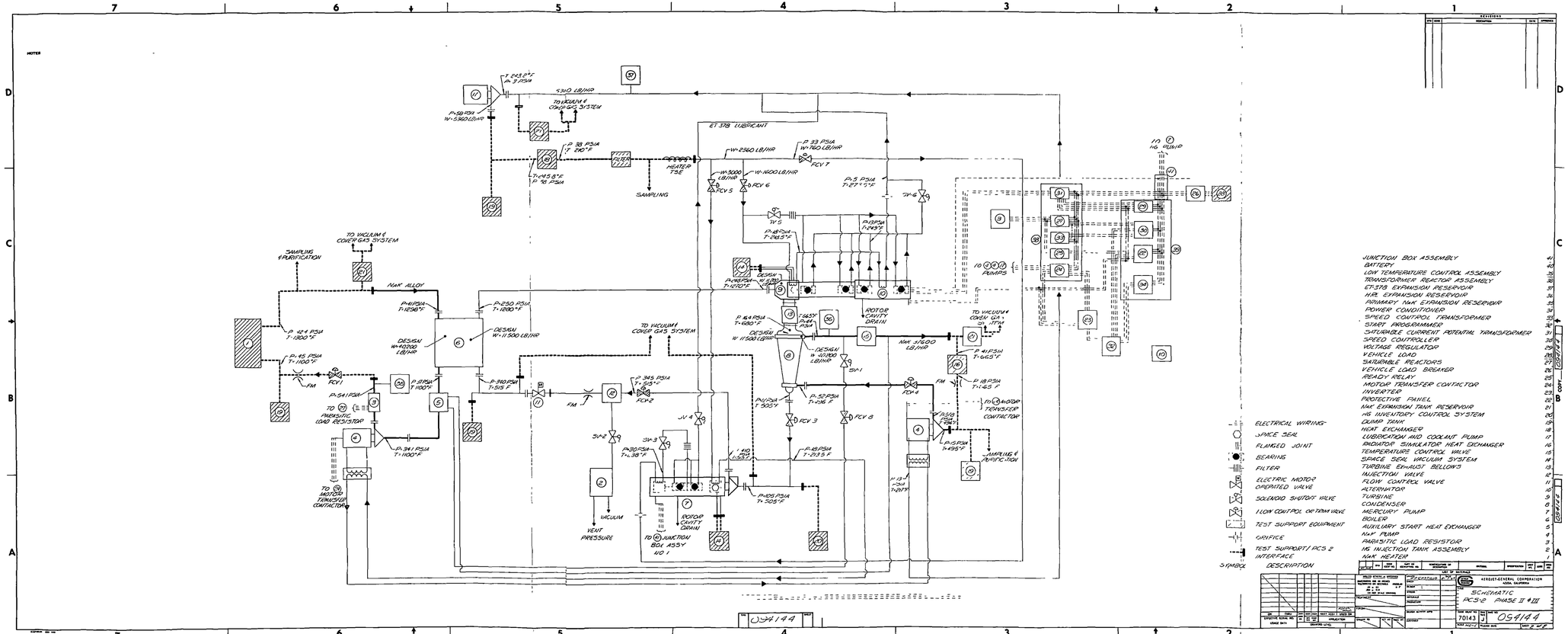

Schematic Diagram PCS-2 - Phases II and III

Figure 8

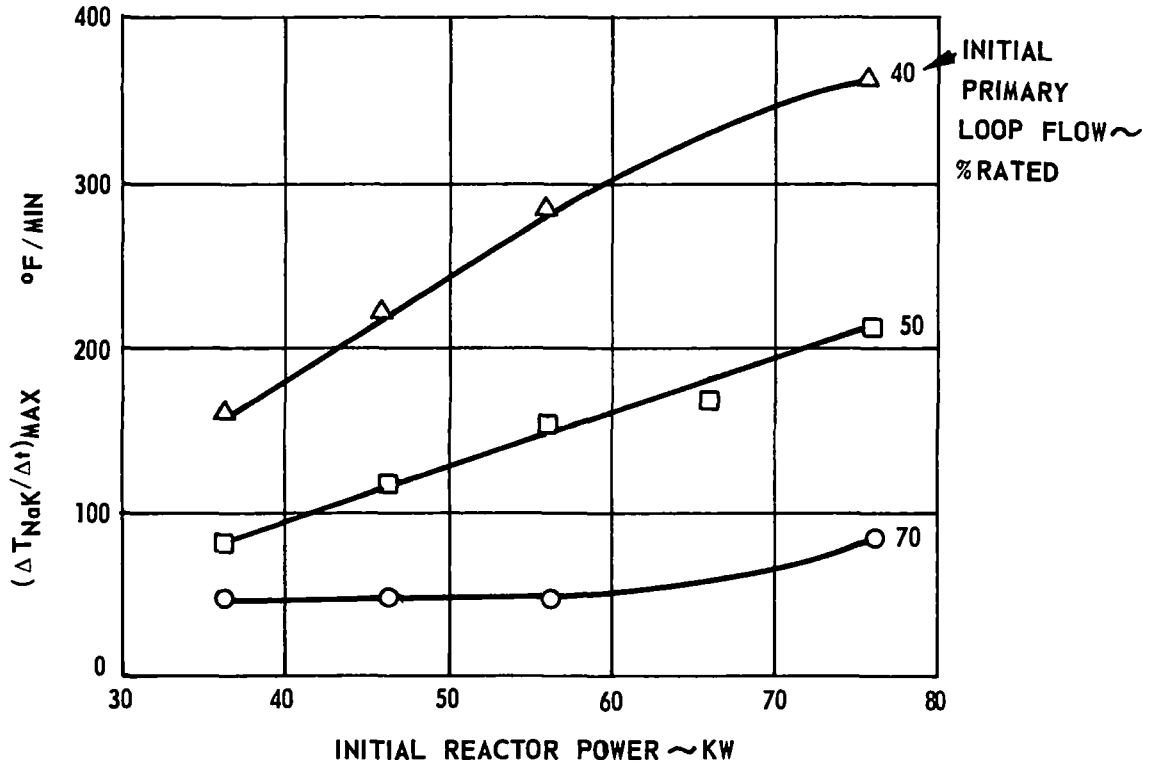

10-067-118

SNAP-8 PCS Start-up Runs, Reference System B, Complete System Simulation - Maximum Rate of Temperature Change vs Internal Reactor Power

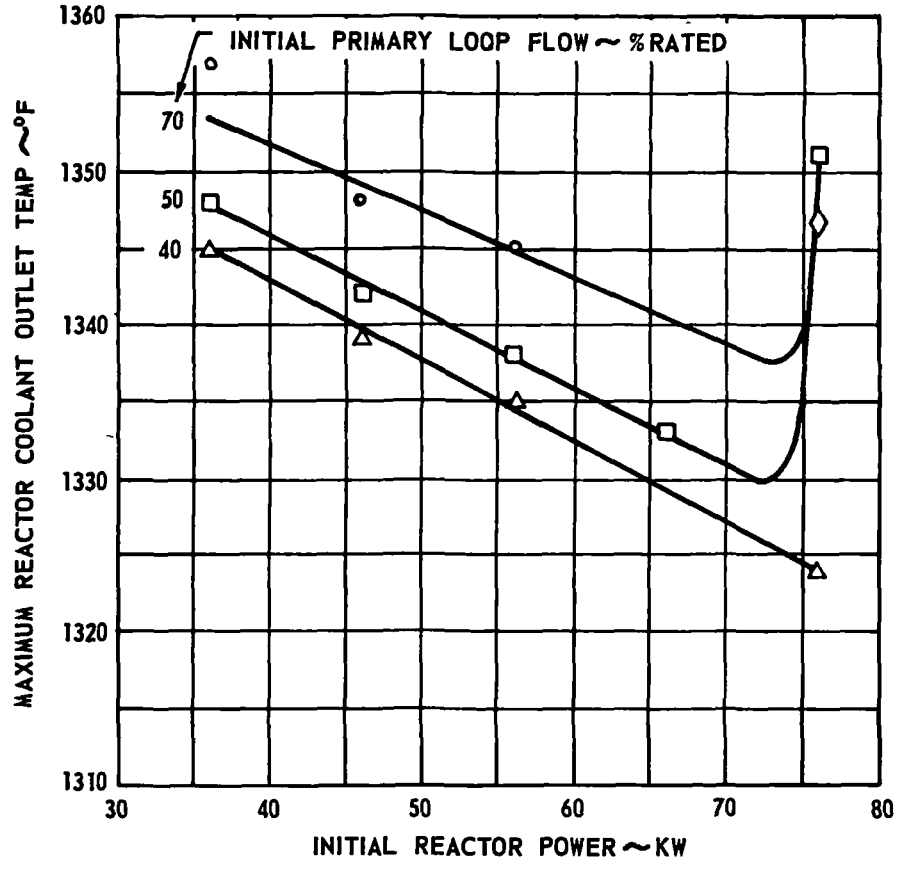

SNAP-8 PCS Start-up Runs, Reference System B, Complete System Simulation - Maximum Reactor Outlet Temperature vs Initial Reactor Power

Figure 10

SNAP-8 PCS Start-up Runs, Reference System B, Complete System Simulation - Effect of Parameter Variations on Maximum Rate of Temperature Change

Figure 11

SNAP-8 PCS Start-up Runs, Reference System B, Complete System Simulation - Effect of Parameter Variations on Maximum Reactor Outlet Temperature

Figure 12

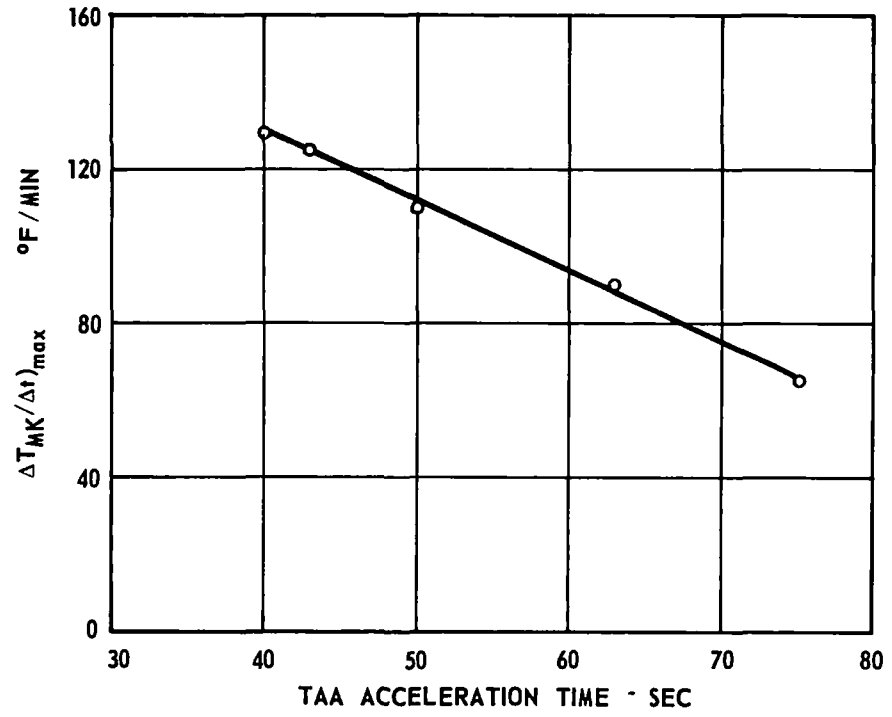

SNAP-8 PCS Start-up Runs, Reference System B, Complete System Simulation - Effect of TAA Acceleration on Maximum Rate of Temperature Change

Figure 13

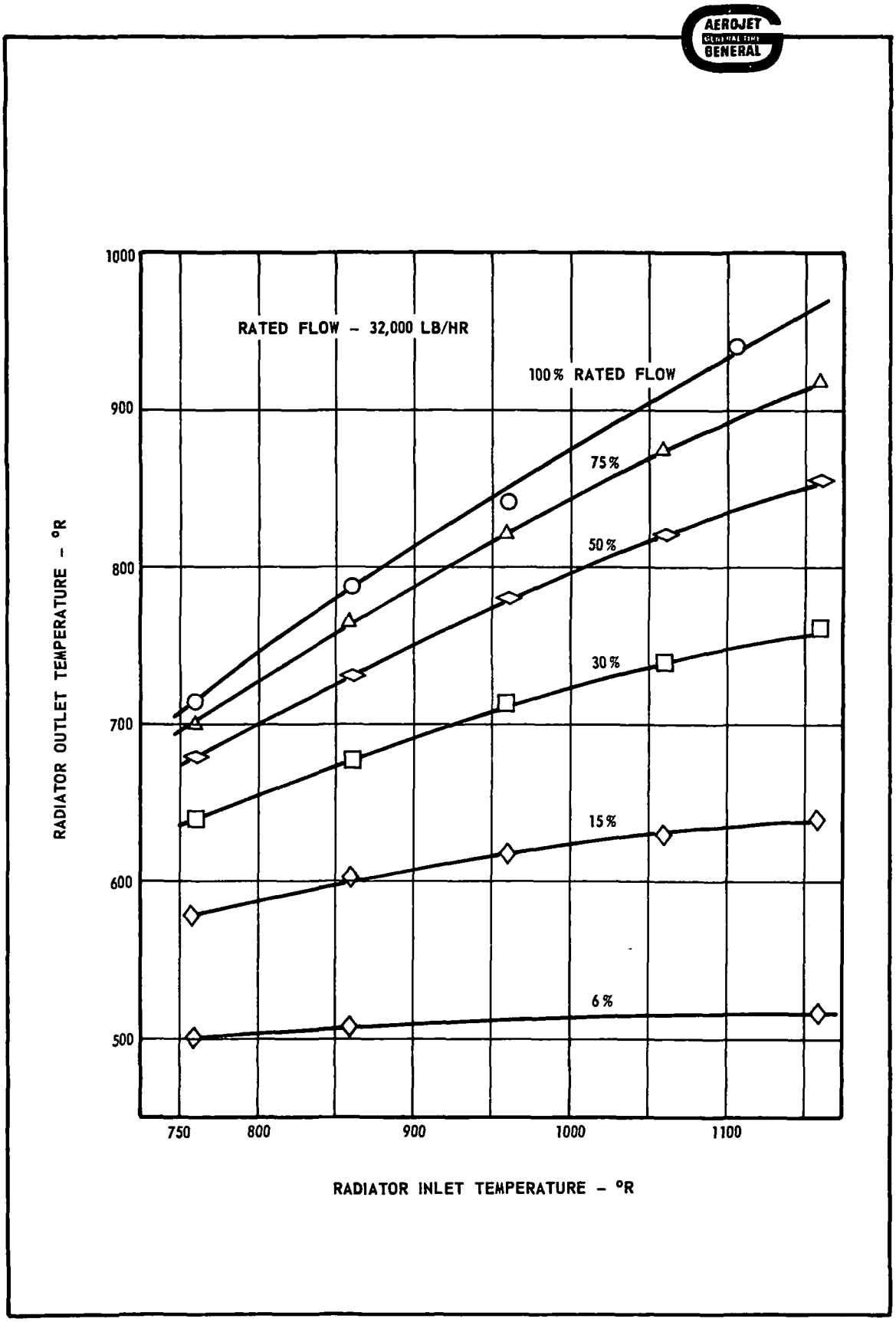

Cylindrical Radiator - Shade Conditions

Figure 14

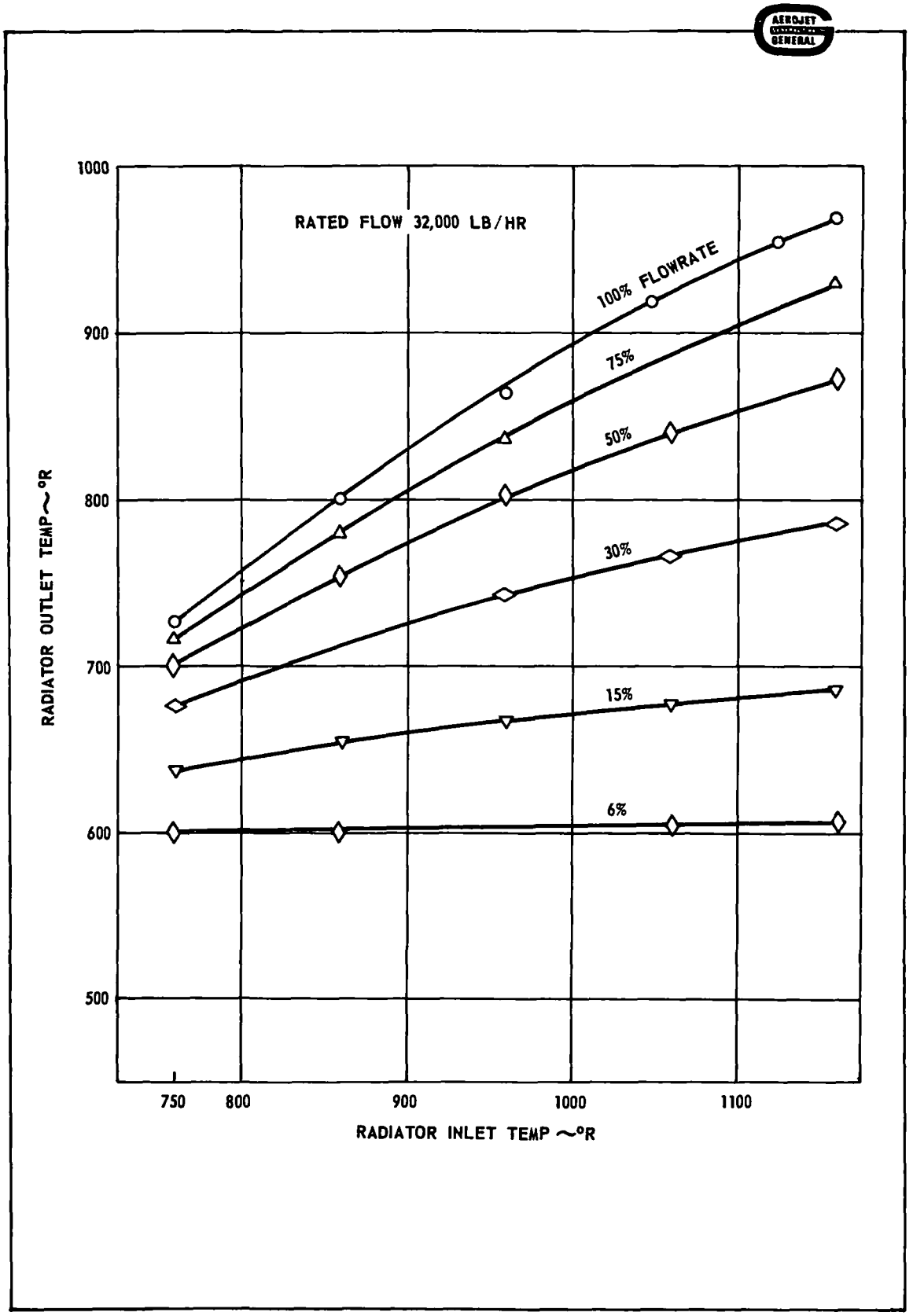

Cylindrical Radiator Performance - Sun Conditions

Figure 15

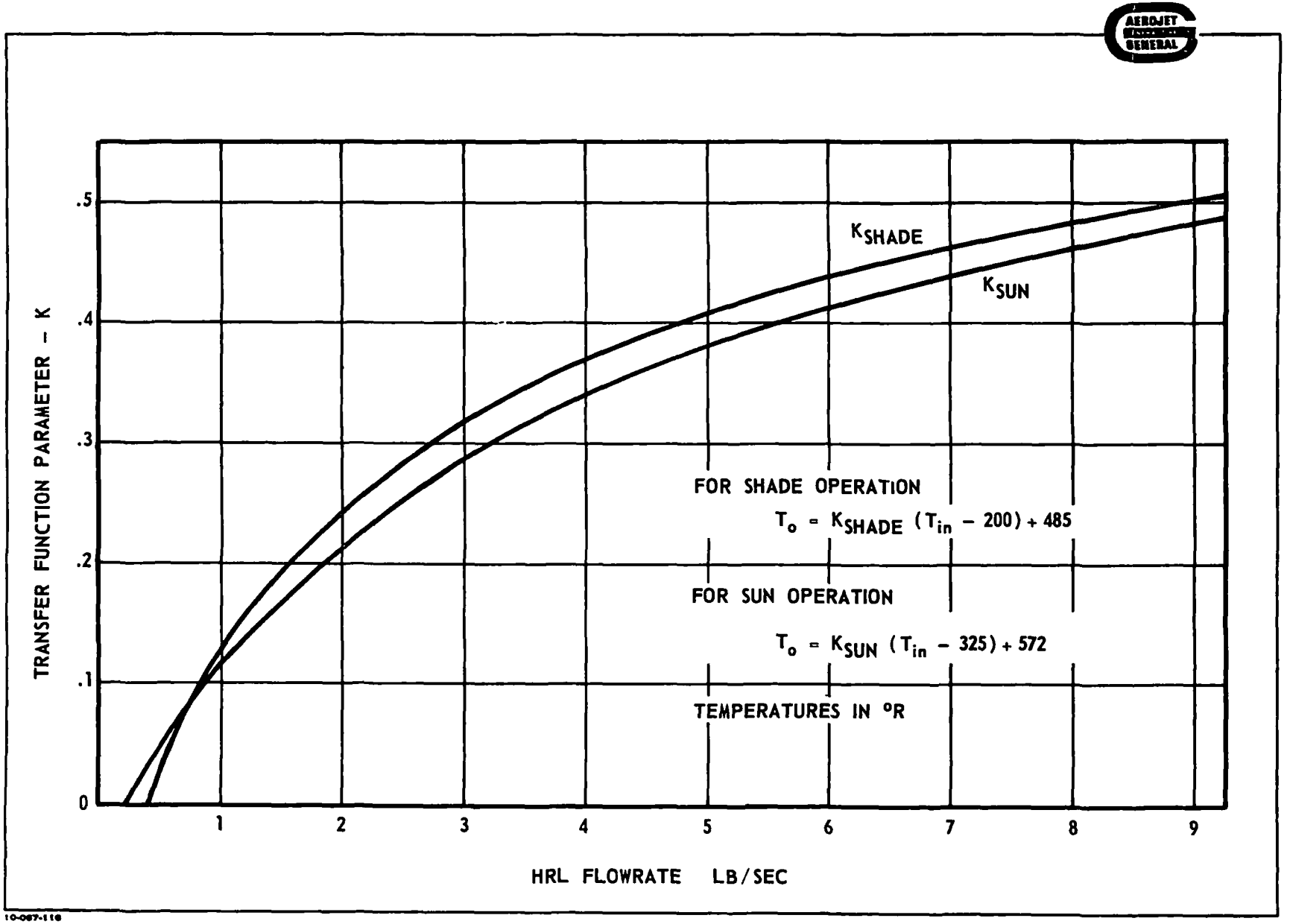

Radiator Transfer Function Parameter

Figure 16

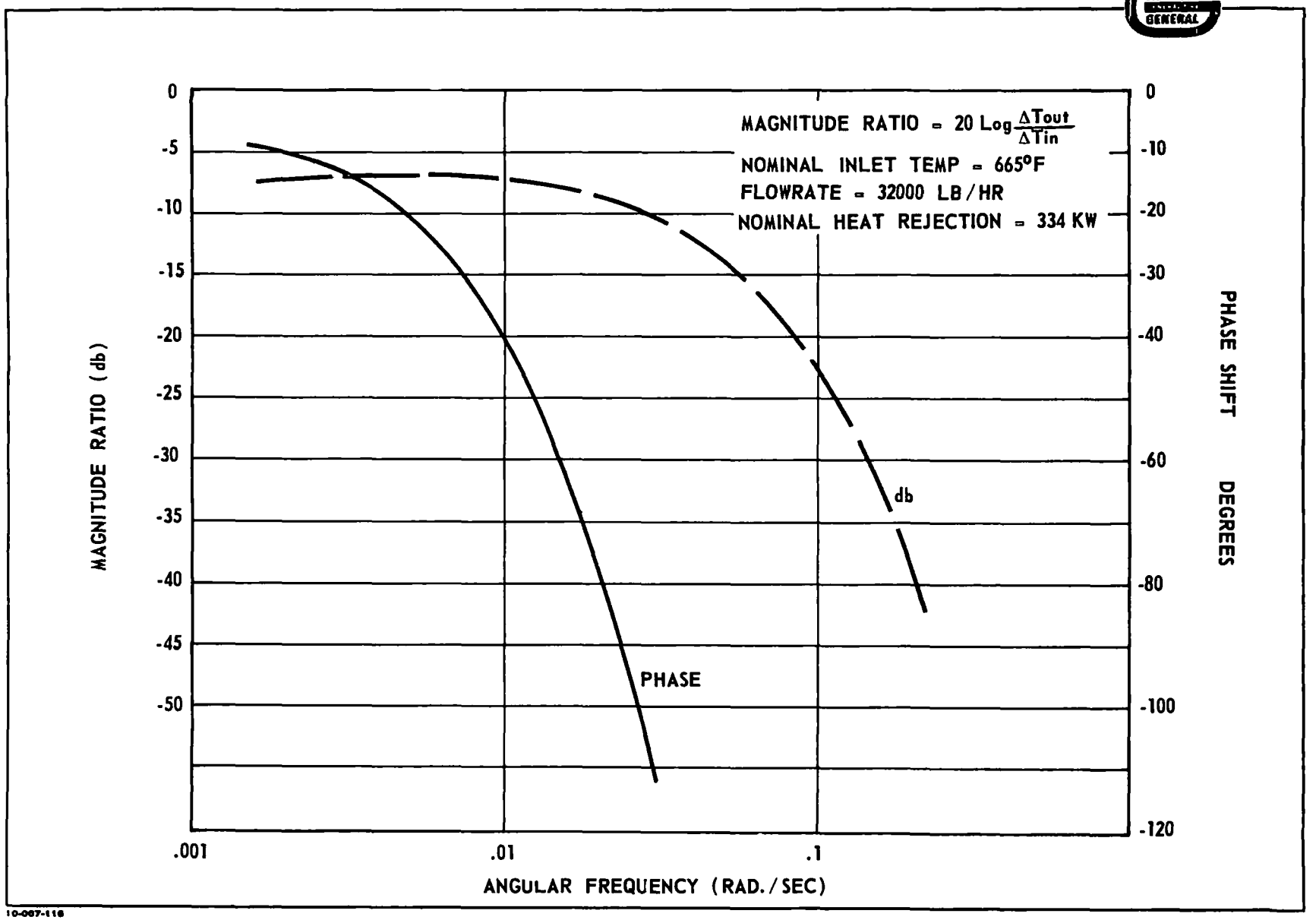

Frequency Response for Cylindrical SNAP-8 Radiator in Sun

Figure 17

FIGURE 18

IN-SUN AND IN-SHADE TRANSFER FUNCTION OF THE SPACE RADIATOR TO BE SIMULATED IN SL-2

IN-SUN TRANSFER FUNCTION SIMULATION OF THE SPACE RADIATOR TO BE SIMULATED IN SL-2 IS AS SHOWN BELOW

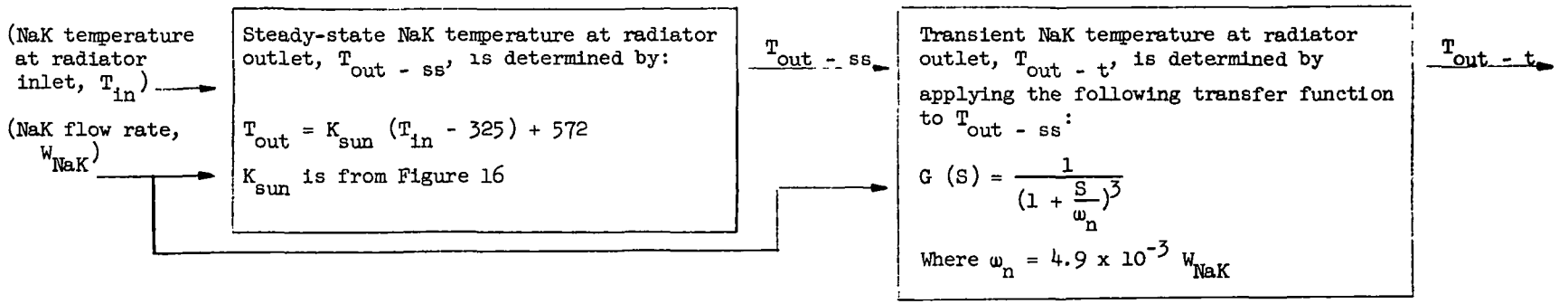

IN-SHADE TRANSFER FUNCTION SIMULATION OF THE SPACE RADIATOR TO BE SIMULATED IN SL-2 IS AS SHOWN BELOW

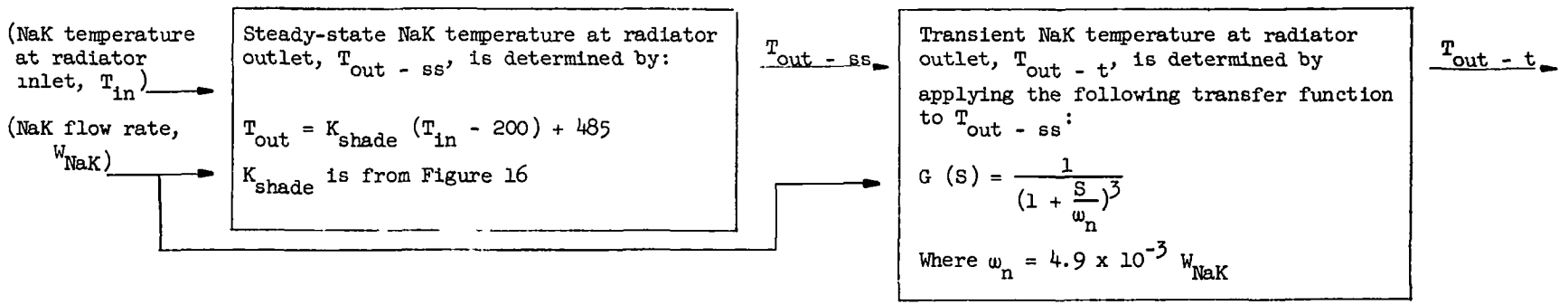

NOTE: Temperatures are in degrees Rankine and W_{NaK} is in lb/sec.

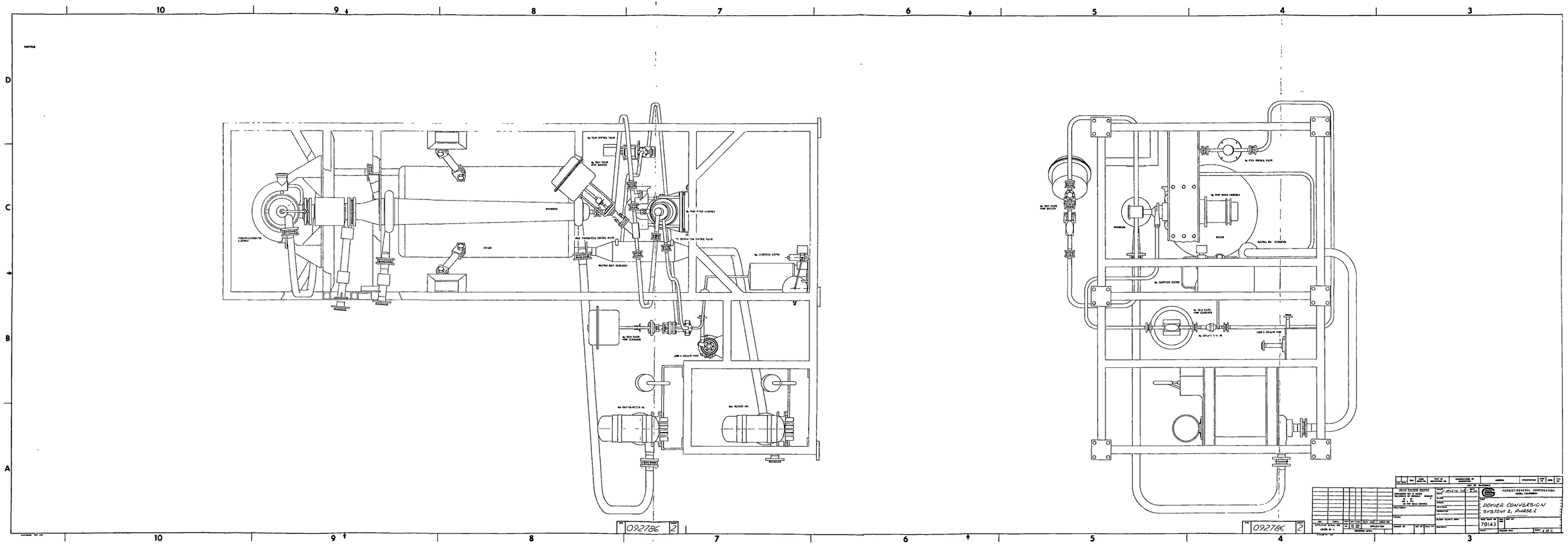

Power Conversion System 2, Phase I

Figure 19

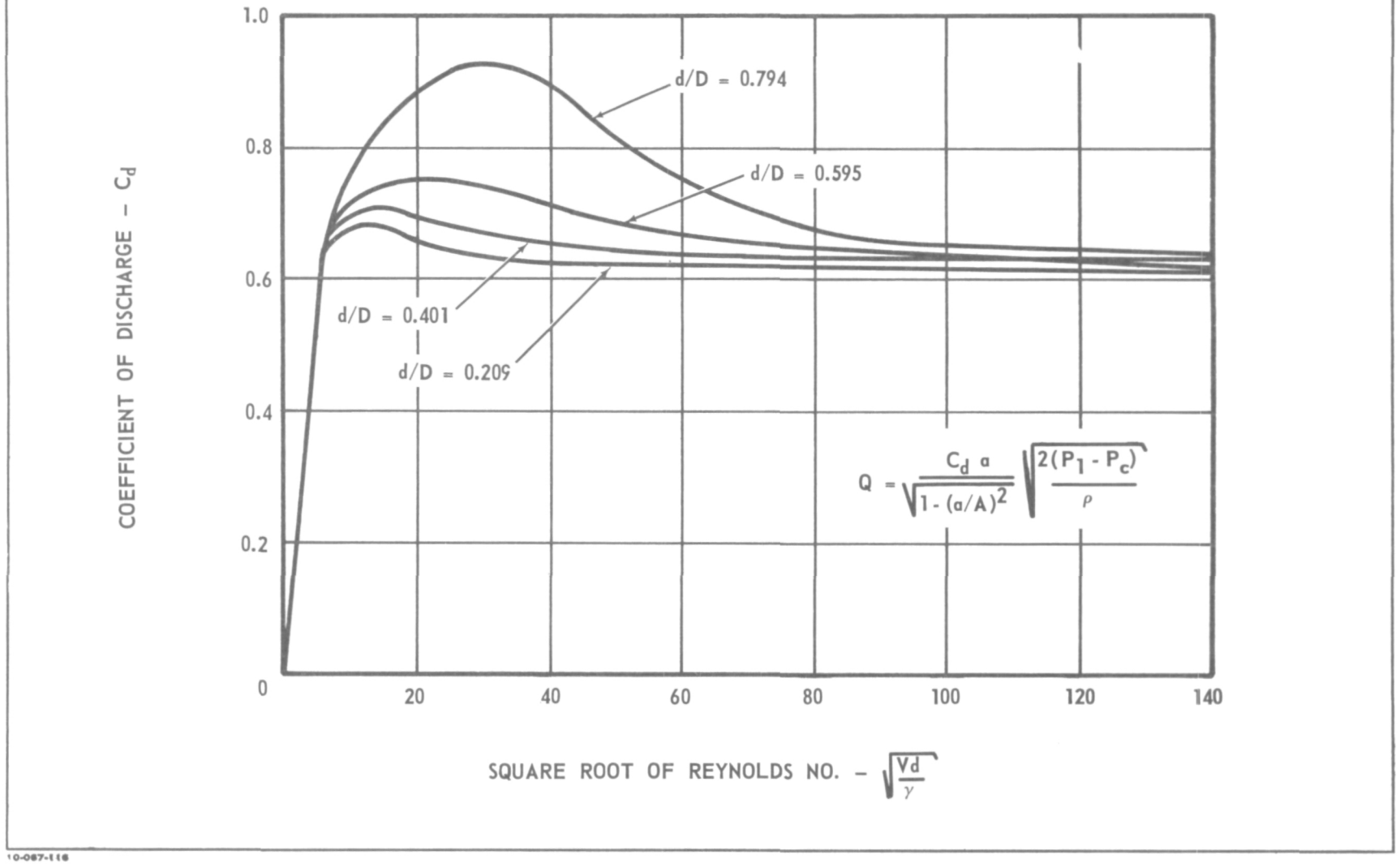

10-067-116

Figure 20

Discharge Coefficients for the Plate Orifice

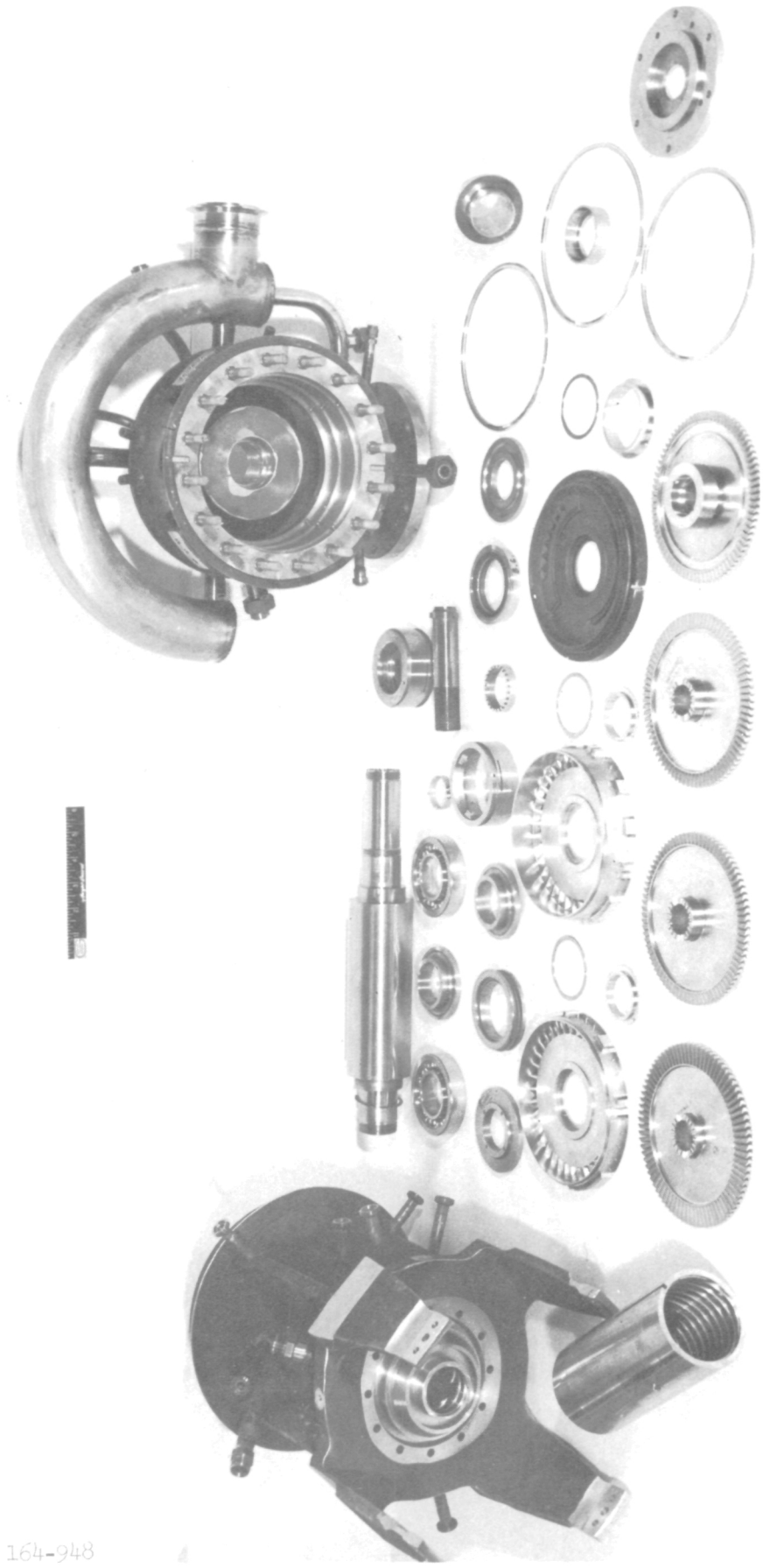

164-948

Turbine Assembly Components - SNAP-8 Turbine Alternator Assembly

Figure 21

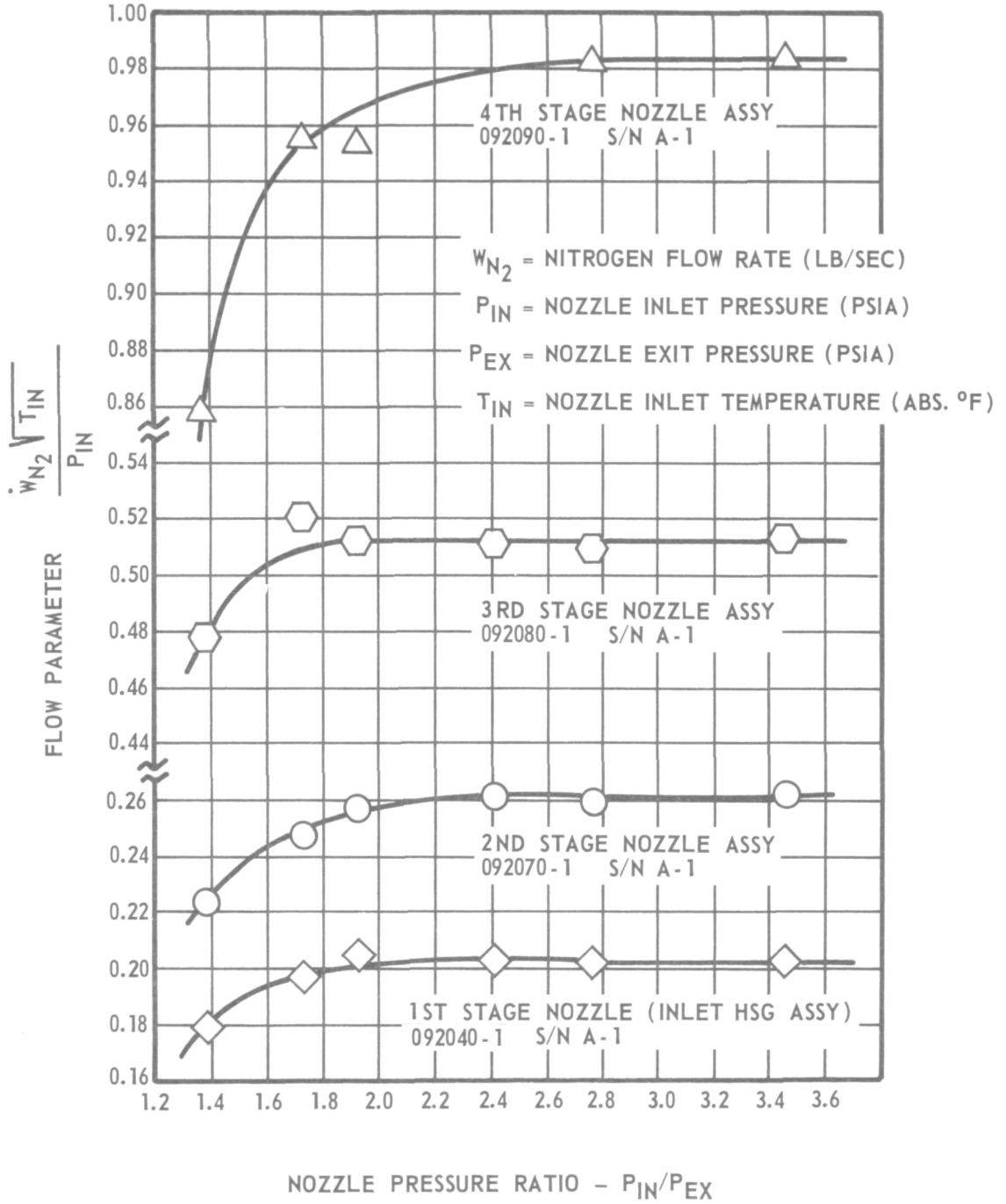

10-067-118

Turbine-Nozzle-Assembly Flow Tests - TAA Buildup No. 1

Figure 22

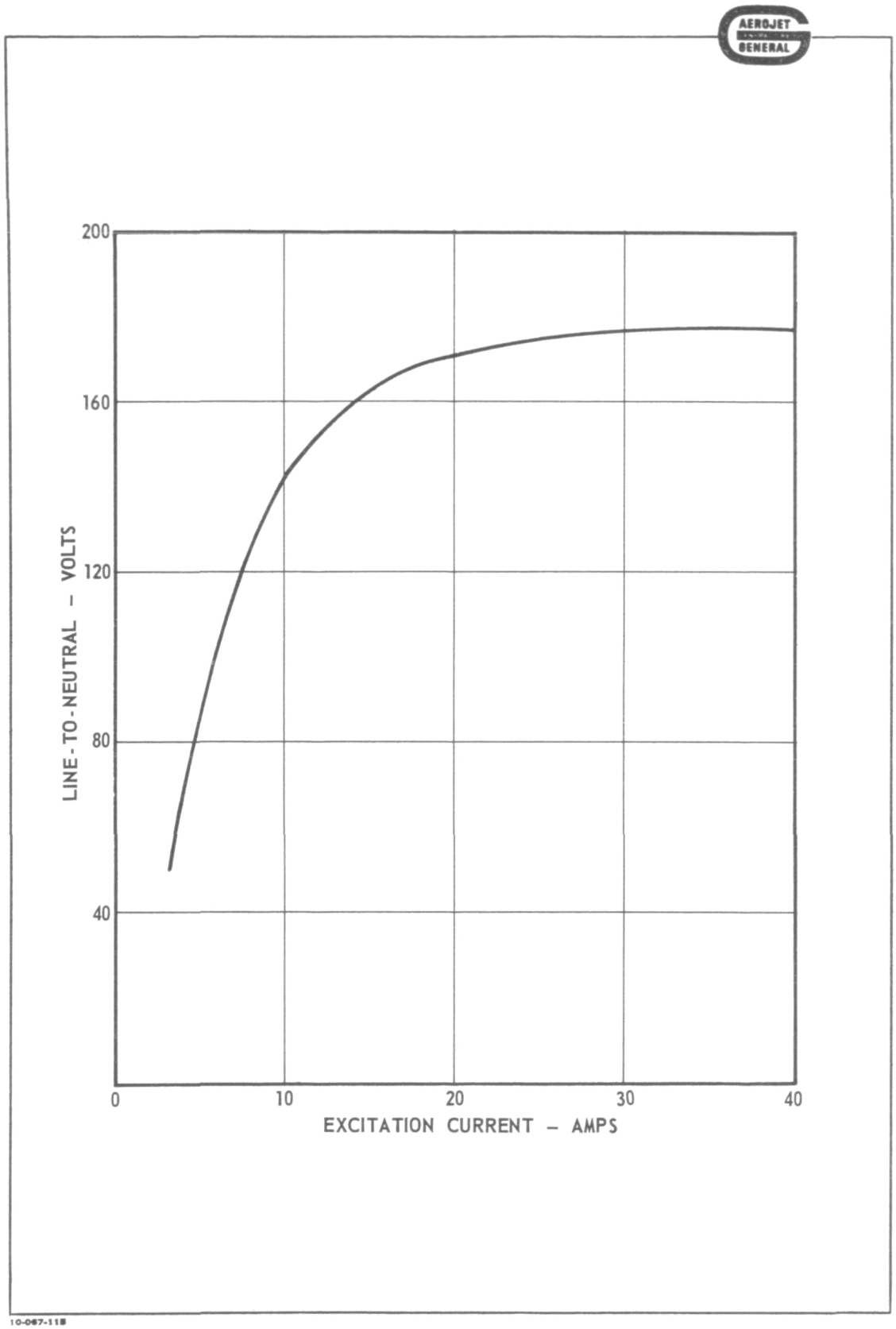

No-Load Saturation - EME Alternator

Figure 23

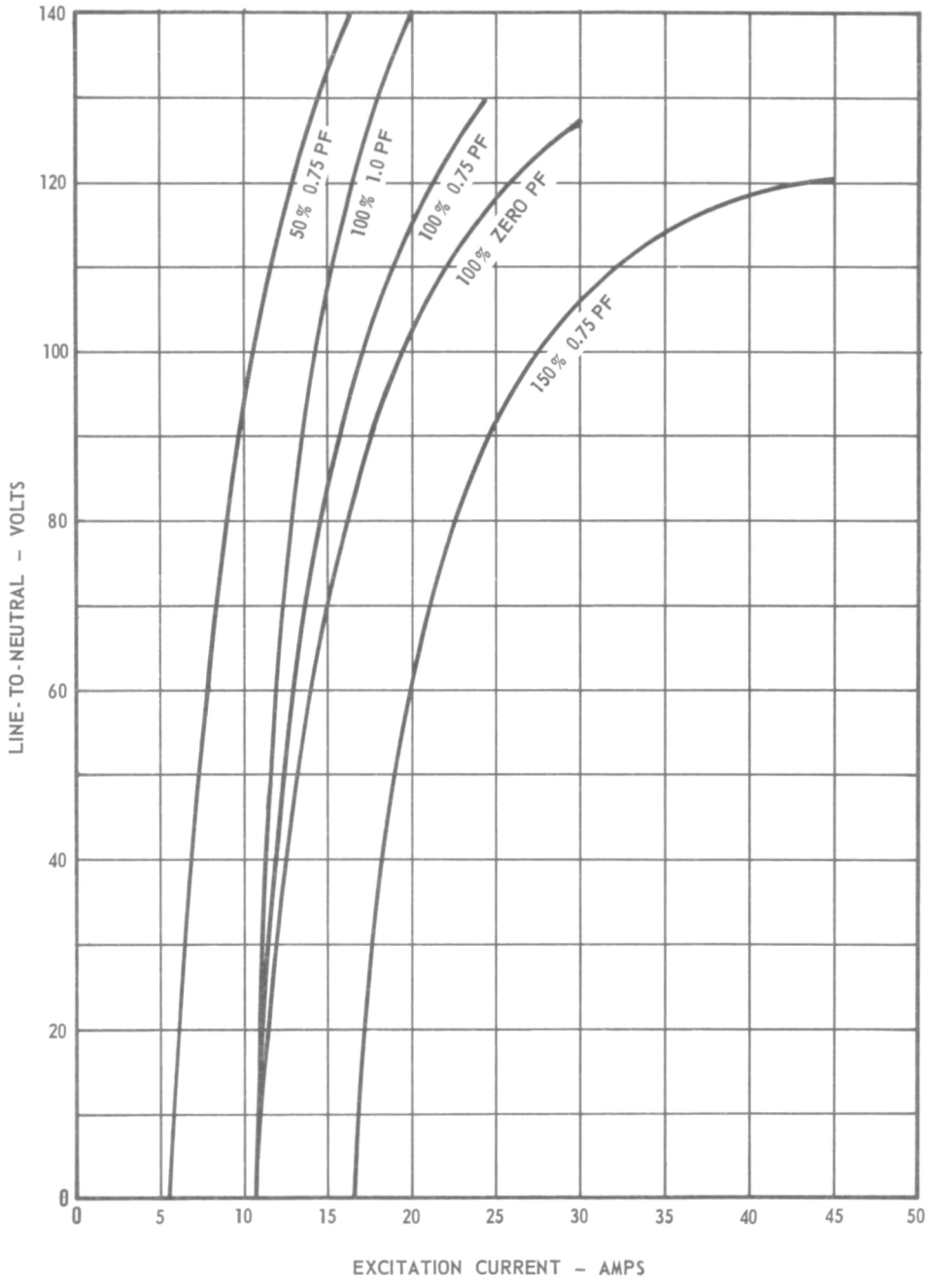

Load Saturation - EME Alternator

Figure 24

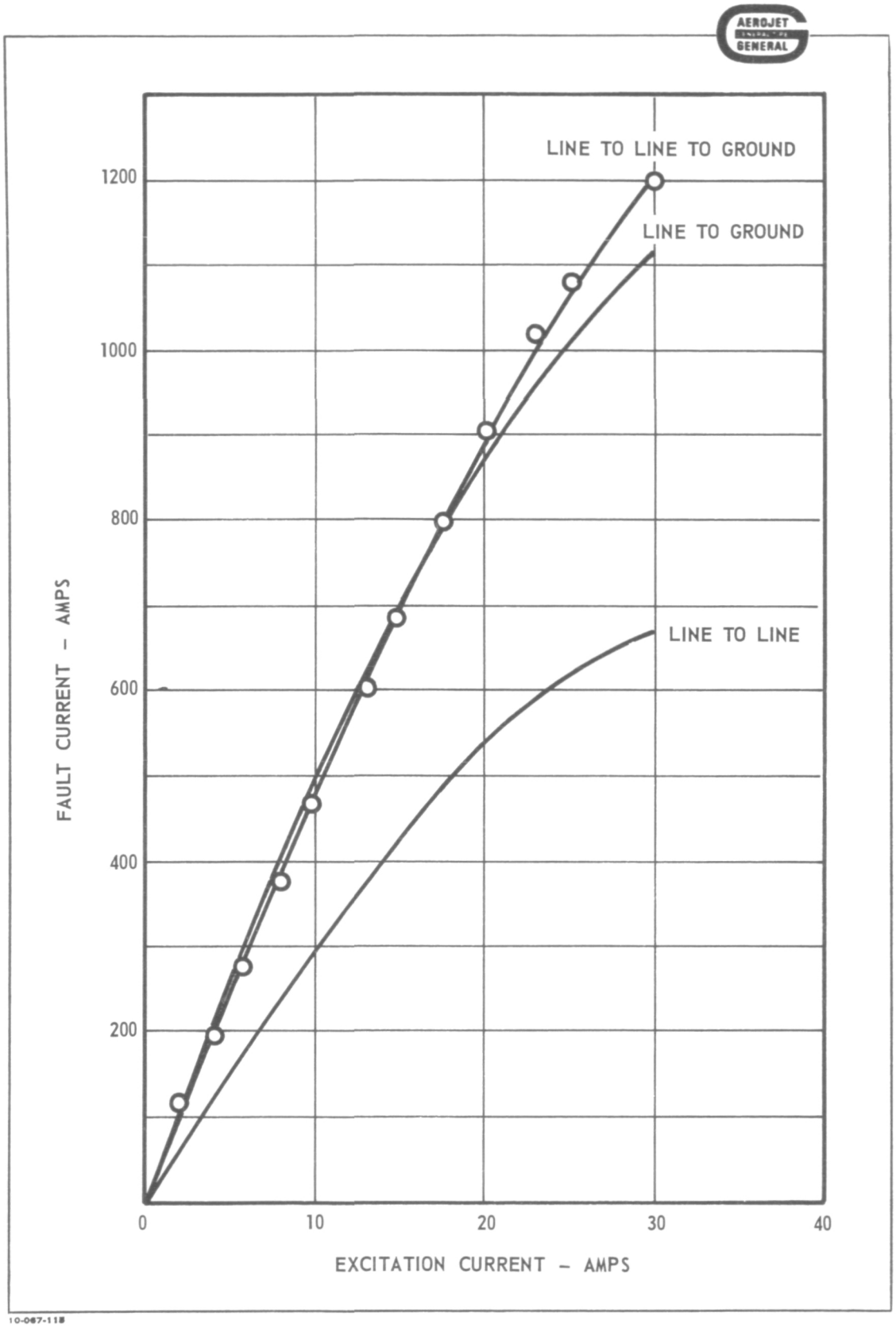

Fault Saturation - EME Alternator

Figure 25

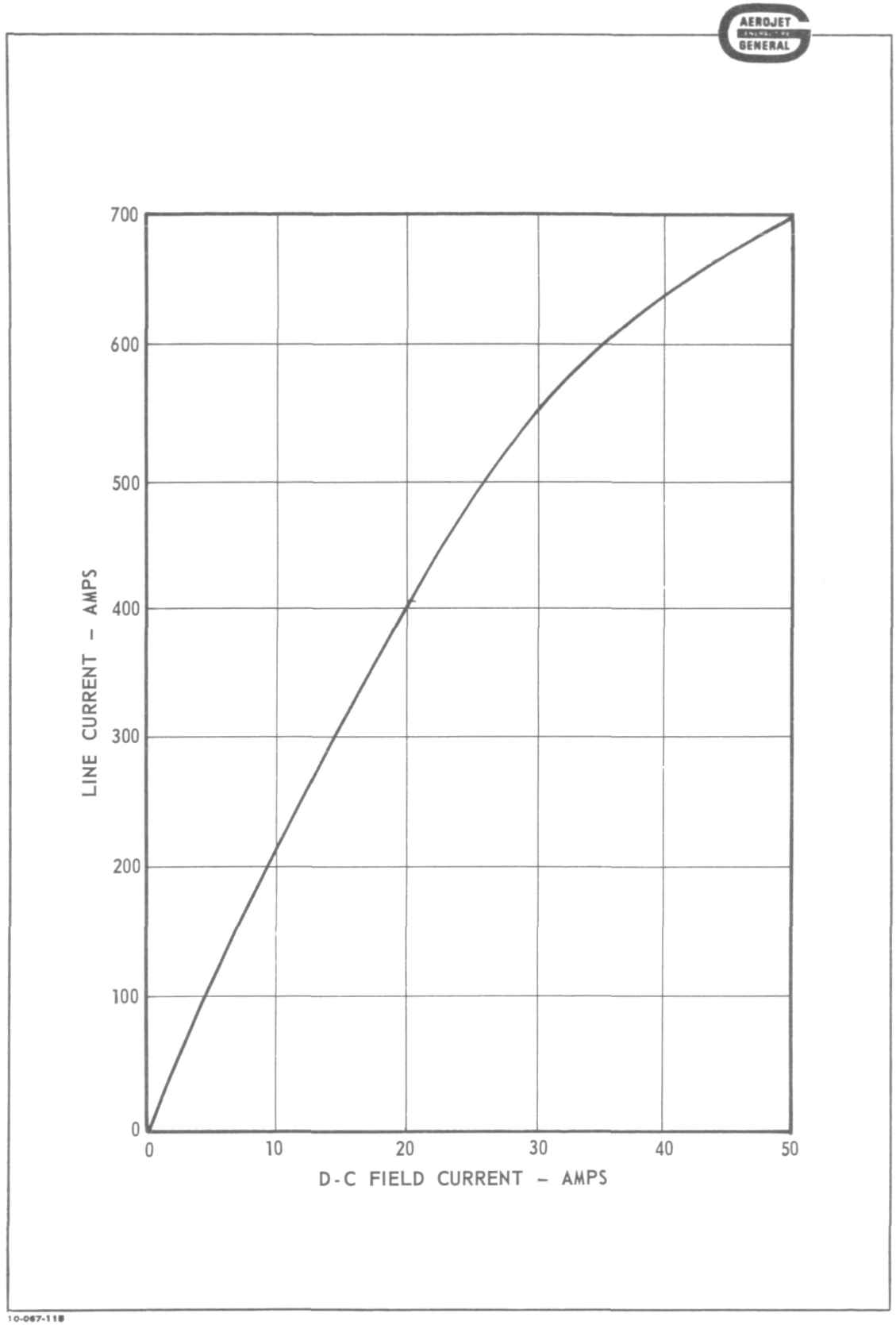

Three-Phase Short-Circuit Saturation - EME Alternator

Figure 26

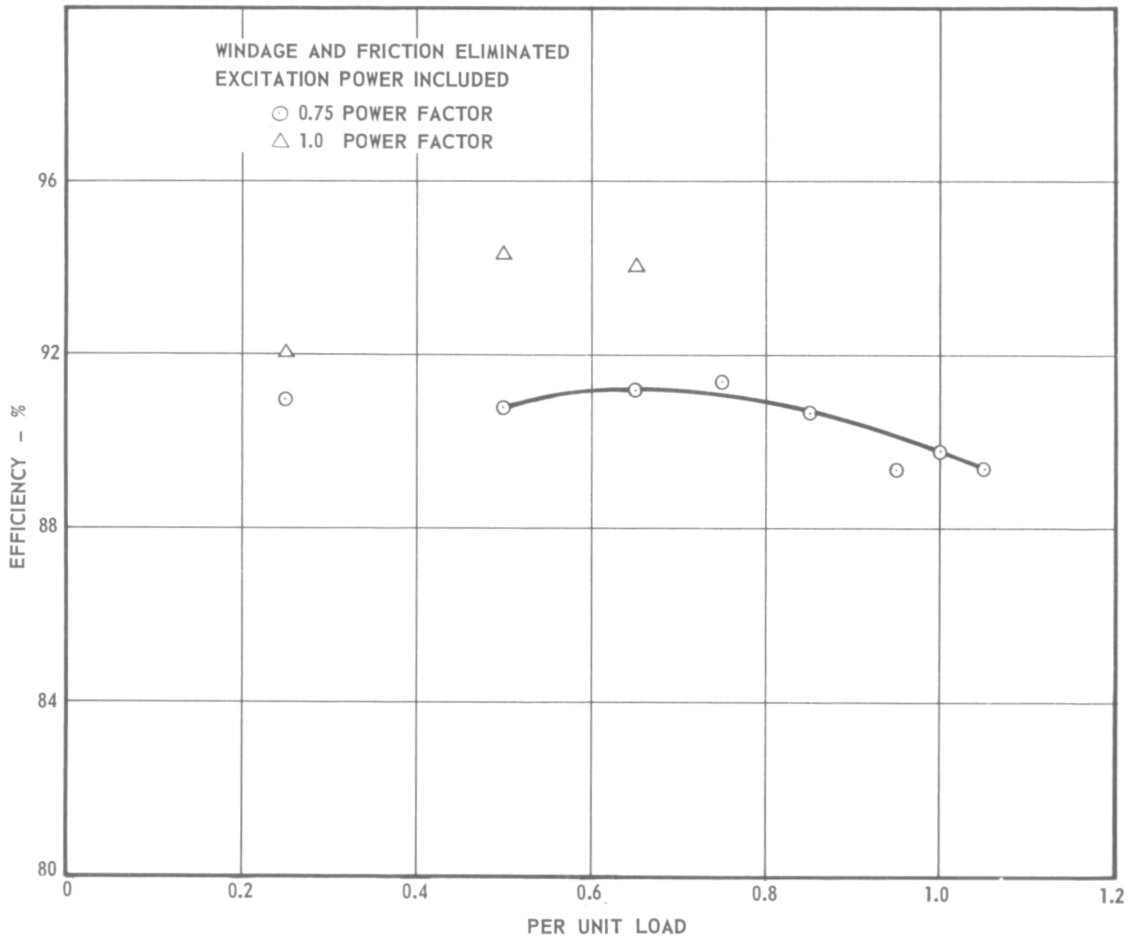

Efficiency - EME Alternator

Figure 27

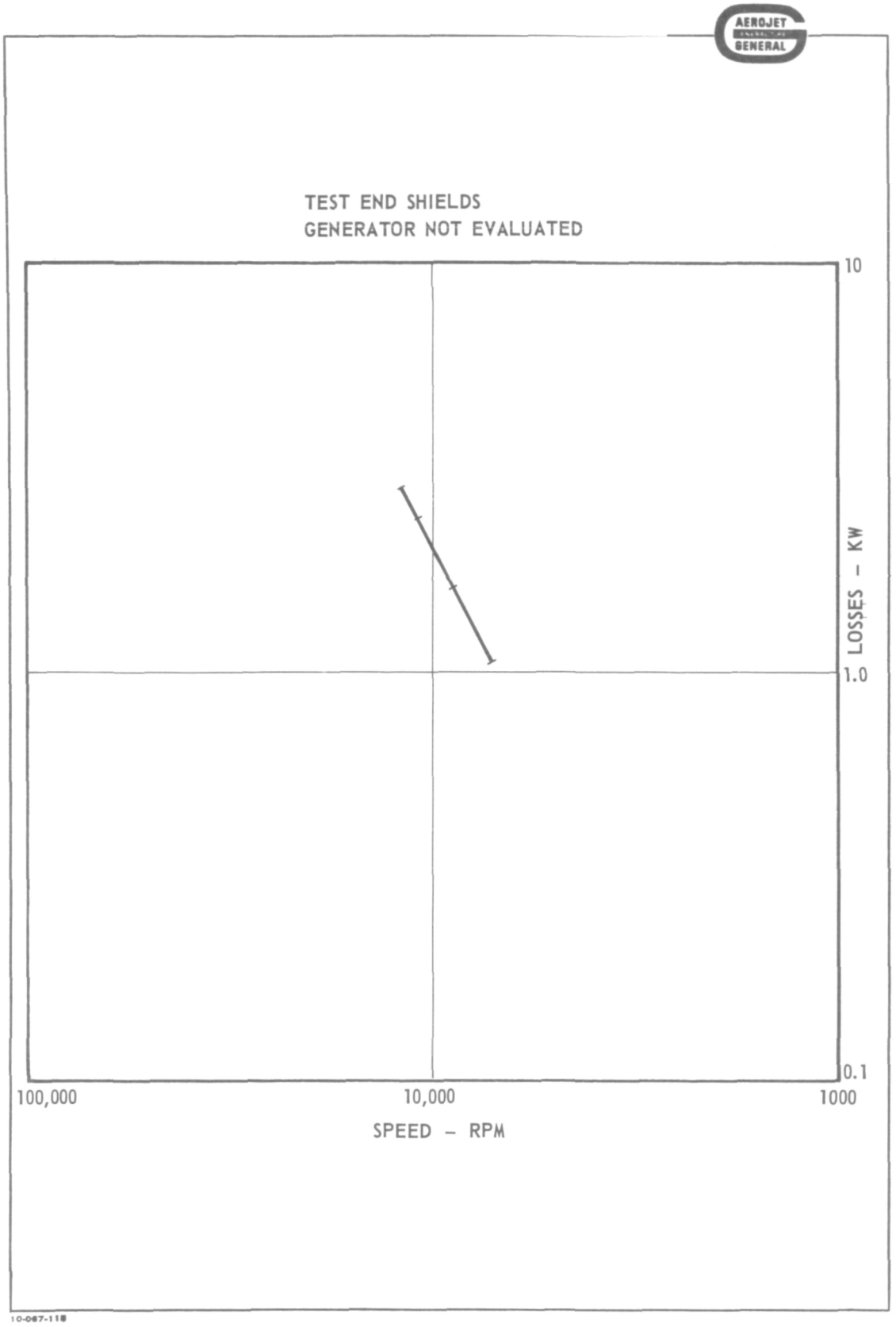

Windage and Friction Losses - EME Alternator

Figure 28

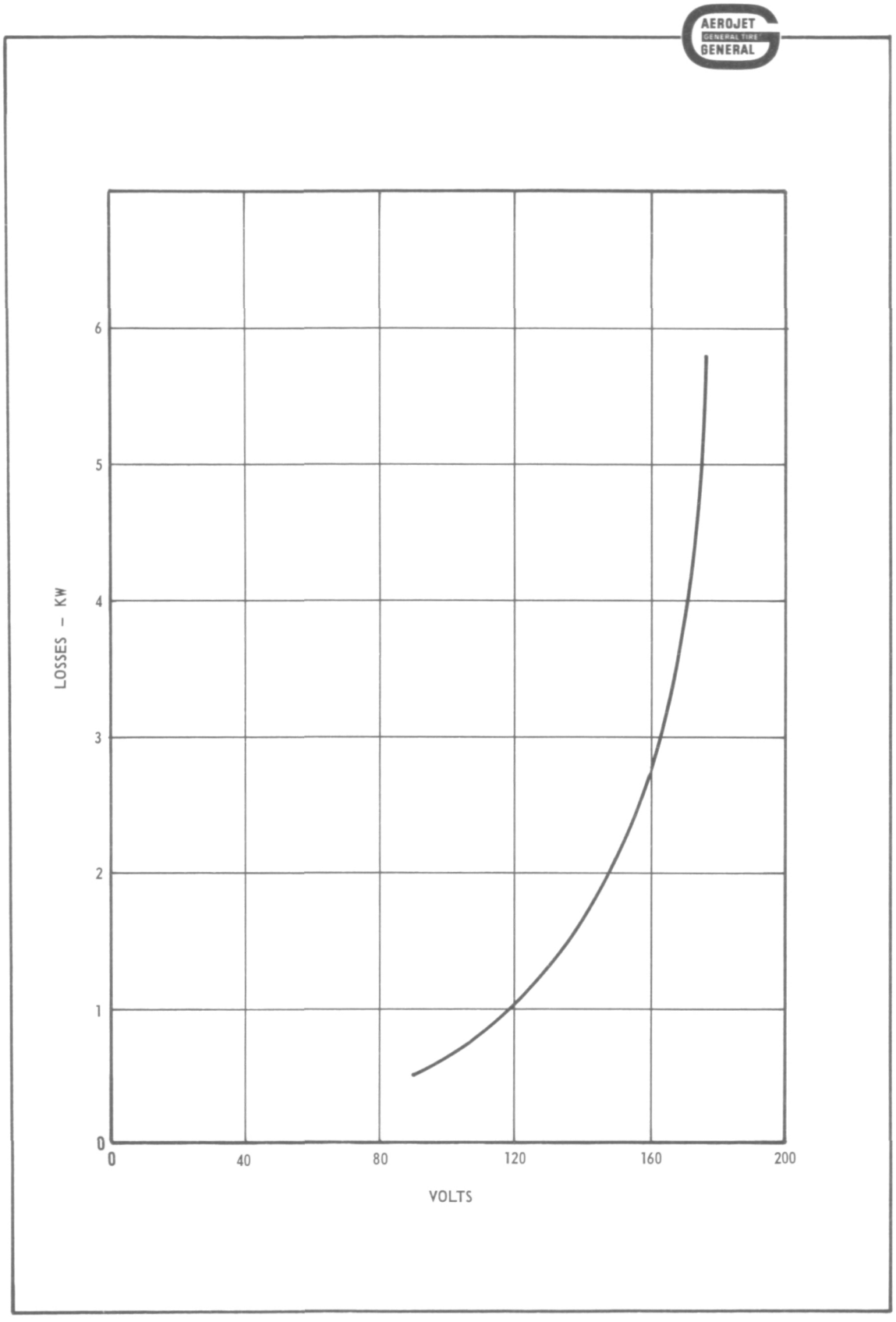

Open-Circuit Core Loss - EME Alternator

Figure 29

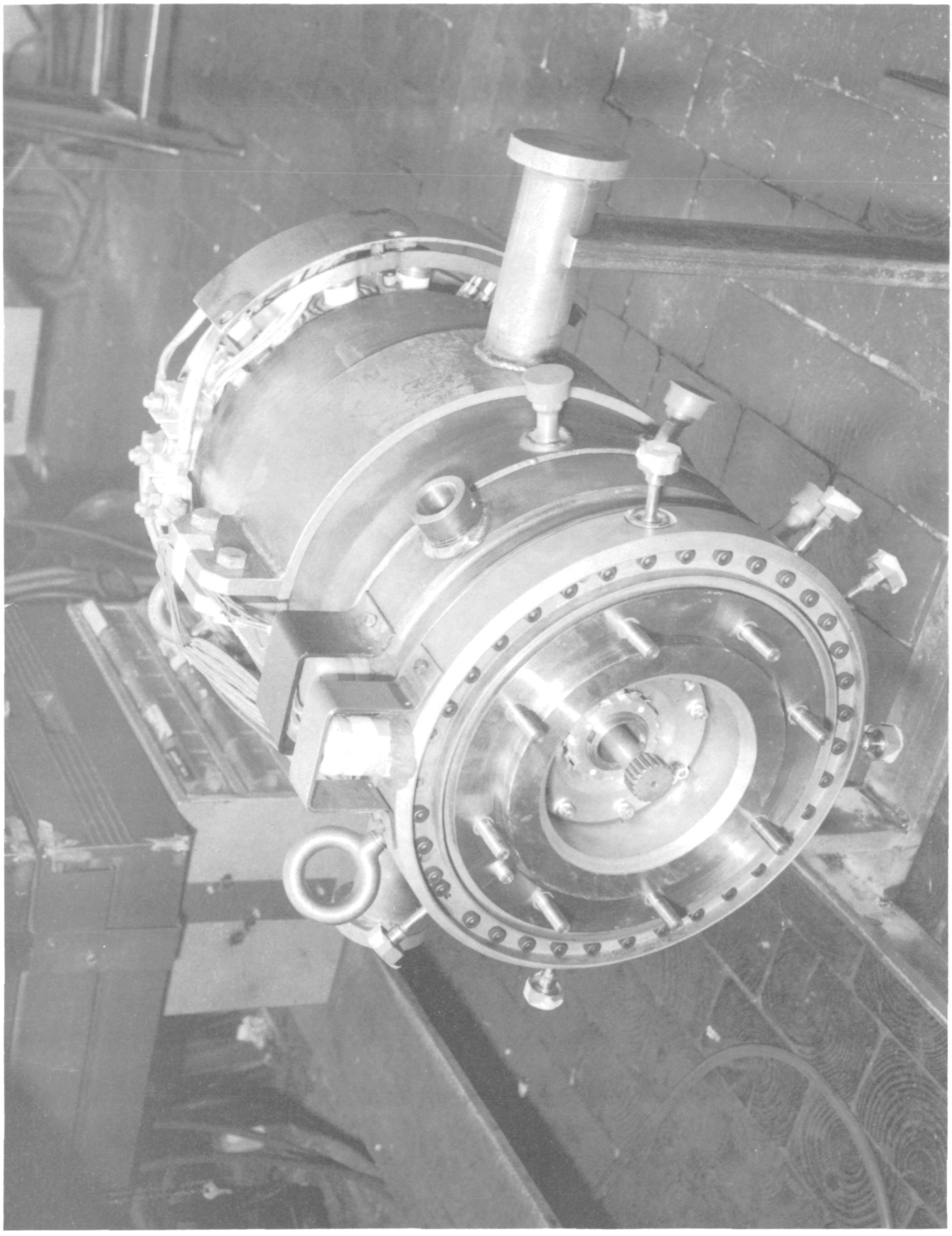

Pre-prototype Alternator

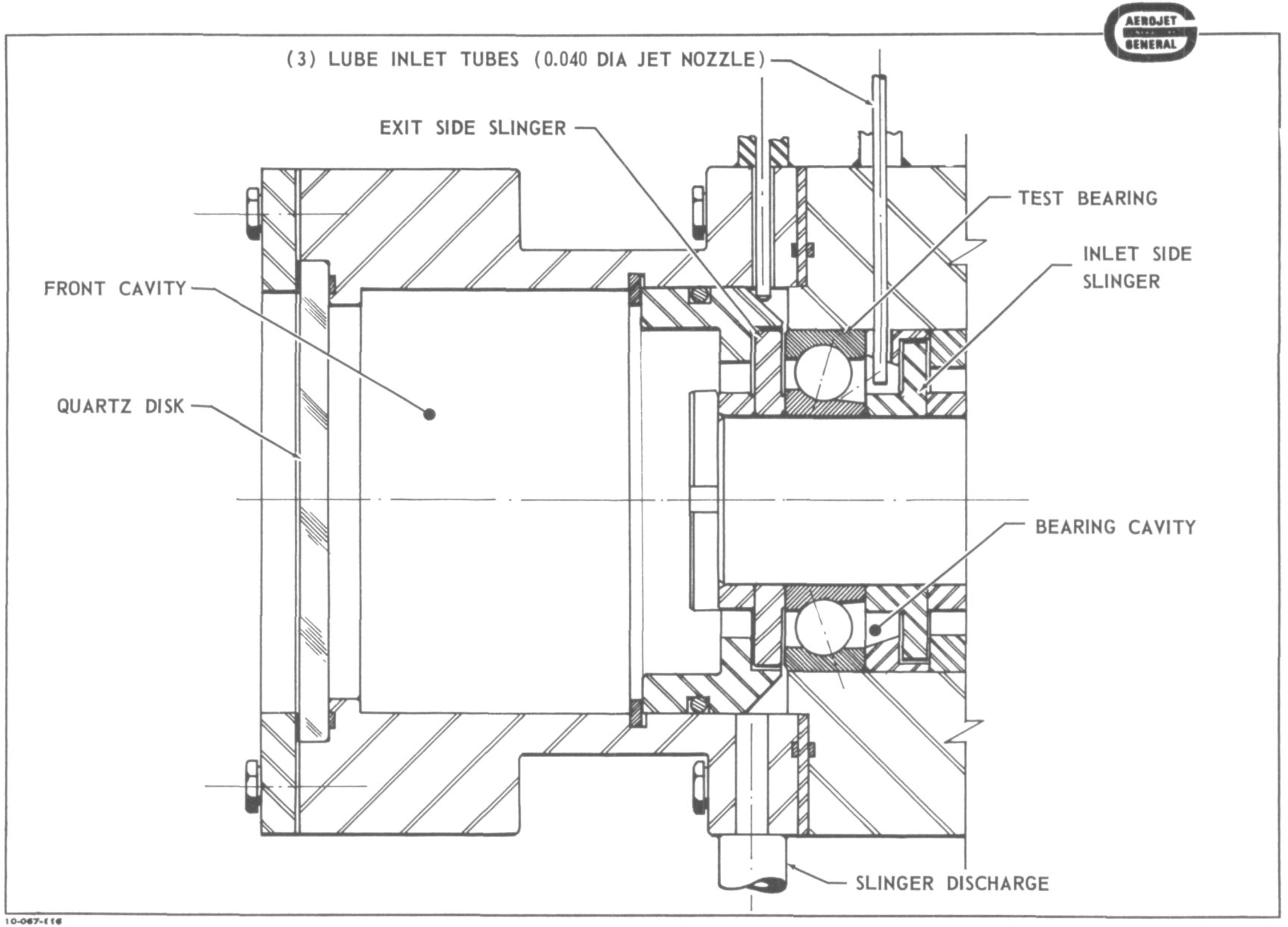

Lubrication Rig No. 1 - Build-up No. 4 and No. 5

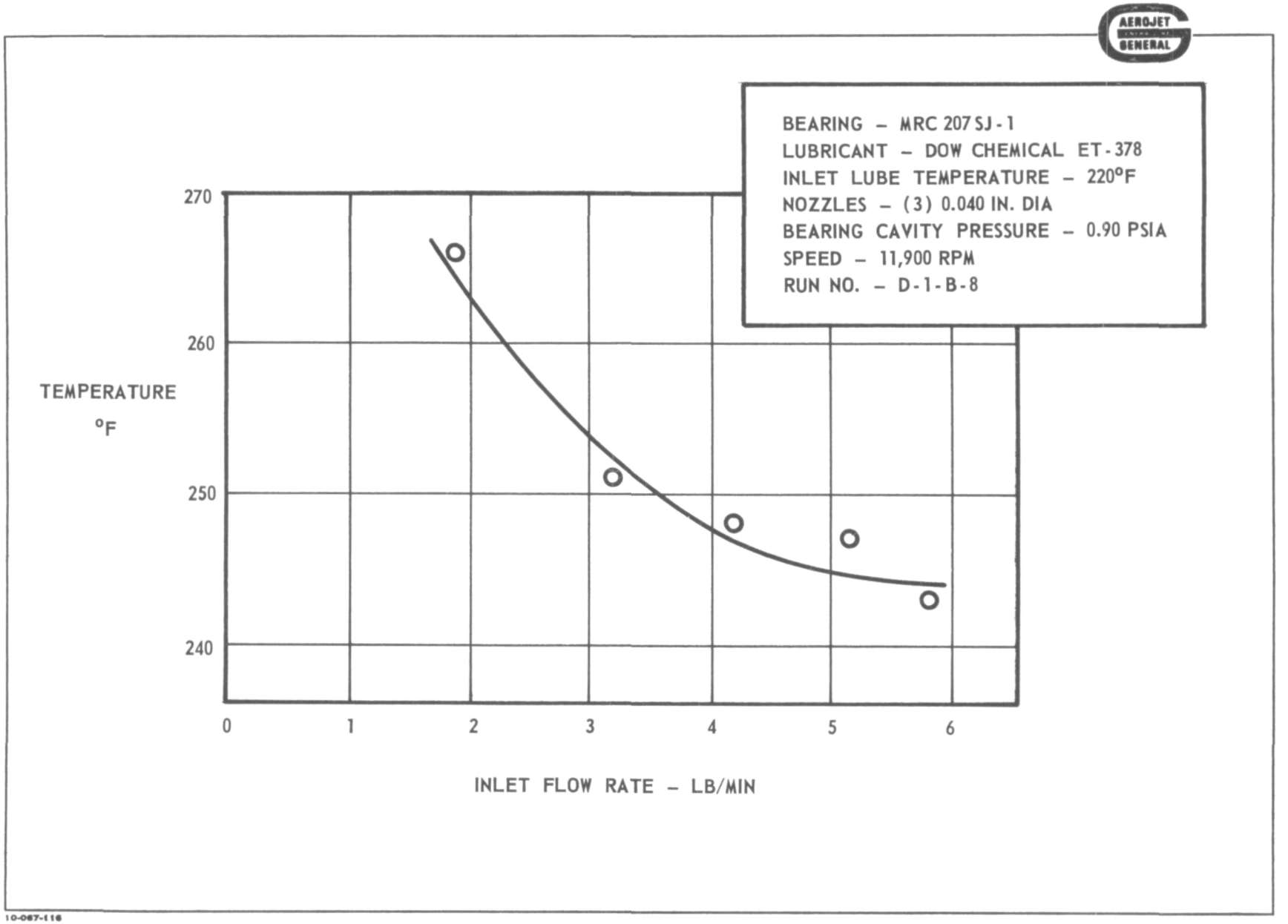

Figure 32

Bearing Outer Race Average Steady-State Temperature vs Inlet Flow Rate

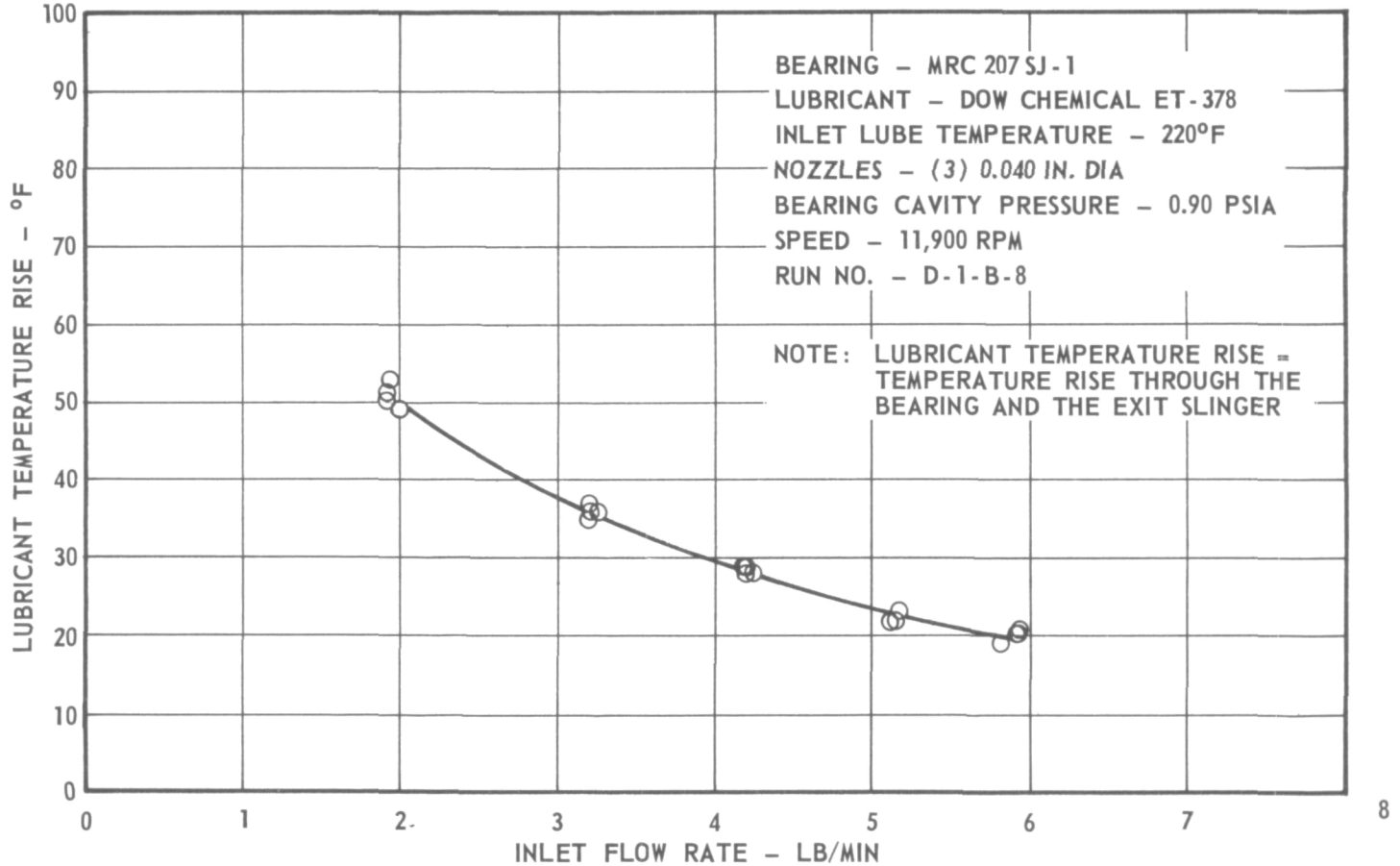

10-067-116

Figure 33

Lubricant Temperature Rise vs Inlet Flow Rate

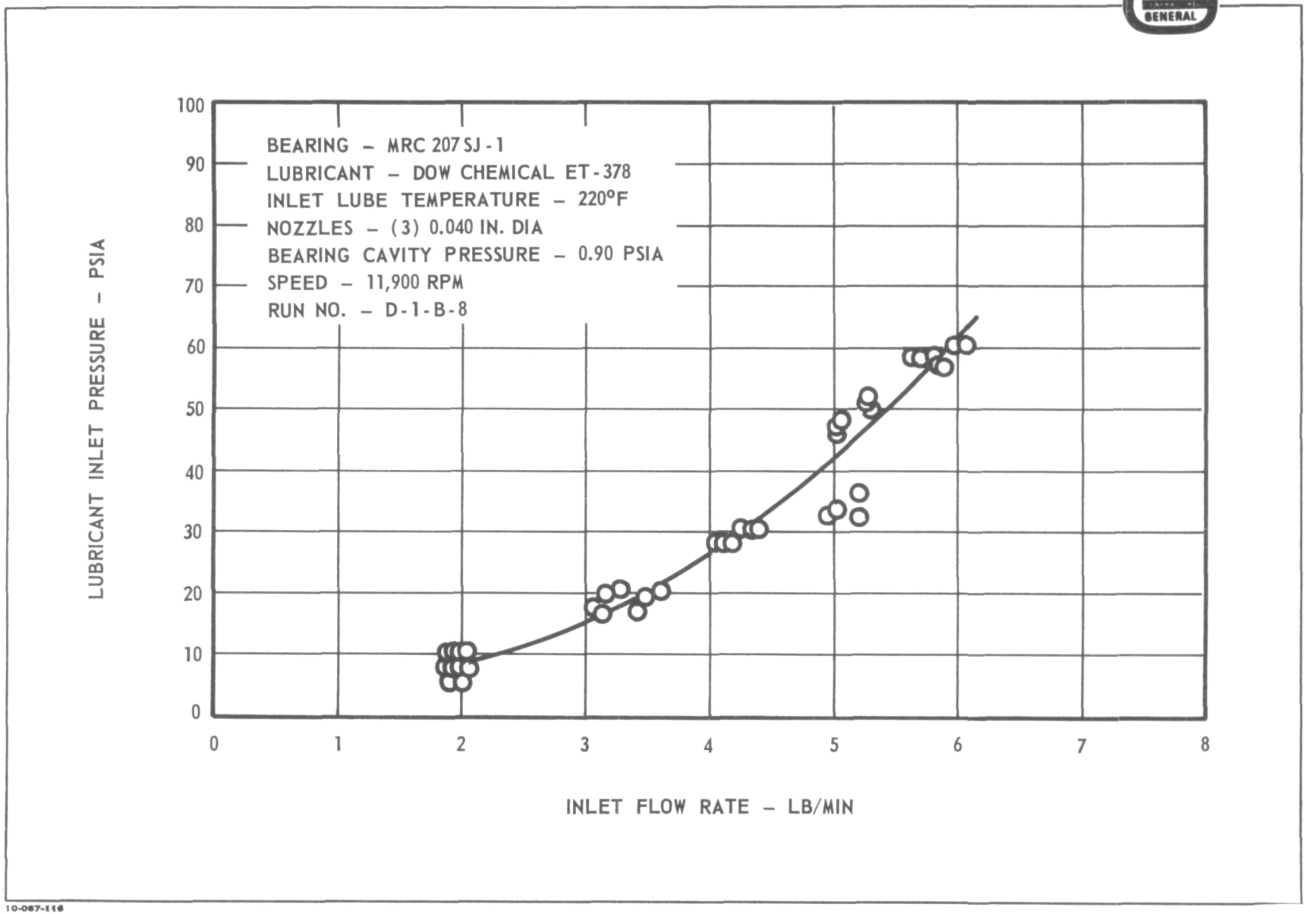

Lubricant Inlet Pressure vs Inlet Flow Rate

Figure 34

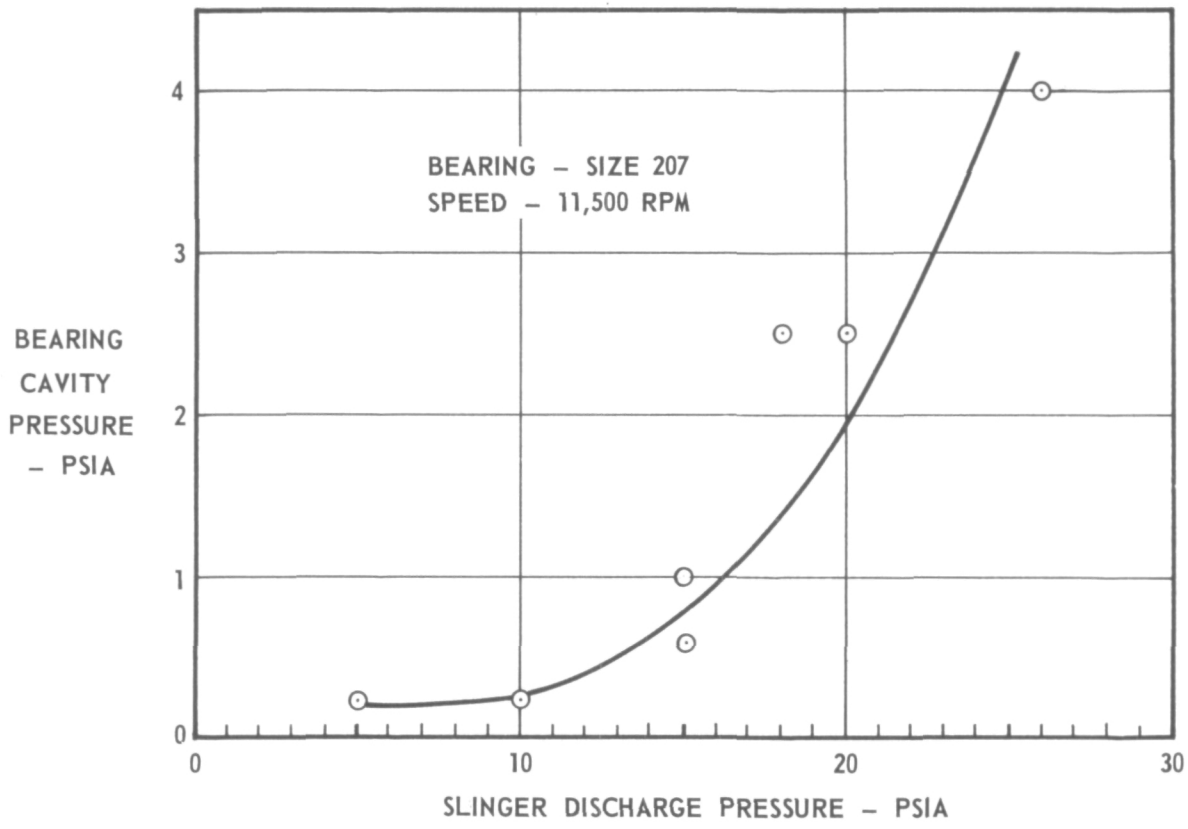

Slinger Scavenging Characteristic - Model A Seal and Lubrication System Simulator

Figure 35

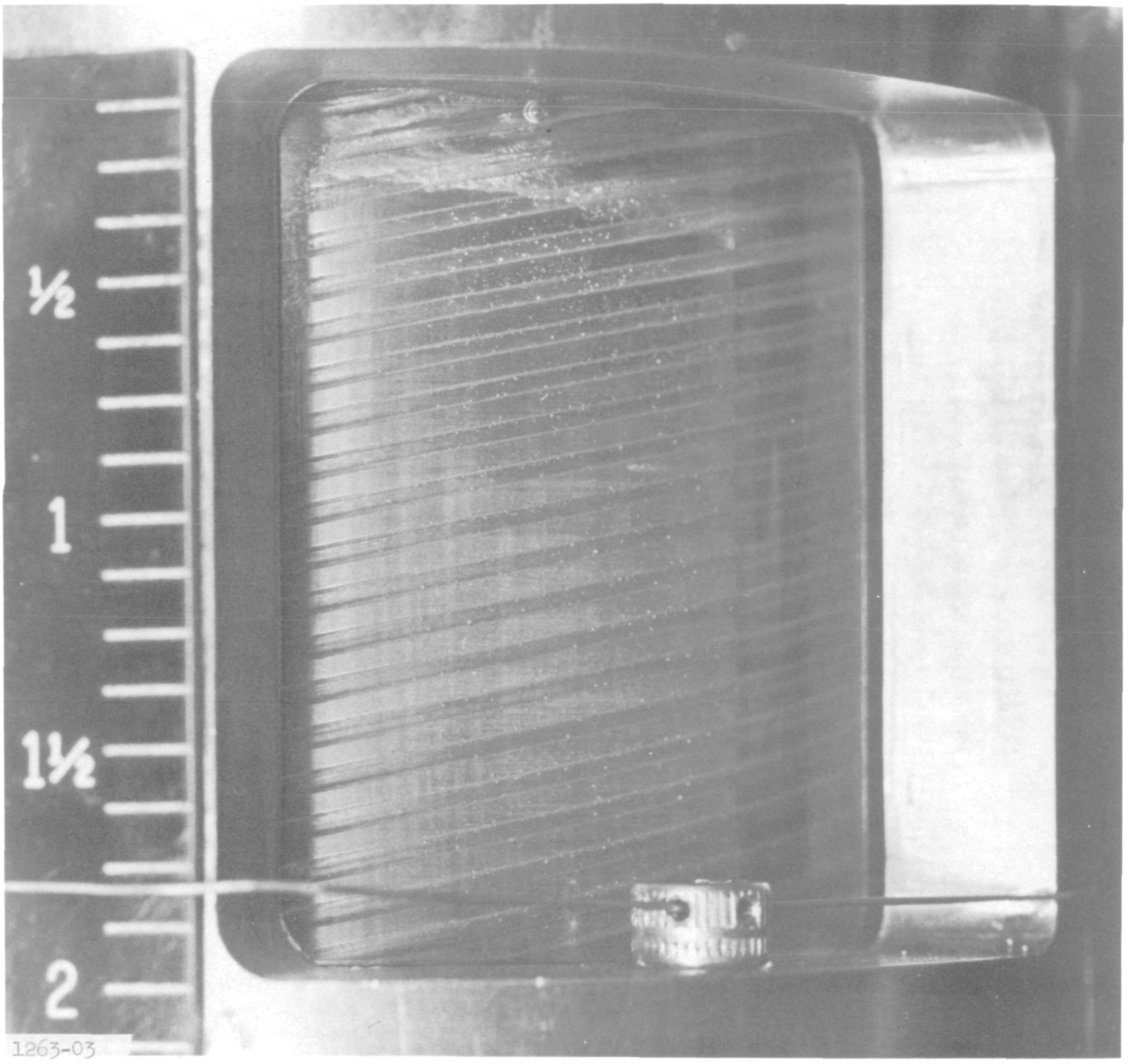

Mercury Visco Pump Interface - Housing Grooves - 11700 rpm
12° helix angle
13 flight thread
ΔP = 100 psi
T = 300°F
Build-Up 1-8
.003-inch radial clearance

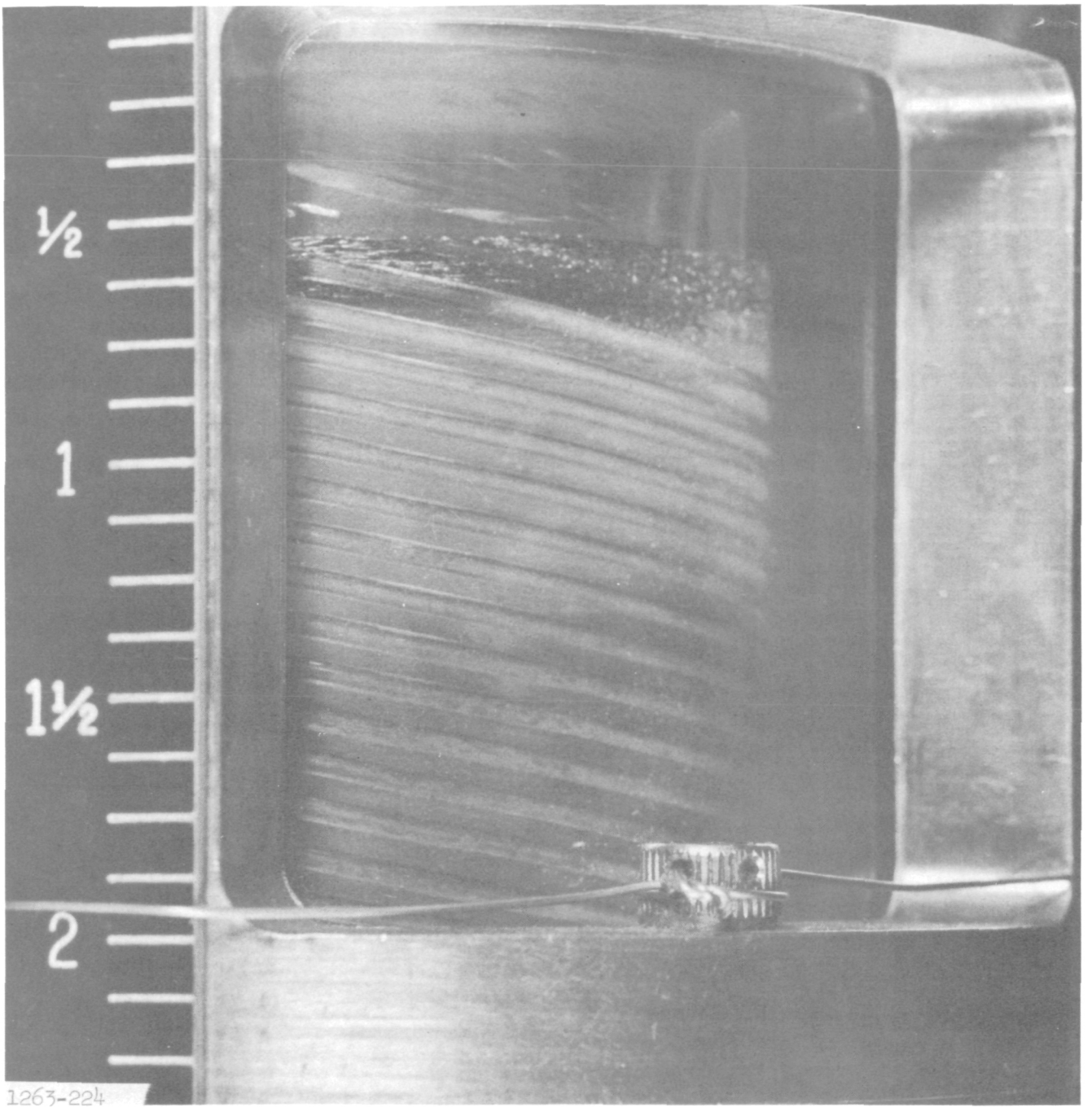

Mercury Visco Pump Interface - Shaft Grooves - 11980 rpm
12° helix angle
13 flight thread
ΔP = 110 psi
T = 287°F
Build-Up 1-9
.003-inch radial clearance

Figure 37

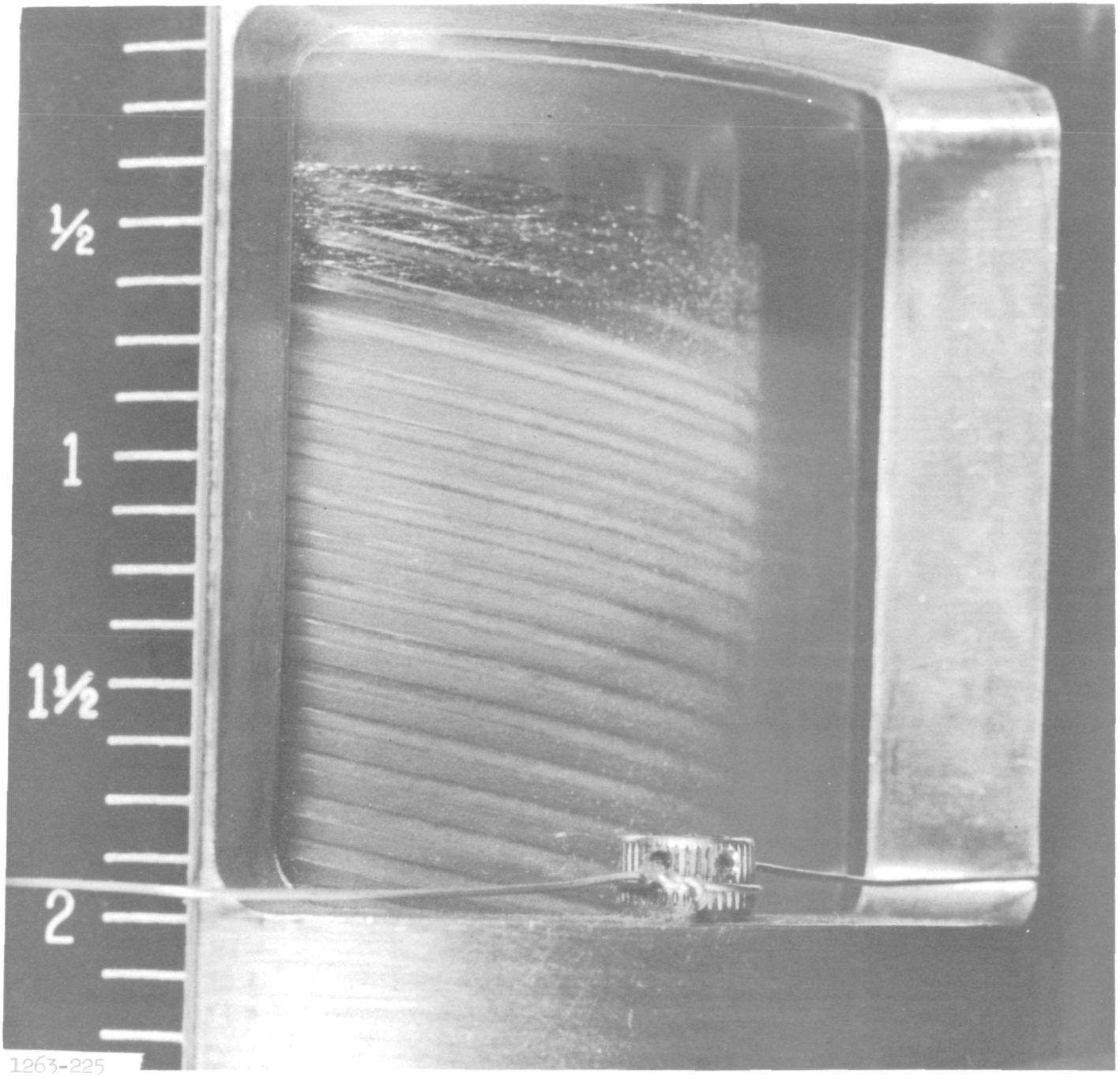

Mercury Visco Pump Interface - Shaft Grooves - 6220 rpm
12° helix angle
13 flight thread
ΔP = 38 psi
T = 126°F
Build-Up 1-9
.003-inch radial clearance

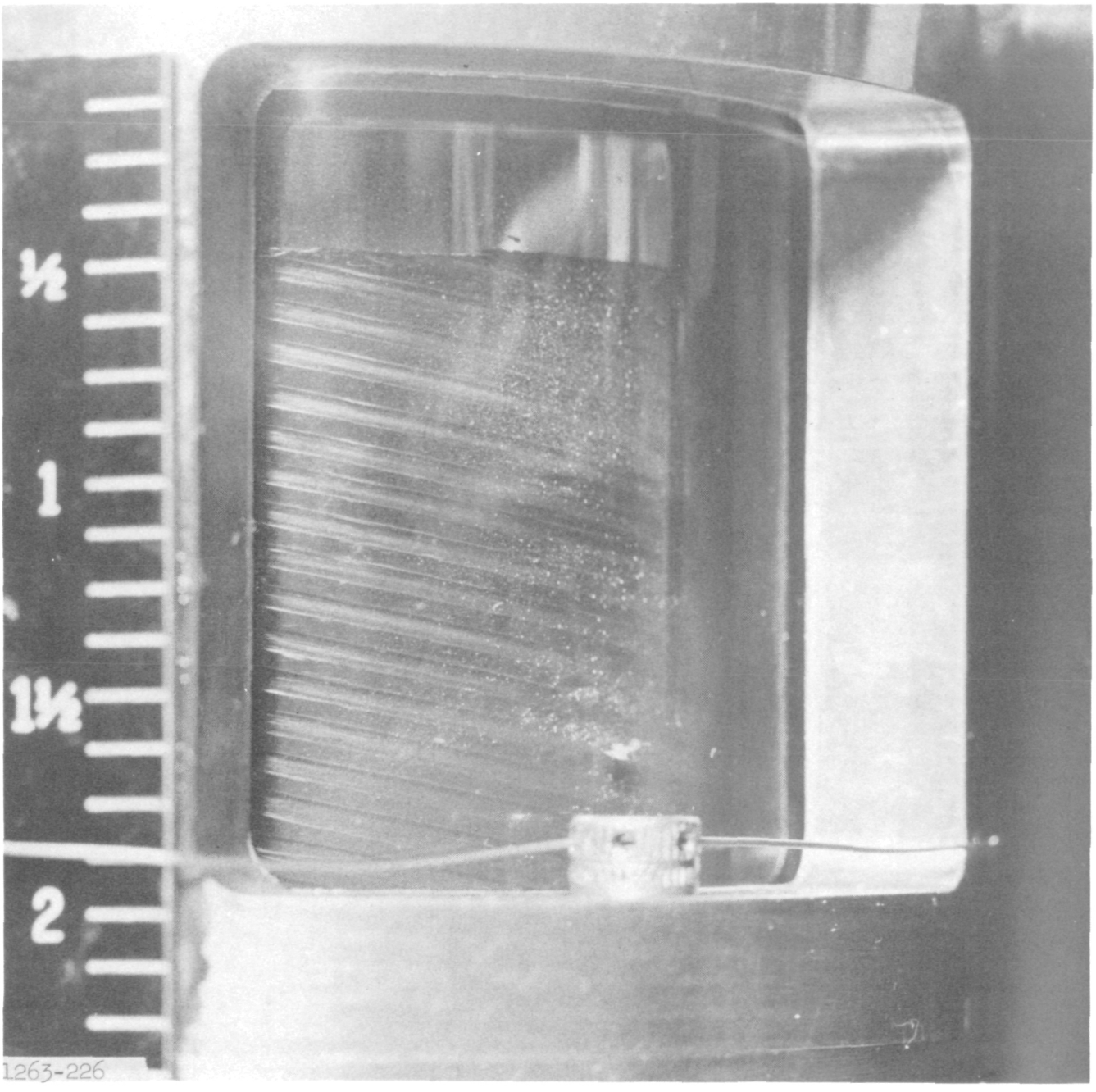

Mercury Visco Pump Interface - Shaft Grooves - 12000 rpm
12° helix angle
13 flight thread
ΔP = 40 psi
T = 250°F
Build-Up 1-11
.005-inch radial clearance

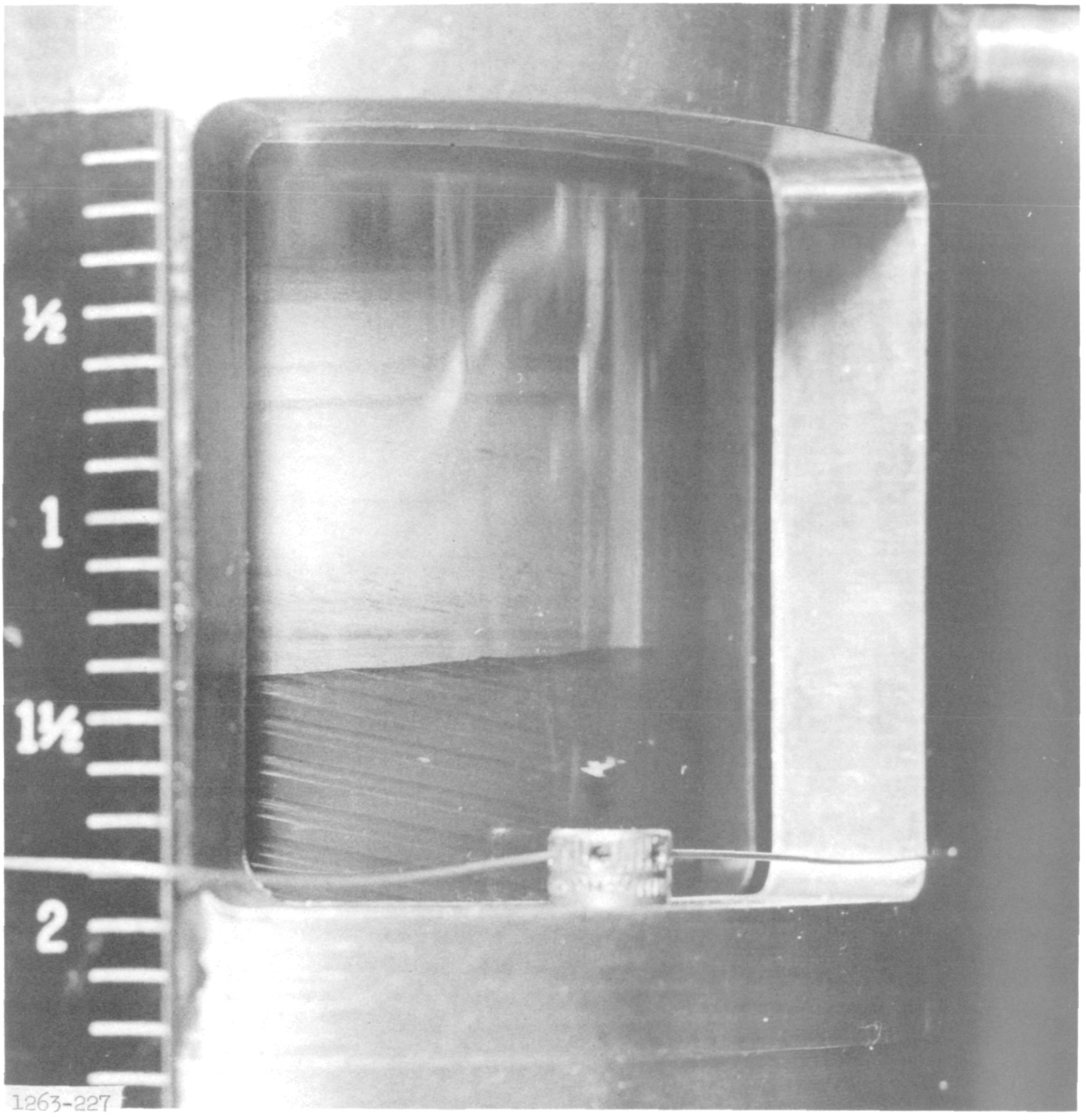

Mercury Visco Pump Interface - Shaft Grooves - 5980 rpm
12° helix angle
13 flight thread
ΔP = 70 psi
T = 145°F
Build-Up 1-11
.005-inch radial clearance

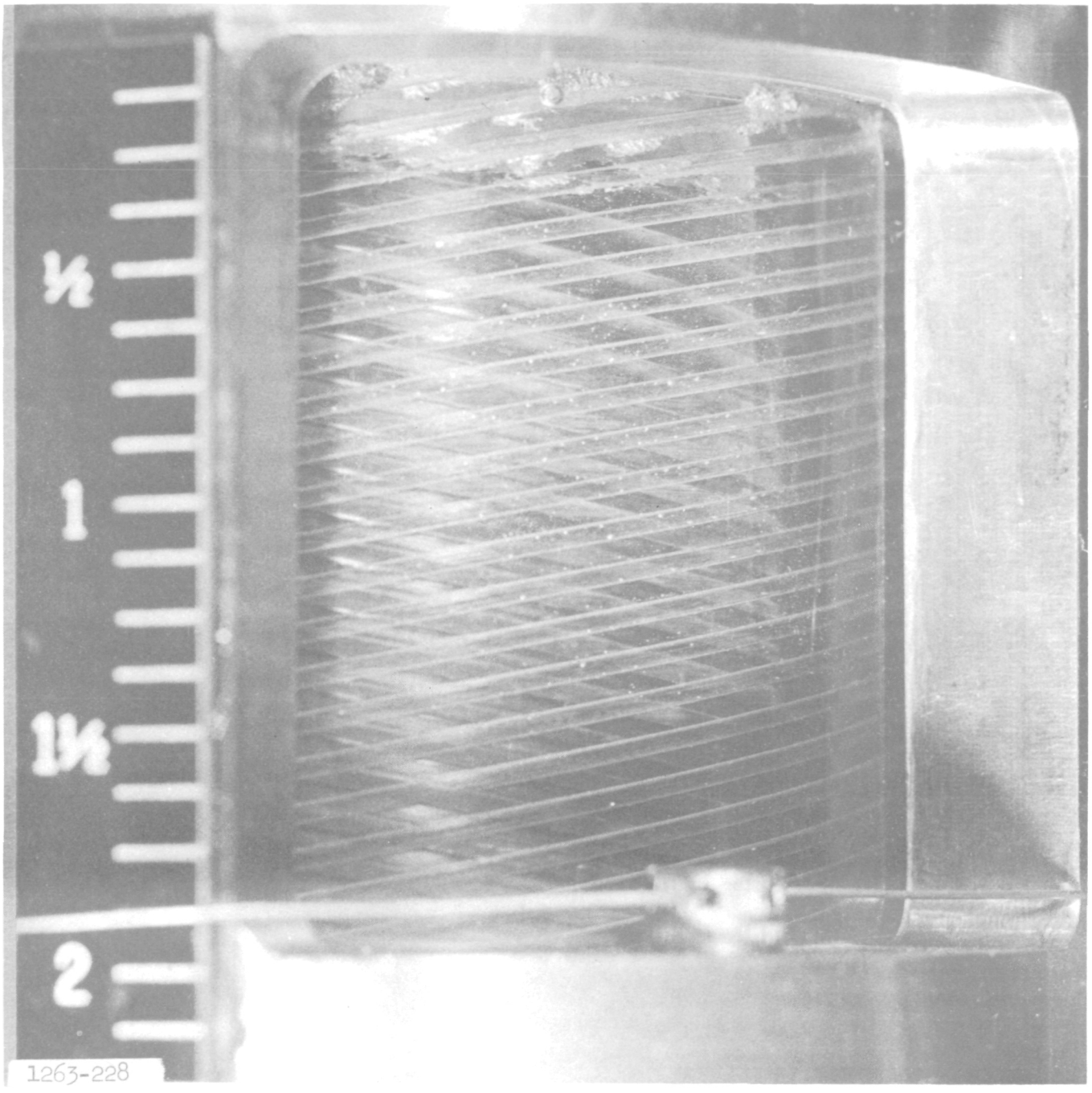

Mercury Visco Pump Interface - Housing and Shaft Grooves - 12000 rpm
12° helix angle
13 flight thread
ΔP = 80 psi
T = 295°F
Build-Up 1-12
.005-inch radial clearance

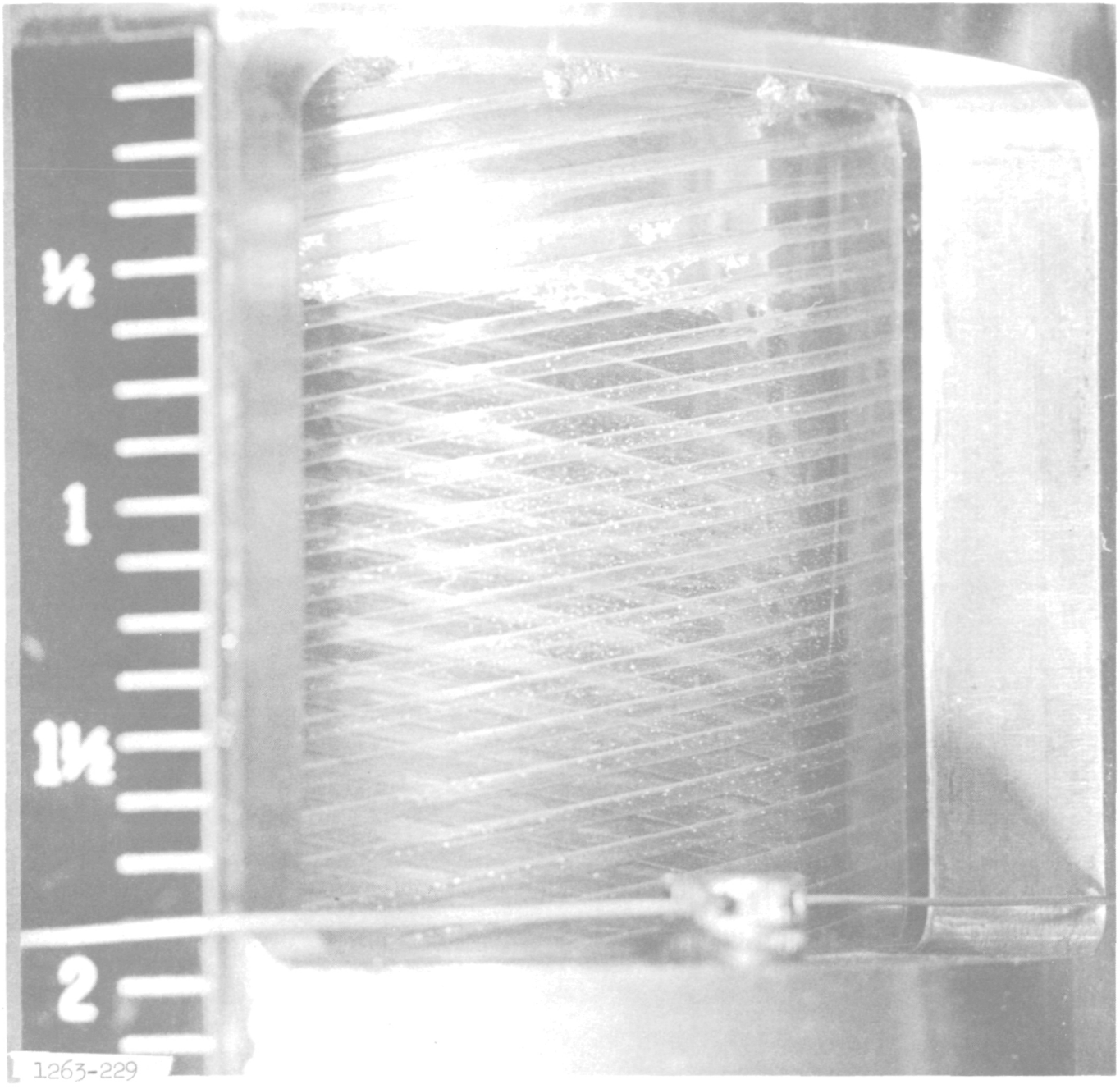

Mercury Visco Pump Interface - Housing and Shaft Grooves - 6000 rpm
12° helix angle
13 flight thread
ΔP = 80 psi
T = 135°F
Build-Up 1-12
.005-inch radial clearance

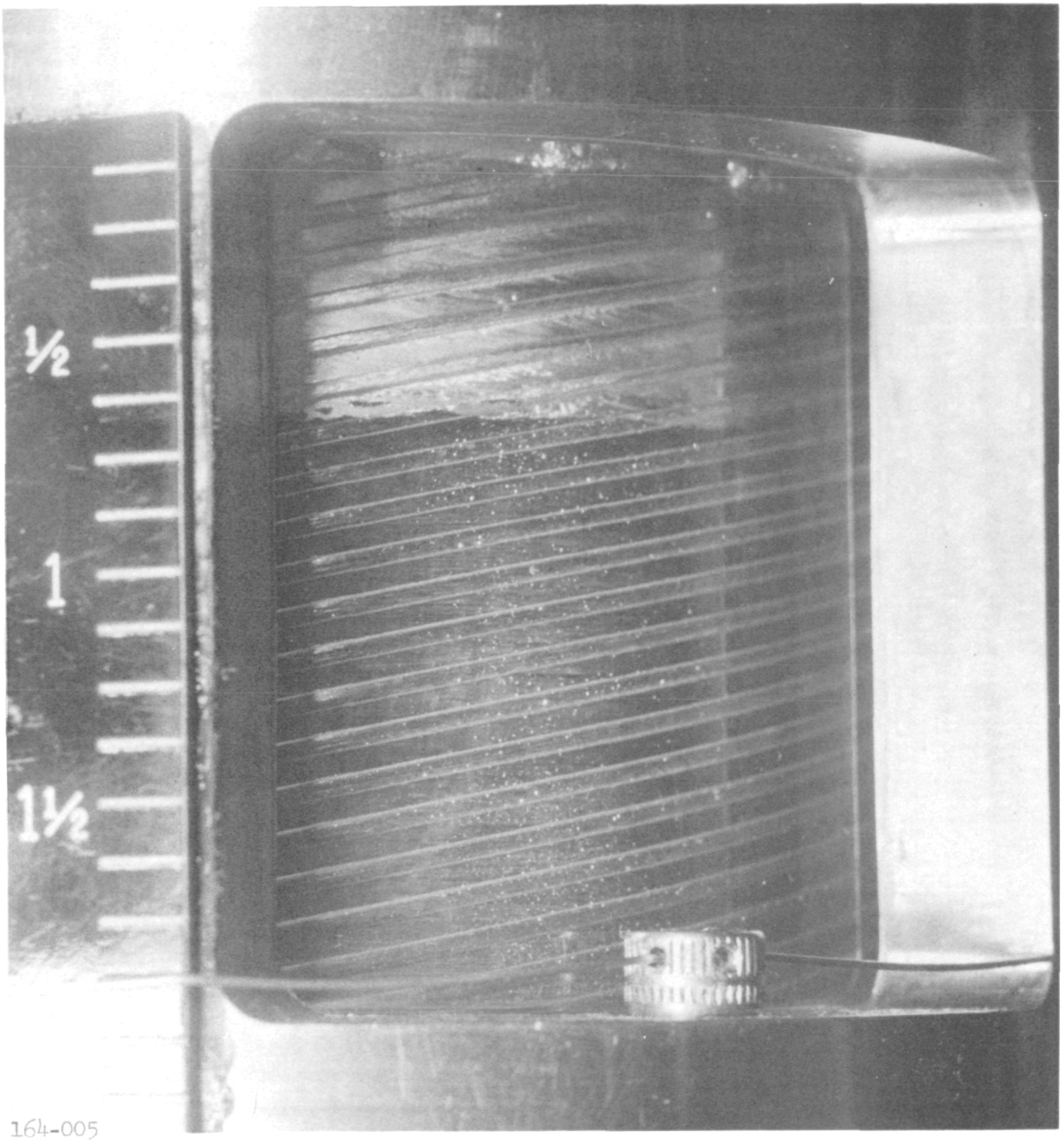

Mercury Visco Pump Interface - Housing Grooves - 12000 rpm
12° helix angle
13 flight thread
ΔP = 110 psi
T = 305°F
Build-Up 1-13
.005 inch radial clearance

Figure 43

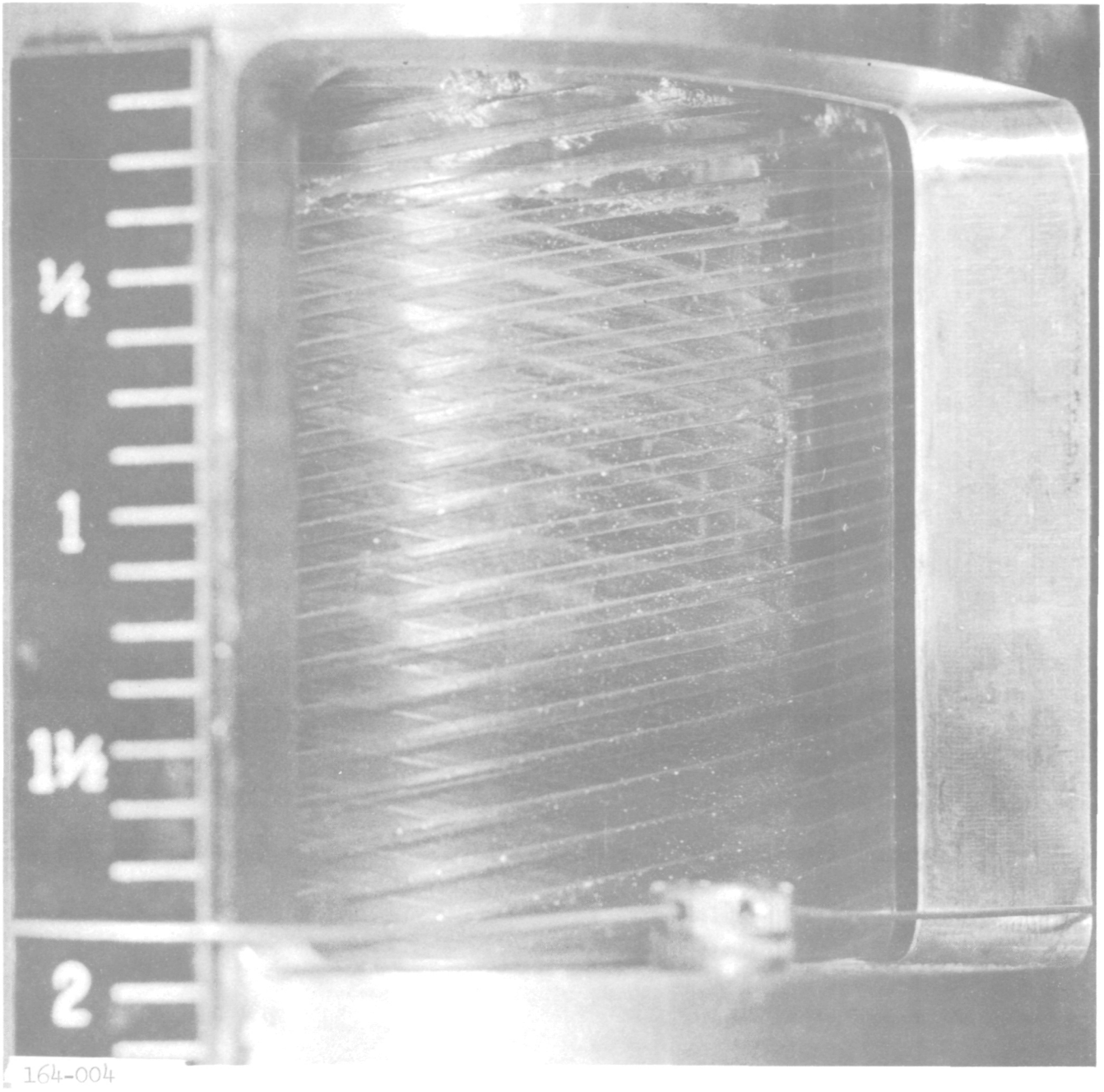

Mercury Visco Pump Interface - Housing and Shaft Grooves - 12000 rpm
12° helix angle
13 flight thread
ΔP = 120 psi
T = 310°F
Build-Up 1-14
.007-inch radial clearance

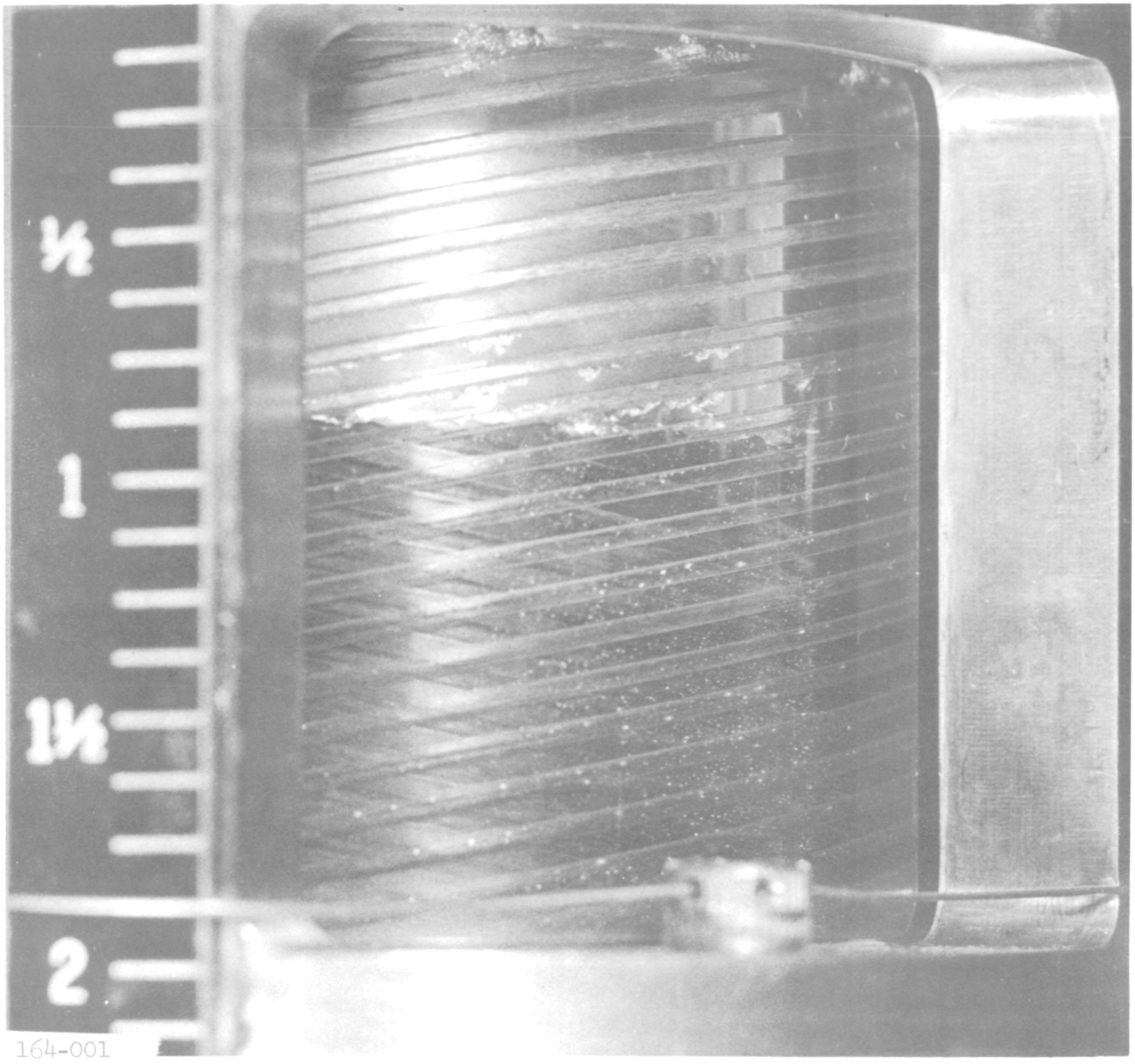

Mercury Visco Pump Interface - Housing and Shaft Grooves - 6000 rpm
12° helix angle
13 flight thread
ΔP = 70 psi
T = 125°F
Build Up 1-14
.007 inch radial clearance

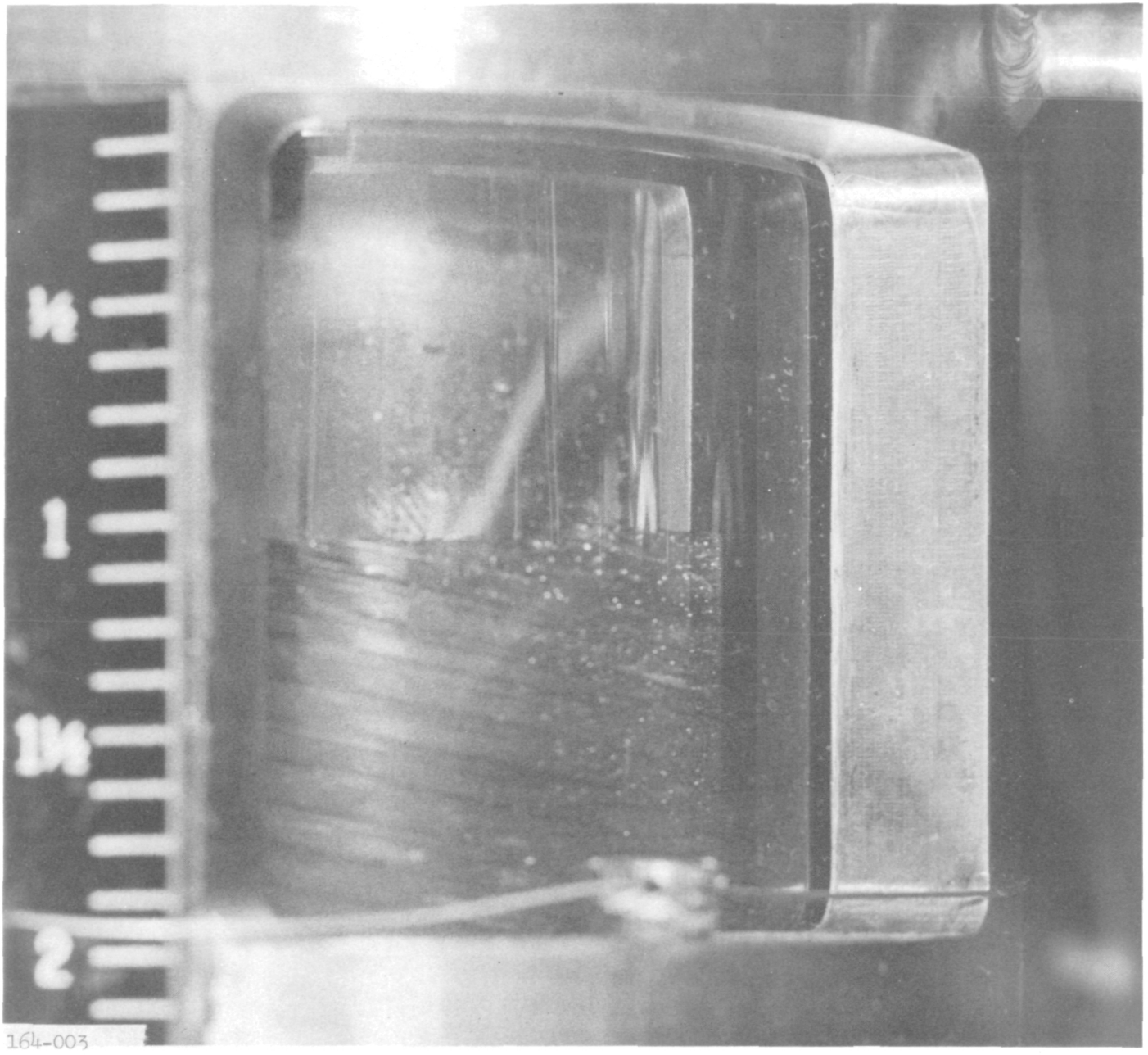

Mercury Visco Pump Interface - Shaft Grooves - 12000 rpm
12° helix angle
13 flight thread
P = 120 psi
T = 330°F
Build-Up 1-15
.007-inch radial clearance

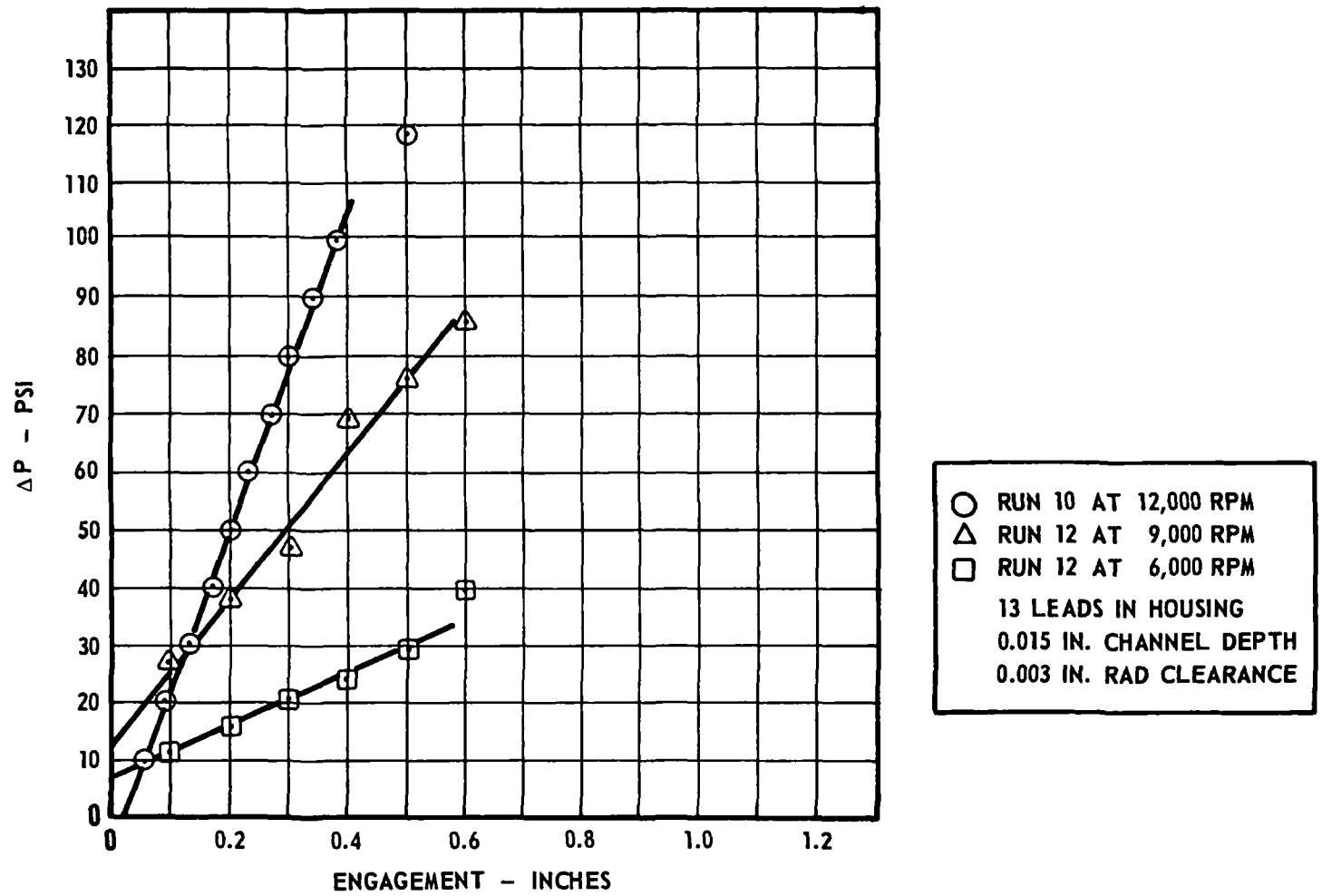

Pressure Differential vs Axial Engagement - Build-Up 1-8

Figure 47

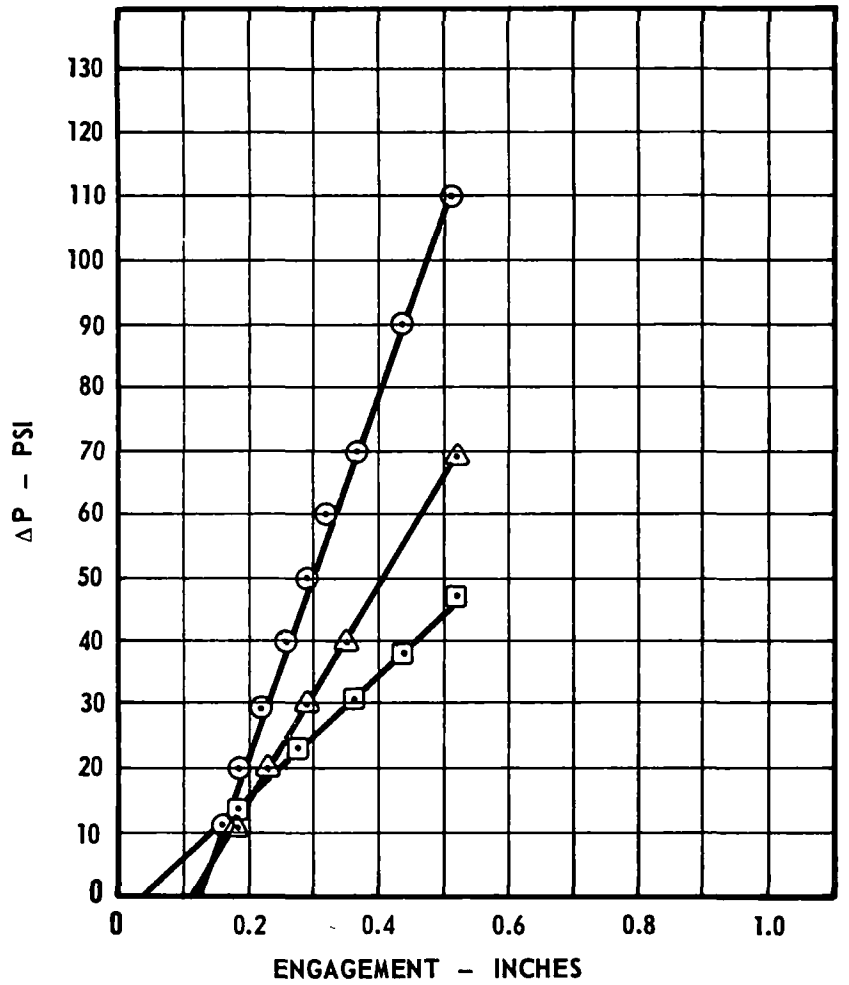

Pressure Differential vs Axial Engagement - Build-Up 1-9

Figure 48

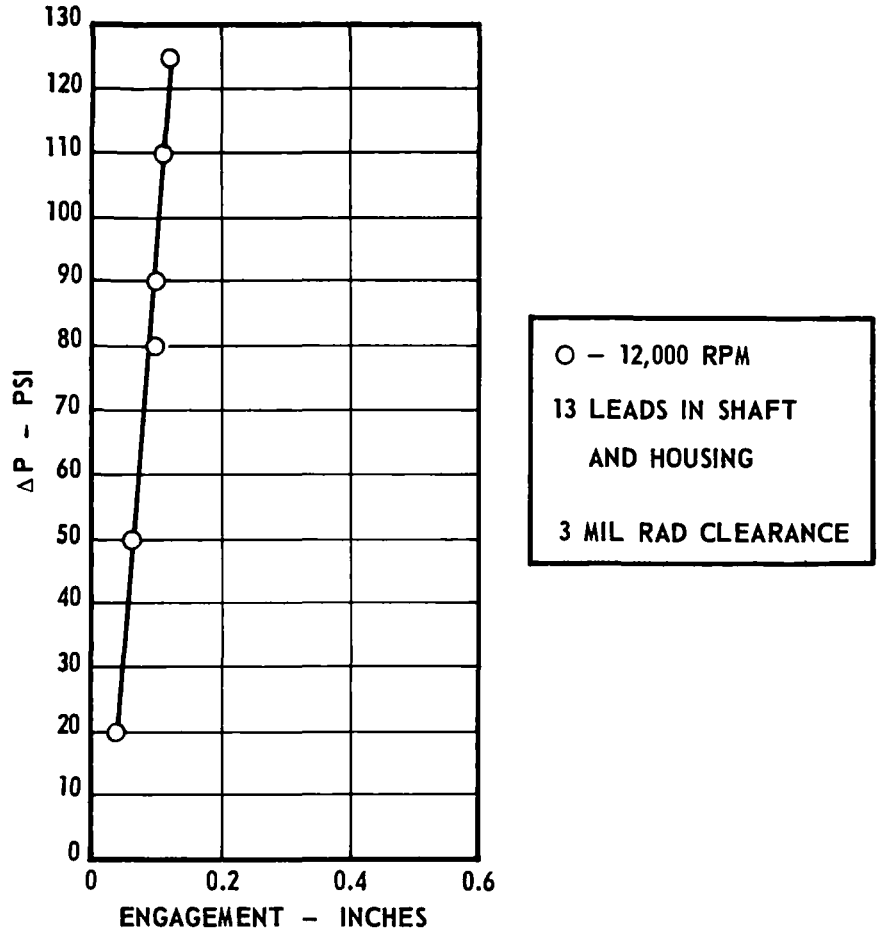

Pressure Differential vs Axial Engagement - Build-up 1-10

10-087-11B

Figure 49

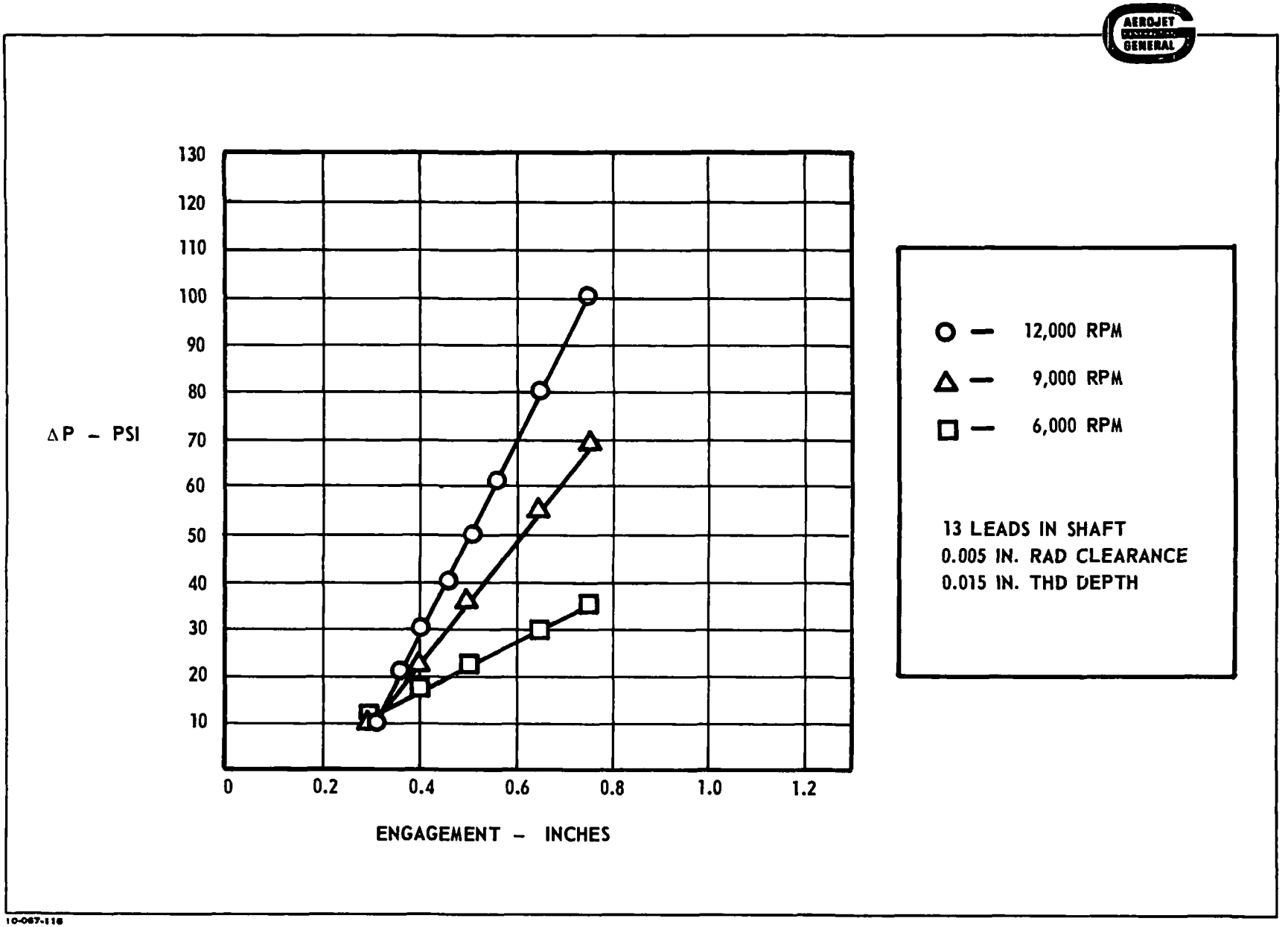

Pressure Differential vs Axial Engagement - Build-Up 1-11

Figure 50

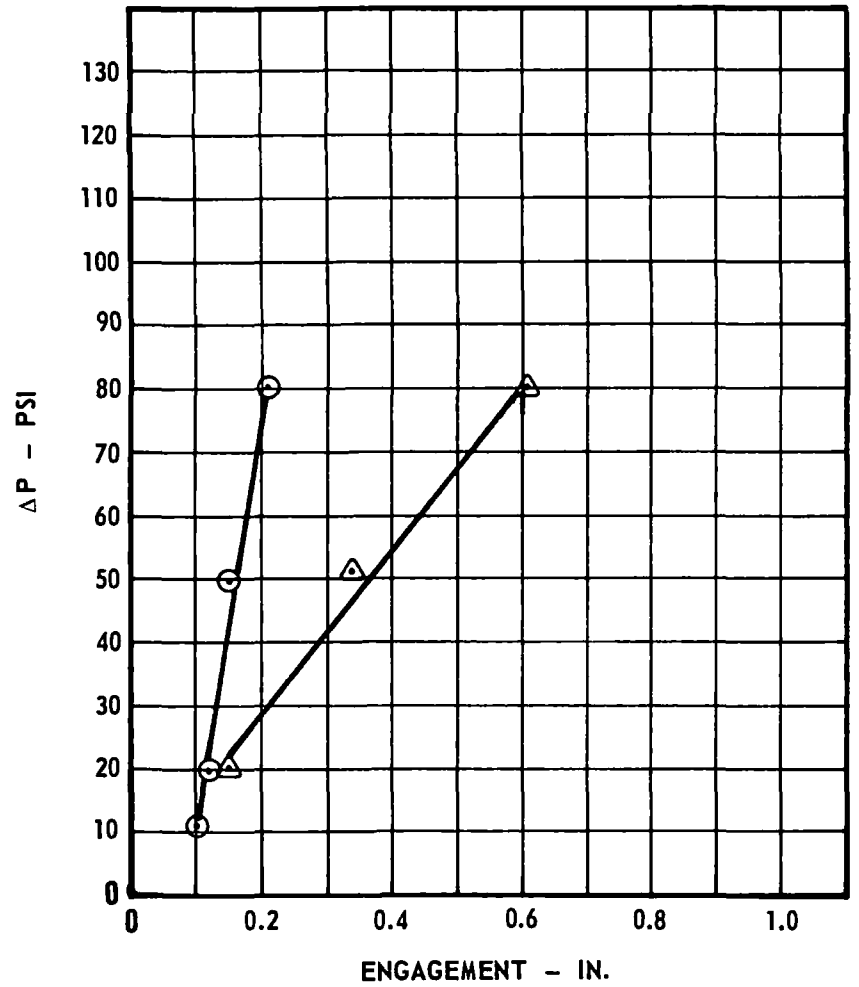

10-067-118

Pressure Differential vs Axial Engagement - Build-Up 1-12

Figure 51

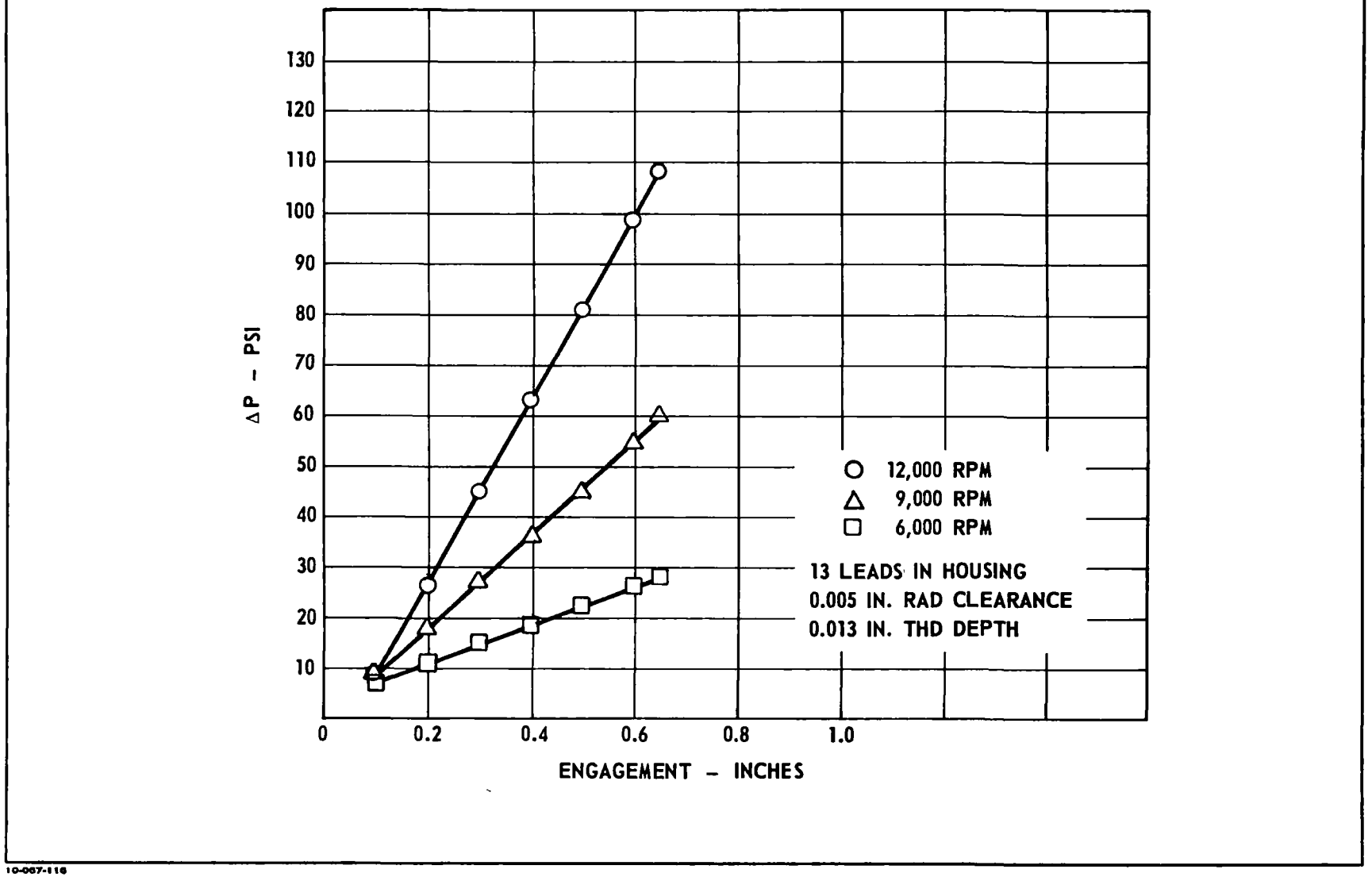

10-067-116

Pressure Differential vs Axial Engagement - Build-Up 1-13

Figure 52

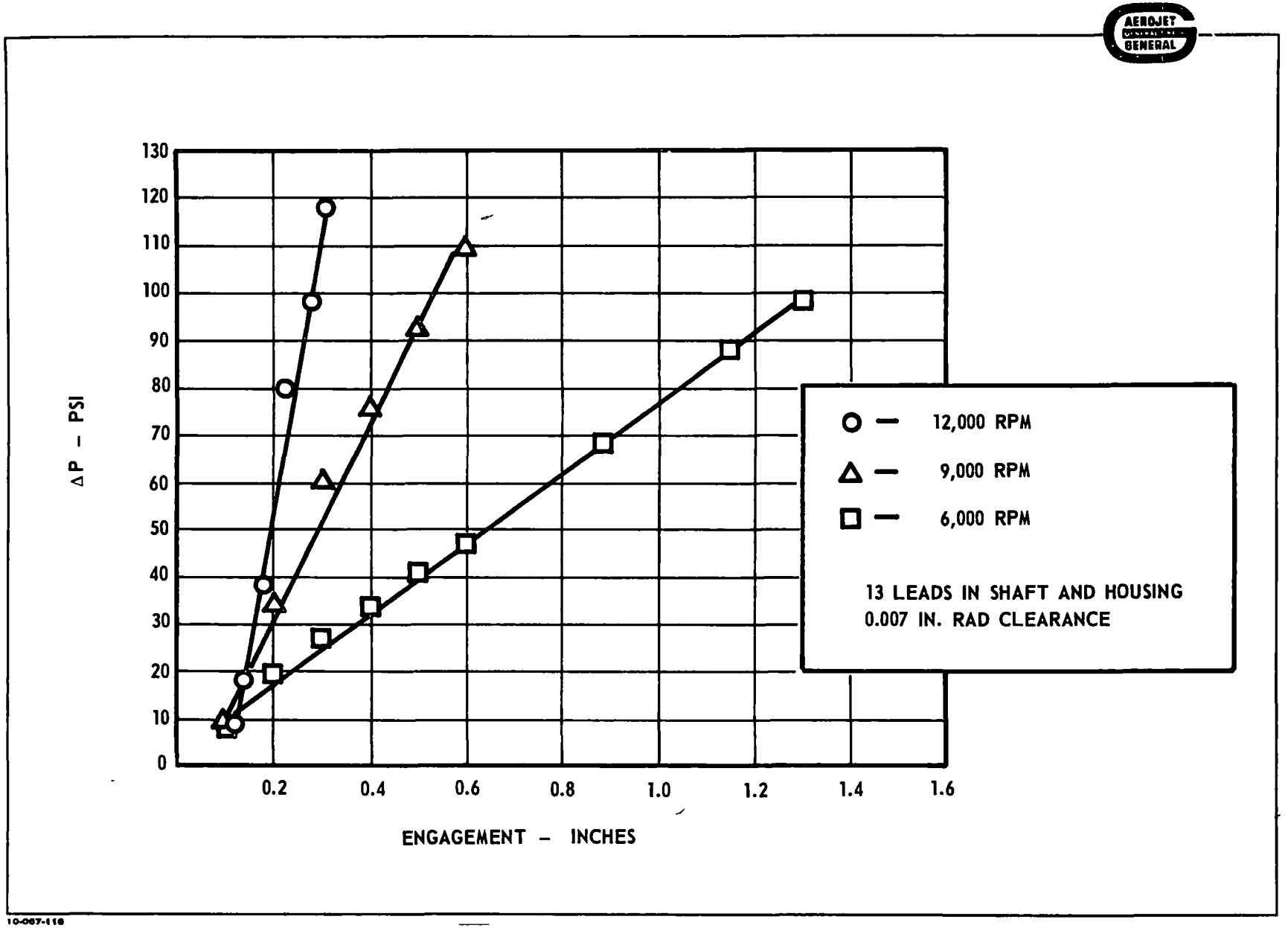

Pressure Differential vs Axial Engagement - Build-Up 1-14

Figure 53

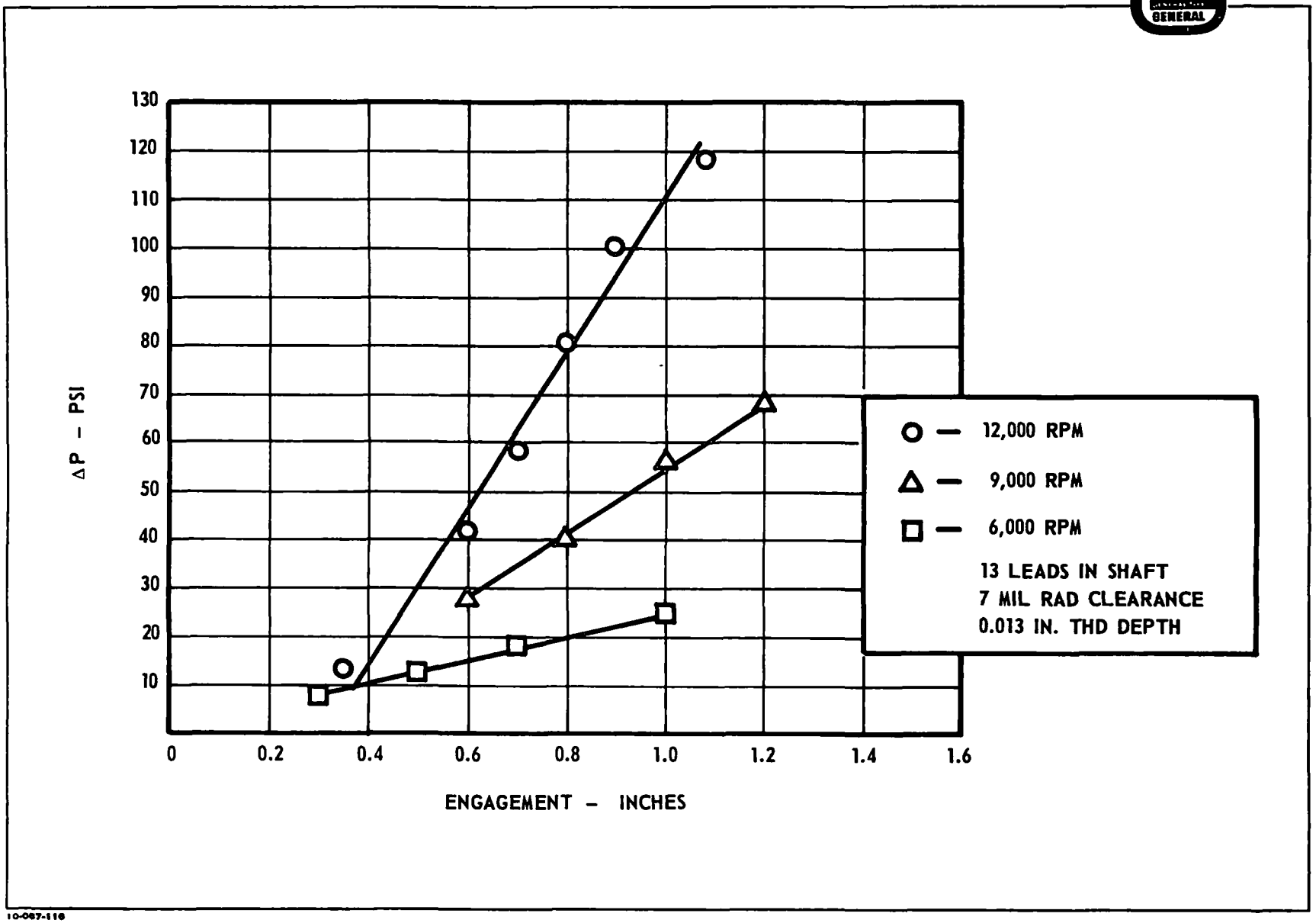

Pressure Differential vs Axial Engagement - Build-Up 1-15

Figure 54

NOTES:
1. TOLERANCE ALL DIMENSIONS PER MIL STD 2_ _ EXCEPT AS NOTED.
2. MATERIAL PER ASSY SPEC.
3. FINISH PER ASSY SPEC.
4. DYNAMICALLY BALANCE COMPLETE ASSY TO 0.0 OZ-IN MAX. AT 10,000 RPM.
5. REMOVE MATERIAL FROM THIS AREA ONLY TO CORRECT DYNAMIC UNBALANCE.
6. IN MATING ALL ROTATING PARTS AFTER OVERALL BALANCE.
7. TORQUE TO BE ESTABLISHED PER CONSTANT SPEED INSTRUCTIONS.
8. THIS DIM TO BE DETERMINED RELATIVE TO SEAL CLEARANCE SHOWN.
9. THIS DIM MUST BE HELD WITH NO TOLERANCE OF AS INSTRUCTED BY CONSTANT SPEED.
10. SCRIBE OF SHIMS TO BE DETERMINED RELATIVE TO CLEARANCE SHOWN.
11. VACUUM LEAK TEST PER MIL STD 2_ _ IN SUCH THAT HOOD TEC WITH HELIUM ON INSIDE PRESSURIZED TO 10 PSIG HELIUM SHALL BE DETECTED USING ANY INSTRUMENT CAPABLE OF MEASURING A LEAKAGE RATE OF 1 X 10 EXP -6 CU FT PER SEC ALL LEAKS SHALL BE LOCATED AND REMOVED.
12. TIME DIM TO BE DETERMINED PER CONSTANT SPEED INSTRUCTIONS
13. IDENTIFY PER ASSY SPEC

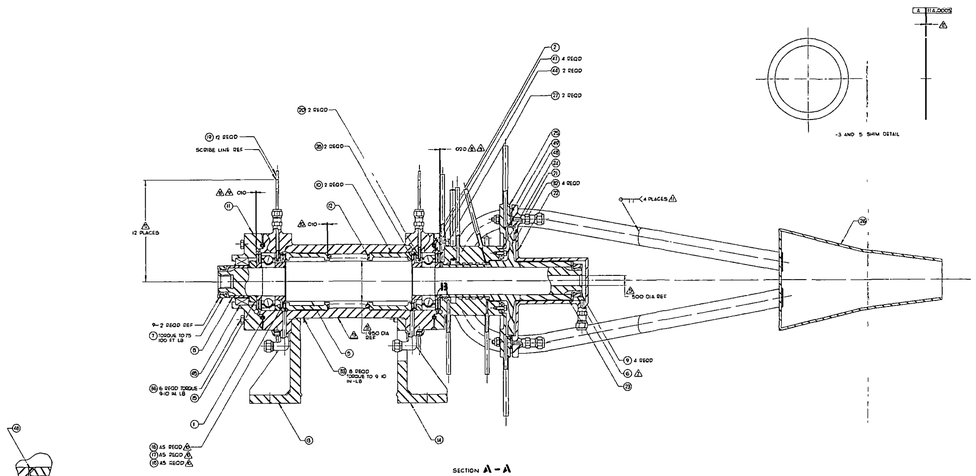
SCRIBE LINE DET
12 PLACES
9-2 RADD DEF
TORQUE 12-15 IN-LB
TORQUE TO 4-10 IN-LB
TORQUE TO 4-10 IN-LB
4 PLACES
.500 DIA REF
.500 DIA REF
.010
.010
.010

NOTES: 1 REMOVE ALL BURRS AND SHARP EDGES
2 63 ALL OVER EXCEPT AS NOTED
3 MACHINE -11 SPACER TO OBTAIN .018/.020 CLEARANCE
4 MACHINE -11 SPACER TO OBTAIN .006/.008 CLEARANCE
5 THIS DIM TO BE MACHINED TO OBTAIN .018/.012 CLEARANCE
6 THIS DIM TO BE OBTAINED PER COGNIZANT BNGG INSTRUCTIONS
7 TIG WELD PER AGC-STD 2795 USING WELD ROD PER MIL-R-5031 CLASS 5A
8 PENETRANT INSPECT WELDS PER MIL-I-6866 TYPE I NO FLAWS ALLOWED
9 HELIUM LEAK TEST PER MIL-STD-271 EXCEPT THAT HOOD TEST WITH HELIUM ON INSIDE PRESSURIZED TO 10 PSIG NO LEAK SHALL BE DETECTED USING AN INSTRUMENT CAPABLE OF MEASURING A FLOW RATE OF 1×10^{-7} CC/SEC (1×10^{-8} FT³ HR) ALL LEAKS SHALL BE IDENTIFIED FOR REMOVAL

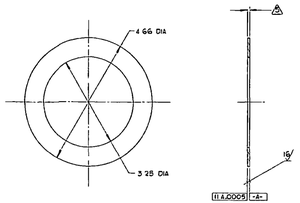

-5 SHIM DETAIL

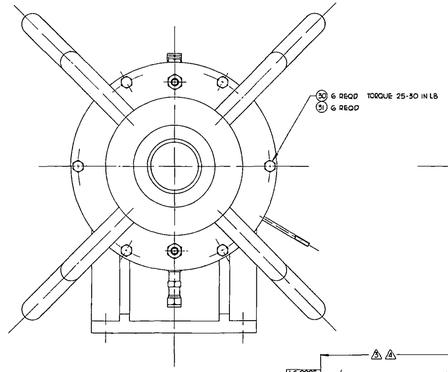

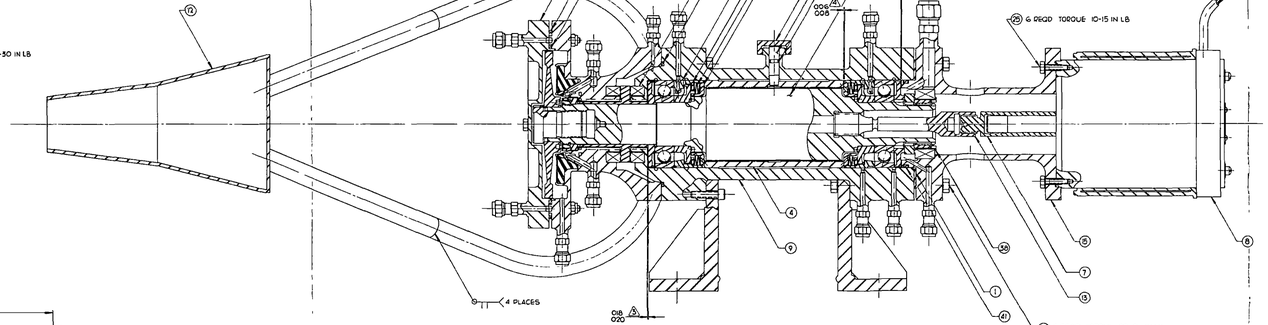

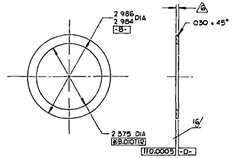

-7 & -9 RING DETAIL

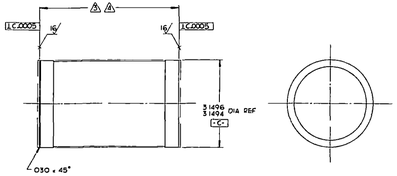

-11 SPACER DETAIL

REVISIONS			
LTR	ZONE	DESCRIPTION	DATE	APPROVED

AD	AD			WELD ROD		MS20900 CL 5A		
								44
								43
								42
1	1	83259	2-233-77 N40	O-RING			5B	41
1	1	83259	2 150-77 N40	O-RING			3C	40
1	1	83259	2-037 N40	O-RING			3C	39
1	1	77842	C-28502 B0-108	SEAL			3B	38
2	2	77842	A-32635	SEAL			4C	37
1	1	07107	3531-66 07100	SEAL			4C	36
1	1	07107	8000-24 07100	SEAL			4C	35
								34
								33
								32
6	6		MS20500 -1052	NUT			GC	31
6	6		MS20085 -14	BOLT			GC	30
								29
								28
6	6		AN4CM15A	BOLT			3B	27
								26
6	6		AN3CM5A	BOLT			2C	25
								24
8	8		091836-1	SPRING			3D	23
1	1		092534-1	RETAINER			5C	22
2			092455 3	MANIFOLD			3C	21
	2		092455 1	MANIFOLD			3C	20
2			092434-3	RETAINER			3C	19
	2		092434 1	RETAINER			3C	18
								17
								16
1	1		092373 1	SEAL HOUSING			2B	15
1	1		092263 1	PIN			3C	14
1	1		092240 1	SHAFT			2B	13
1	1		092105 1	MANIFOLD ASSY			3C	12
1	1		091906 1	HOUSING ASSY			4C	11
1	1		091885-1	SHAFT ASSY			3C	10
1	1		091854-1	HOUSING ASSY			3B	9
1	1		091582-1	MOTOR ASSY			2B	8
1	1		091562 1	COUPLER			2B	7
								6
								5
1	1		-11	SPACER	ALTED FROM 092263 1		5B	4
2			-9	RING	250 PLATE 4340 STL	MIL-6369	3C	3
	2		-7	RING	187 PLATE CRES 410	AMS 5504	3C	2
1	1		-5	SHIM	.125 SHEET CRES STL	300-S-606	3B	1

091883 COPY

-5	1							
QTY/ASSY	REV	ZONE	PART OR IDENTIFYING NO.	NOMENCLATURE OR DESCRIPTION	MATERIAL	SPECIFICATION	PART OR IDENT NO.	ITEM NO.

LIST OF MATERIALS

UNLESS OTHERWISE SPECIFIED
DIMENSIONS ARE IN INCHES
TOLERANCES ON DECIMALS: ANGLES ±1°
.X ± .1
.XX ± .03
.XXX ± .010
SEE NEXT DRAWING

	NAME	SIGNATURE	DATE
DRAWN	R.D. LEDBETTER		7-2-63
CHECKED			7-2-63
ENGR APPR			7-2-63
MFG APPR			7-2-63
QA			7-2-63
PROJ ENGR			7-2-63
ADD'L SIGNATURES			

FINISH
MATERIAL
HEAT TREATMENT

AEROJET GENERAL CORPORATION
AZUSA, CALIFORNIA

INTEGRATED SEAL ASSY- TYPE B MODEL X

SIZE A | CAGE CODE 70143 | DWG NO. J 091883

SCALE 1/2 | WEIGHT | SHEET 1 OF 1

ZONE	REVISION RECORD	APPROVED	DATE

DRAWING LEVEL 1

NEXT ASSY USED ON
APPLICATION

DO NOT SCALE DRAWING

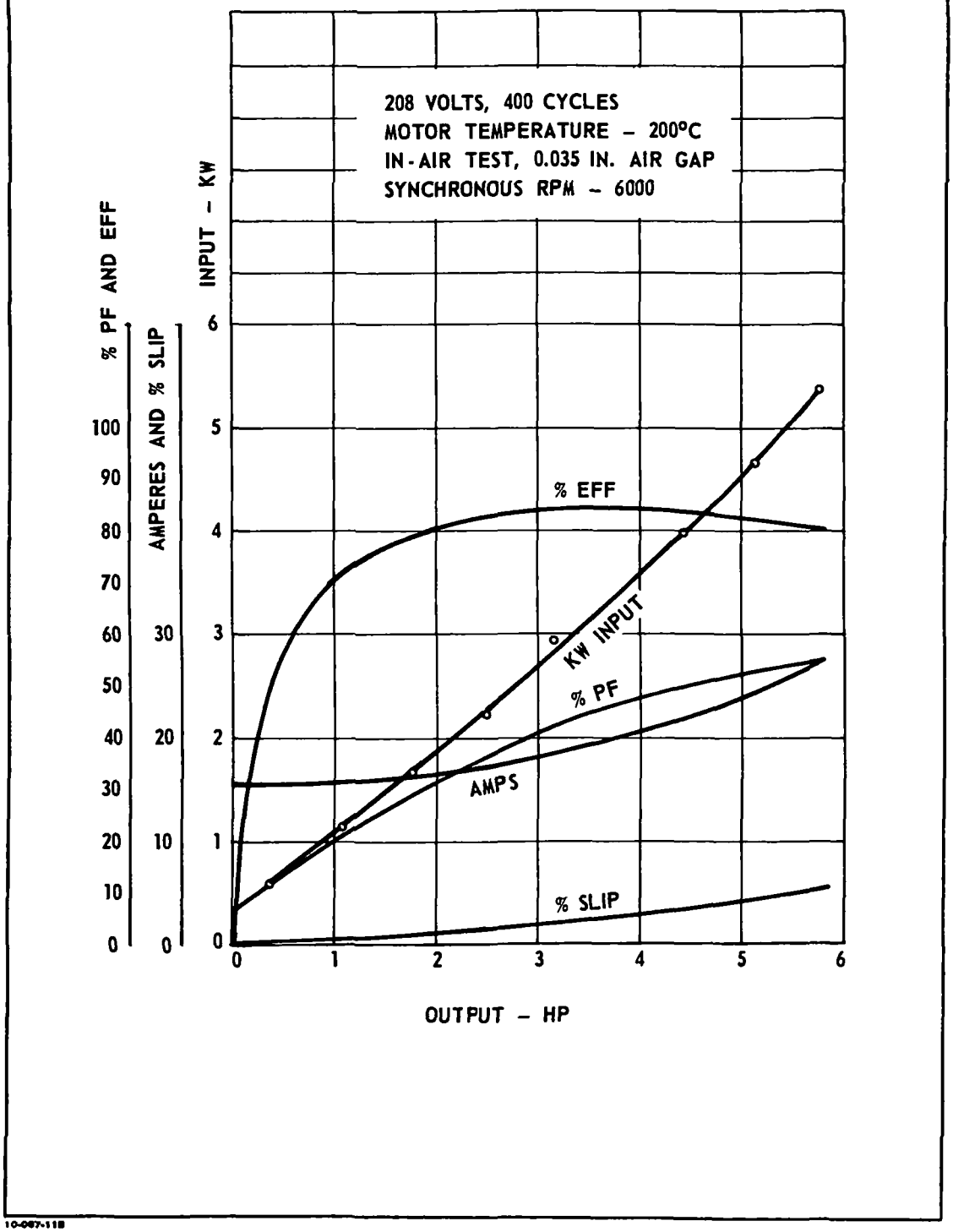

Motor Load Test - Heat Rejection Loop NaK PMA

Figure 57

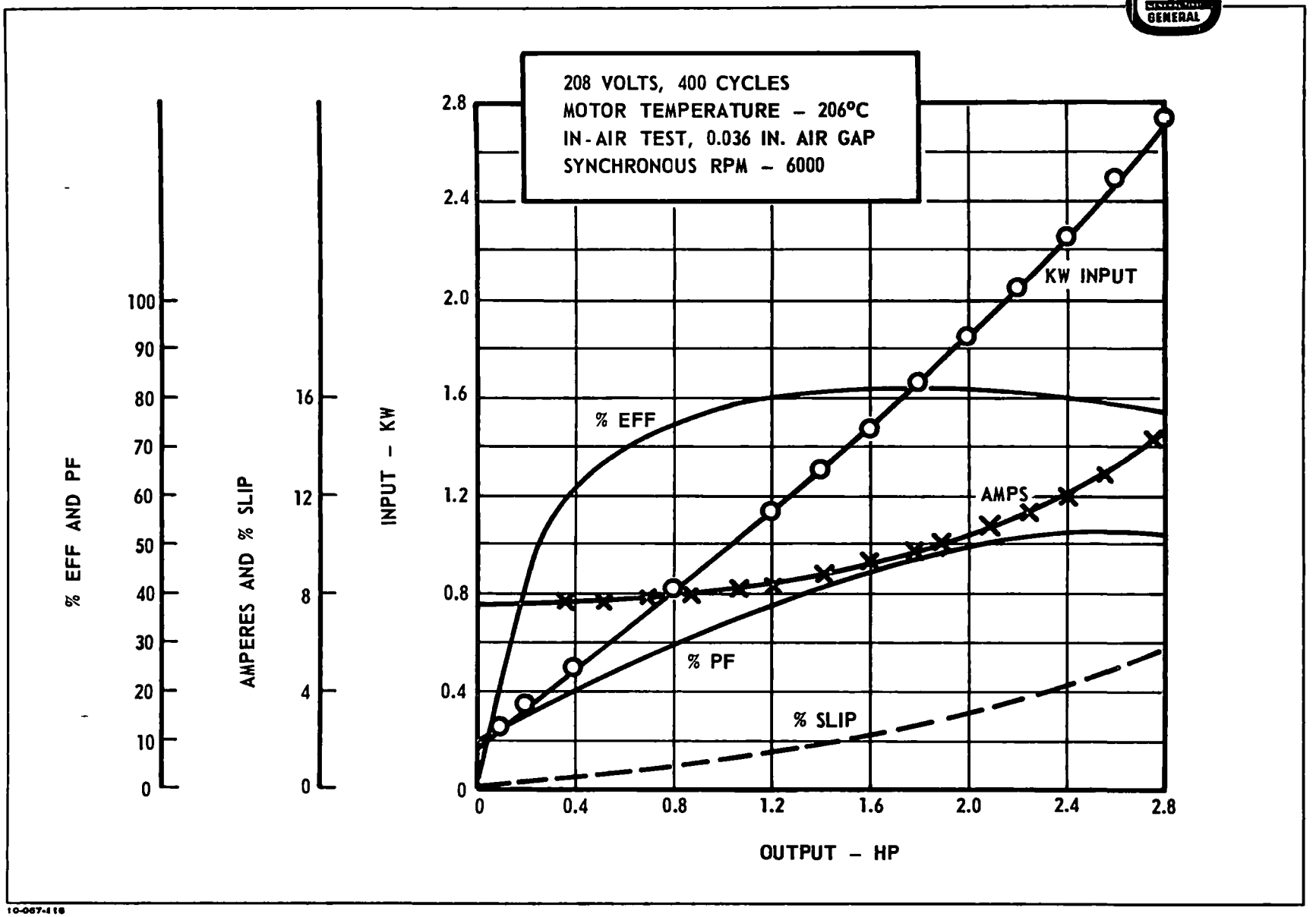

Motor Load Test - Primary Loop NaK PMA

Figure 58

UNCLASSIFIED

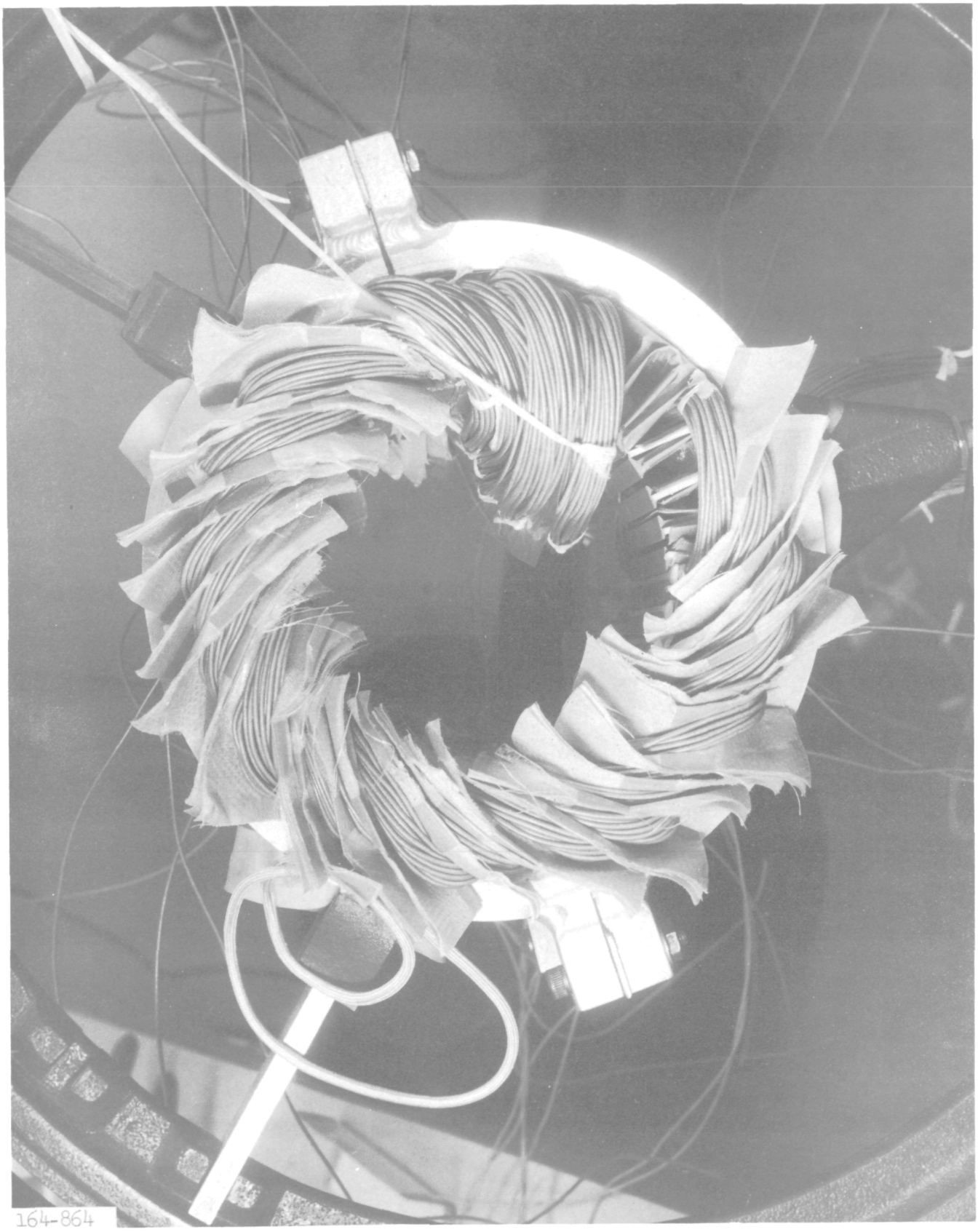

Prototype HRL Motor Stator Assembly

Figure 59

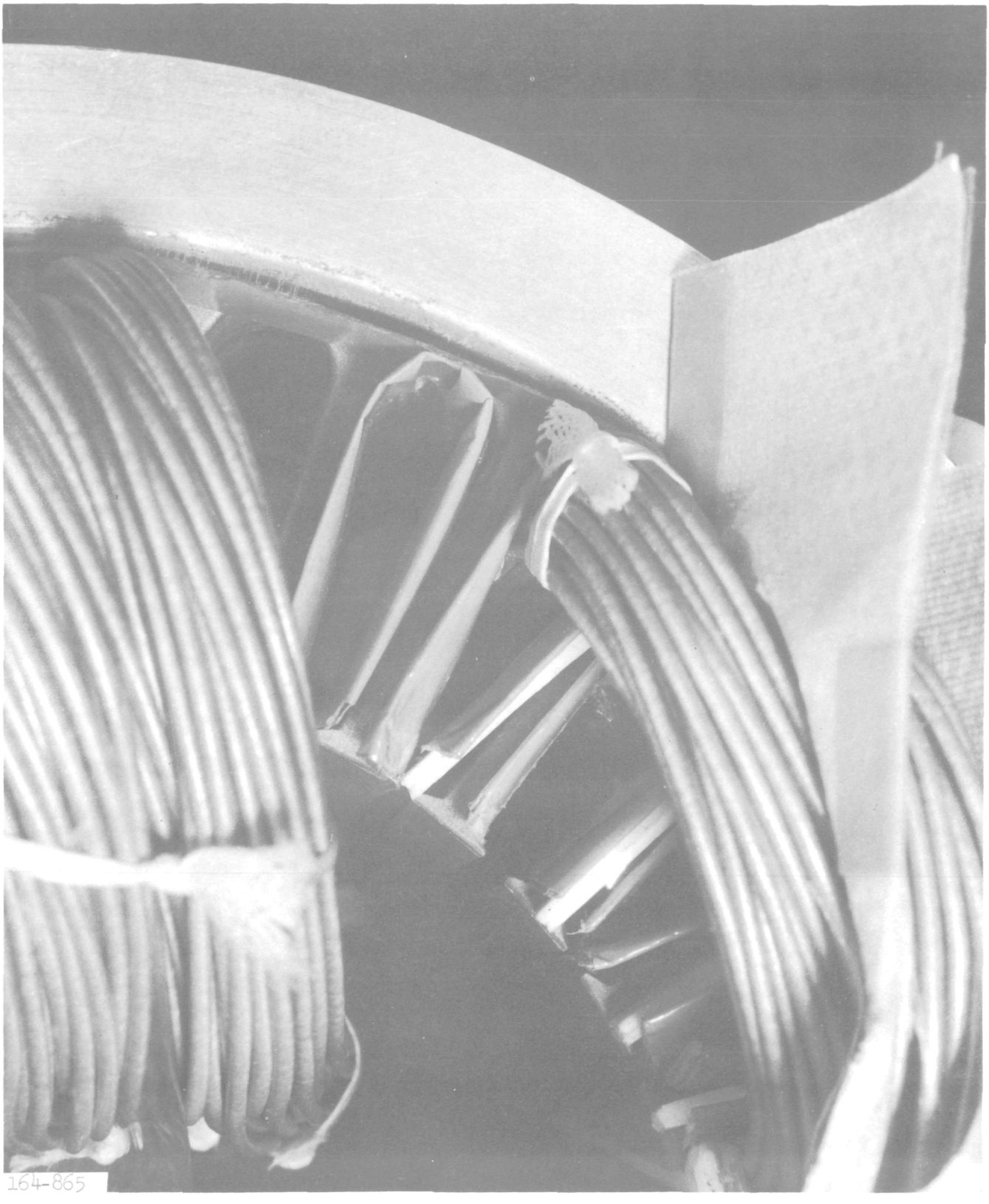

Prototype HRL Motor Stator Assembly - Close-up of Slot Portion

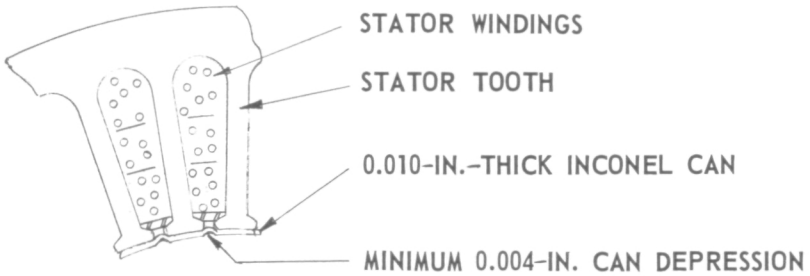

END VIEW OF CANNED STATOR

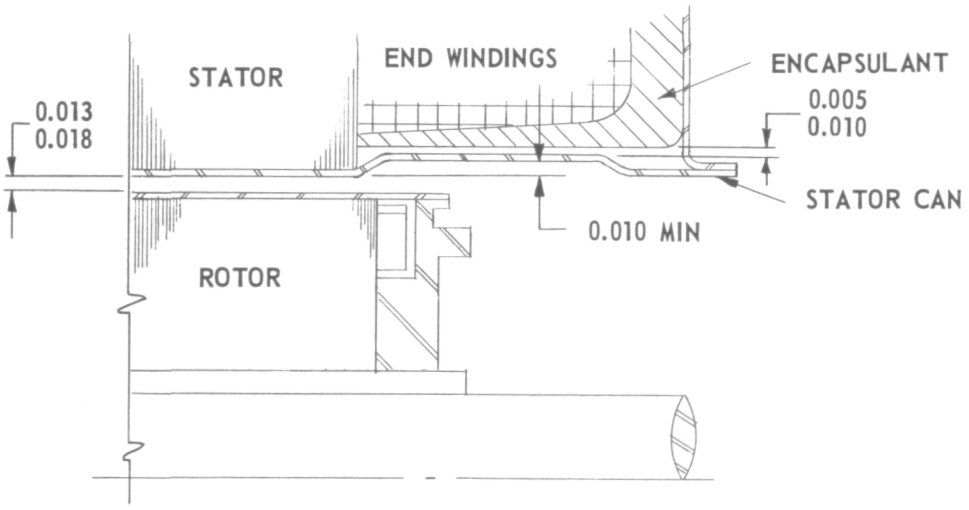

SECTION VIEW OF CANNED STATOR

10-087-11B

End View and Section View of Canned Stator

Figure 61

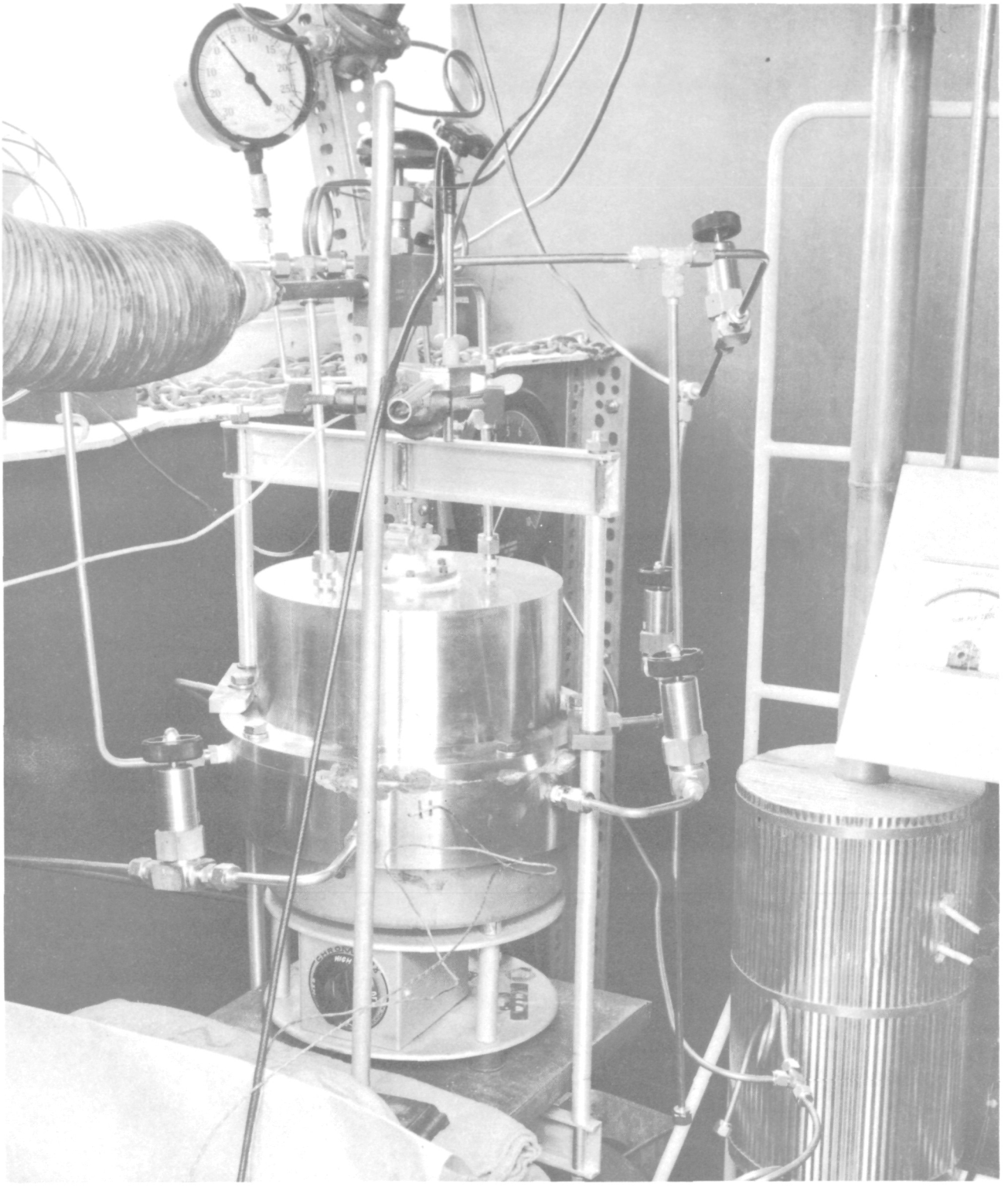

Pivot Fretting Test Apparatus

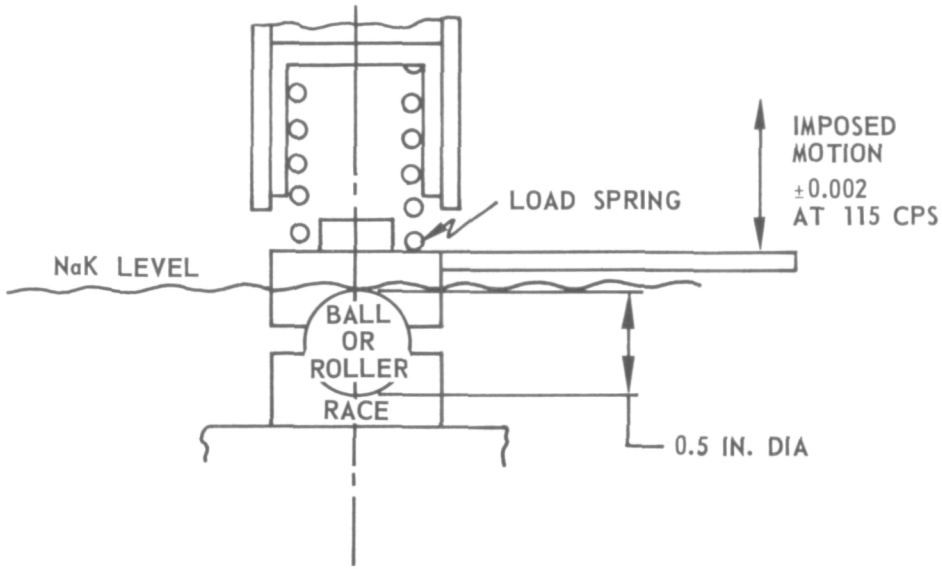

10-067-116

Schematic - Pivot Fretting Test Apparatus

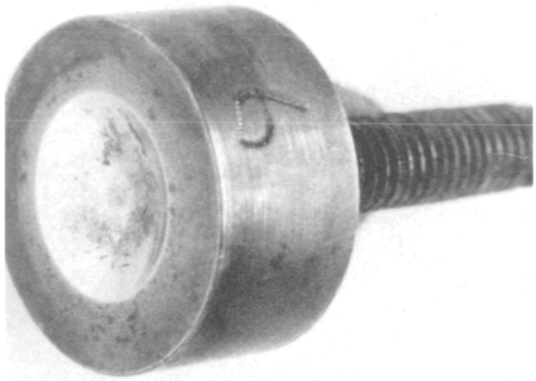

(a) M2 Socket

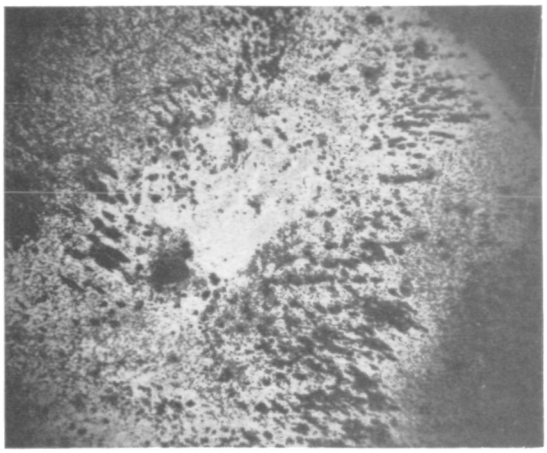

(b) Enlarged View of Socket Damage

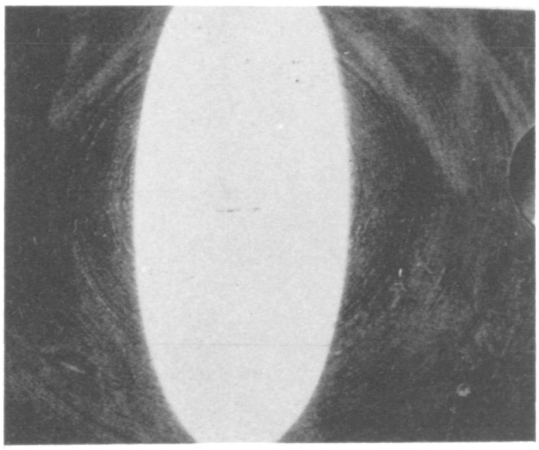

(c) M2 Race

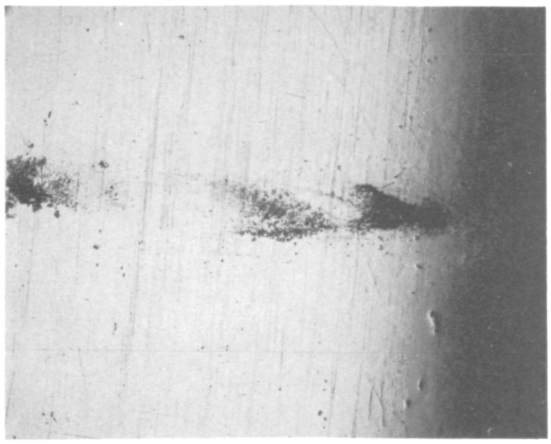

(d) Enlarged View of Race Damage

M2-T1-M2 Bearing Test Specimens Following 99 Hours in 600°F NaK

Figure 64

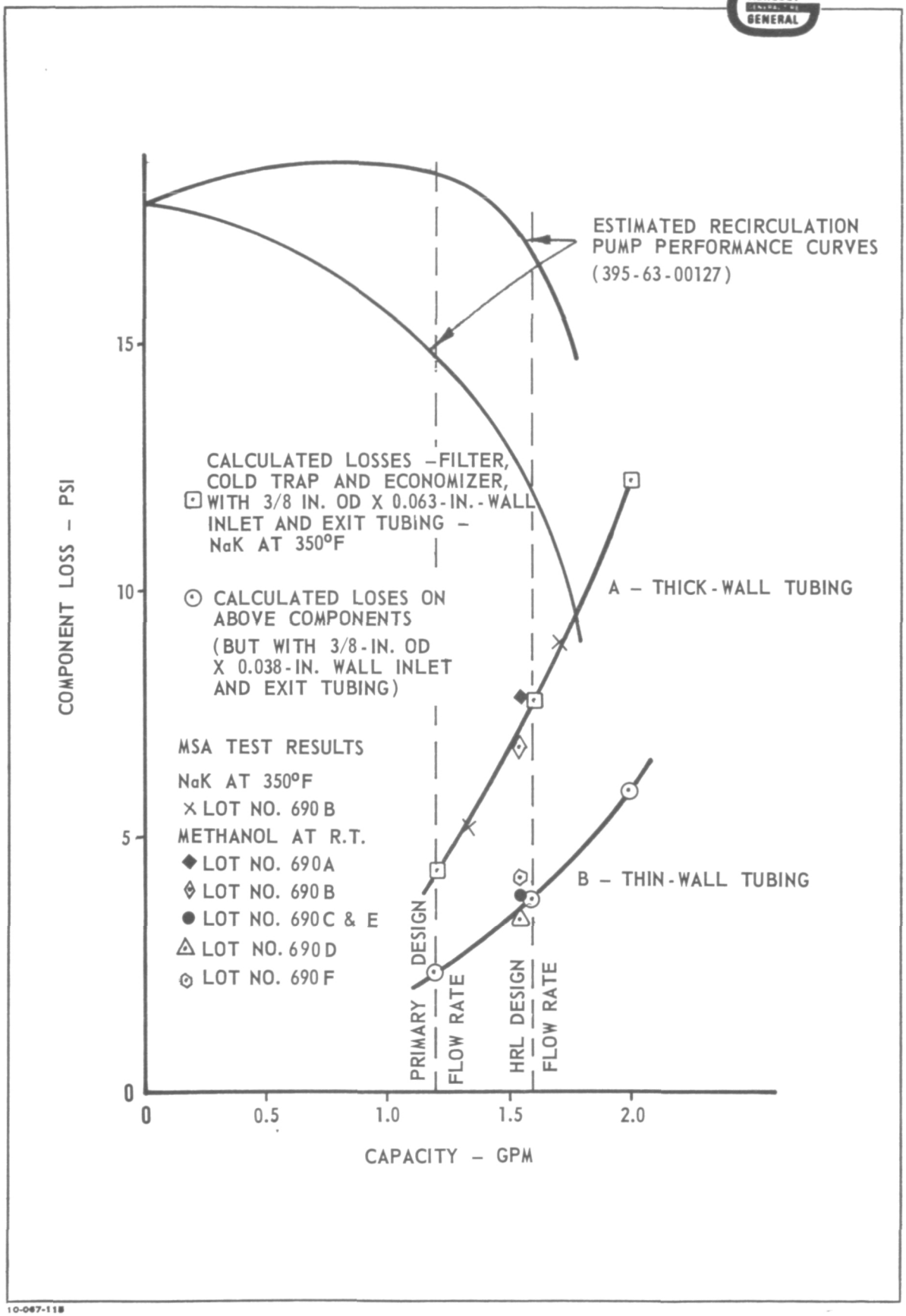

10-067-118

Component Losses, NaK PMA Recirculation System - Capacity vs Component Losses

Figure 65

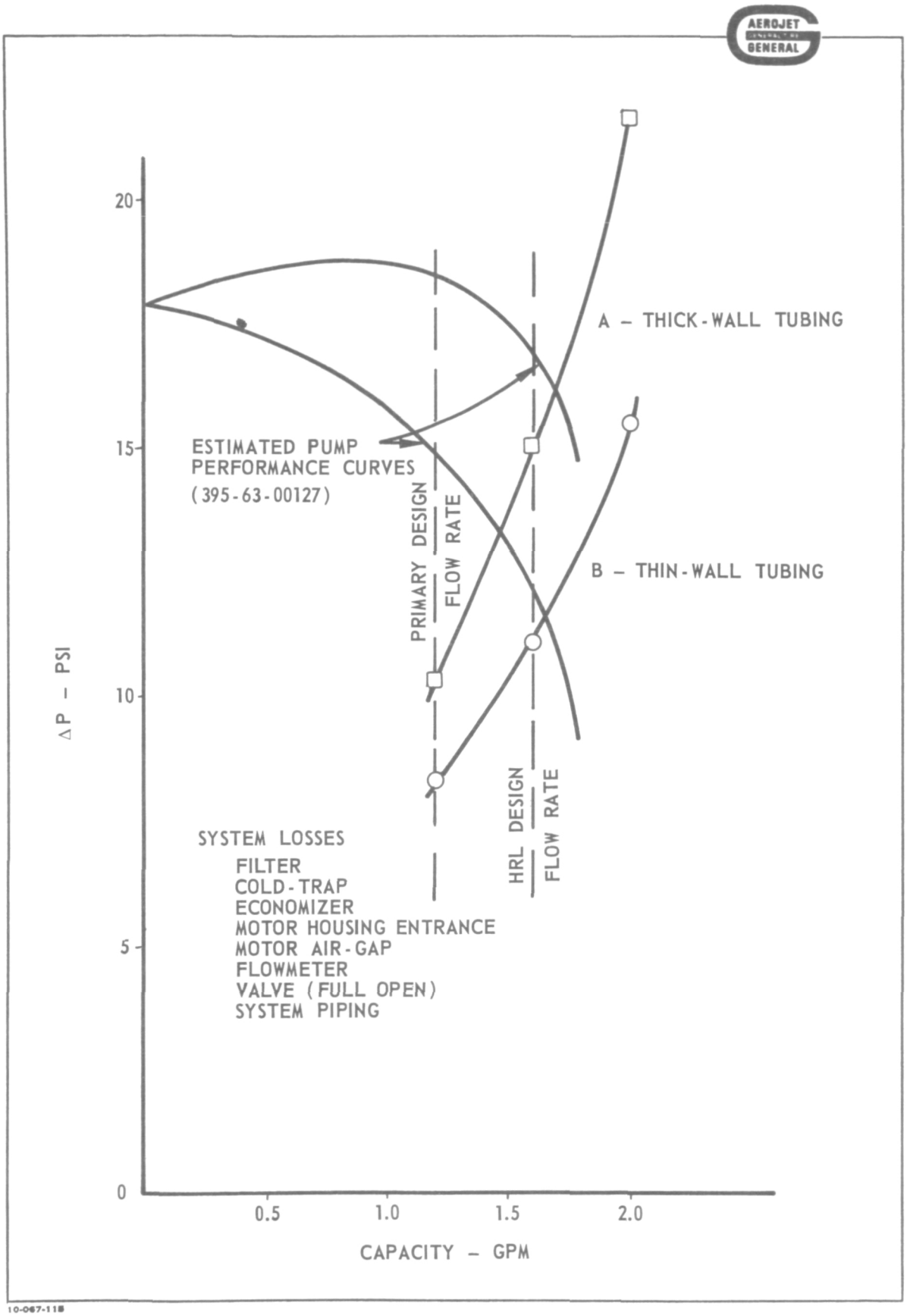

NaK PMA Recirculation Loop Losses - Capacity vs ΔP

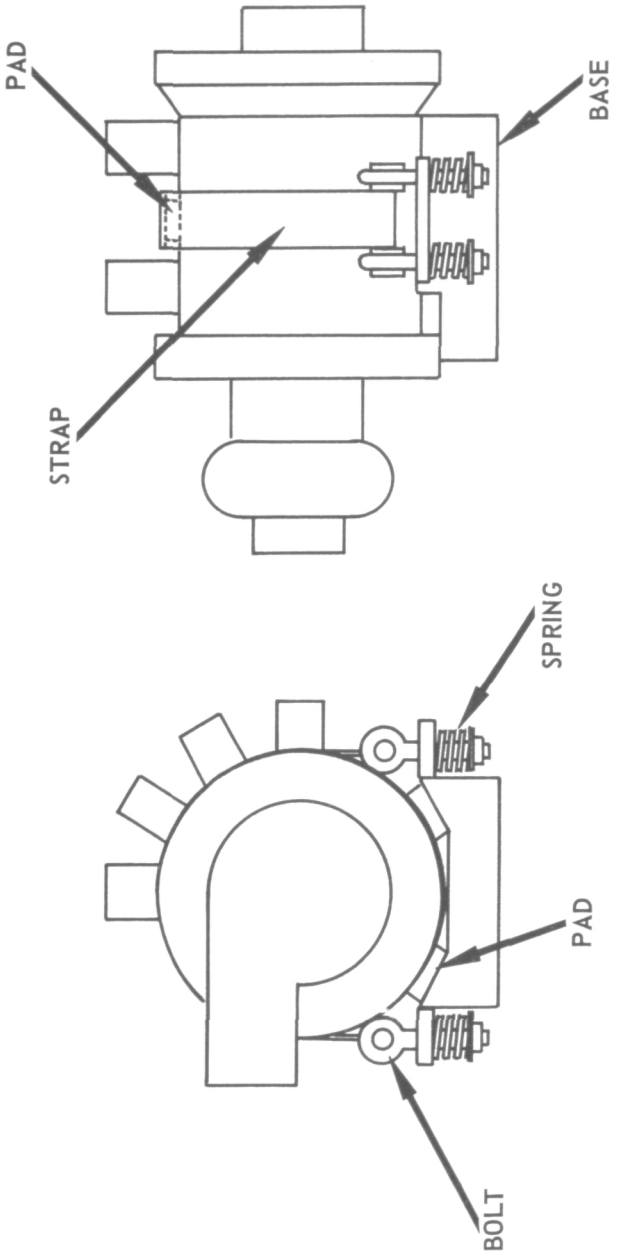

NaK PMA Mounting Arrangement

Figure 67

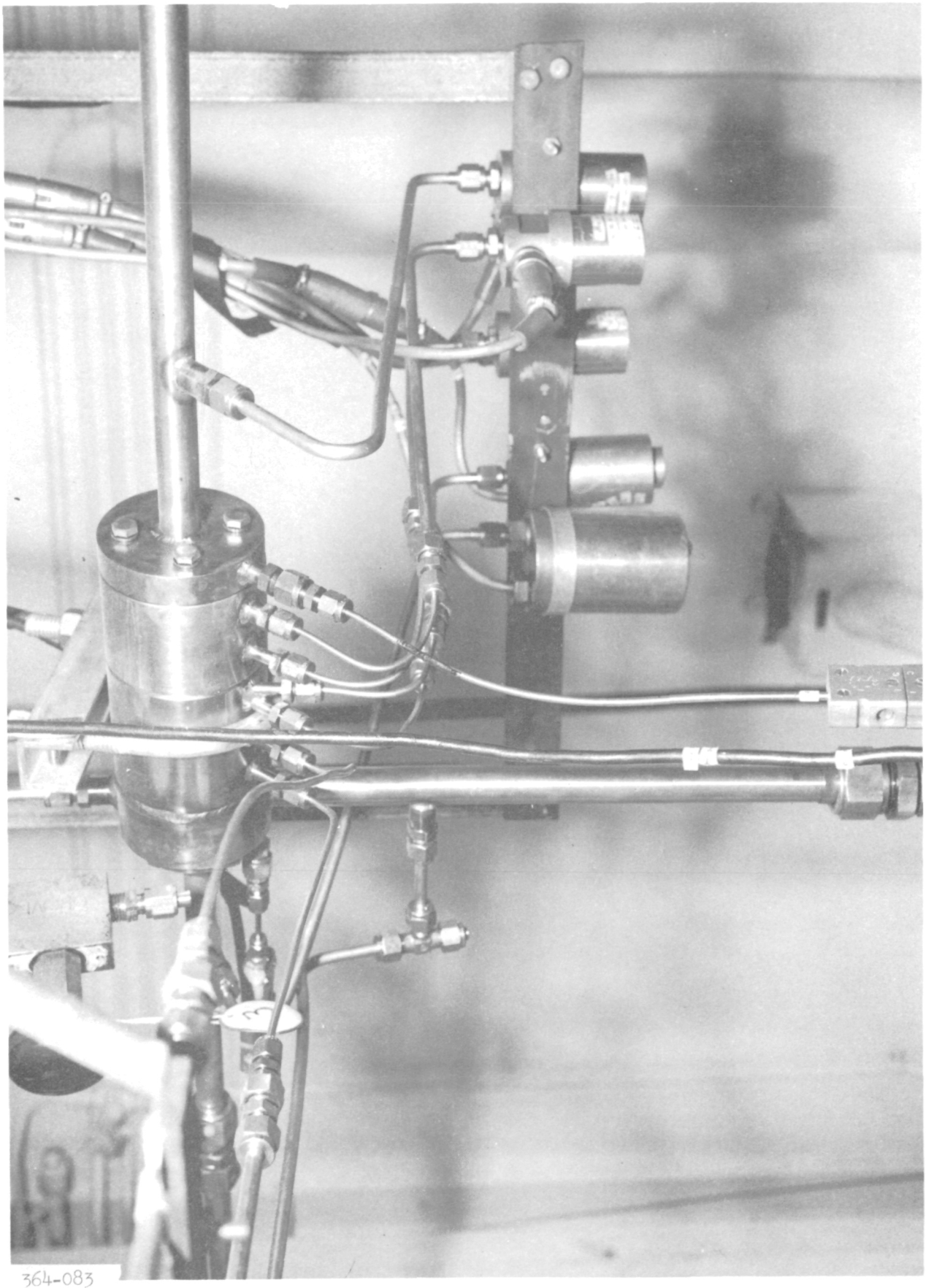

364-083

Mercury Jet Pump - Test Setup

Figure 68

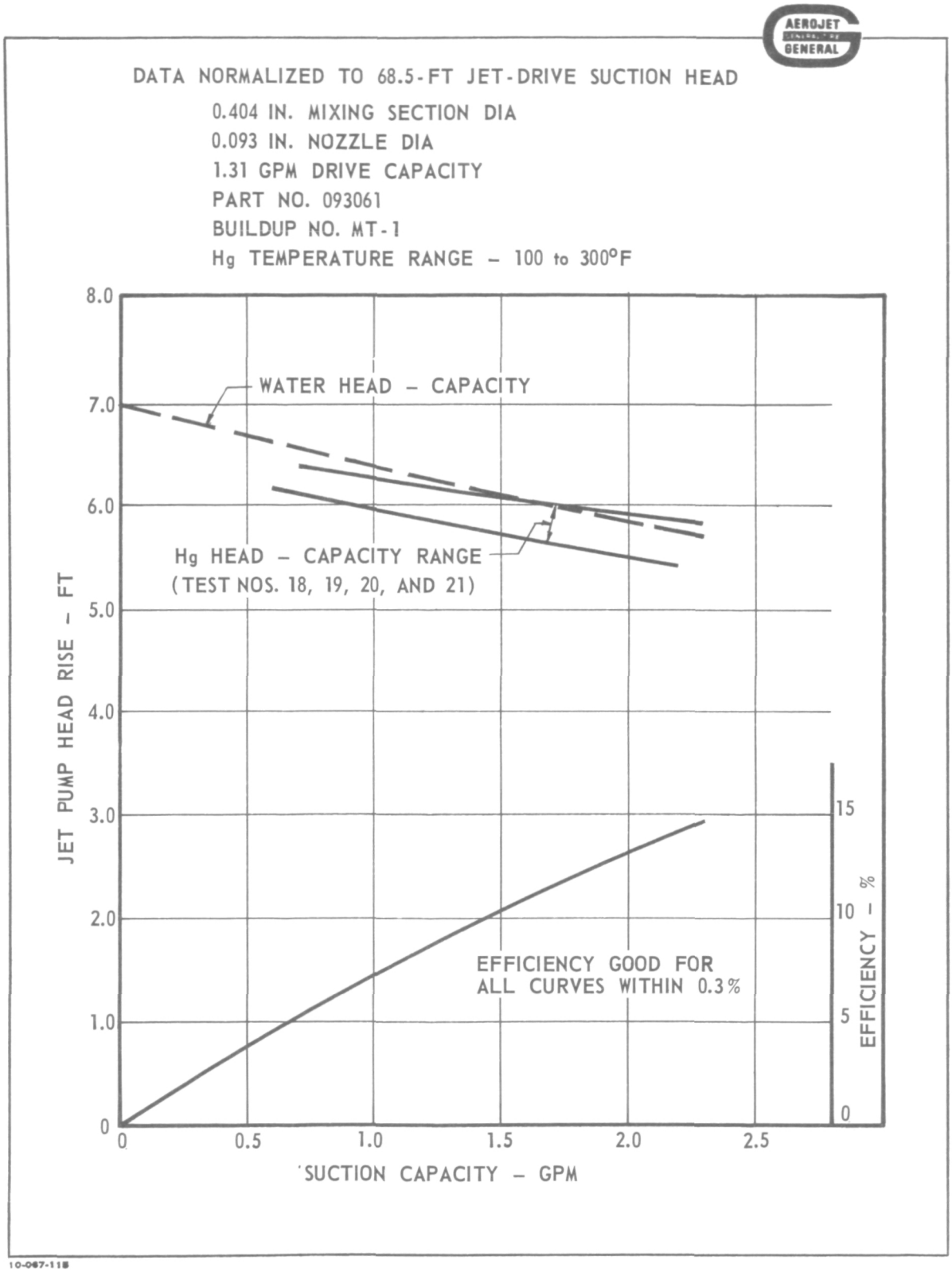

Mercury Jet Pump - Performance Curves for Water and Mercury Tests

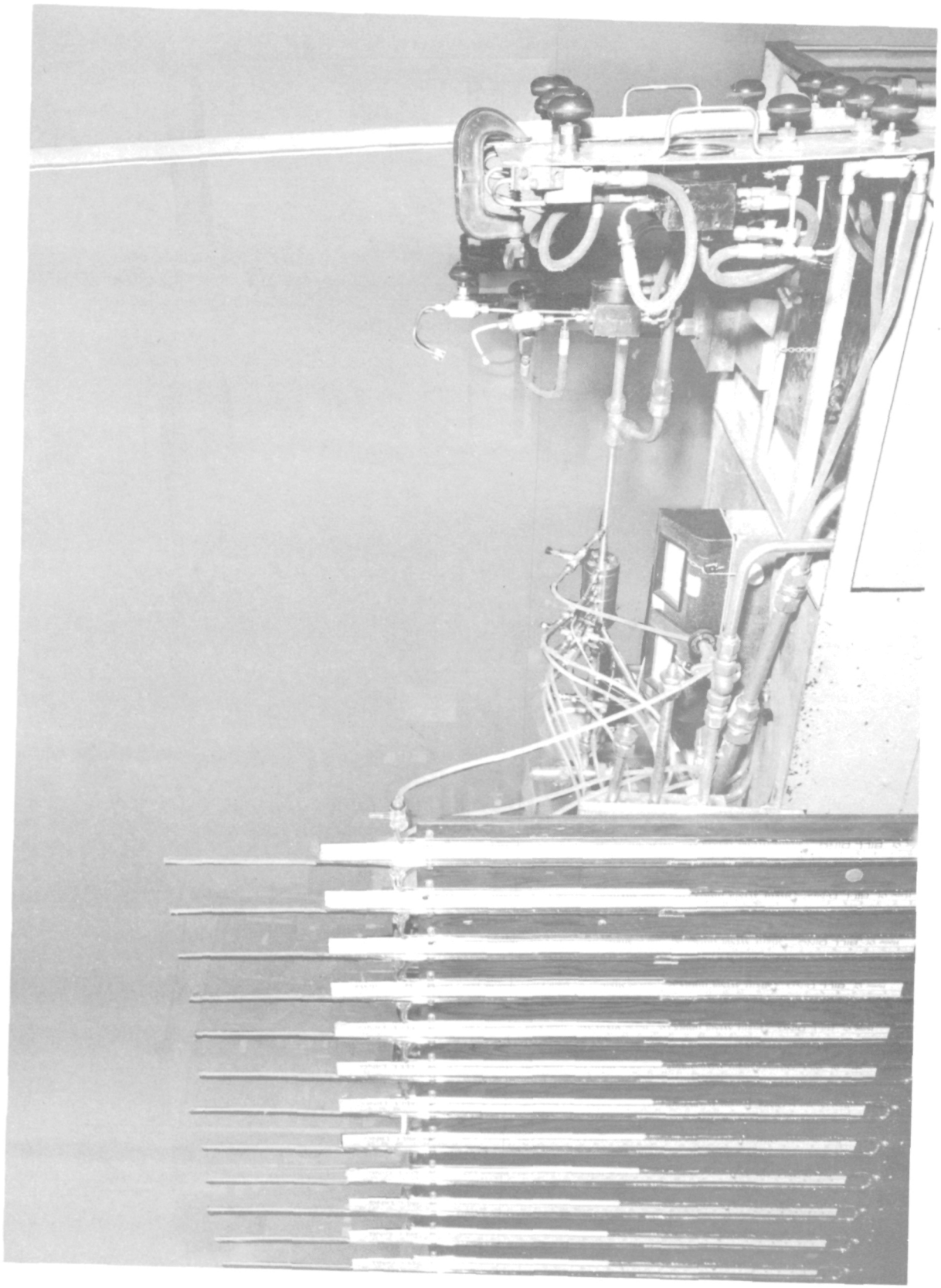

Mercury Jet Pump, -X Model, Water Test Setup

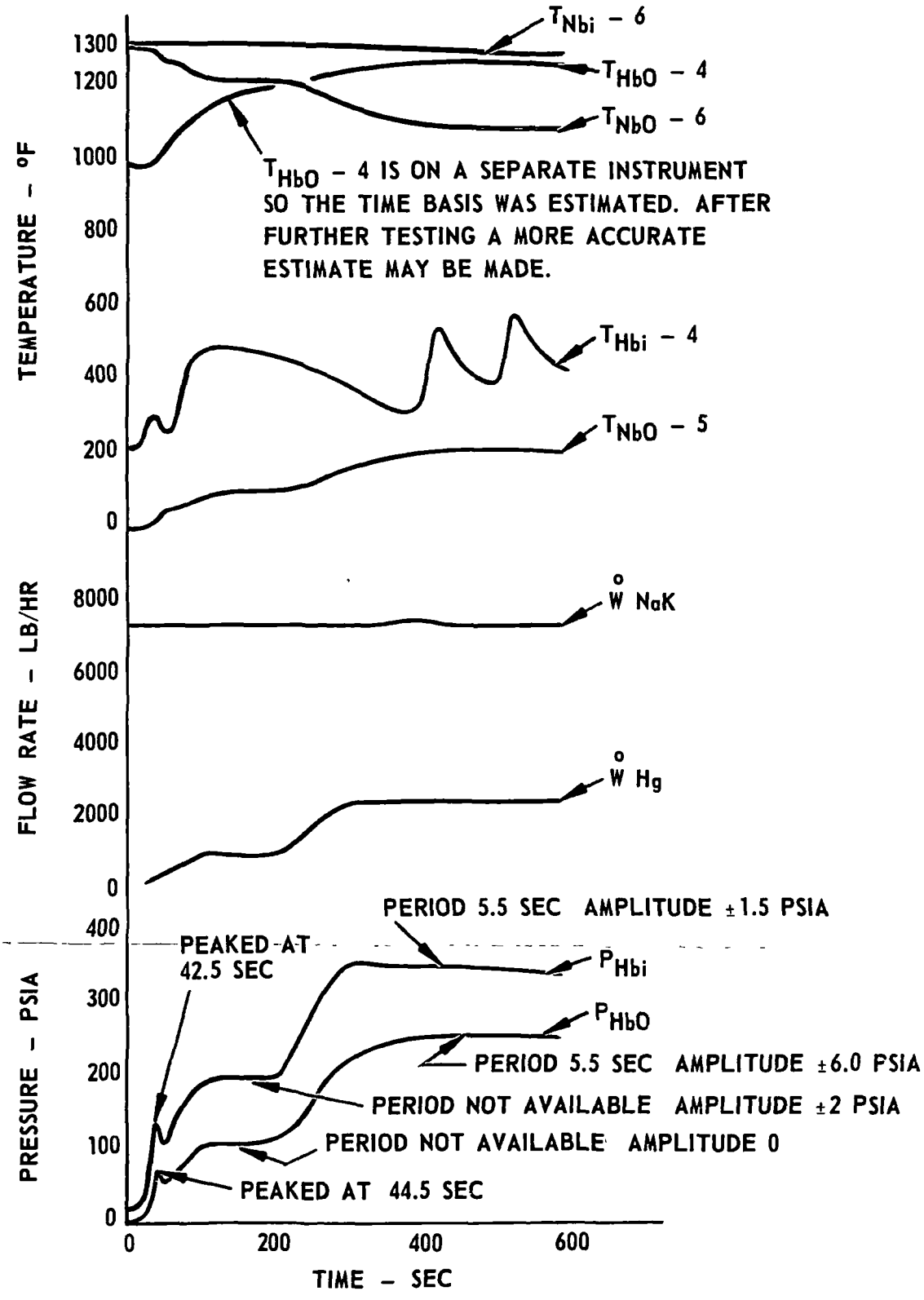

Boiler Hot-Start Test No. 1

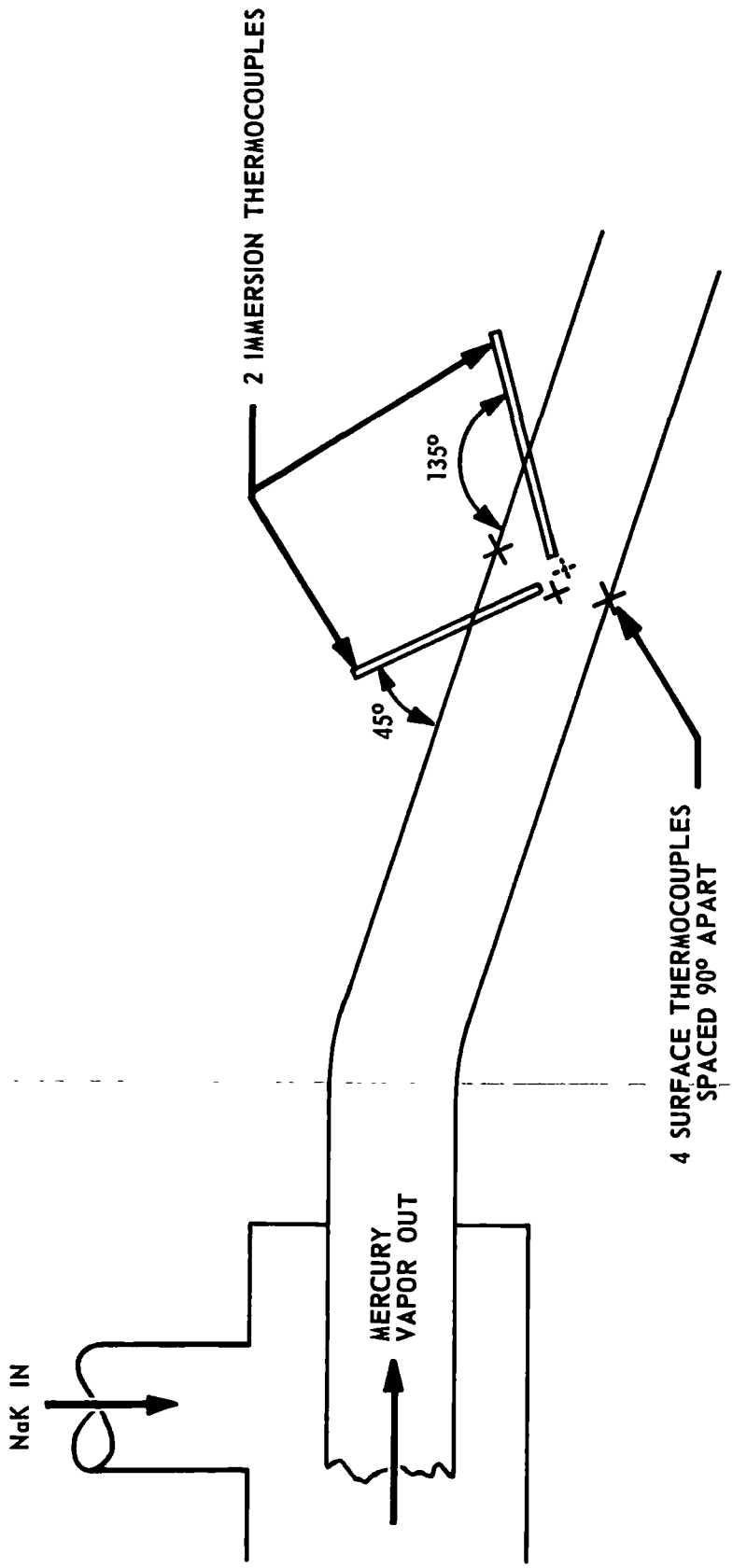

Thermocouple Location, Mercury Boiler Outlet

Figure 71B

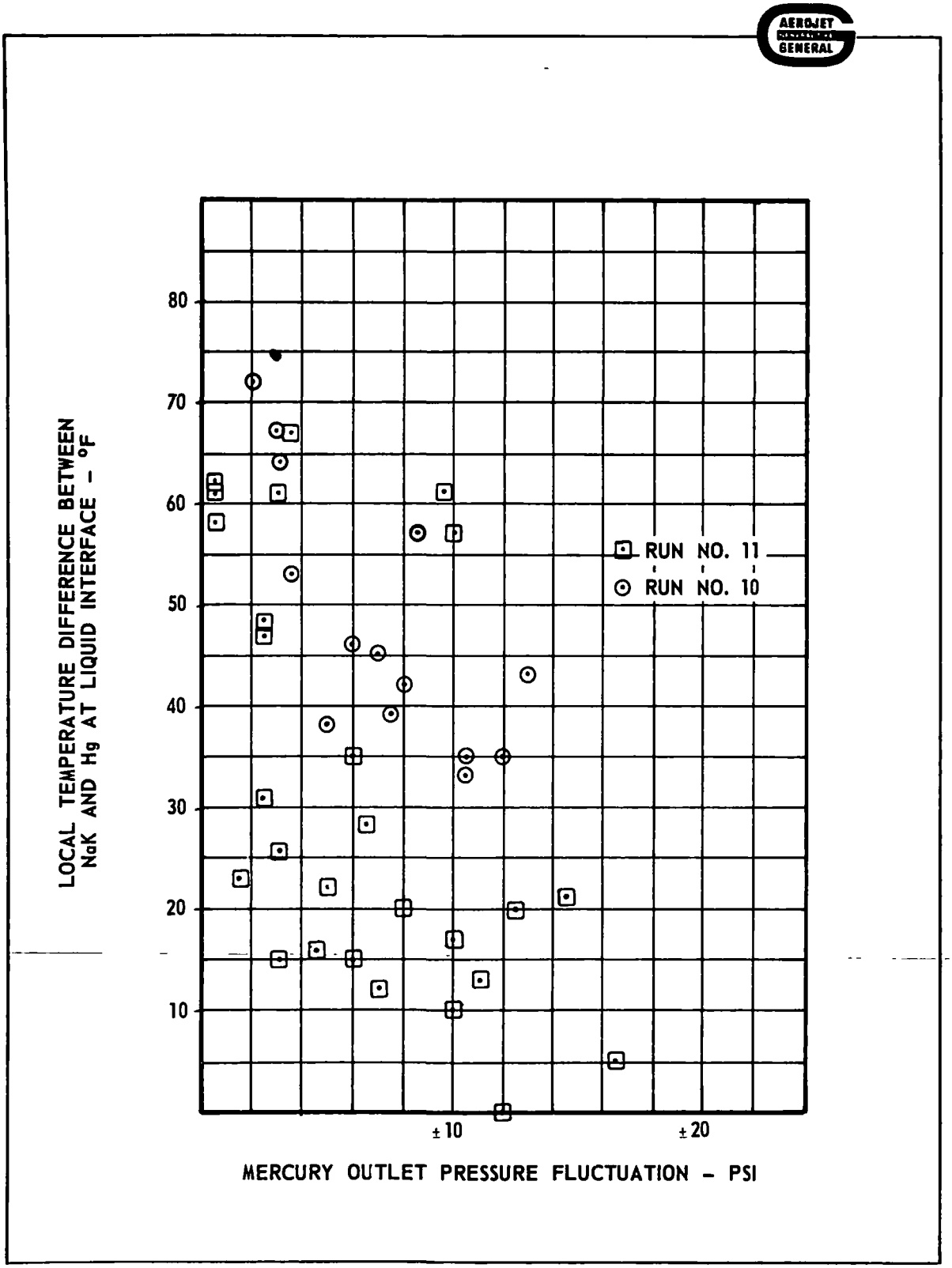

Local Temperature Difference Between NaK and Mercury at Liquid Interface vs Mercury Outlet Pressure Fluctuation - TS-2B Test Section with 0.135-in.-dia Wire in Plug Section

Figure 72

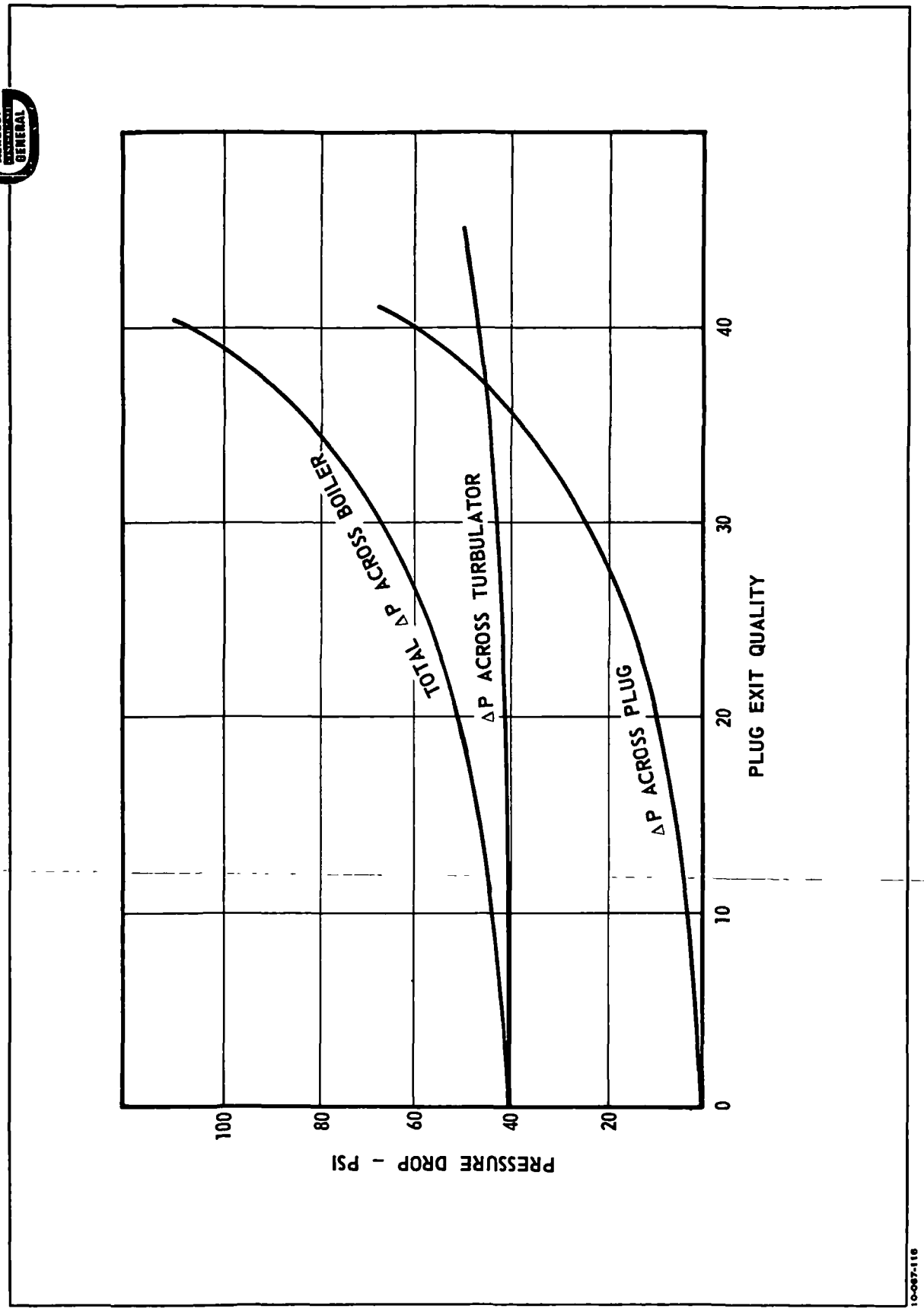

Boiler Pressure Drop With Varied Plug Exit Quality

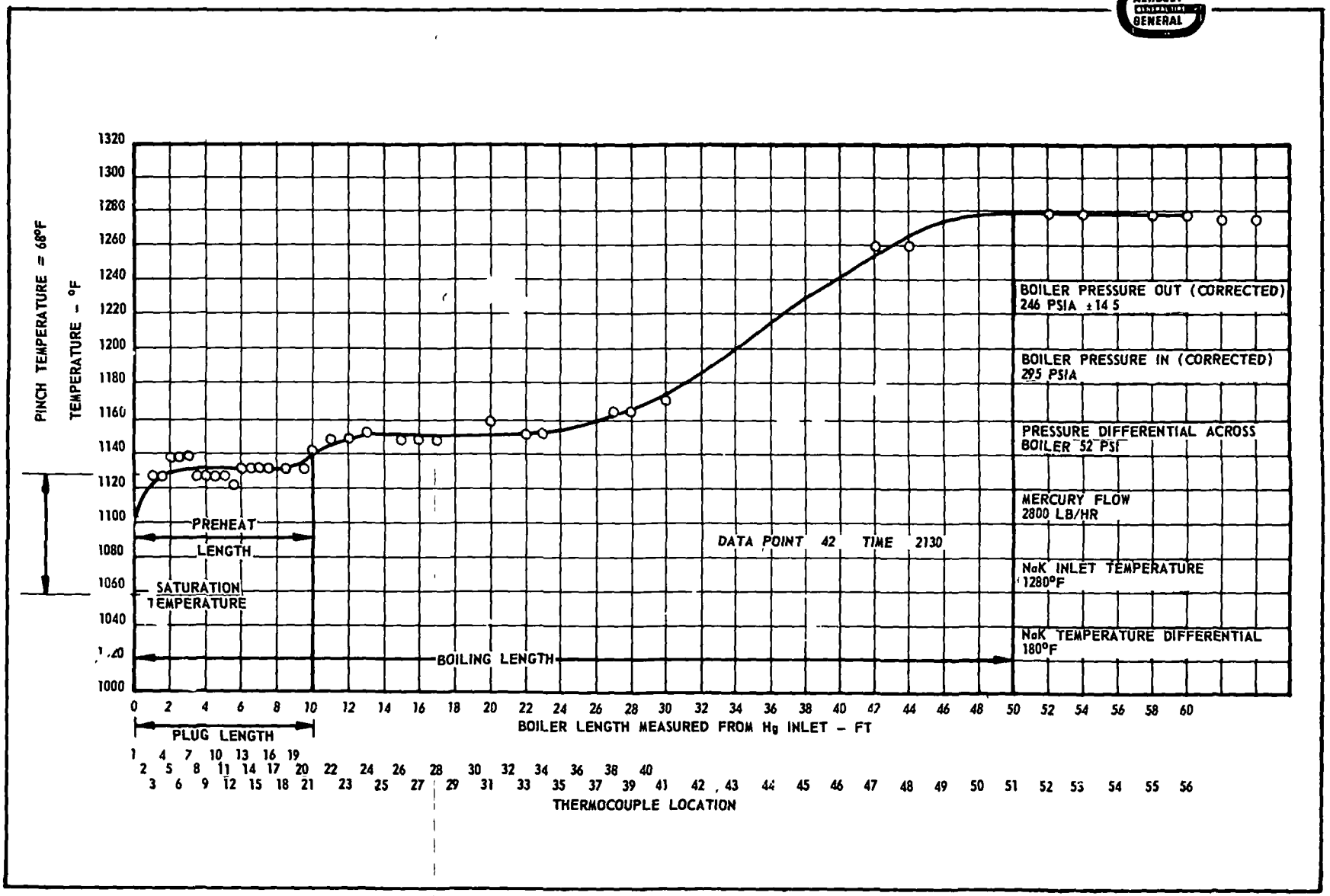

Boiler Thermal Profile, Boiler Test Section - Data Point 42

Figure 74

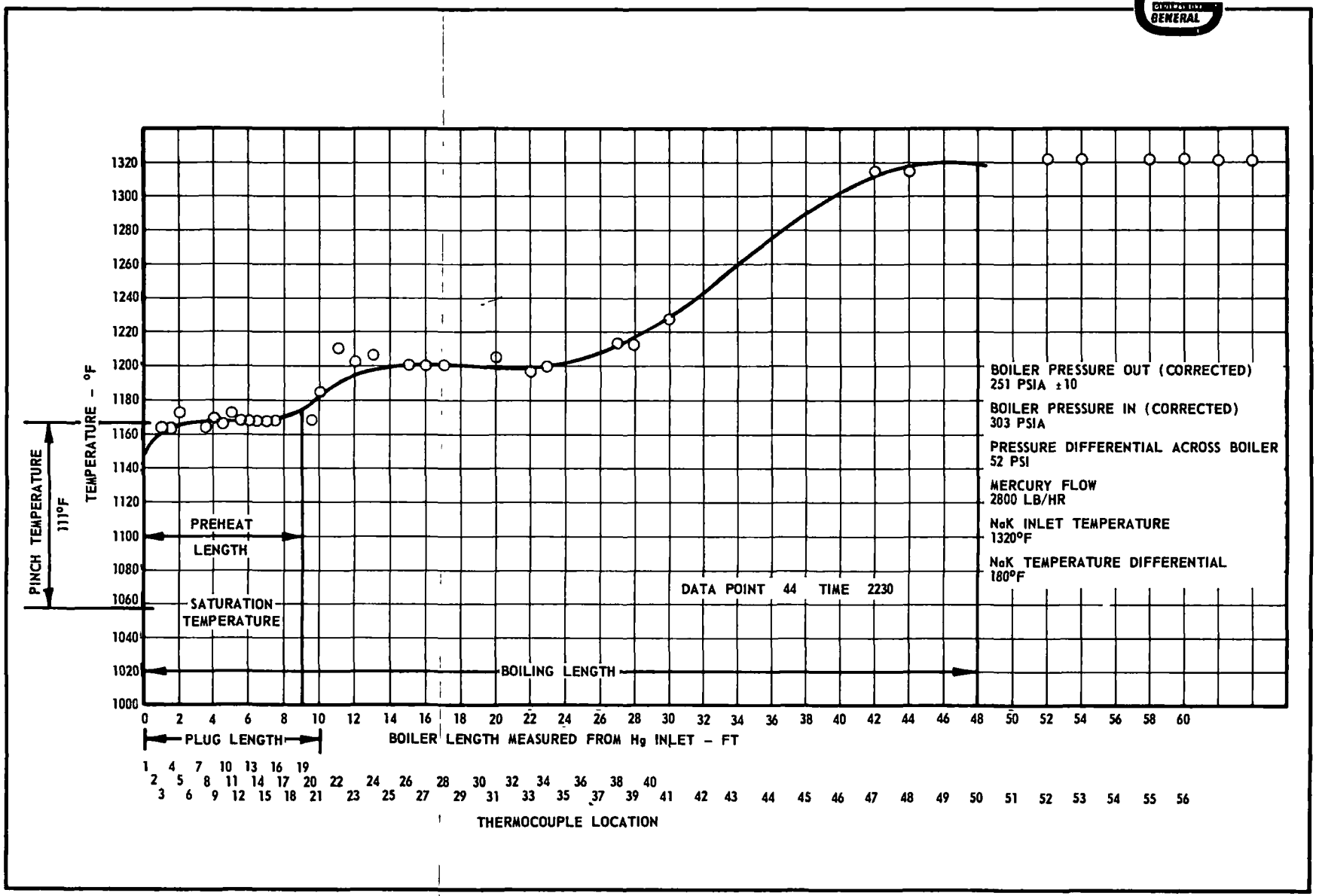

Boiler Thermal Profile, Boiler Test Section - Data Point 44

Figure 75

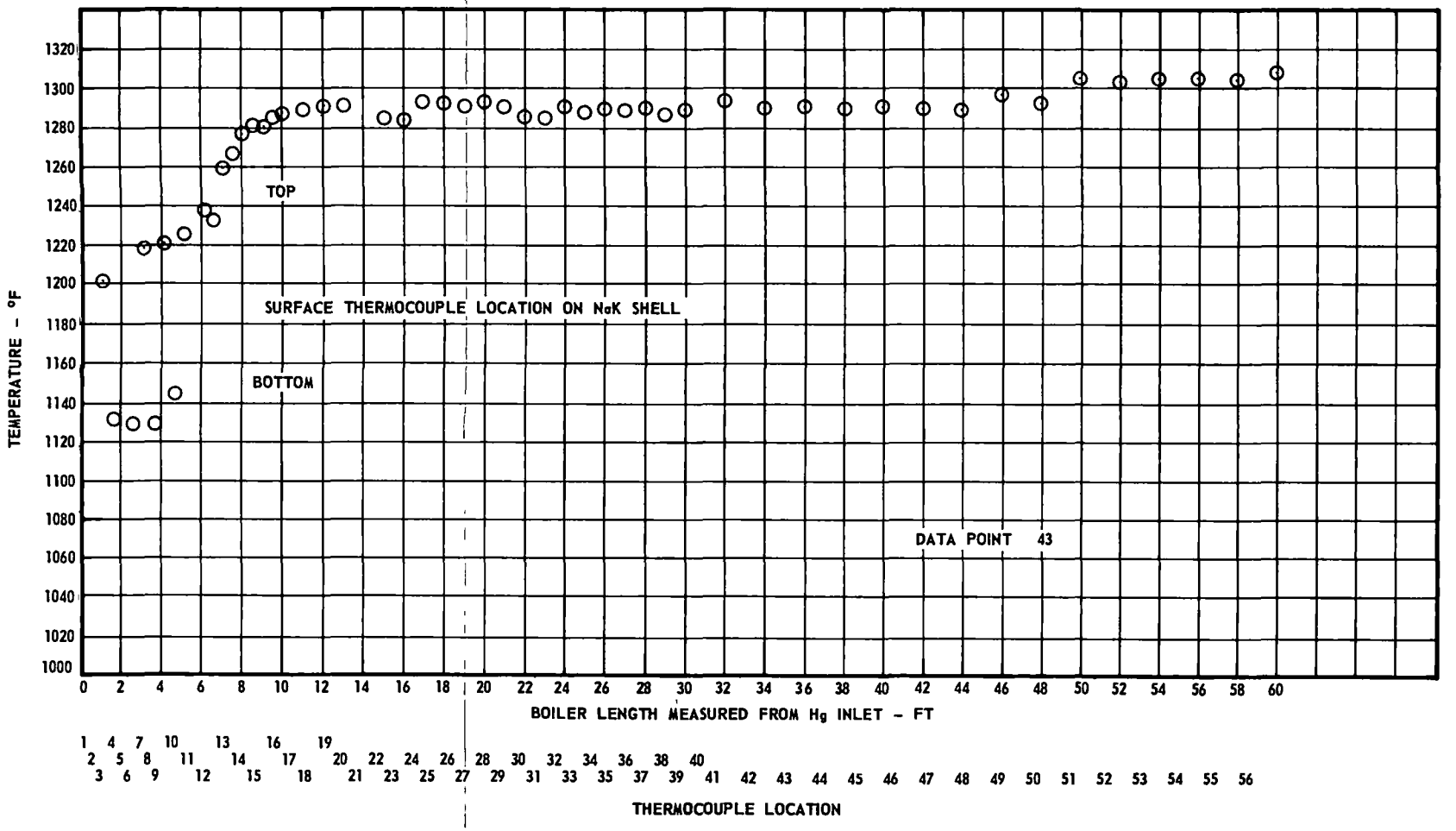

Boiler Thermal Profile, Boiler Test Section - Data Point 43

Figure 76

REVISIONS				
STA	ZONE	DESCRIPTION	DATE	APPROVED
A		SEE A CHANGE DCN		

NOTES: 1. REMOVE ALL BURRS AND SHARP EDGES
2 INTERPRET DWG PER J STD PRESCRIBED IN MIL-D-70327
3 MACHINED SURFACES TO BE 125
4 MARK PER AEDS 815 C WITH PART No 094202-1 AND ASSIGNED AGC SERIAL NO
5 COAT WITH OIL PER MIL-L-644 & PROTECTIVELY PACKAGE PER MIL-P-116, METHOD C
6 RADIOGRAPHICALLY INSPECT WELDS PER AGC-13859, INTERPRET PER AGC-13860, TABLE I, CLASS IV
7 PENETRANT INSPECT WELDS PER MIL-G866, TYPE II
8 TIG WELD PER AGC STD-2795 & AGC 10227 CLASS A, USING WELD ROD ASTM-A371-53T CLASS ER 310
9 PRIOR TO FINAL MACHINING, STRESS RELIEVE PER MIL-H-6875 AT 1350°F ±25°F FOR GO TO 75 MINUTES IN ARGON ATMOSPHERE HAVING A MINIMUM OF -40°F OR LOWER DEW POINT AS READ AT THE EXHAUST OF THE MUFFLE. RETAIN ARGON ATMOSPHERE UNTIL TEMP DROPS TO 800°F. STILL AIR COOL
10 ITEM 2 MUST HAVE .010 TO .013 CLEARANCE WITH ITEM 1

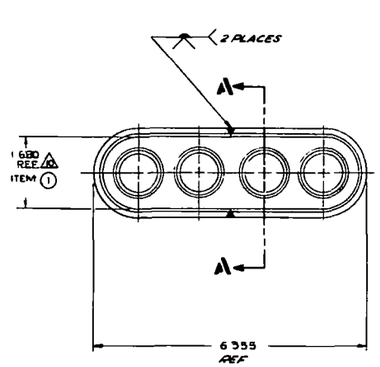

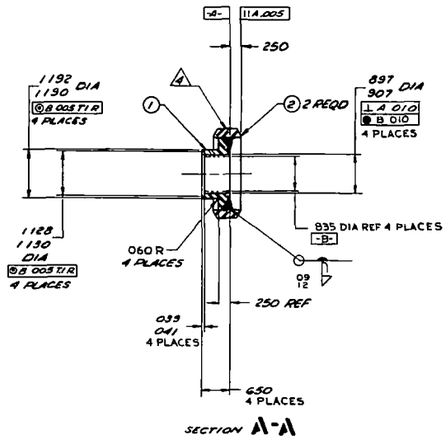

SECTION A-A

ITEM	QTY	CODE IDENT NO.	PART OR IDENTIFYING NO.	NOMENCLATURE OR DESCRIPTION	SPECIFICATION	UNIT WT.	ZONE	ITEM NO.
6	AR			WELD ROD	AMS 5787 CLASS ER 310			5
5	AR			OIL	MIL-L-644			4
4	2		094225-1	COVER				3
3	1		094171-1	HEADER				2
2	1		094202-1	ASSEMBLY				1
QTY REQD	ITEM	CODE IDENT NO.	PART OR IDENTIFYING NO.	NOMENCLATURE OR DESCRIPTION	SPECIFICATION	UNIT WT.	ZONE	ITEM NO.

LIST OF MATERIALS

UNLESS OTHERWISE SPECIFIED: DIMENSIONS ARE IN INCHES; TOLERANCES ON DECIMALS: .XX ± .03, .XXX ± .010; DO NOT SCALE DRAWING; ANGULAR ± 1°

TREATMENT 3

FINISH

NEXT ASSY | USED ON | APPLICATION

DRAWING LEVEL 1

DRAWN R. LITTLE 9-29-64
ENGR
CHECKED
STRESS
MATERIALS
PROCESS
DESIGN ACTIVITY APPR.
QUALITY

AEROJET-GENERAL CORPORATION
AZUSA, CALIFORNIA

CODE IDENT NO. 70143 | SIZE E | DWG NO. 094202 | SCALE 1 | SHEET

094202 A

094202 A

COPY

Mercury Outlet Tube Header, -1 Boiler

Figure 77

REVISIONS				
STN	ZONE	DESCRIPTION	DATE	APPROVED

NOTES 1 REMOVE ALL BURRS AND SHARP EDGES
2 INTERPRET DWG PER STANDARDS PRESCRIBED IN MIL-D-70327
3 MACHINED SURFACES TO BE 125 UNLESS OTHERWISE SPECIFIED
4 ALL FILLET RADII TO BE .025 R
5 TIG WELD PER AGC-STD-2795 USING WELD ROD MIL-R-5632, CLASS I.
6 PENETRANT INSPECT WELDS MIL-I-6866, TYPE II
7 PROTECTIVELY COAT WITH OIL PER MIL-L-644
8 MARK PER ASD 5215 F WITH 094300-1 AND APPLICABLE DASH No AND ASSIGNED AGC LOT OR SERIAL No.
9 DIA TO BE DETERMINED BE COGNIZANT ENGINEER AS A RESULT OF A WATER FLOW CHECK TO GIVE 25 TO 35 PSI DROP AT AN EQUIVALENT MERCURY FLOW RATE OF 2500 LB/M.

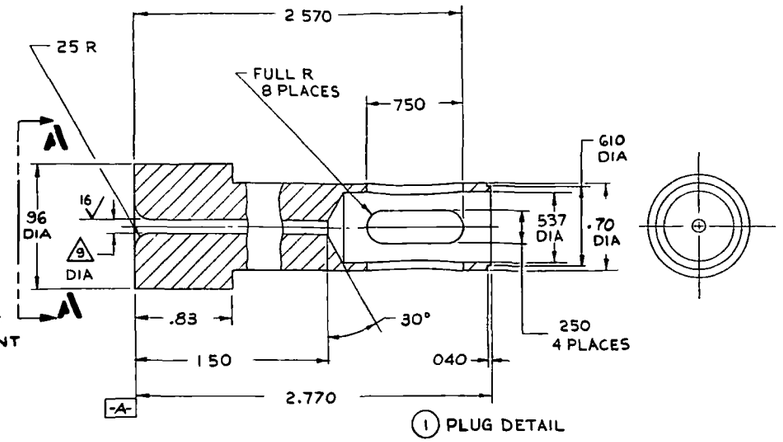

1 PLUG DETAIL

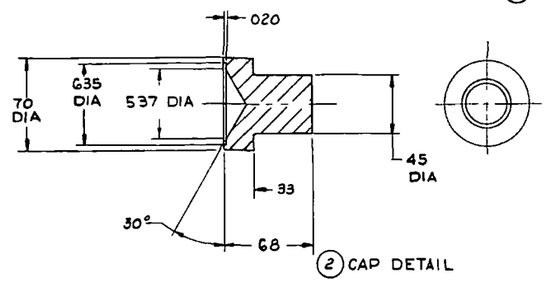

2 CAP DETAIL

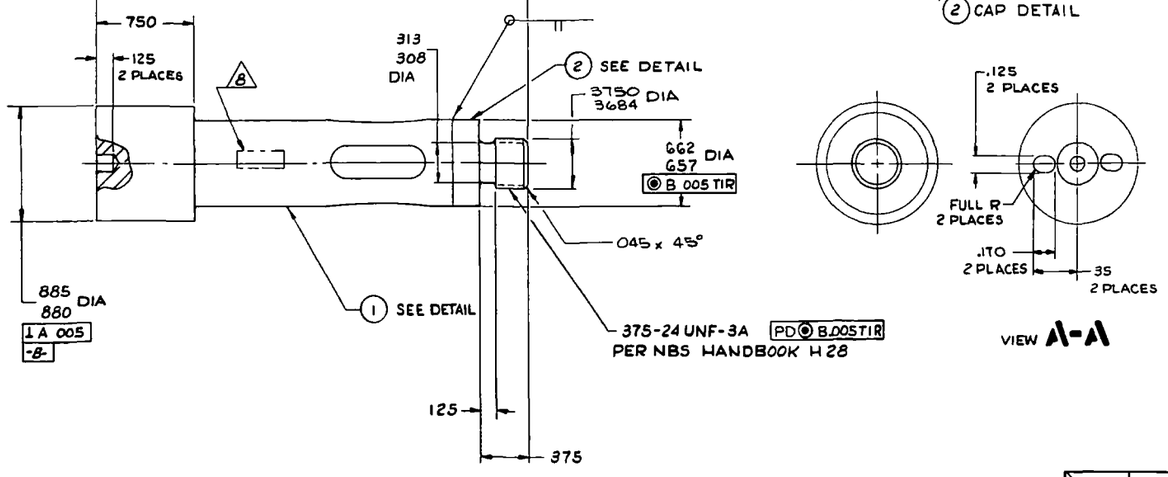

VIEW A-A

QTY REQD	SYM	CODE IDENT NO.	PART OR IDENTIFYING NO.	NOMENCLATURE OR DESCRIPTION	MATERIAL	SPECIFICATION	UNIT WT	ZONE	ITEM NO.
AR				WELD ROD		MIL-R 5632 CLASS I			6
AR				OIL, LUBRICATION		MIL-L-644			5
									4
									3
1			-5	CAP	750 DIA BAR M 1020	ASTM-A-7			2
1			-3	PLUG	1 250 DIA BAR M 1020	ASTM-A-7			1

LIST OF MATERIALS

ON	THRU	-1	4	4	092020-1	AGAN 0010
EFFECTIVE SERIAL NO		PART ASSY NO.	NEXT ASSY	FINAL ASSY	NEXT ASSY	USED ON
USAGE DATA			QTY REQD PER ASSY		APPLICATION	
		DRAWING LEVEL			1	

UNLESS OTHERWISE SPECIFIED
DIMENSIONS ARE IN INCHES
TOLERANCES ON DECIMALS ANGULAR
.XX = 03 = 2°
.XXX = 010
DO NOT SCALE DRAWING

TREATMENT
FINISH
SIMILAR TO — ACT WT — CALC WT

DRAWN	H T HIDALGO	DATE 1-10-64
CHECK		
DESIGN		1-15-64
STRUCTURE/STRESS		1-14-64
MATERIALS		1-14-64
PROJECT ENGINEER		1-14-64
DESIGN ACTIVITY APPD		1-14-64

AEROJET GENERAL CORPORATION
AZUSA, CALIFORNIA

TITLE
PLUG ASSY, INLET
BOILER, -1 MODEL

CODE IDENT NO.	DWG SIZE	DWG NO.
70143	D	094300

SCALE — RELEASE DATE 1-30-64 — SHEET

094300 COPY

Plug Assembly, -1 Boiler Inlet

Figure 78

SNAP-8 -1 Boiler Assembly, No. A-1. Mercury Outlet End Shown Near Completion of Final Hand Welding and Assembly

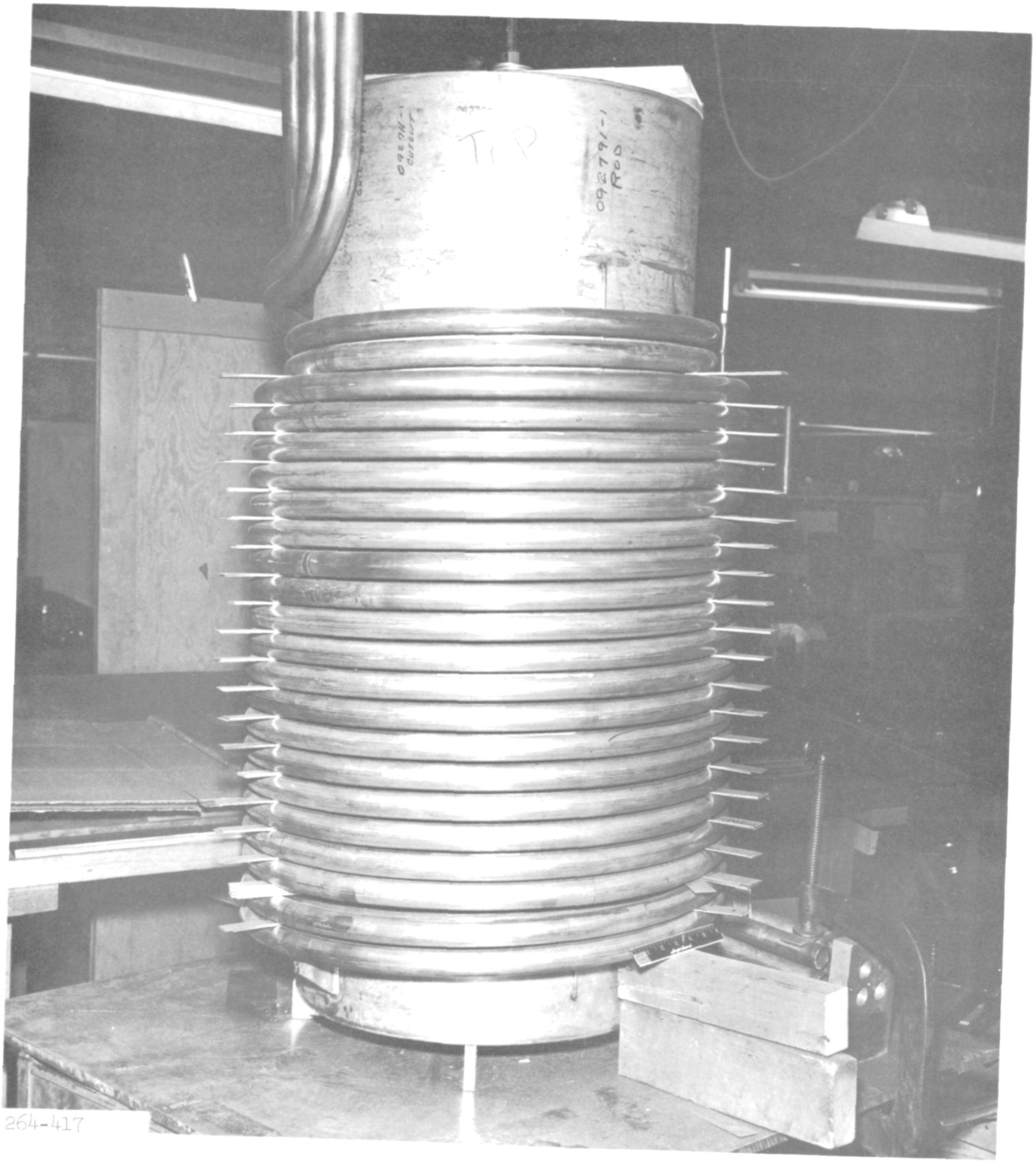

SNAP-8 -1 Boiler Assembly, No. A-2. Side View Showing Partially Assembled Boiler with Tubes Mounted on Inner Shell

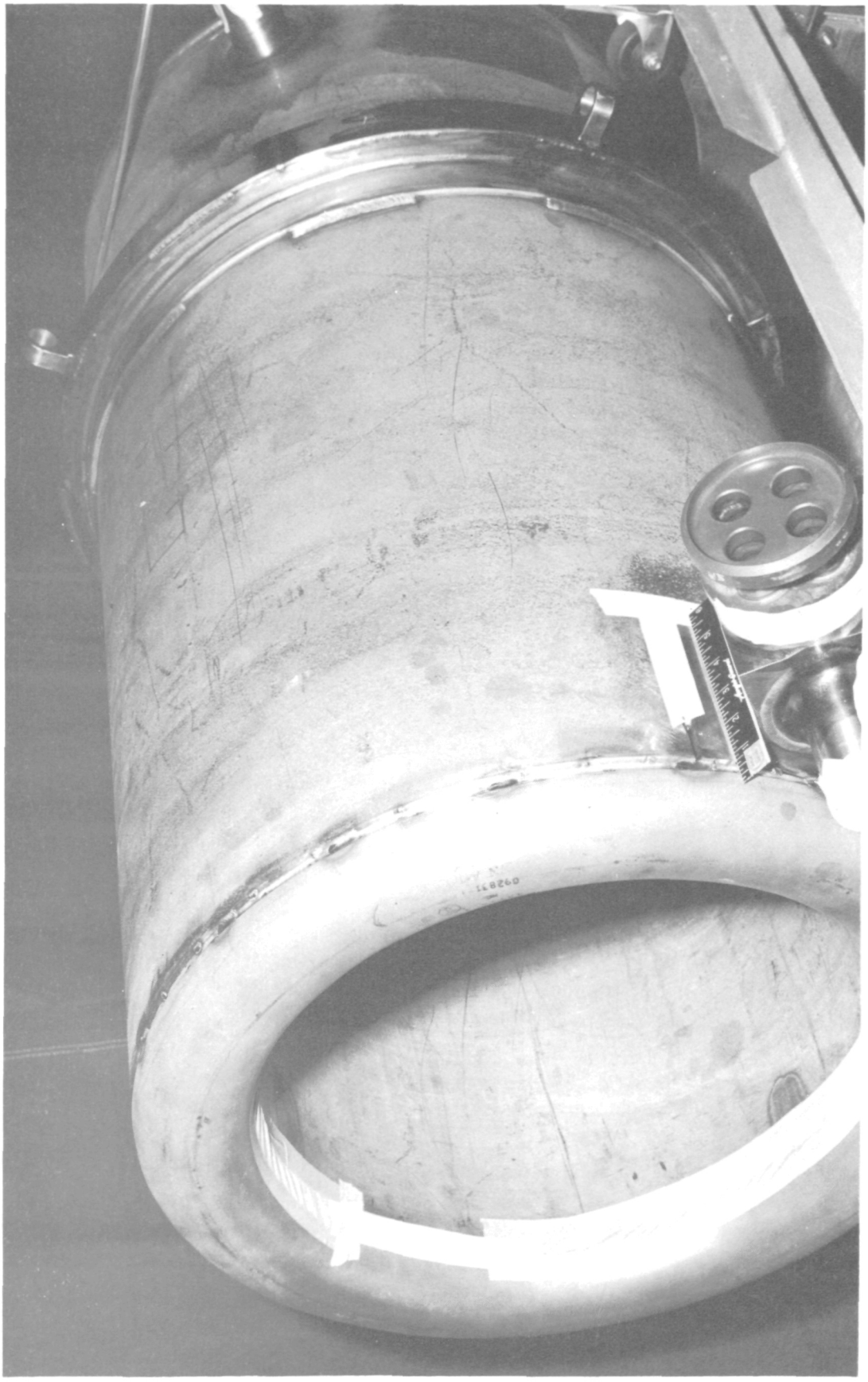

SNAP-8 -1 Boiler Assembly, No. A-1. Mercury Inlet at Lower Center. Boiler Shown Near Completion of Final Hand Welding and Assembly

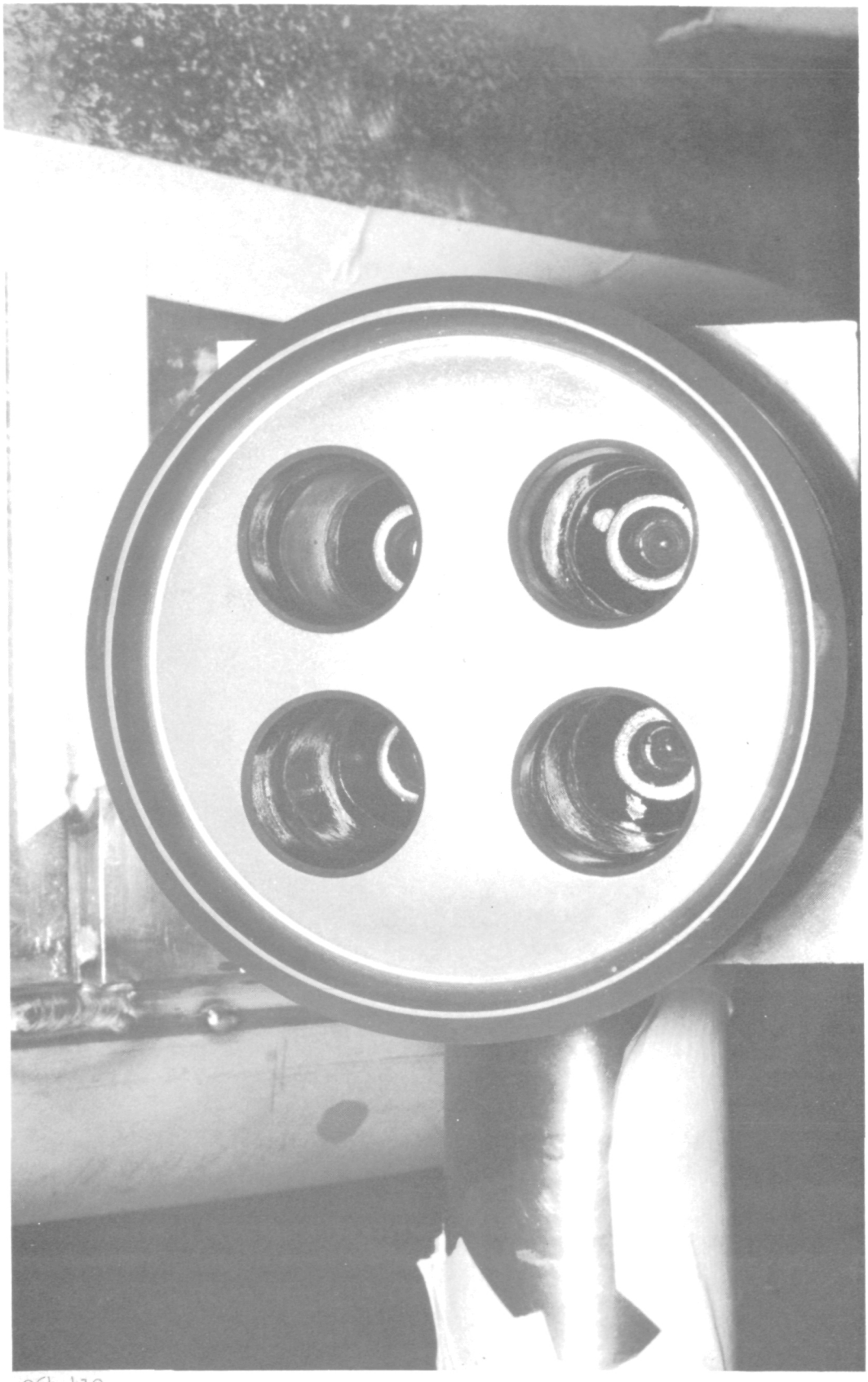

264-419

SNAP-8 -1 Boiler Assembly, No. A-1. Closeup of Mercury Inlet Header (Center) and NaK Outlet (Tube at Left) in Process of Final Assembly

Wood Mockup of SNAP-8 -1 Boiler Assembly

164-471

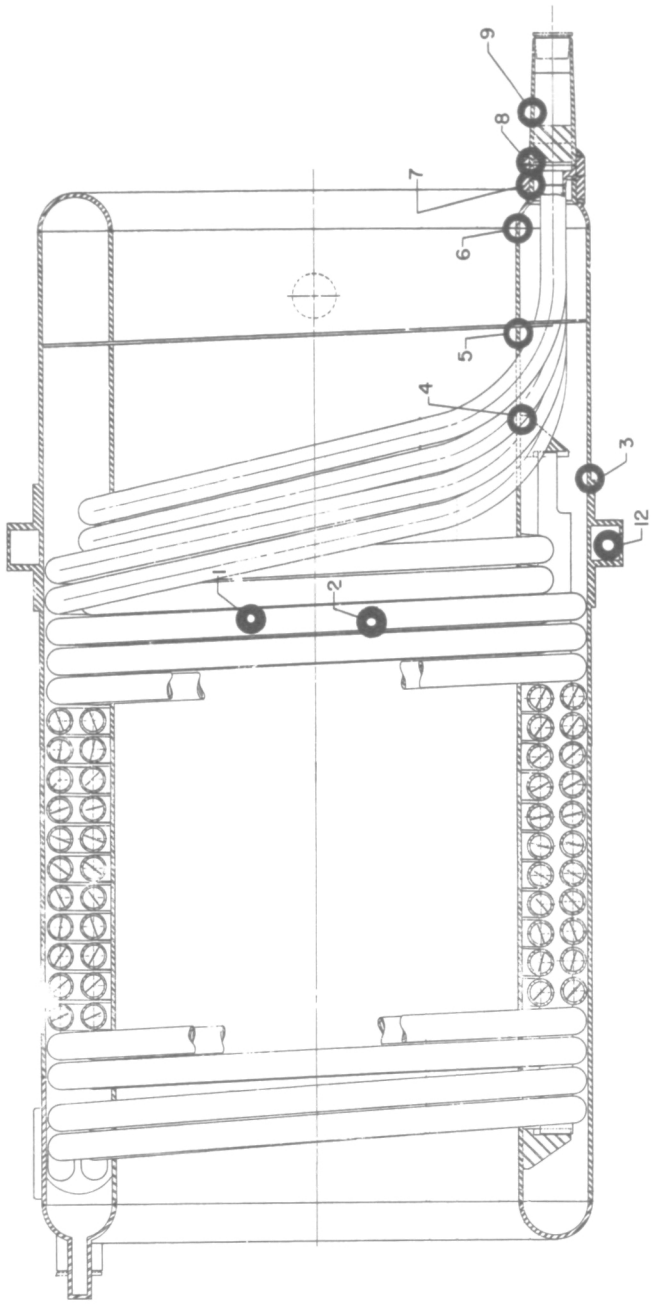

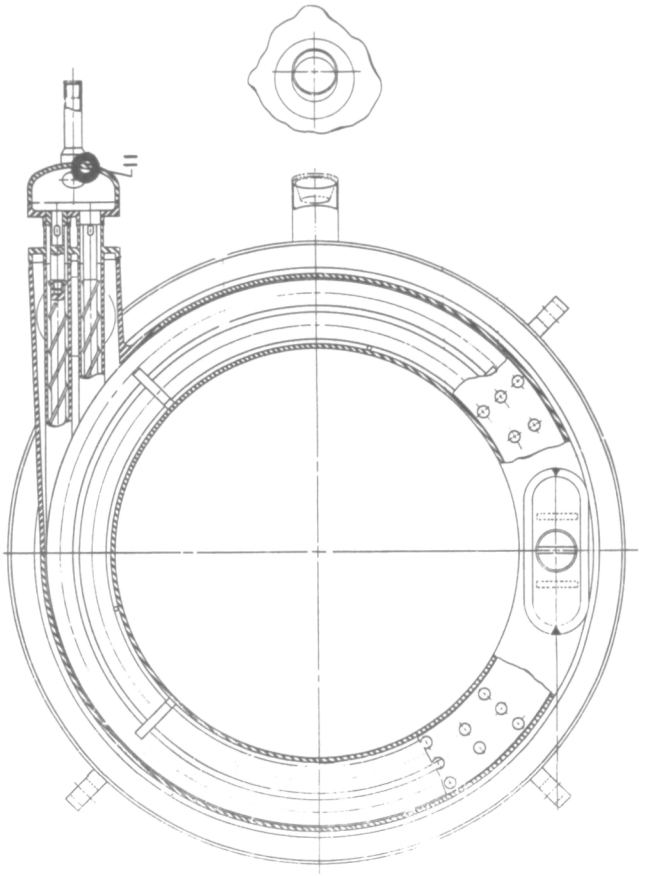

1. MAXIMUM HEAT FLUX ZONE
2. TUBE BUTT WELD
3. OUTER SHELL
4. TUBE BEND
5. INNER SHELL
6. TORUS-TO-SHELL CONNECTION
7. & 8. 316 S.S. TO 9 Cr-1 Mo TRANSITION WELD
9. MERCURY OUTLET
10. TUBE-TO-TUBE SHEET CONNECTION
11. MERCURY INLET
12. MOUNTING RING ASSEMBLY

SNAP-8 -1 Boiler, Major Stress Areas

264-853

SNAP-8 -1 Condenser

Figure 85

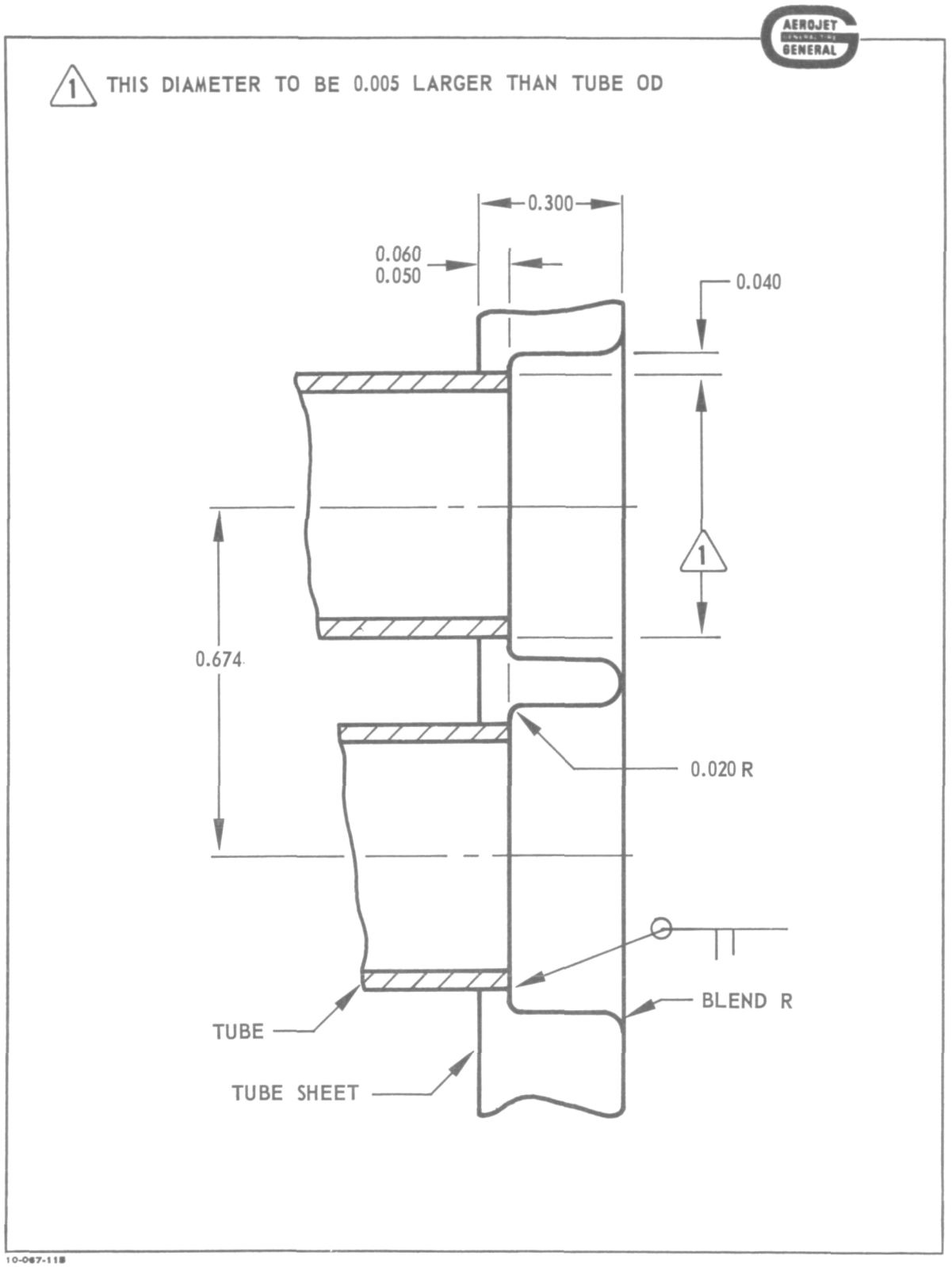

SNAP-8 -1 Condenser. Tube-to-Tube Sheet Weld. Sample Development No. 2

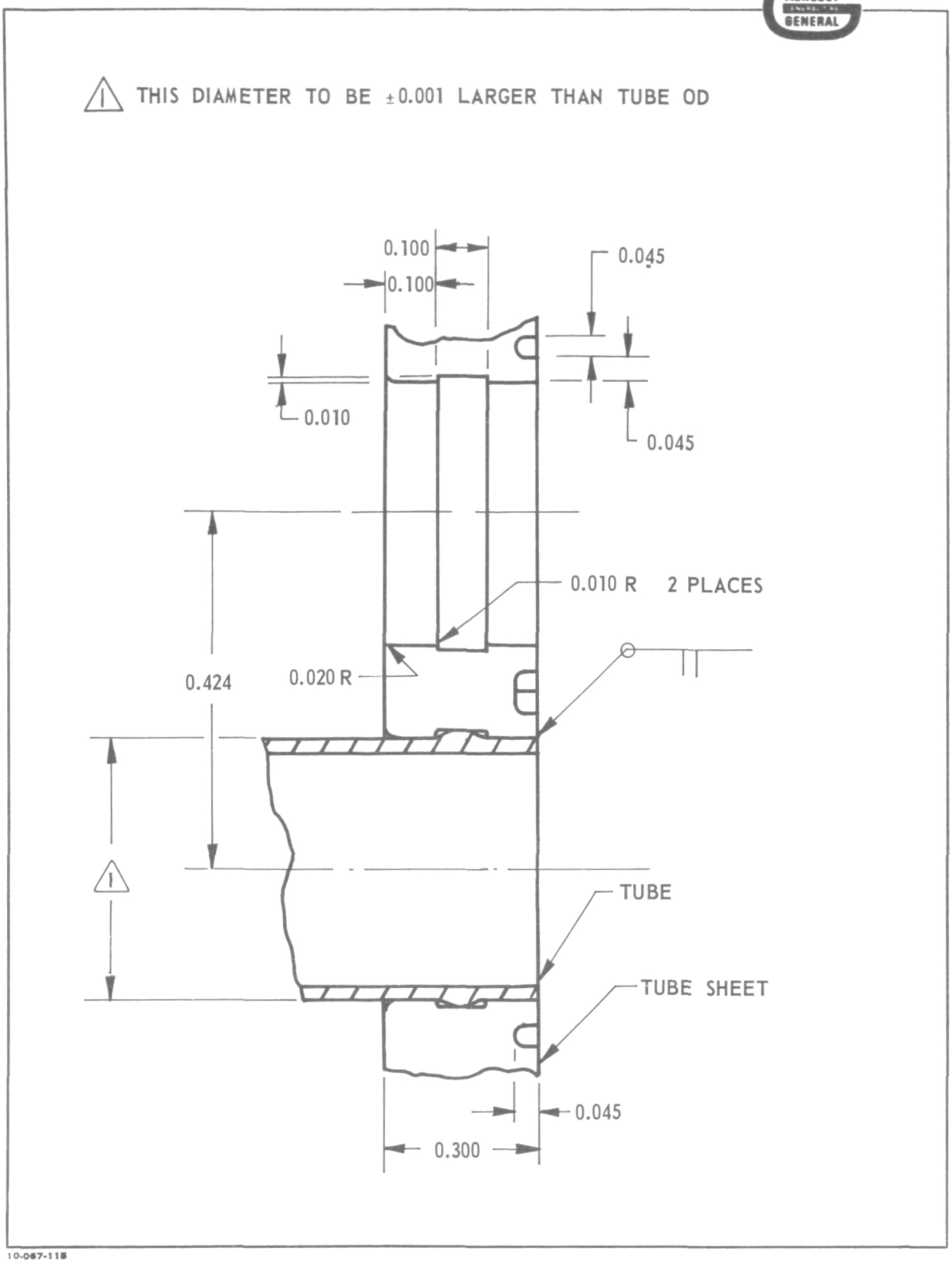

SNAP-8 -1 Condenser. Tube-to-Tube Sheet Weld. Sample Development No. 6

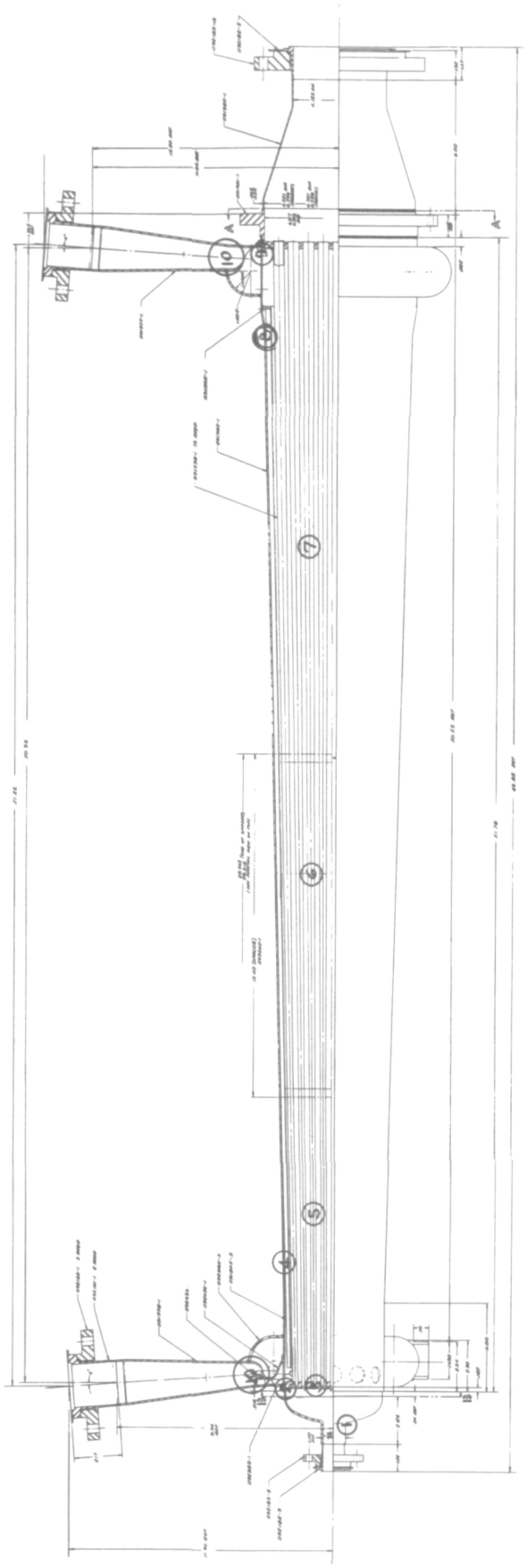

SNAP-8 -1 Condenser Structural Analysis. Numbered Points Show Parts Analyzed.

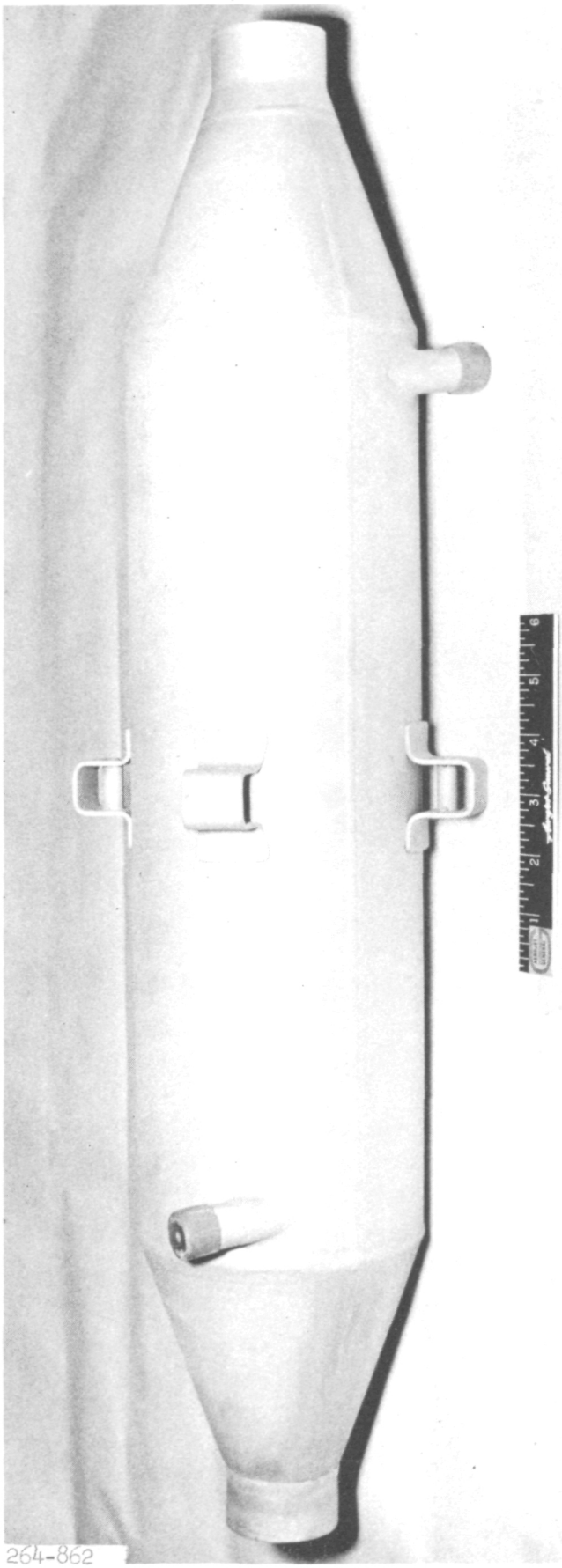

SNAP-8 -1 Auxiliary Start Loop Heat Exchanger

Figure 89

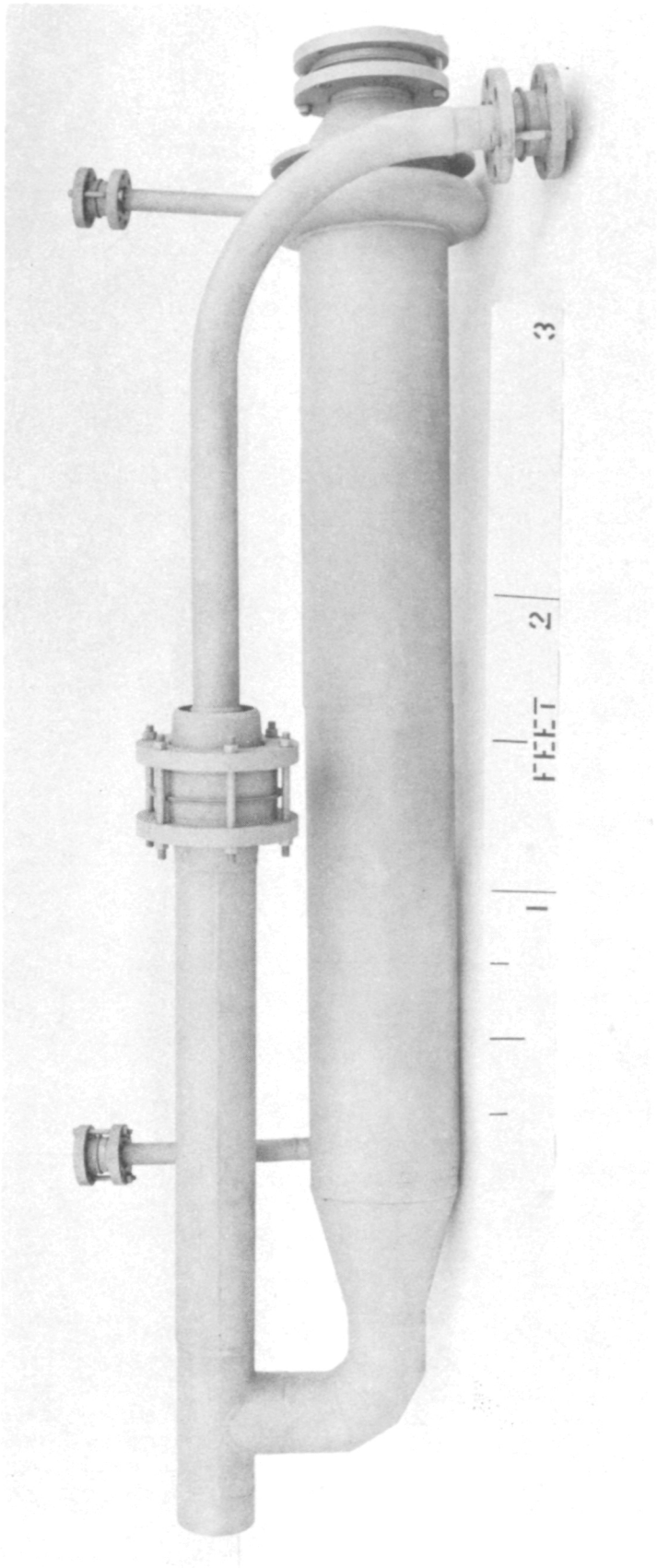

264-928

SNAP-8 Turbine Simulator

Figure 90

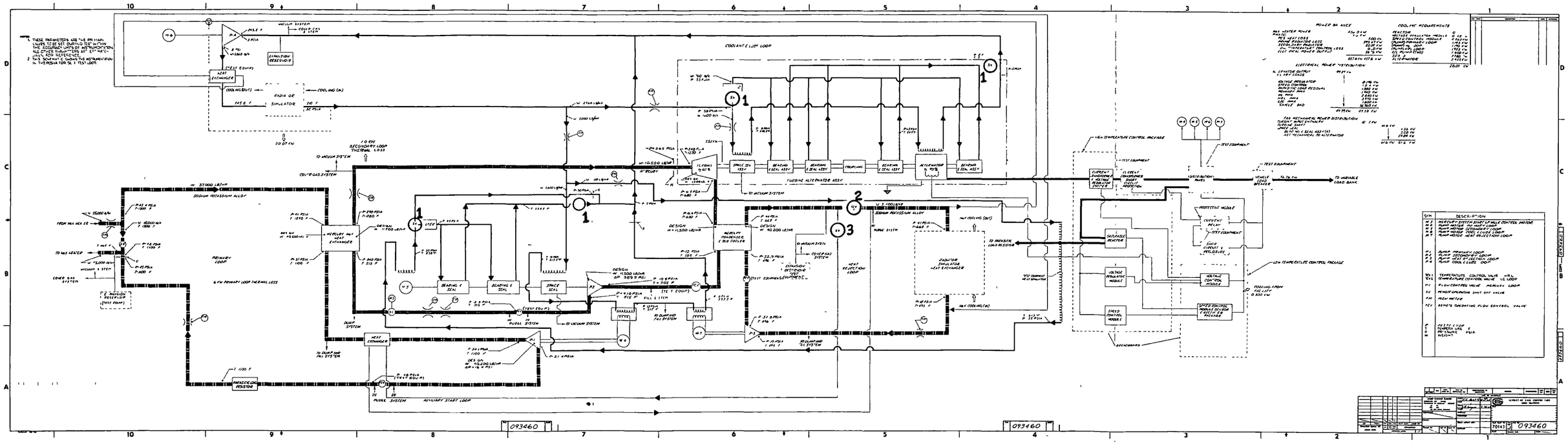

SNAP-8 PCS-1A Schematic Showing Location of Valves

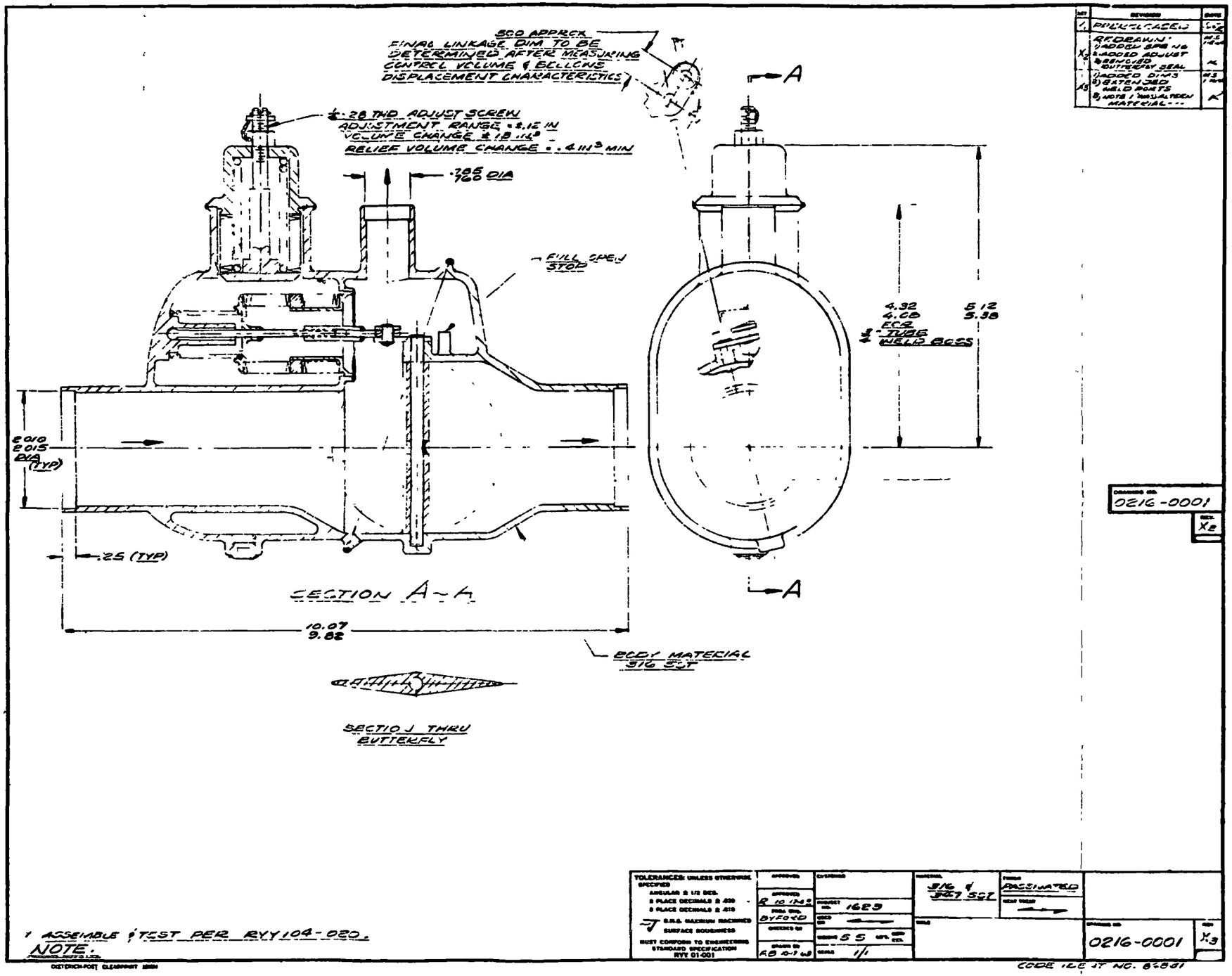

Figure 92

Preliminary Design - SNAP-8 Heat-Rejection-Loop Temperature Control Valve

UNCLASSIFIED

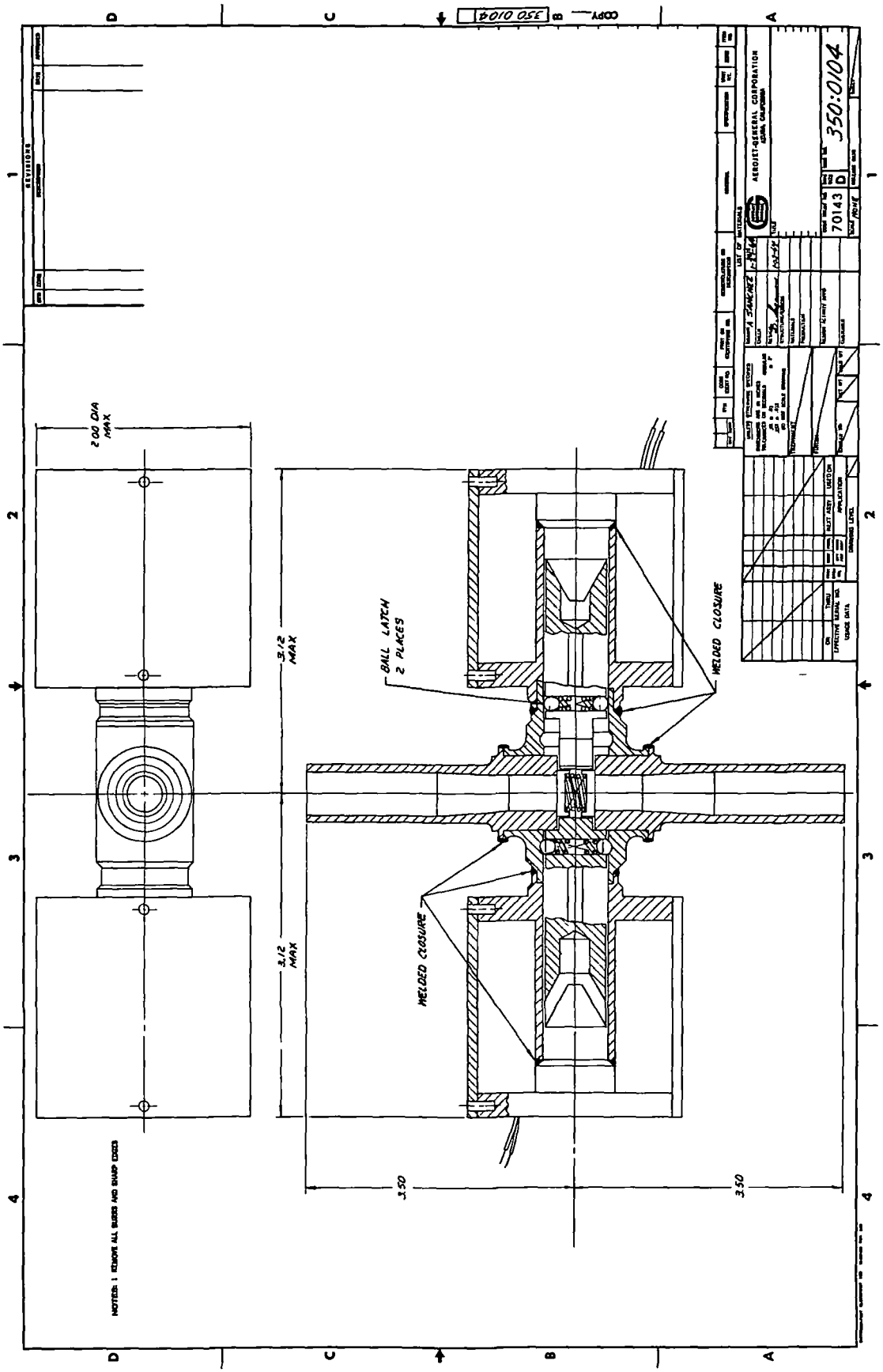

Preliminary Design - SNAP-8 Lubricant-Coolant and Auxiliary Shutoff Valves

Figure 93

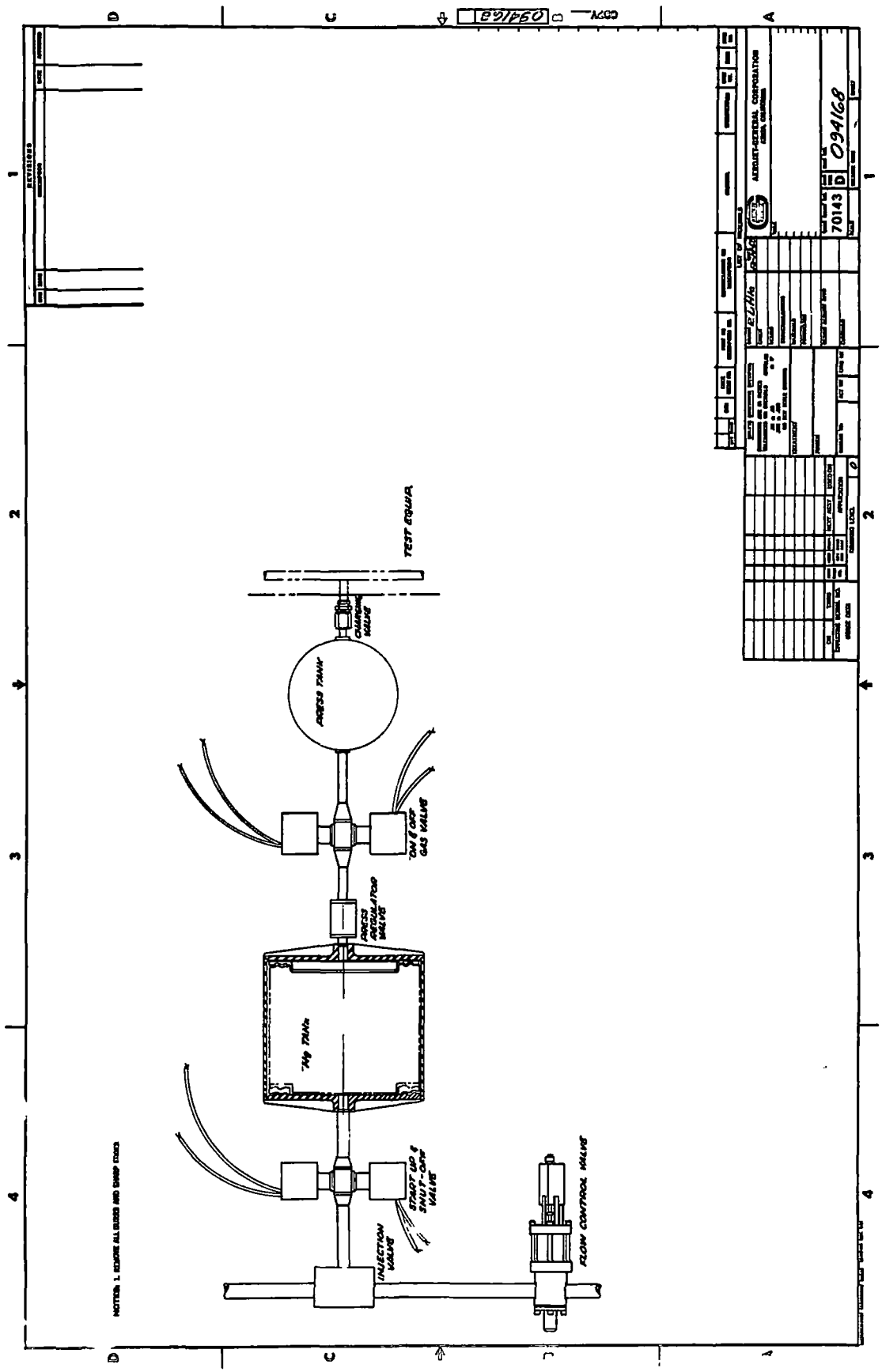

SNAP-8 Mercury Injection System

Figure 94

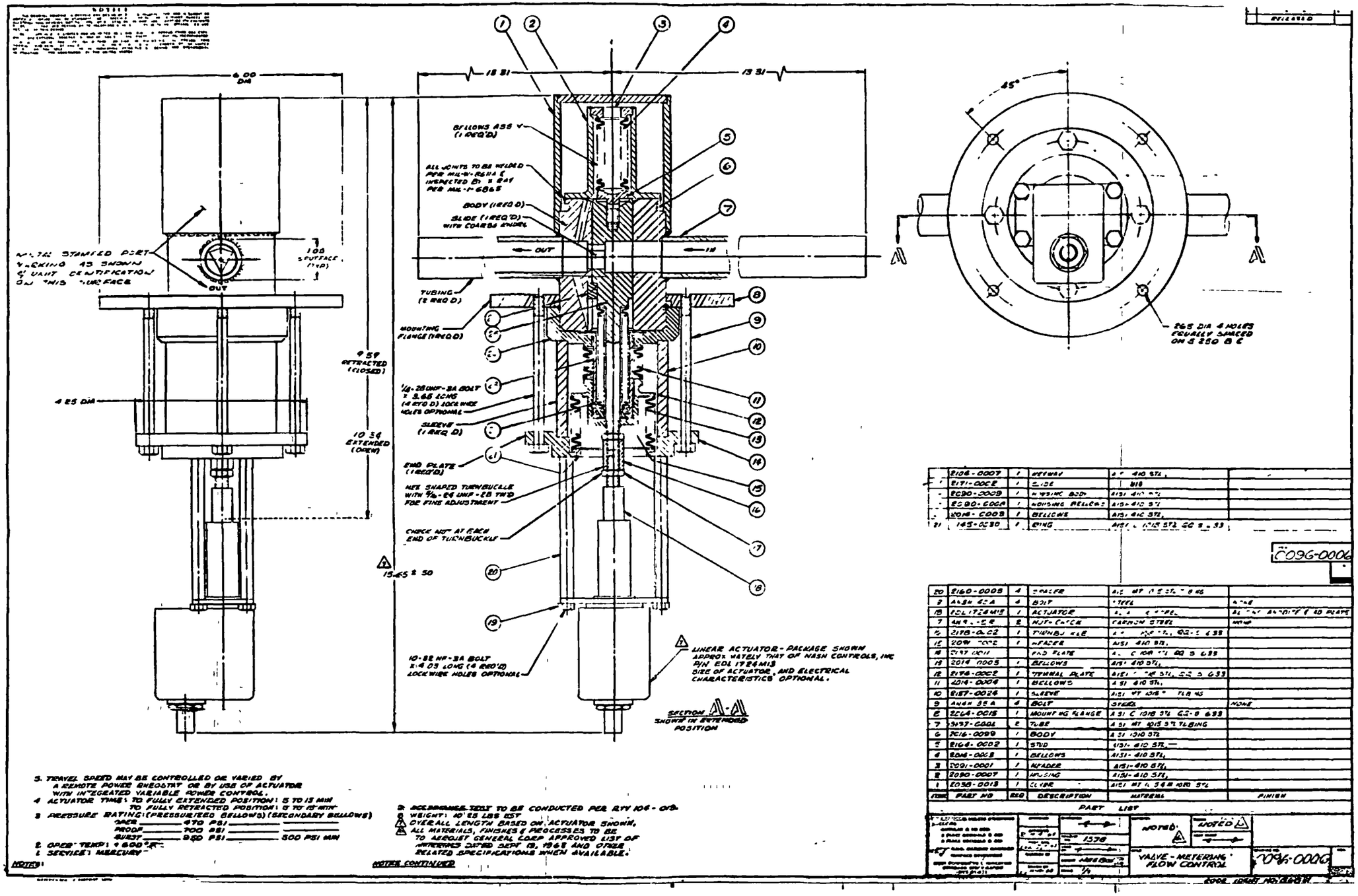

ITEM	PART NO	REQ	DESCRIPTION	MATERIAL	FINISH
21	145-0030	1	RING	AISI 4 [illegible] STL QQ S 633	
-	2080-0003	1	BELLOWS	AISI 410 STL	
-	EC80-0008	1	HOUSING BELLOWS	AISI 410 STL	
-	EC80-0009	1	HOUSING BODY	AISI 410 STL	
-	2171-0002	1	SLIDE	918	
-	2106-0007	1	BODY/AN	A-286	
20	2160-0008	4	SPACER	AISI MT 15 STL - 8 MS	
3	AN34 4-A	4	BOLT	STEEL	NONE
19	EDL 1724 M13	1	ACTUATOR	A-4 C TYPE	SEE NOTE 4 AND NOTE 6 ON PLATE
7	AN9-2-B	2	NUT-CAP	CARBON STEEL	NONE
14	2178-0002	1	TURNBUCKLE	A-286 NF-3A, 10-32 X 4.38	
15	2094-0002	1	HEADER	AISI 410 STL	
18	2197-0011		END PLATE	A-286 NF-3A QQ S 633	
13	2014-0005	1	BELLOWS	AISI 410 STL	
12	2176-0002	1	TERMINAL PLATE	AISI [illegible] STL QQ S 633	
11	2014-0004	1	BELLOWS	AISI 410 STL	
10	2157-0024	1	SLEEVE	AISI 9T 4316 TUBING	
9	AN34 3S-A	4	BOLT	STEEL	NONE
8	2144-0015	1	MOUNTING FLANGE	AISI C 1018 STL QQ-S 633	
7	2137-0004	2	TUBE	AISI MT 4015 STL TUBING	
6	2106-0009	1	BODY	AISI 1010 STL	
5	2164-0002	1	STUD	AISI-410 STL	
4	2014-0003	1	BELLOWS	AISI-410 STL	
3	2091-0001	1	HEADER	AISI-410 STL	
2	2090-0007	1	HOUSING	AISI-410 STL	
1	2038-0013	1	CLOSER	AISI MT 4 340 1018 STL	

Mercury Flow Control Valve for the SNAP-8

Mercury Injection System

Figure 95

UNCLASSIFIED

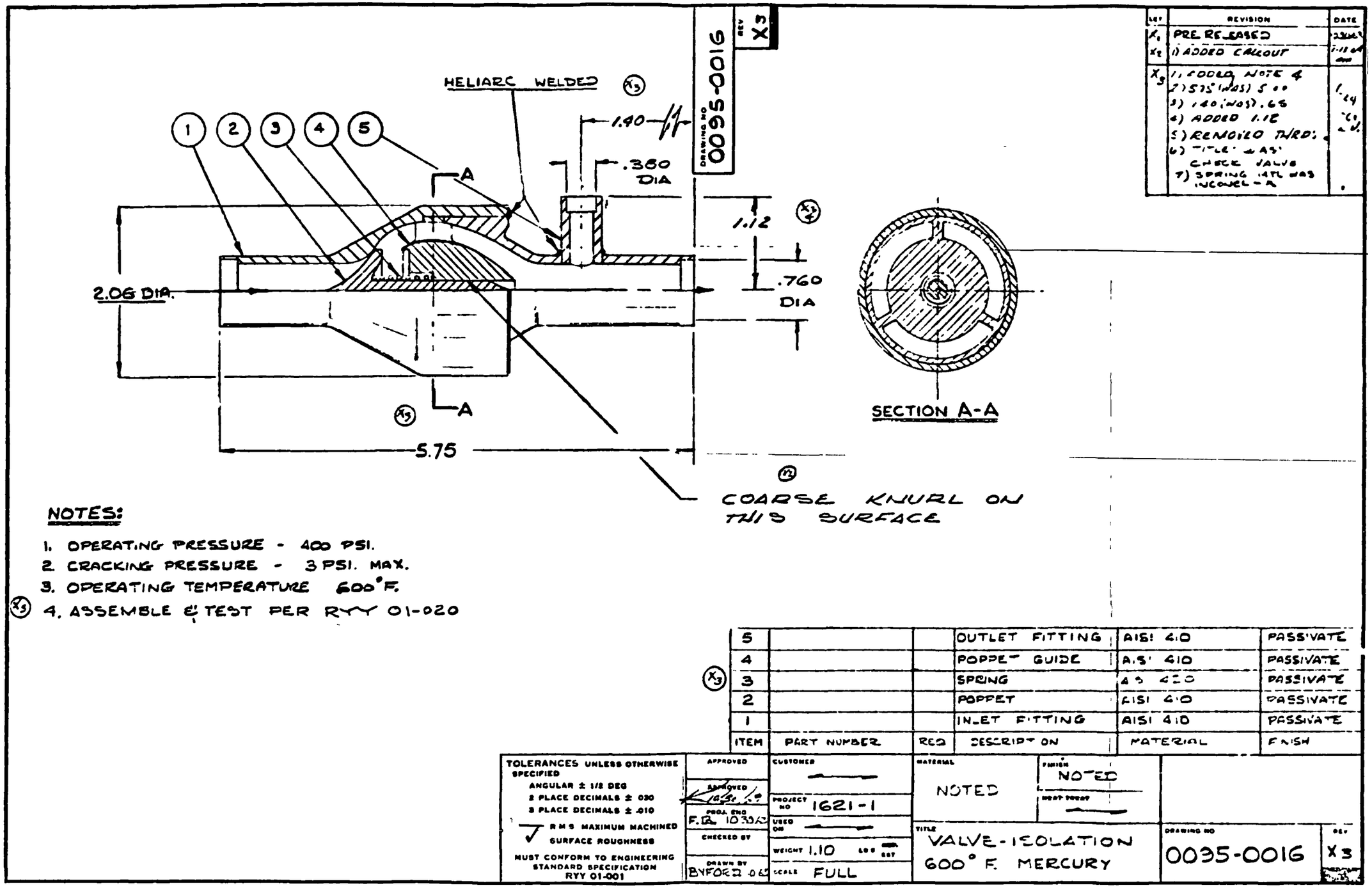

Figure 96

Isolation Valve for SNAP-8 Mercury Injection System.

PCS-1 and PCS-2 Use.

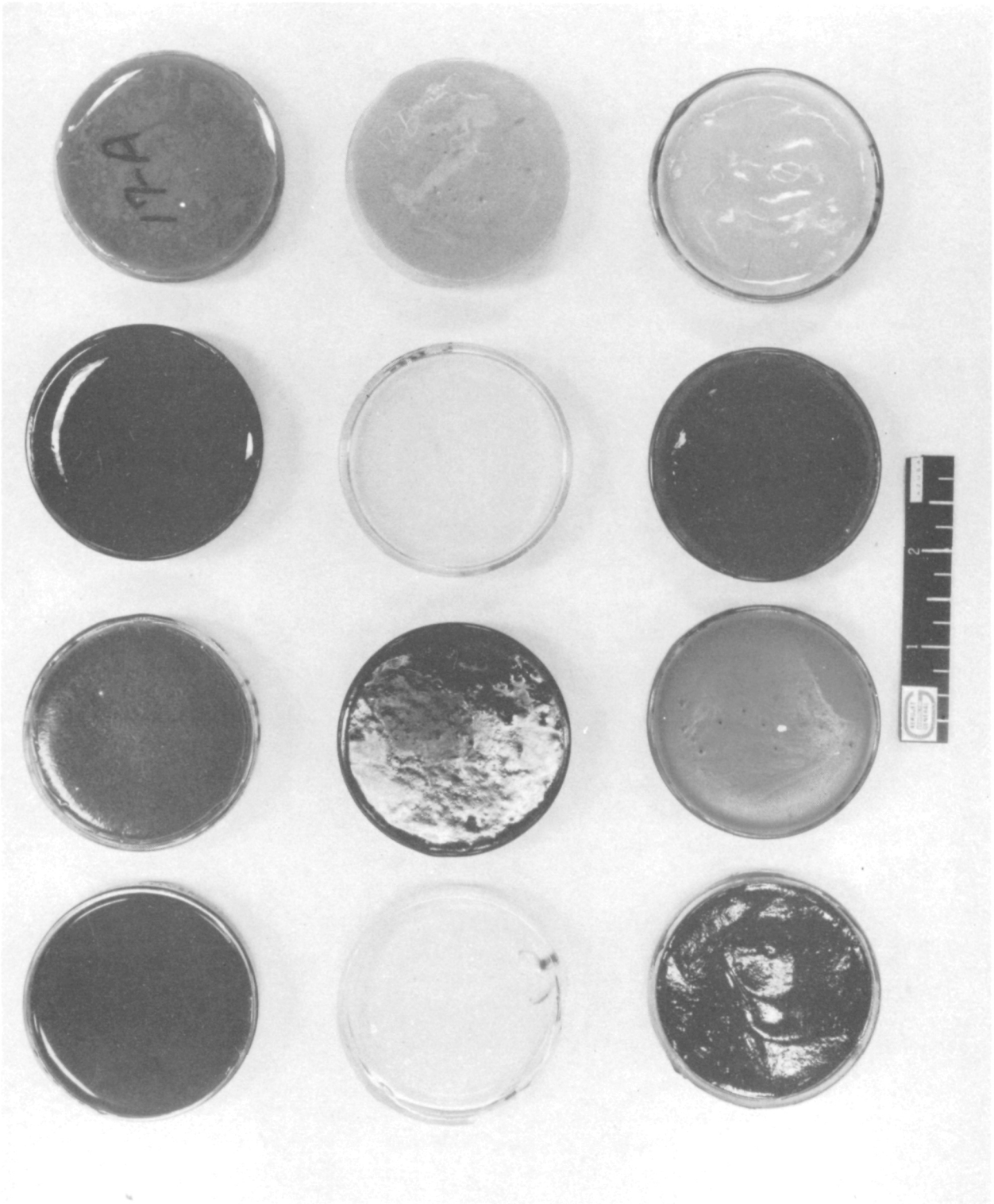

ORGANIC ENCAPSULANT SMAPLES READY FOR WEIGHT-LOSS STUDY

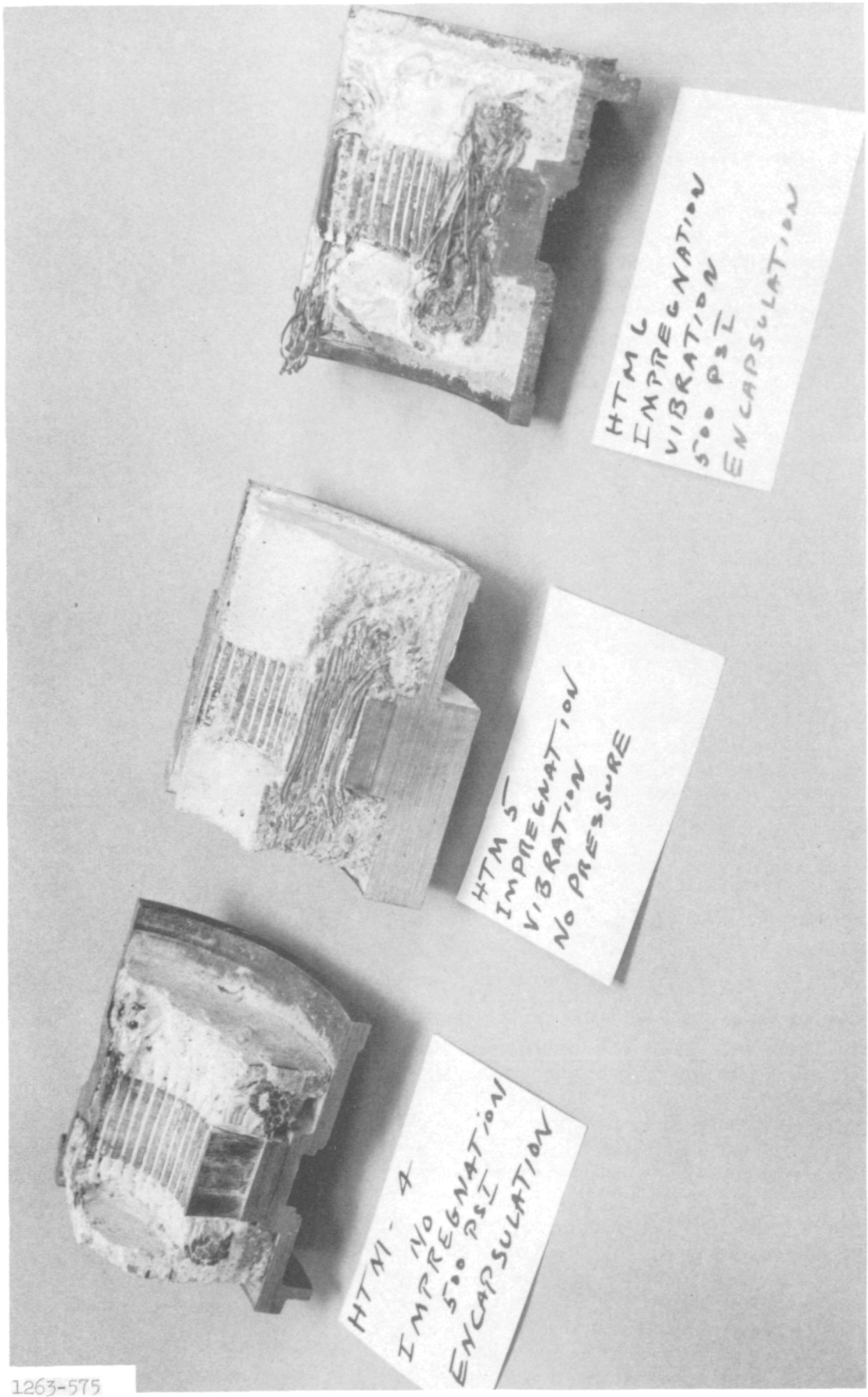

ENCAPSULATION TRIALS - HTM SERIES USING LM-1625 CEMENT

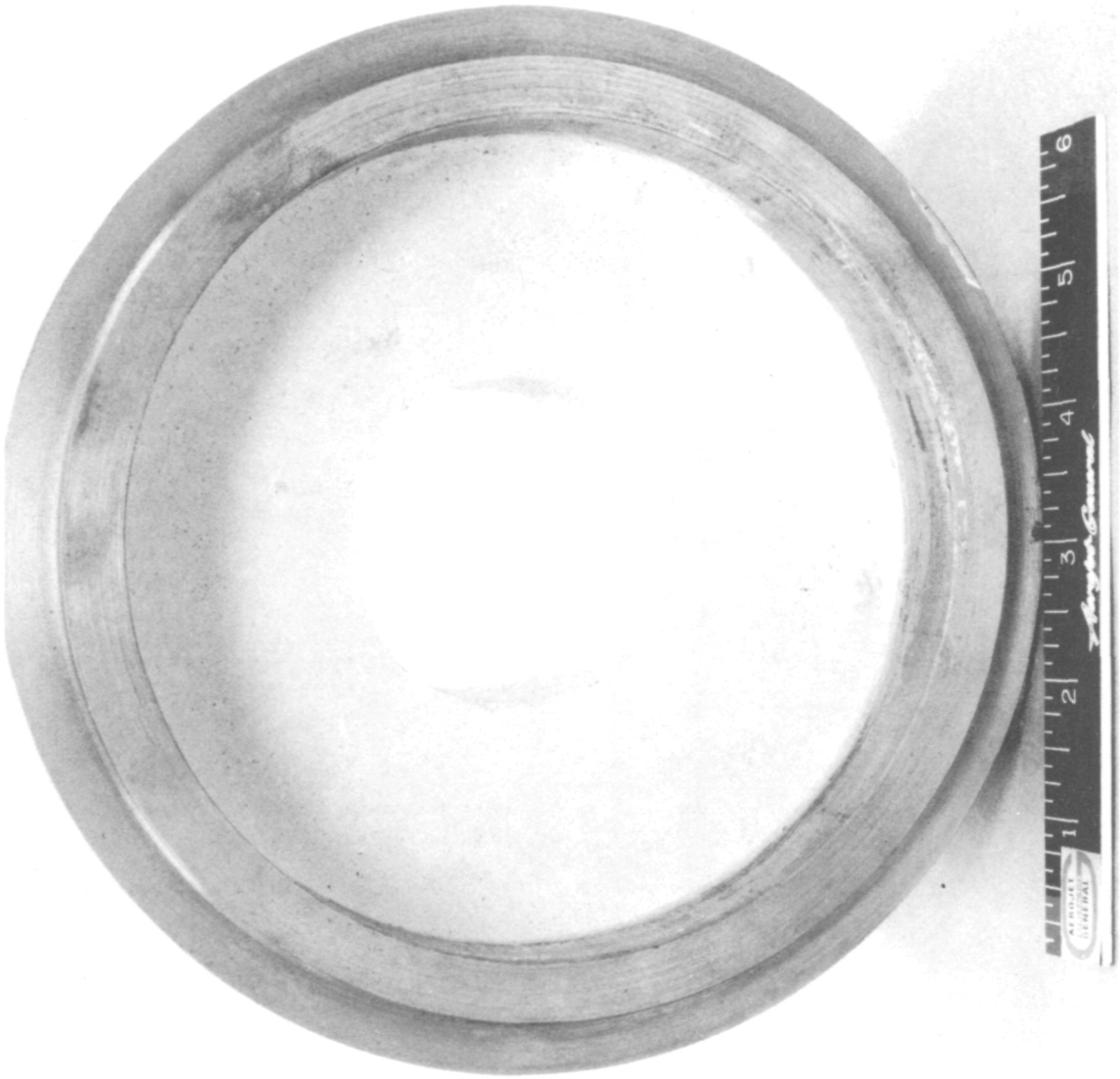

ENCAPSULANT STUDY TRIAL - LM-1625
PRESSED AT 250 PSI AFTER FINAL CURE

1263-137

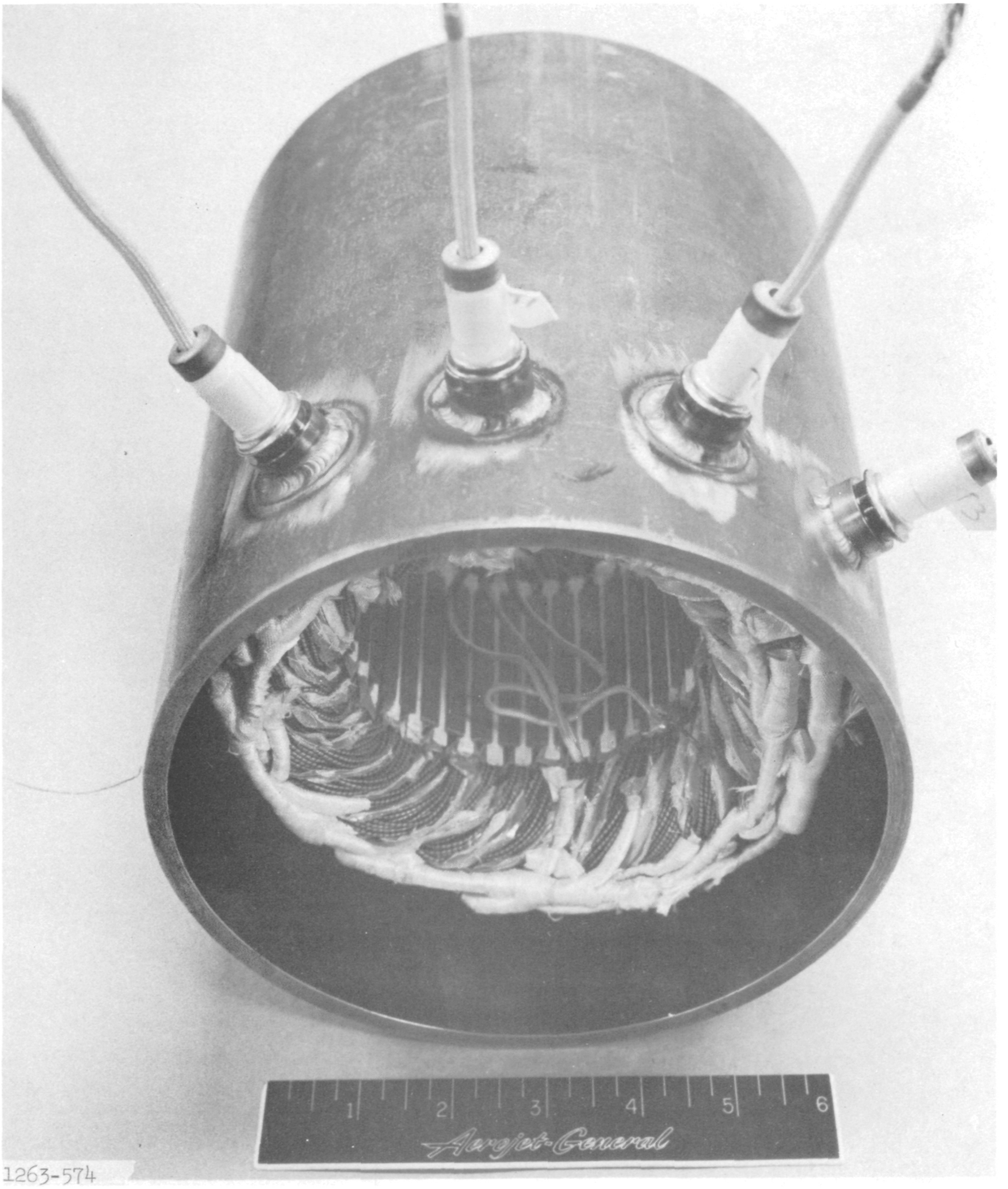

HRL Trial Stator in Dummy Housing

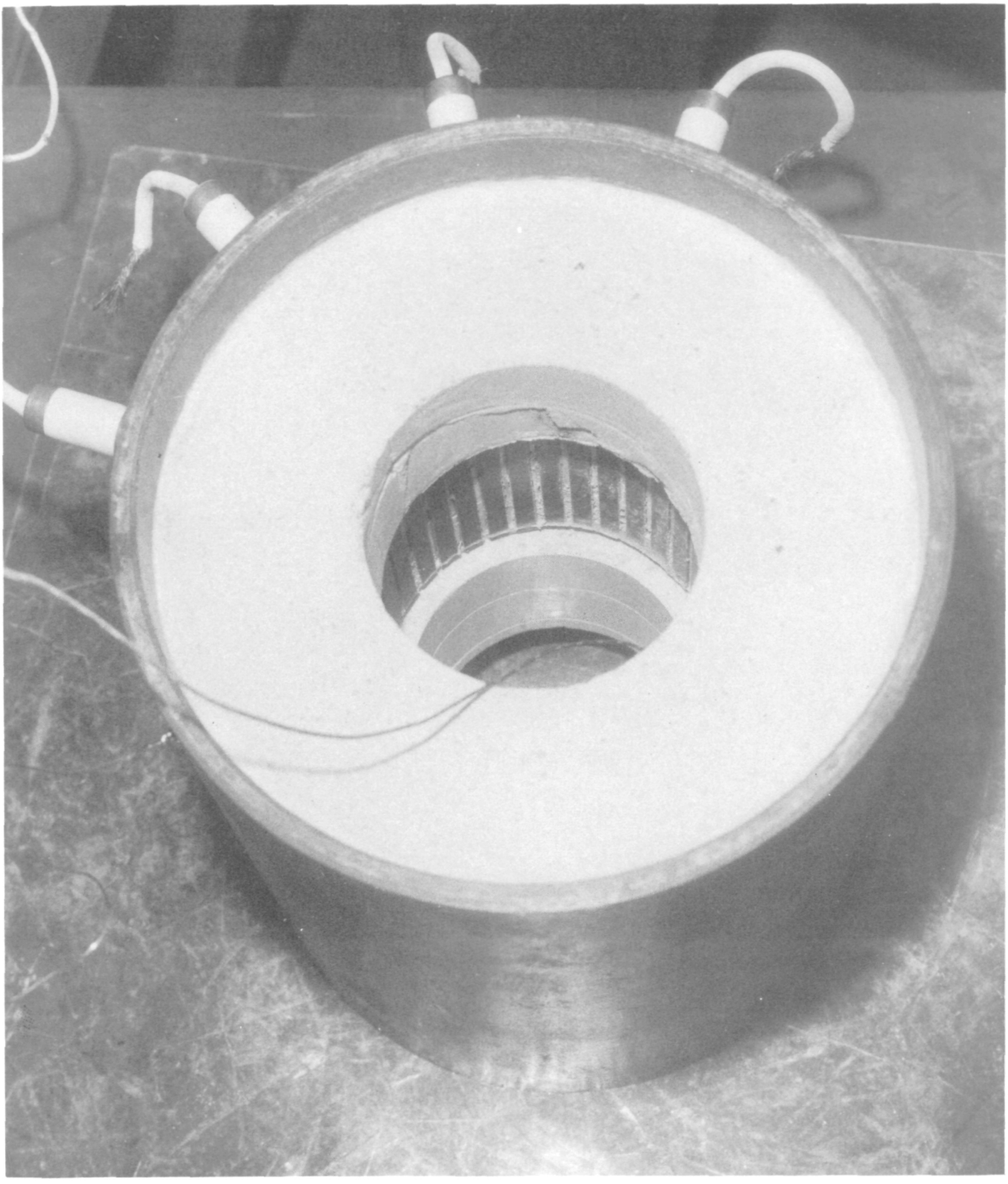

164-863

HRL Trial Stator in Dummy Housing - Following Test

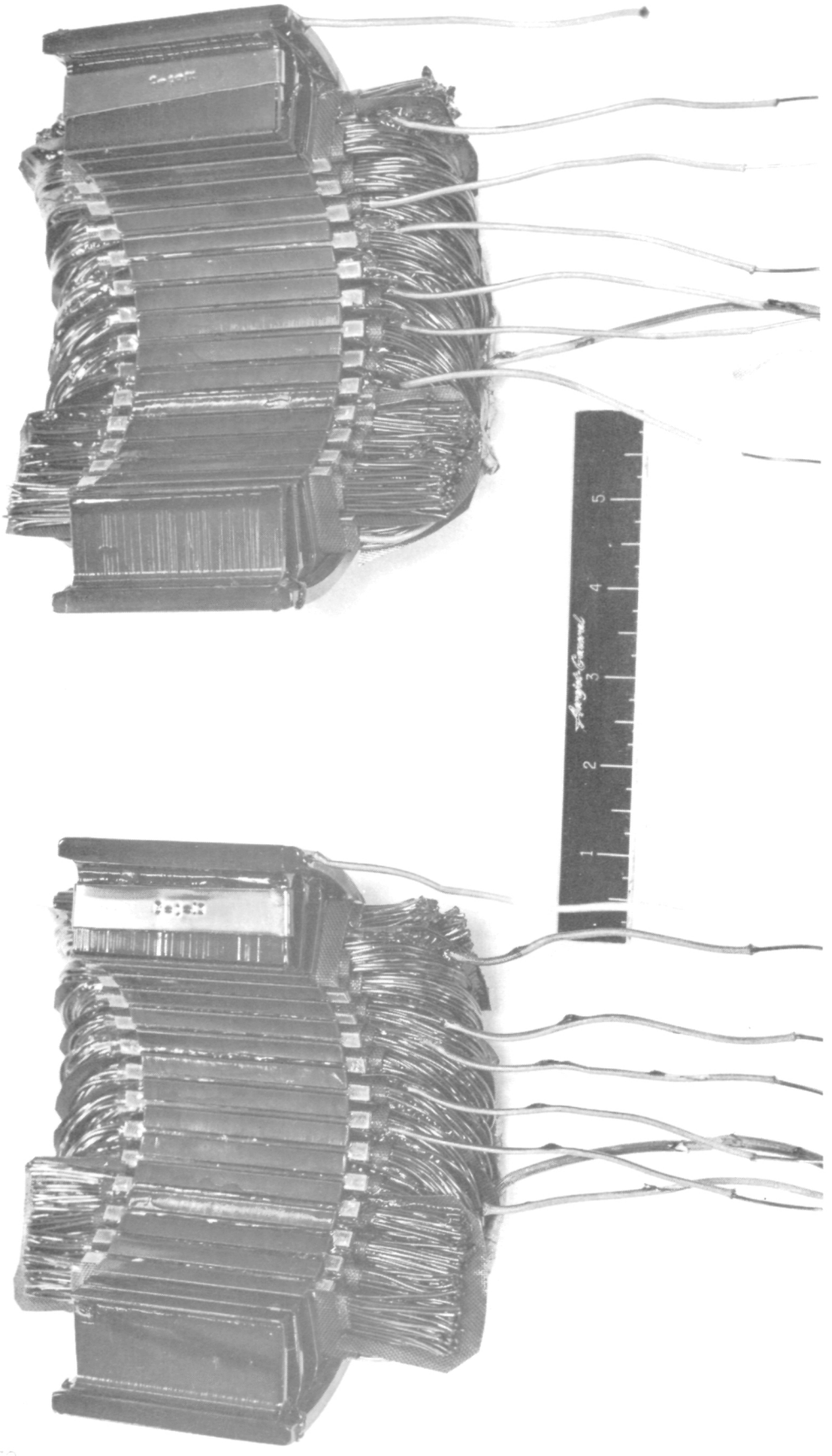

ORGANIC STATORETTES FOR RADIATION EFFECTS PROGRAM

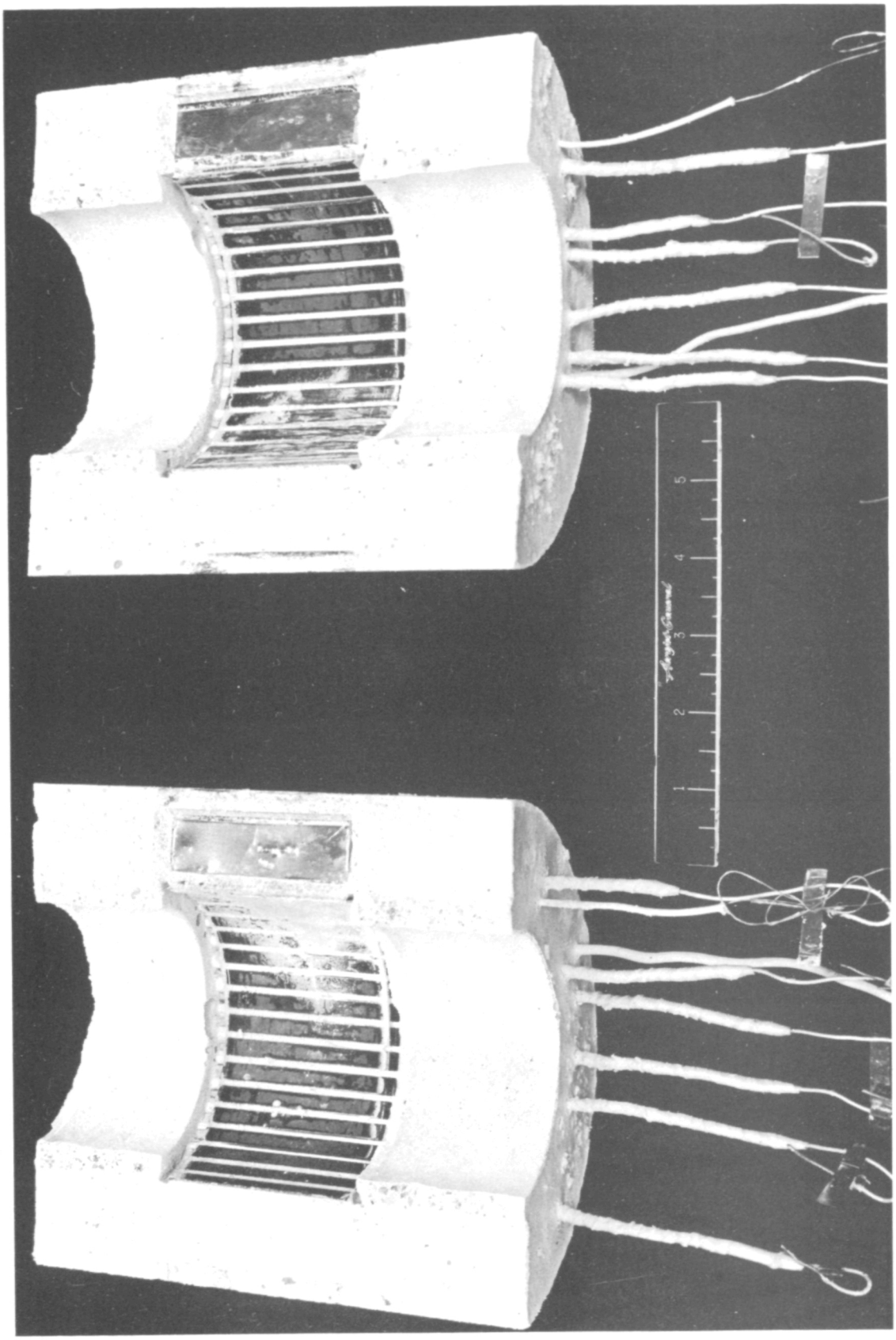

INORGANIC STATORETTES FOR RADIATION EFFECTS PROGRAM

264-731

Figure 103

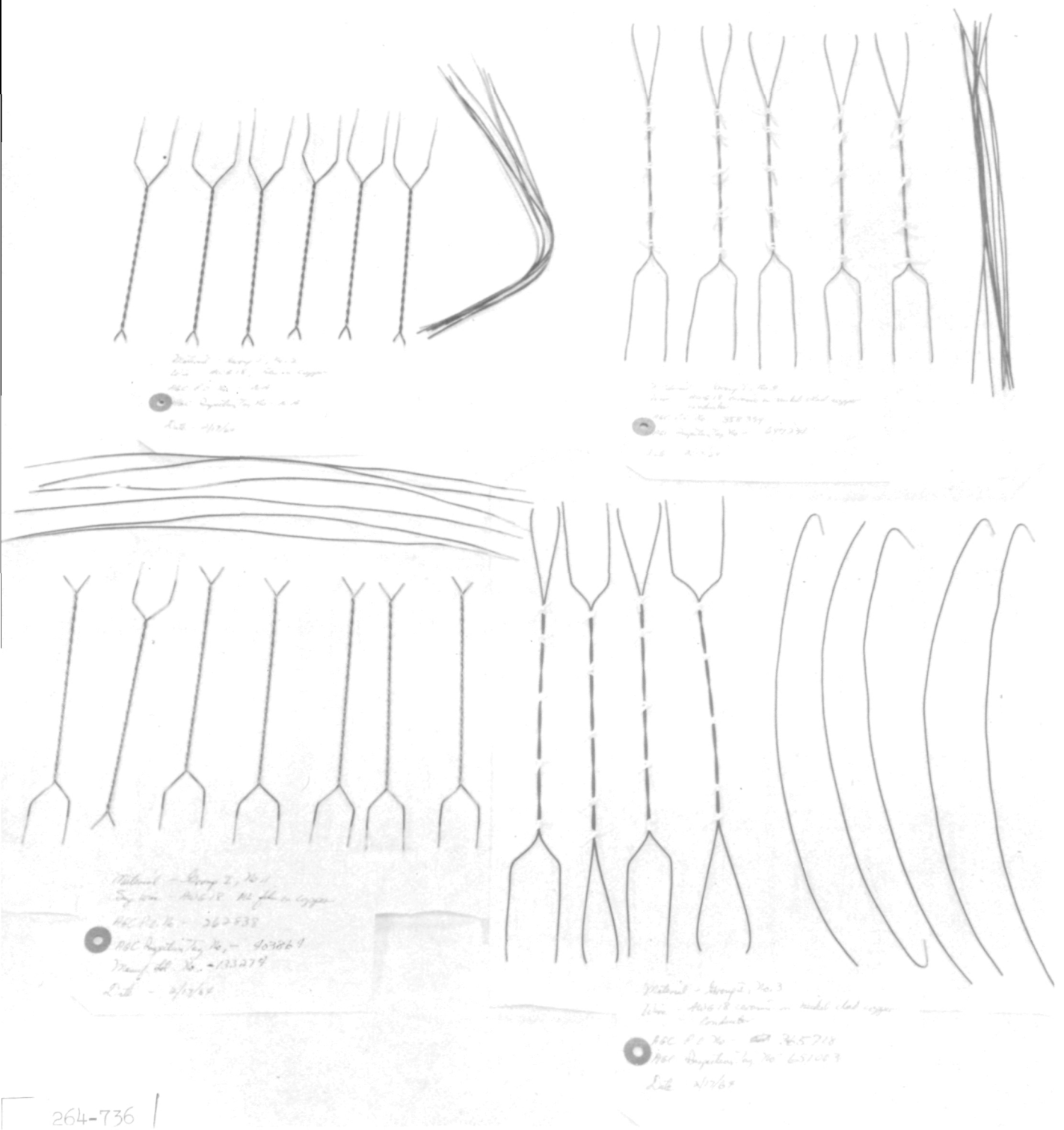

264-736

TWISTED WIRE INSULATION TEST SAMPLES FOR RADIATION EFFECTS PROGRAM

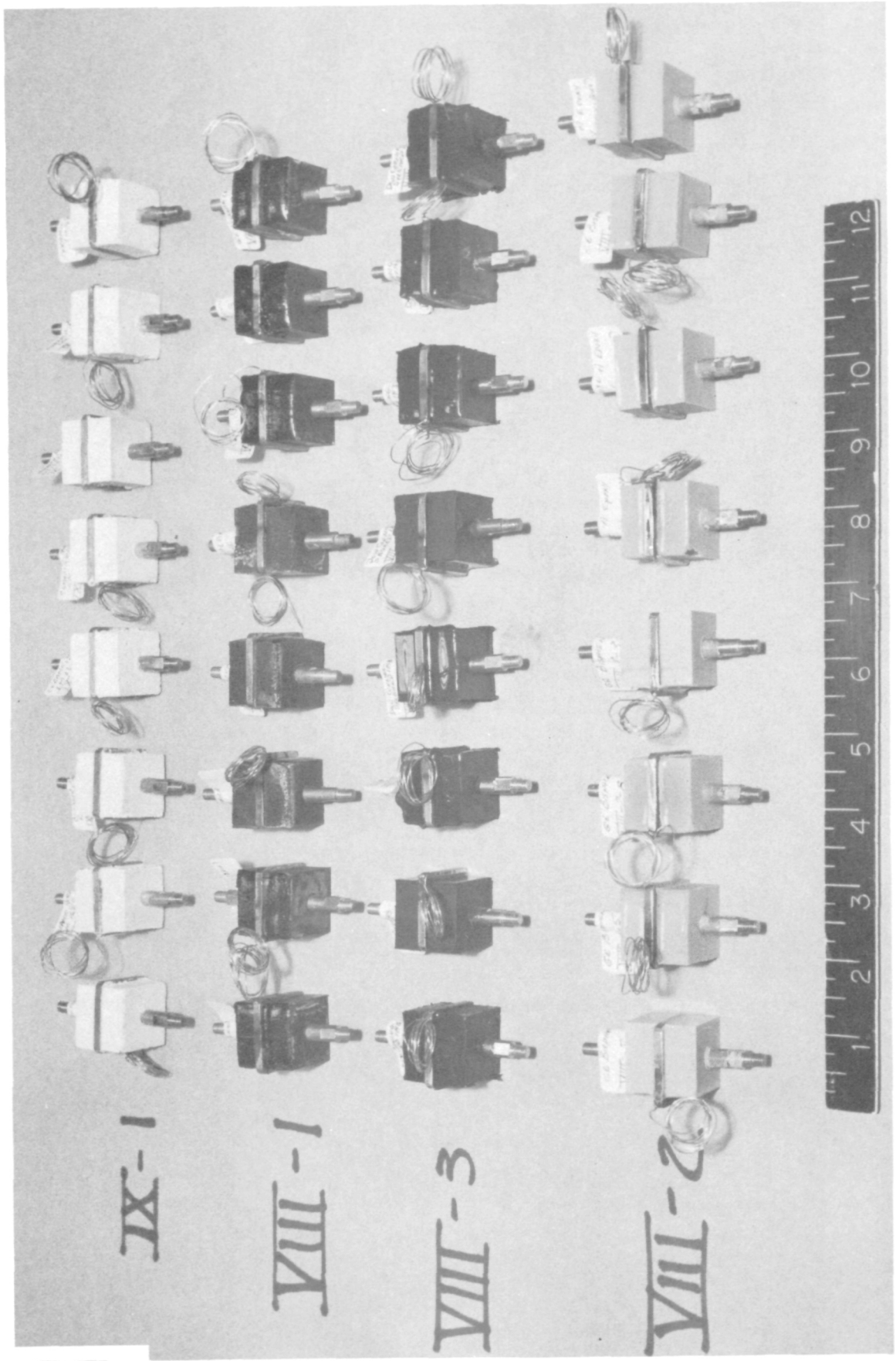

264-735

ORGANIC AND INORGANIC ENCAPSULANTS IN ELECTRICAL SAMPLE CUBE FOR RADIATION EFFECTS PROGRAM

Figure 105

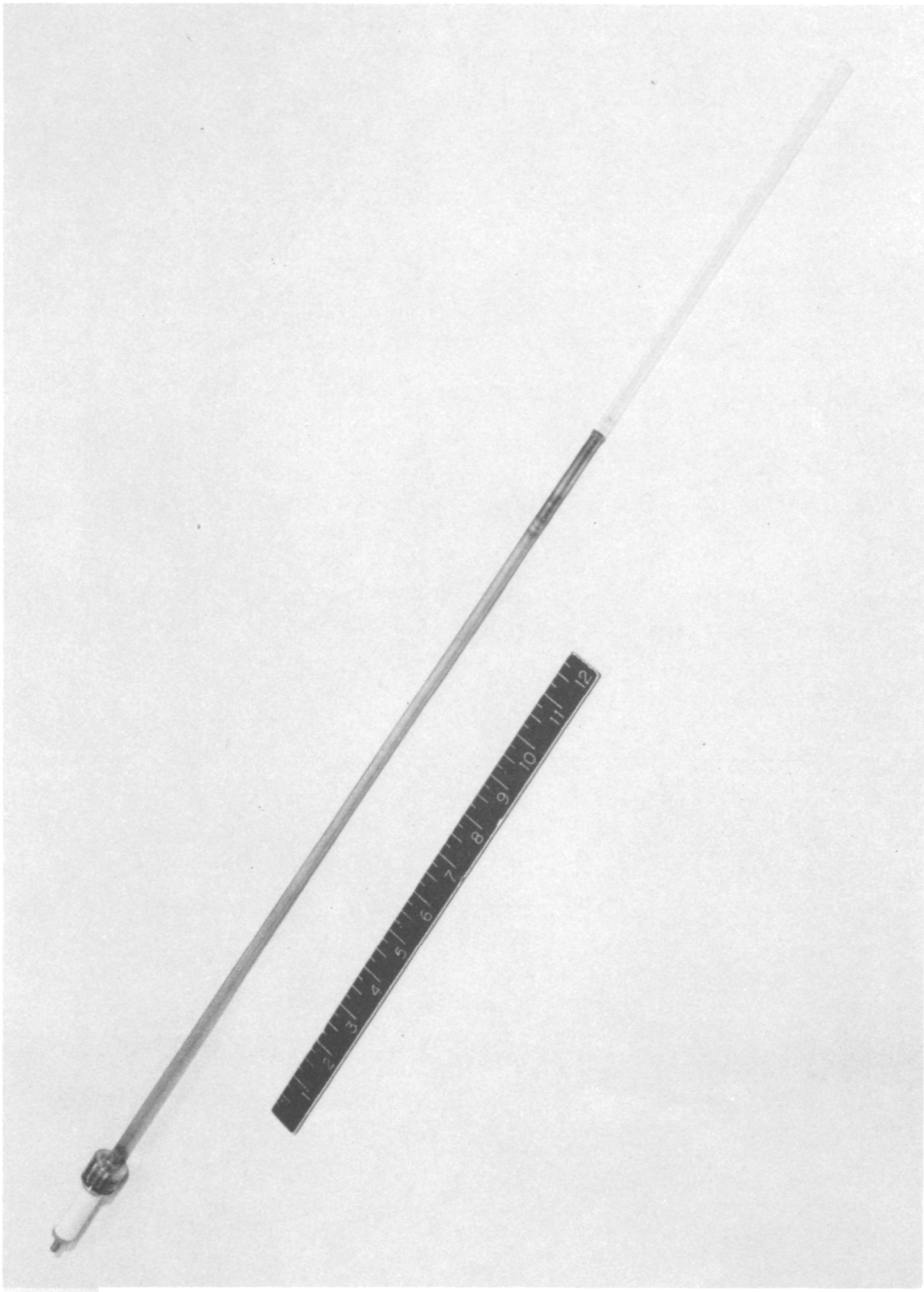

264-733

Ceramic Terminal Trial Assembly Ready for Long-Term Vacuum Aging at 1000°F

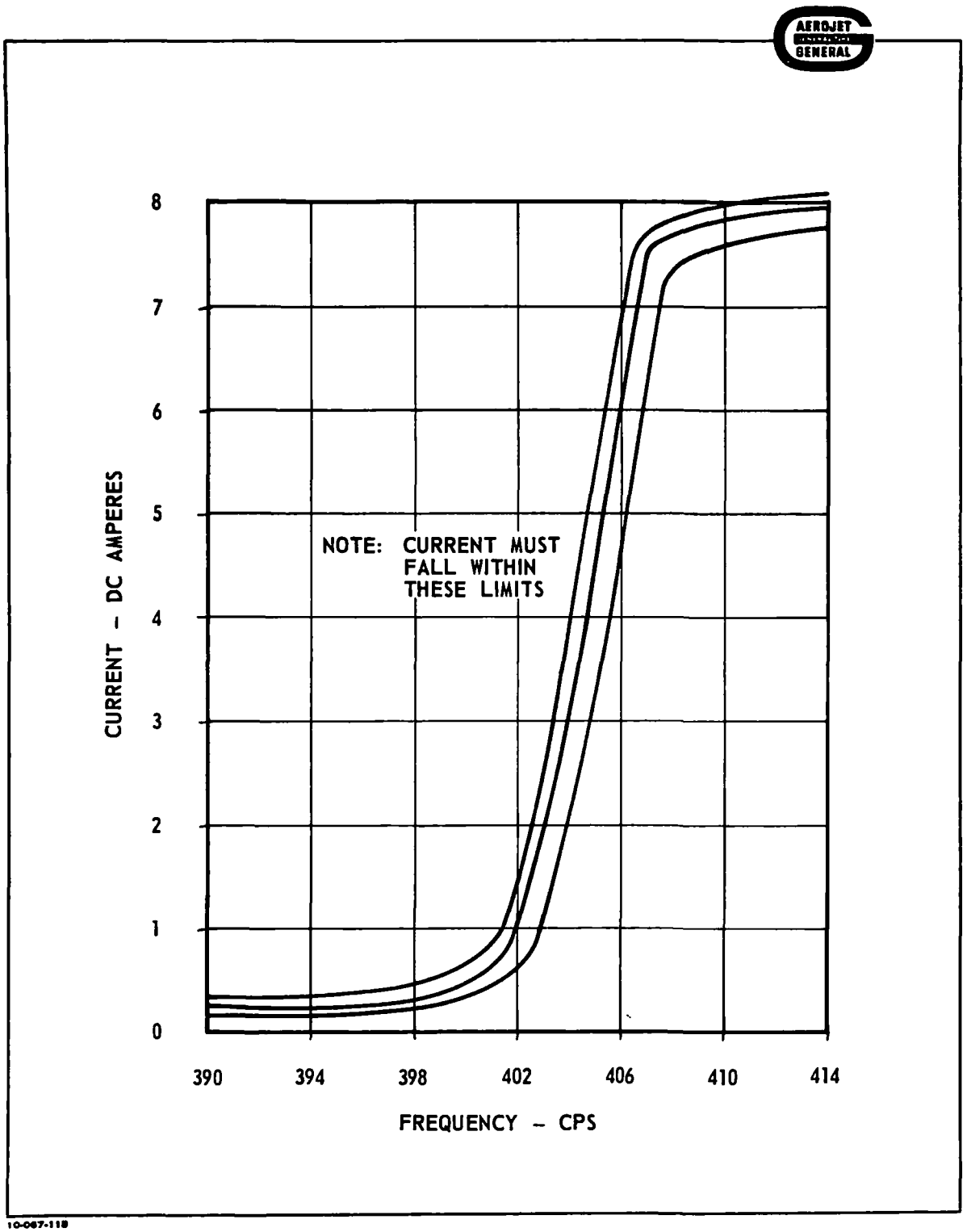

Speed Control, Serial No. 3 - Frequency vs Magnetic Amplifier Output (Current vs Maximum Gain)

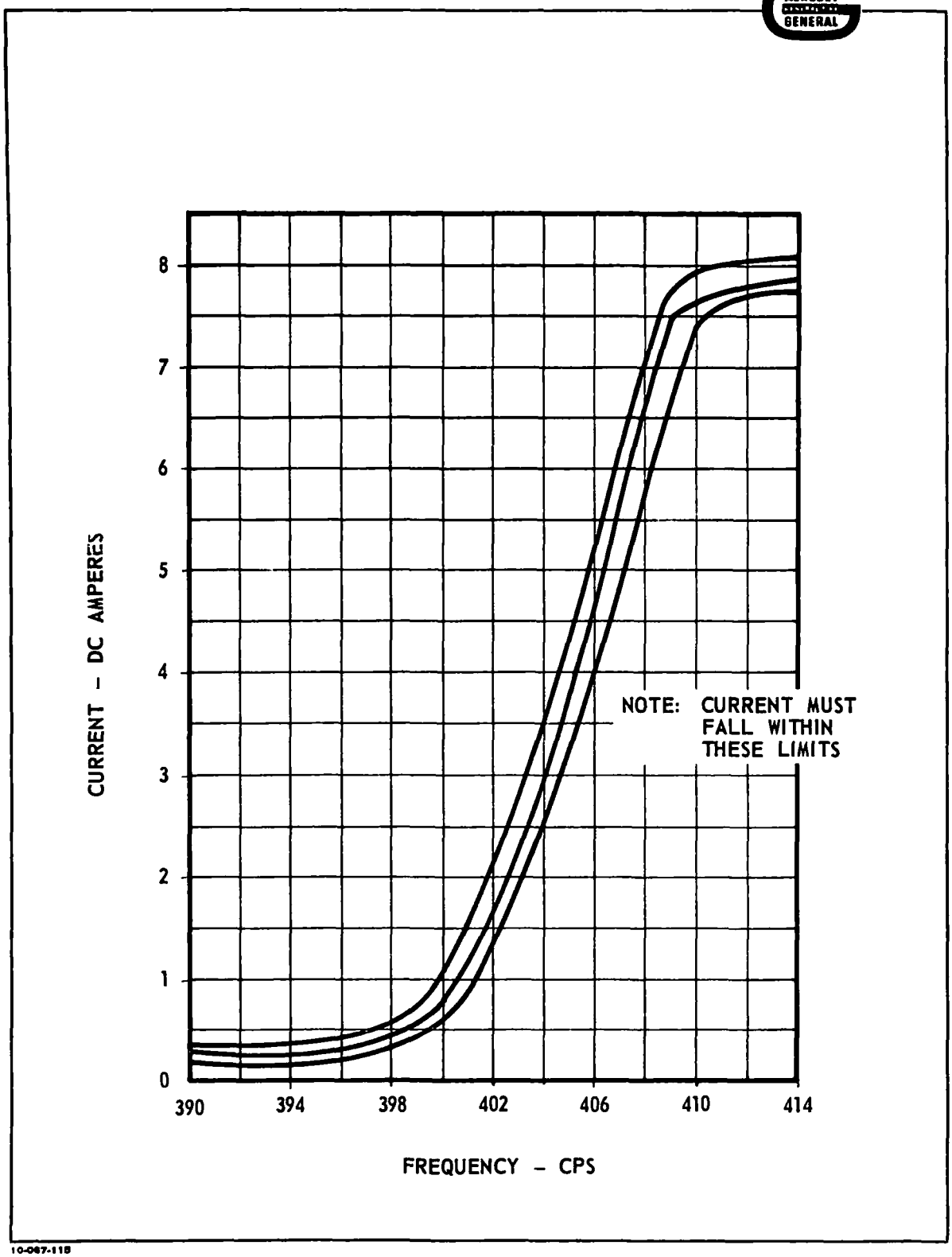

Speed Control, Serial No. 3 - Frequency vs Magnetic Amplifier Output
(Current vs Minimum Gain)

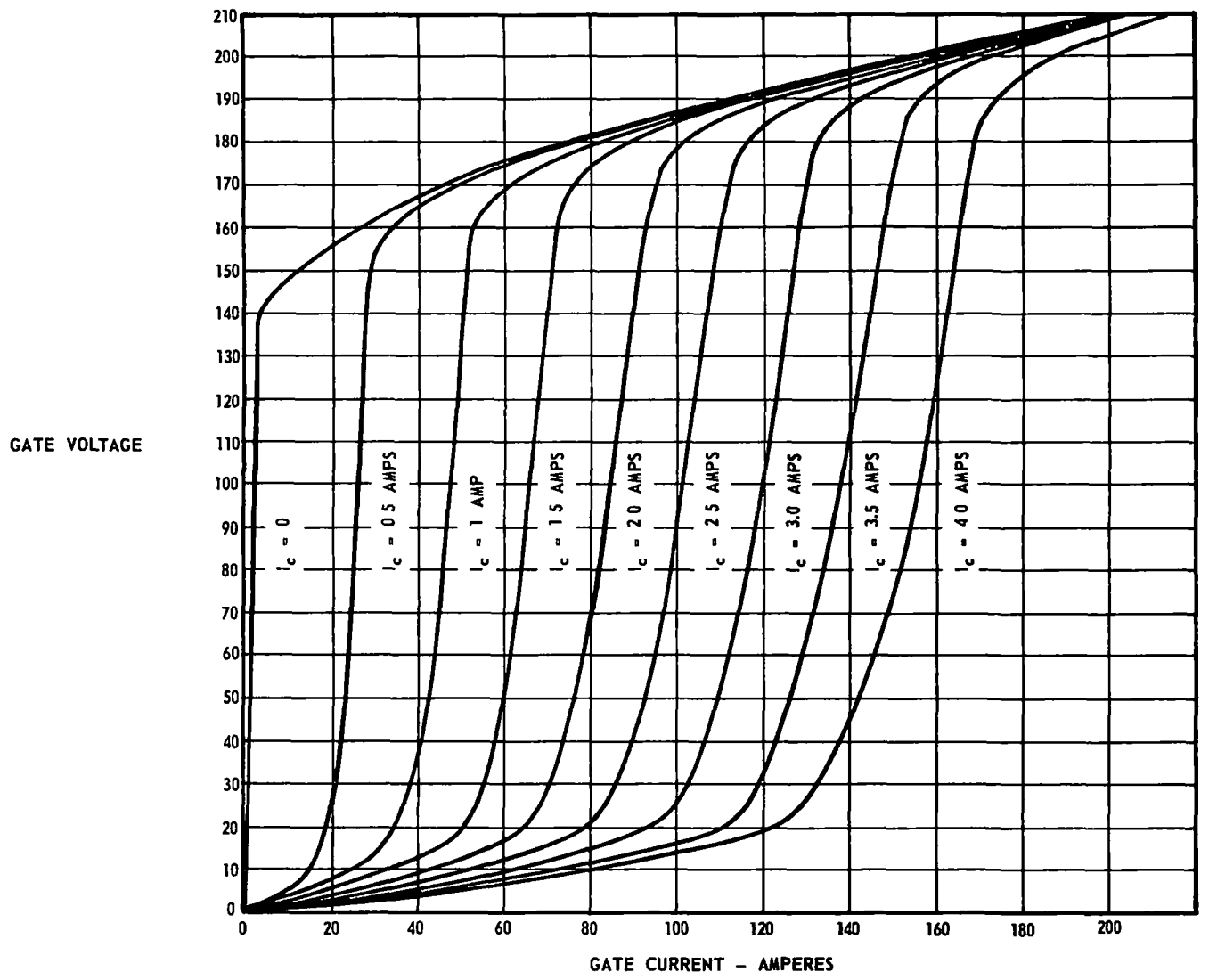

Transfer Curves for the -X Saturable Reactor - Gate Voltage vs Gate Current

Figure 109

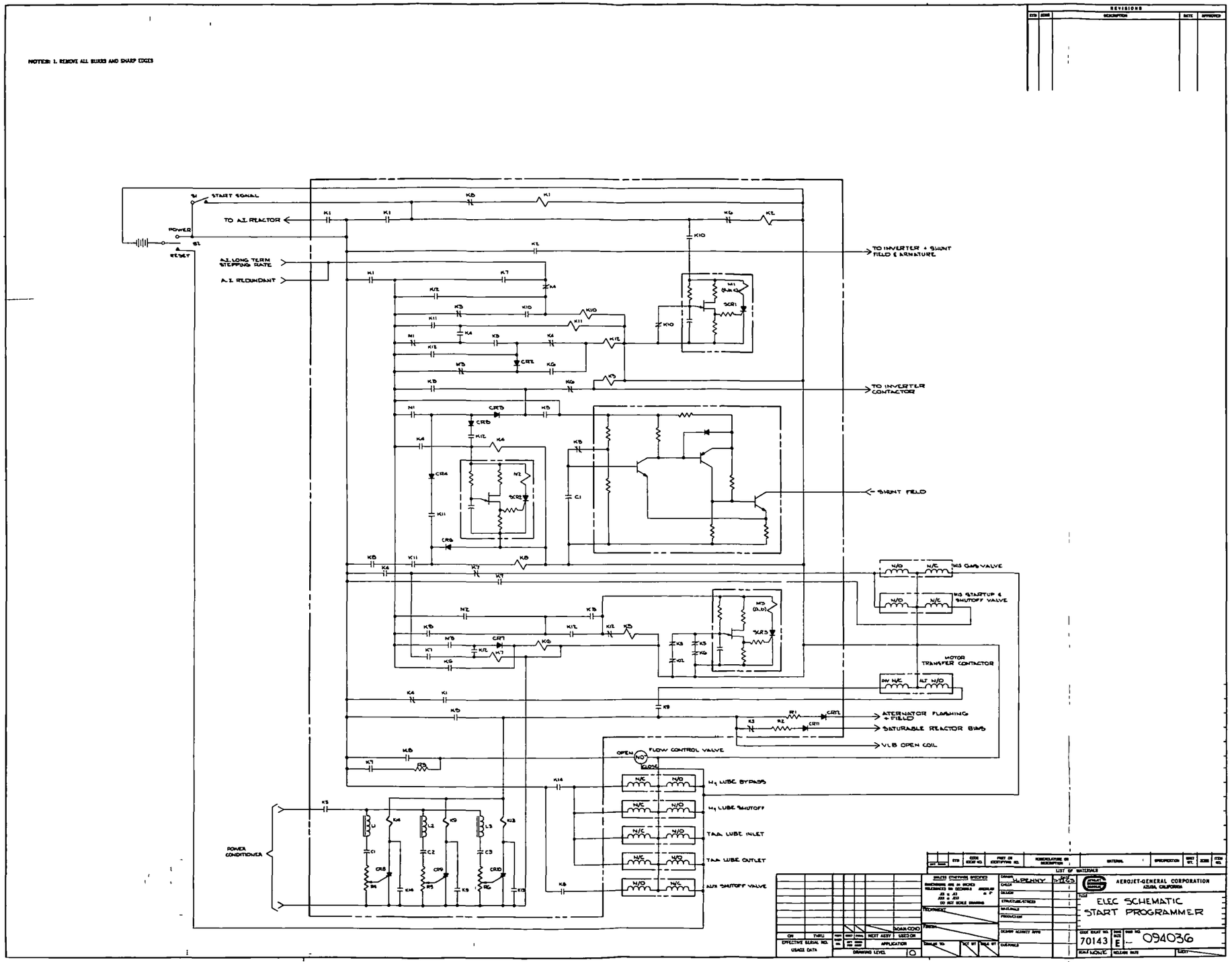

Figure 110

Electrical Schematic - Start Programer

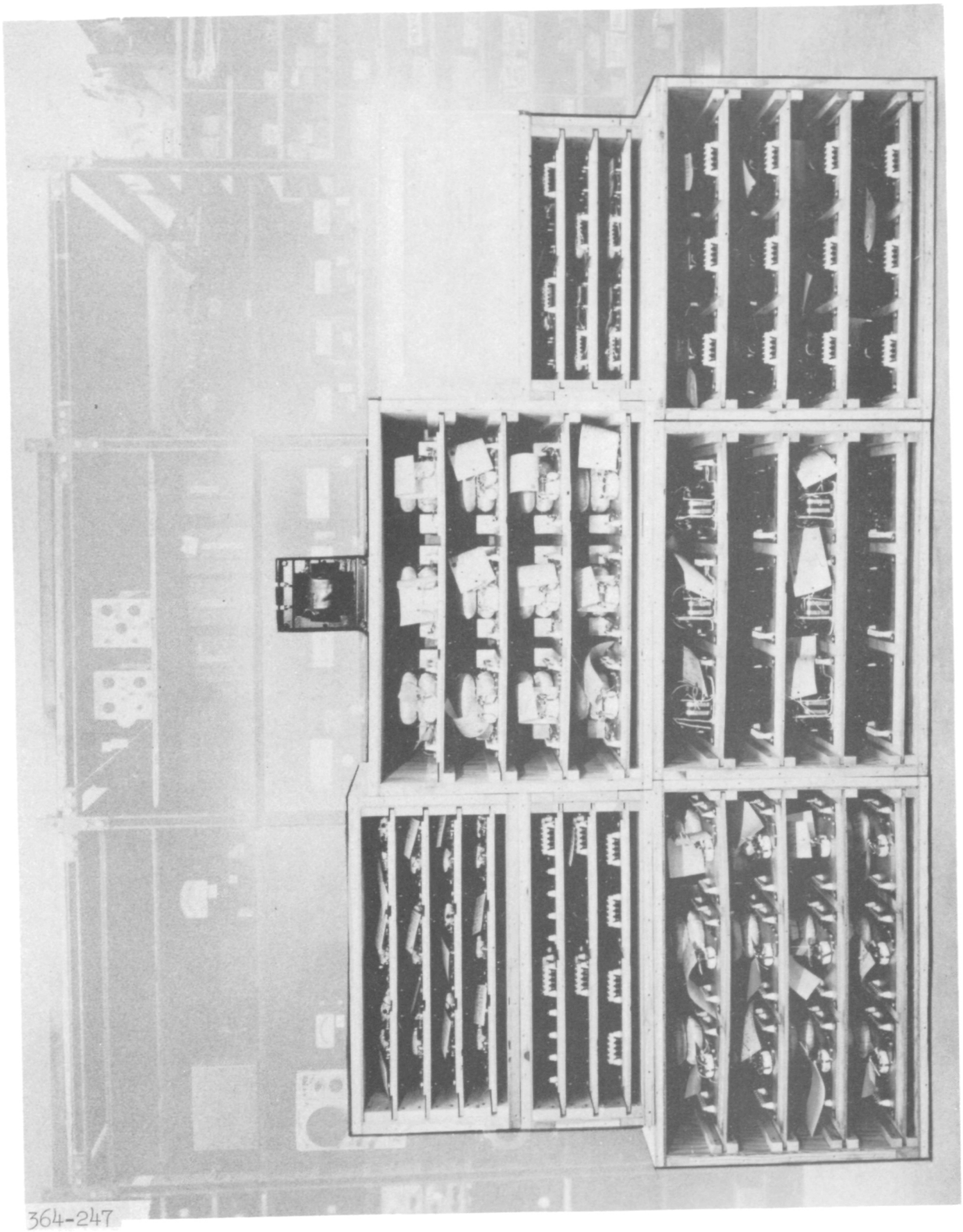

Electrical Components for Radiation Tests, Prior to Shipment

Materials for Radiation Effects Test Program

Figure 112

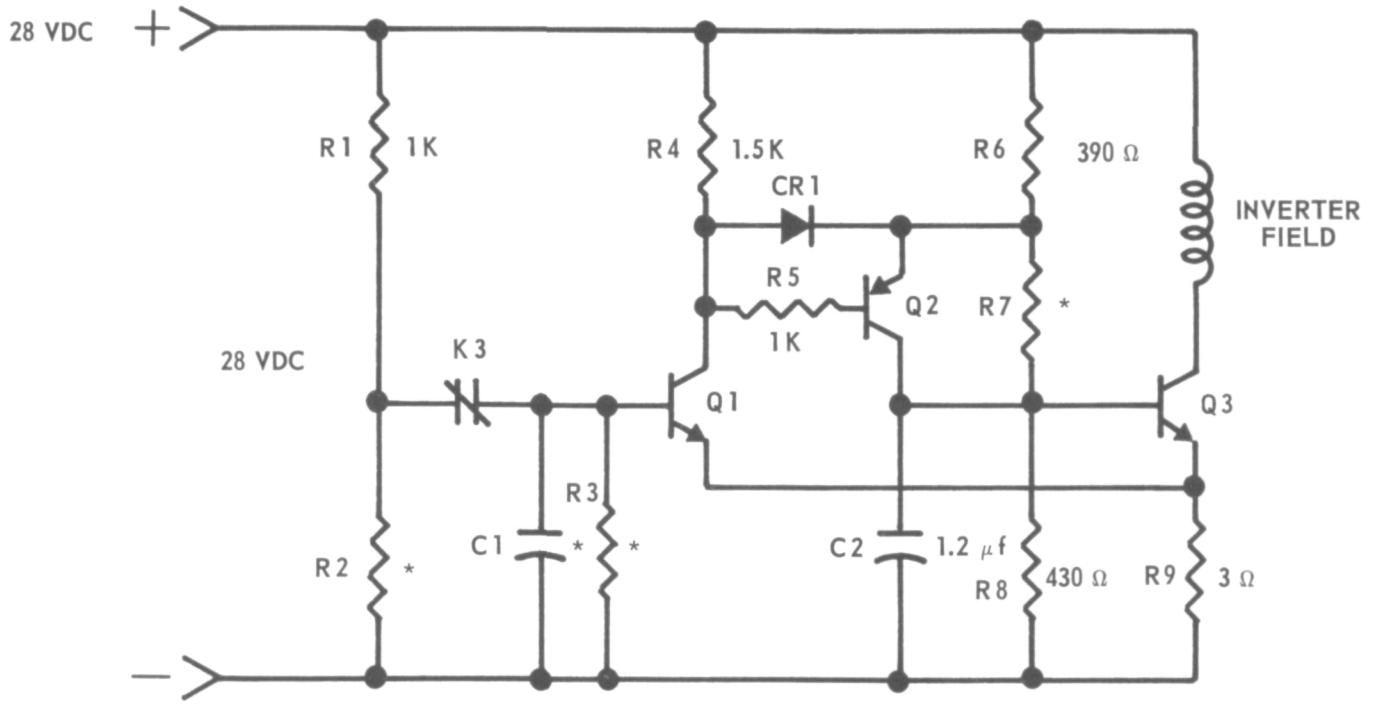

10-067-115

Schematic - Three-Transistor Inverter Frequency Control

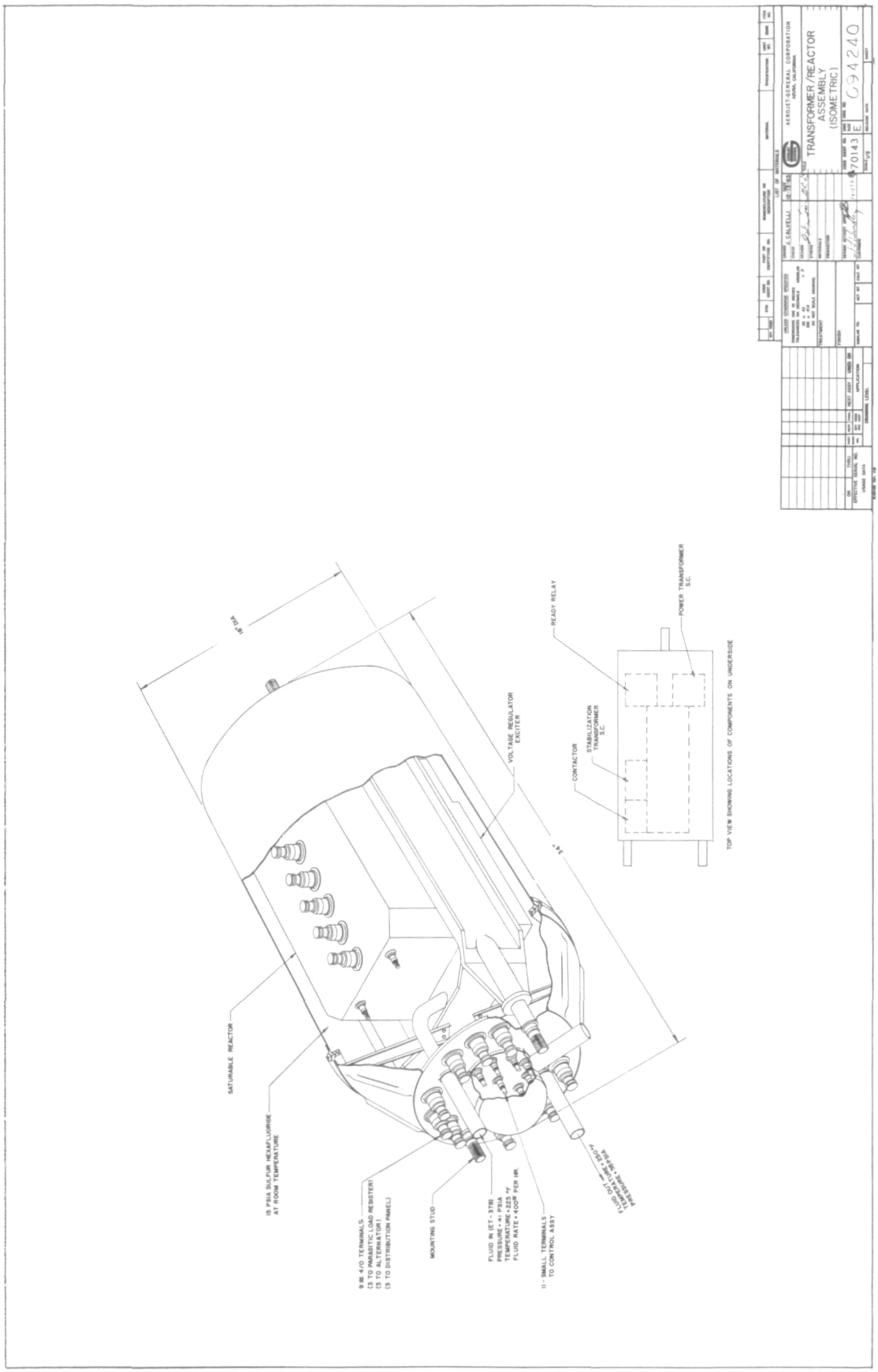

Transformer-Reactor Assembly

Figure 114

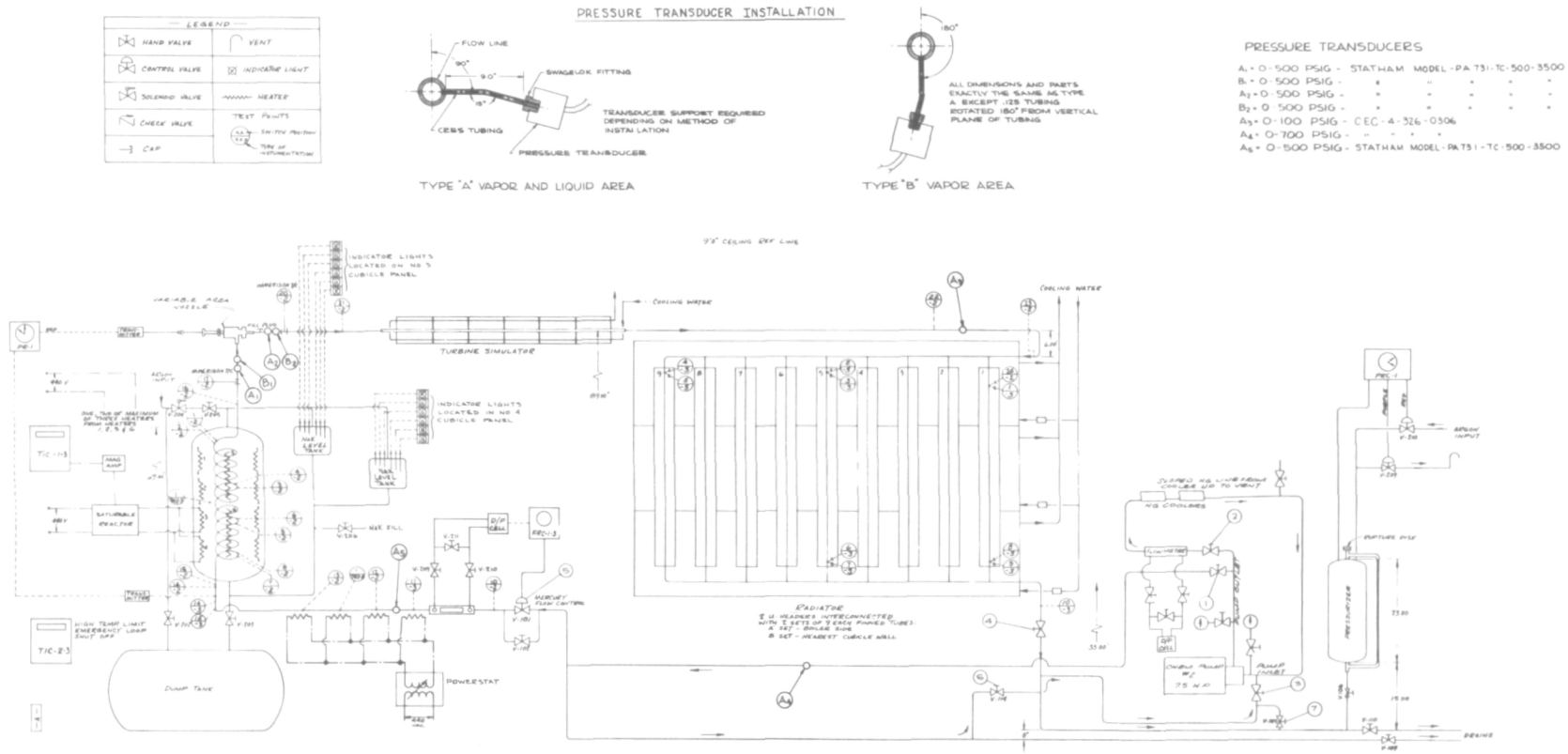

Schematic Diagram of Component Test Loop 2, Showing Location of Pressure Transducers

Figure 115

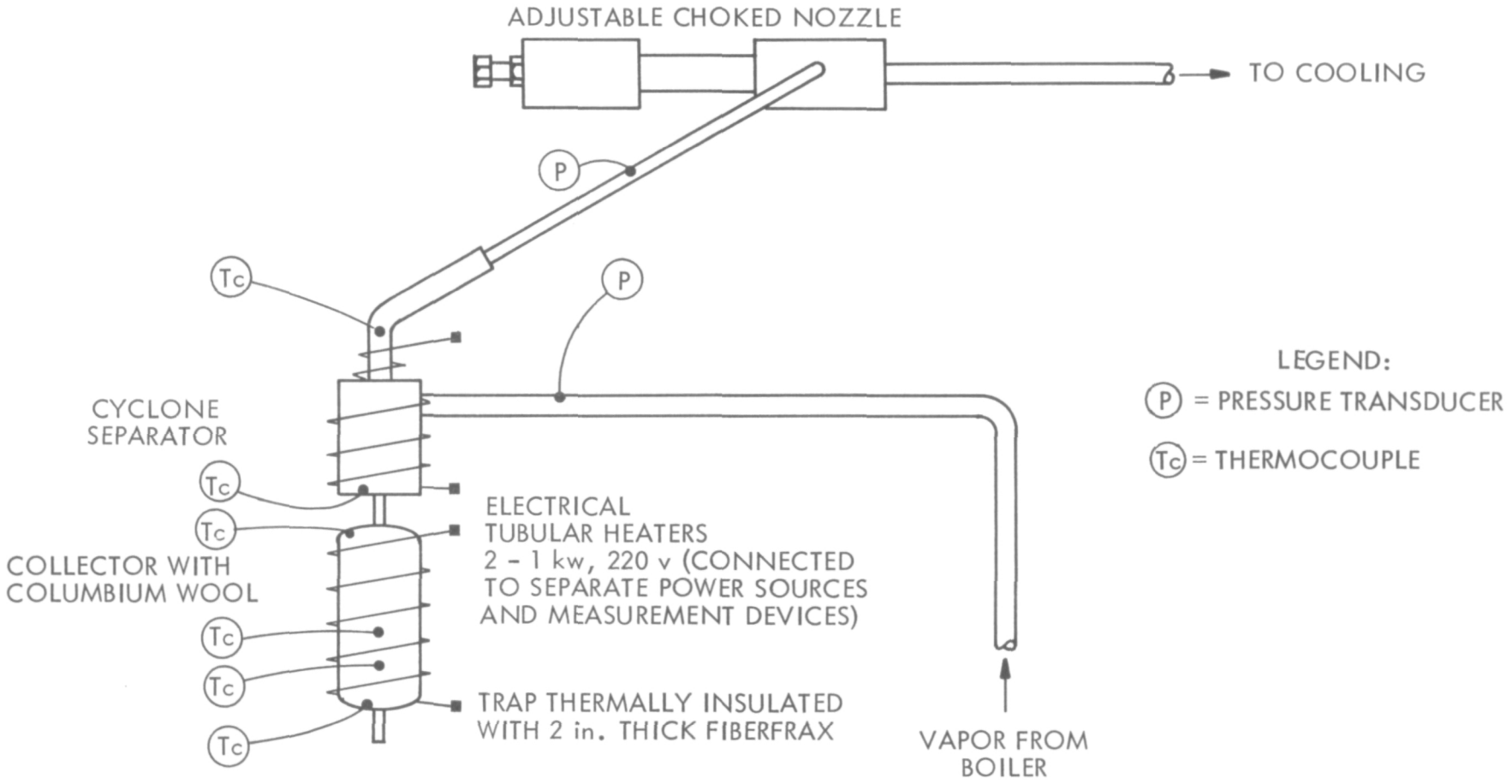

Corrosion Product Cyclone Separator, As Installed in Component Test Loop 2 for Run 11

Figure 116

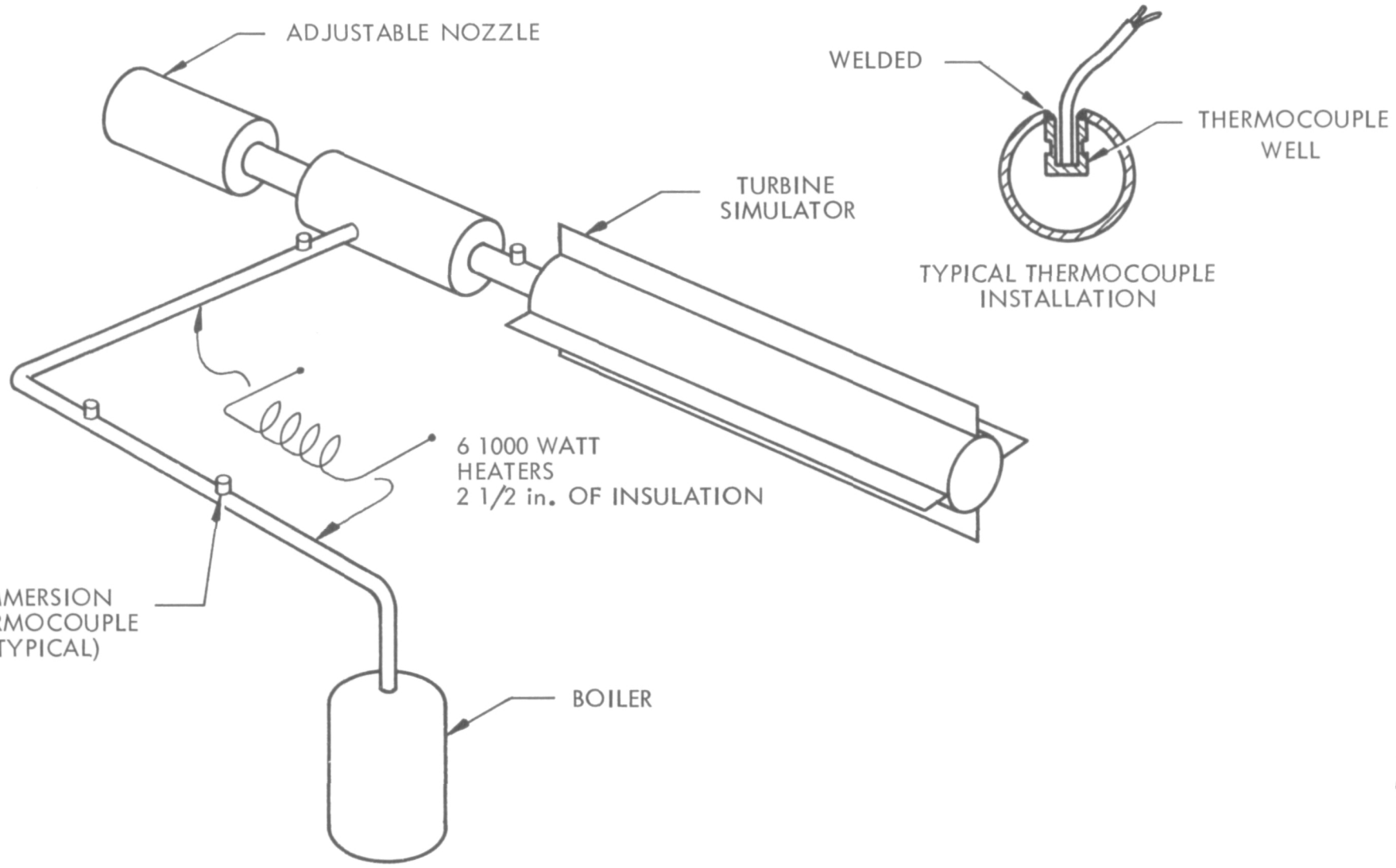

THERMOCOUPLE WELL AS MODIFIED FOR RUN 12

Figure 117

UNCLASSIFIED

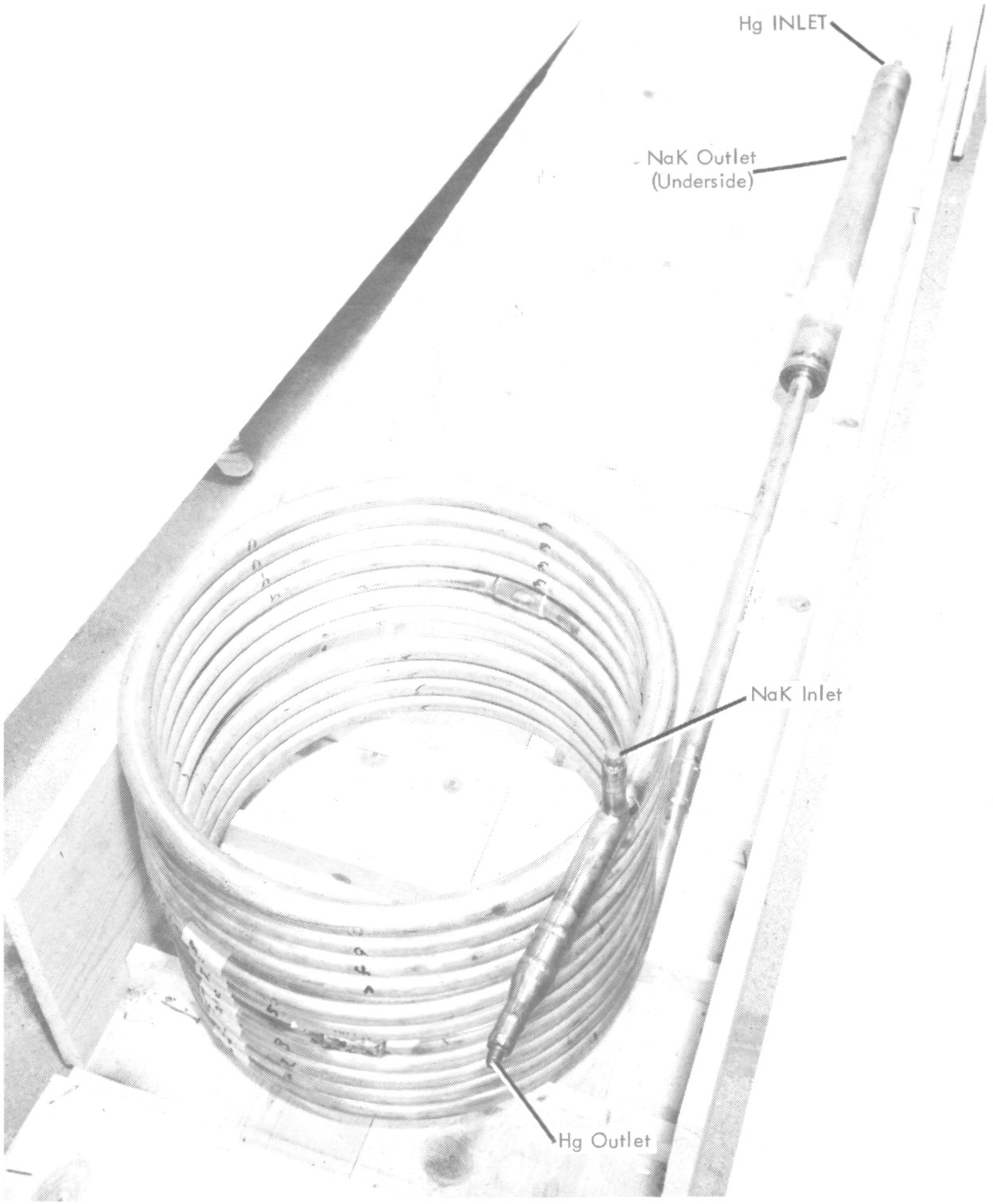

Mercury Boiler

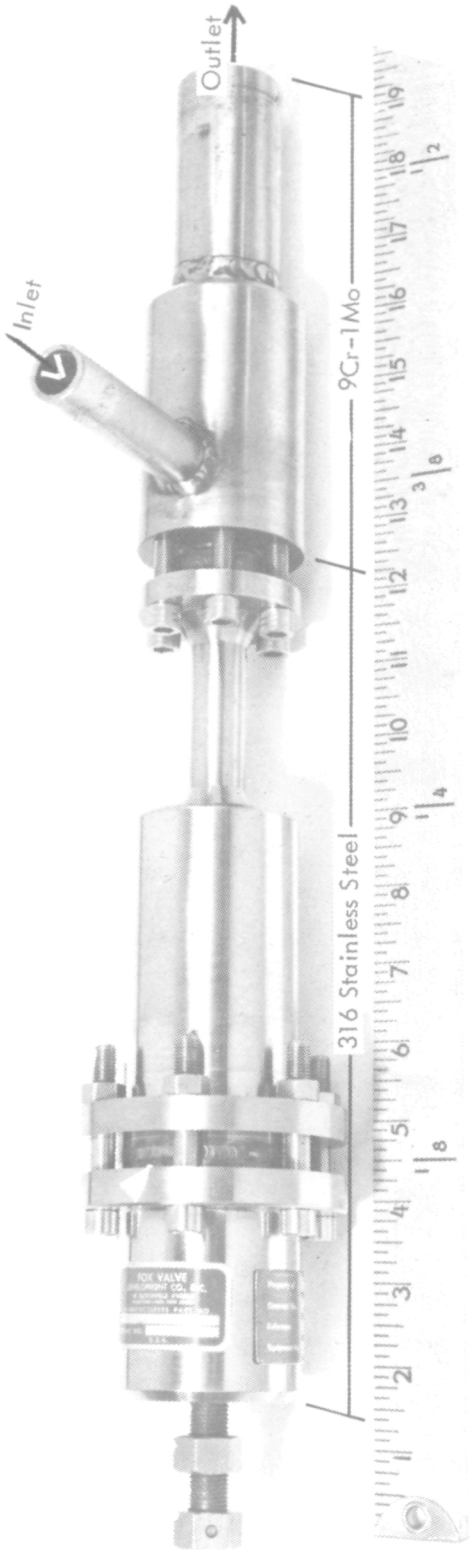

Adjustable Choked Nozzle for Expanding Mercury Vapor

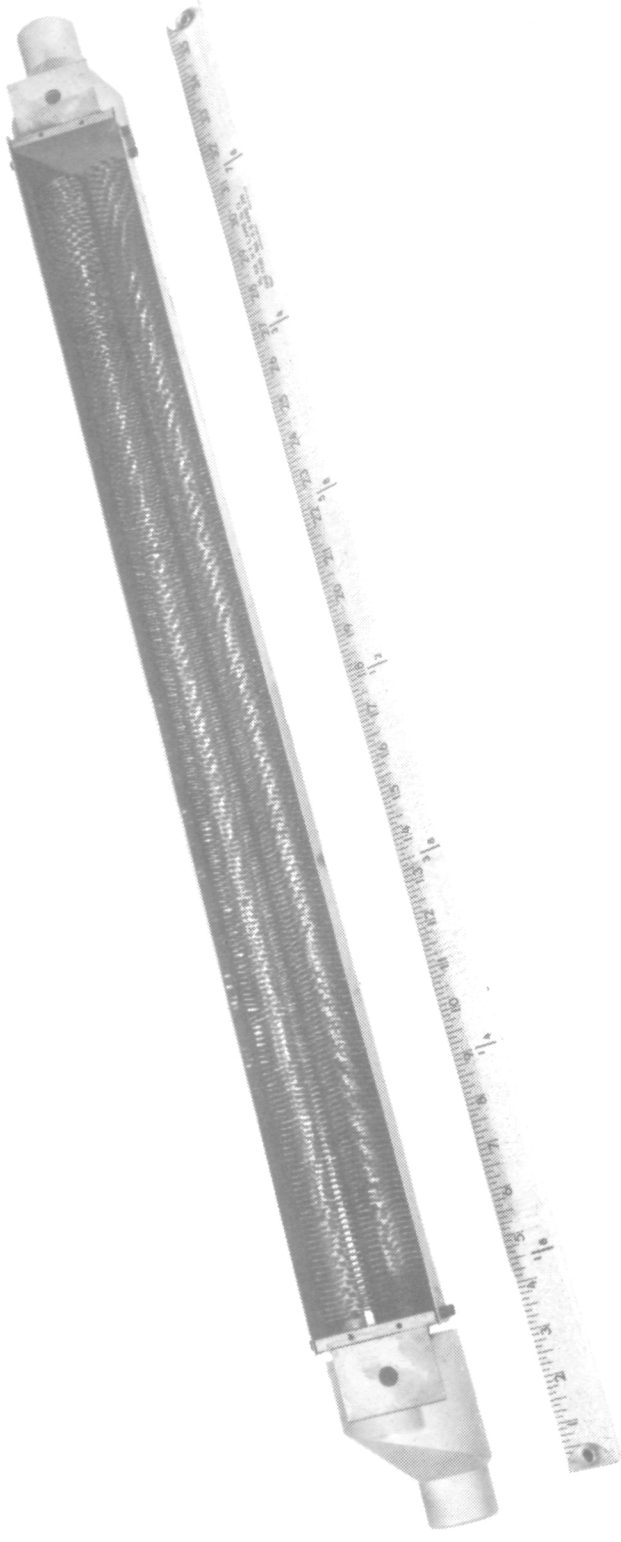

Turbine Simulator Heat Exchanger

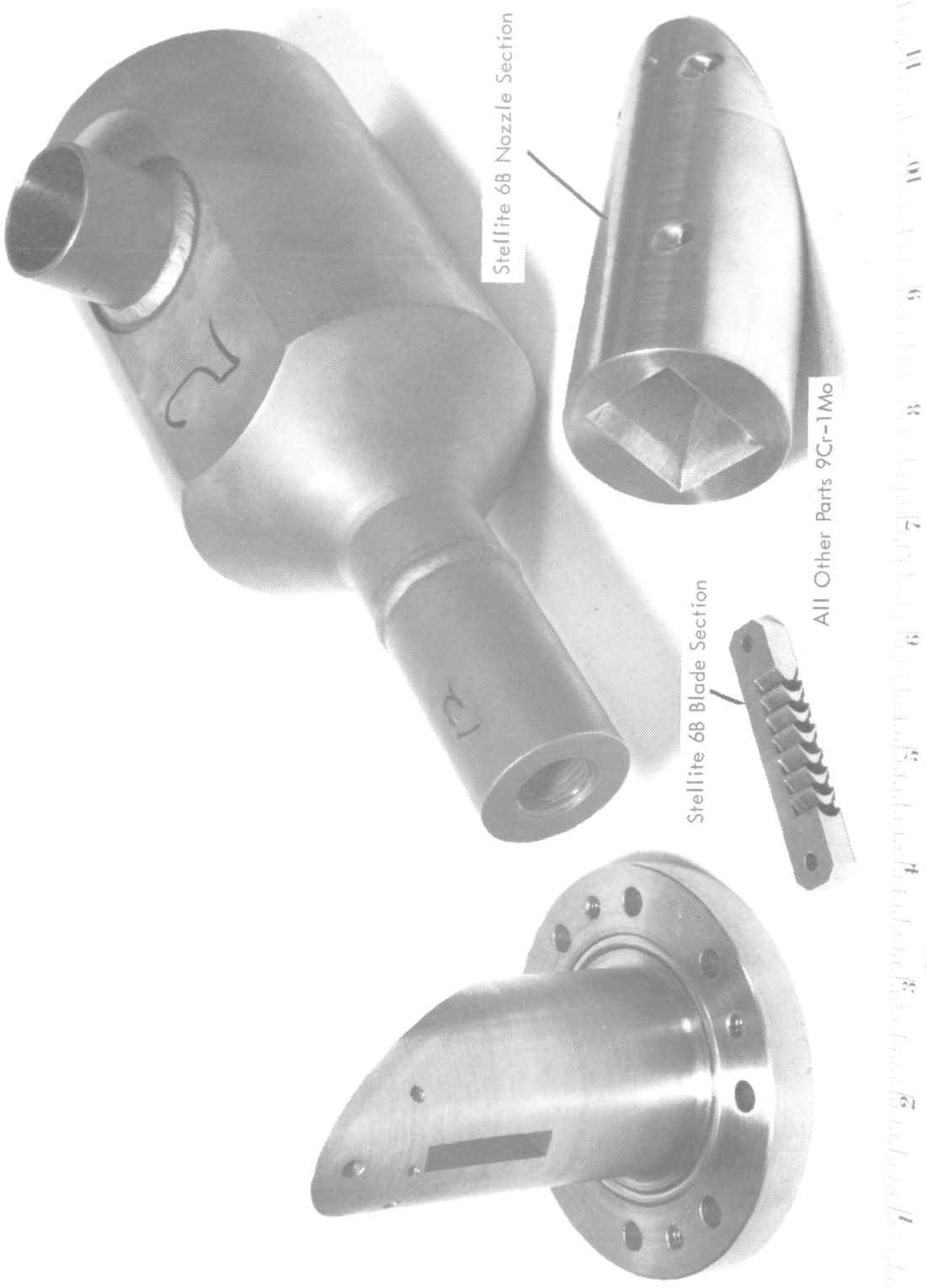

Turbine Simulator Blade Mockup

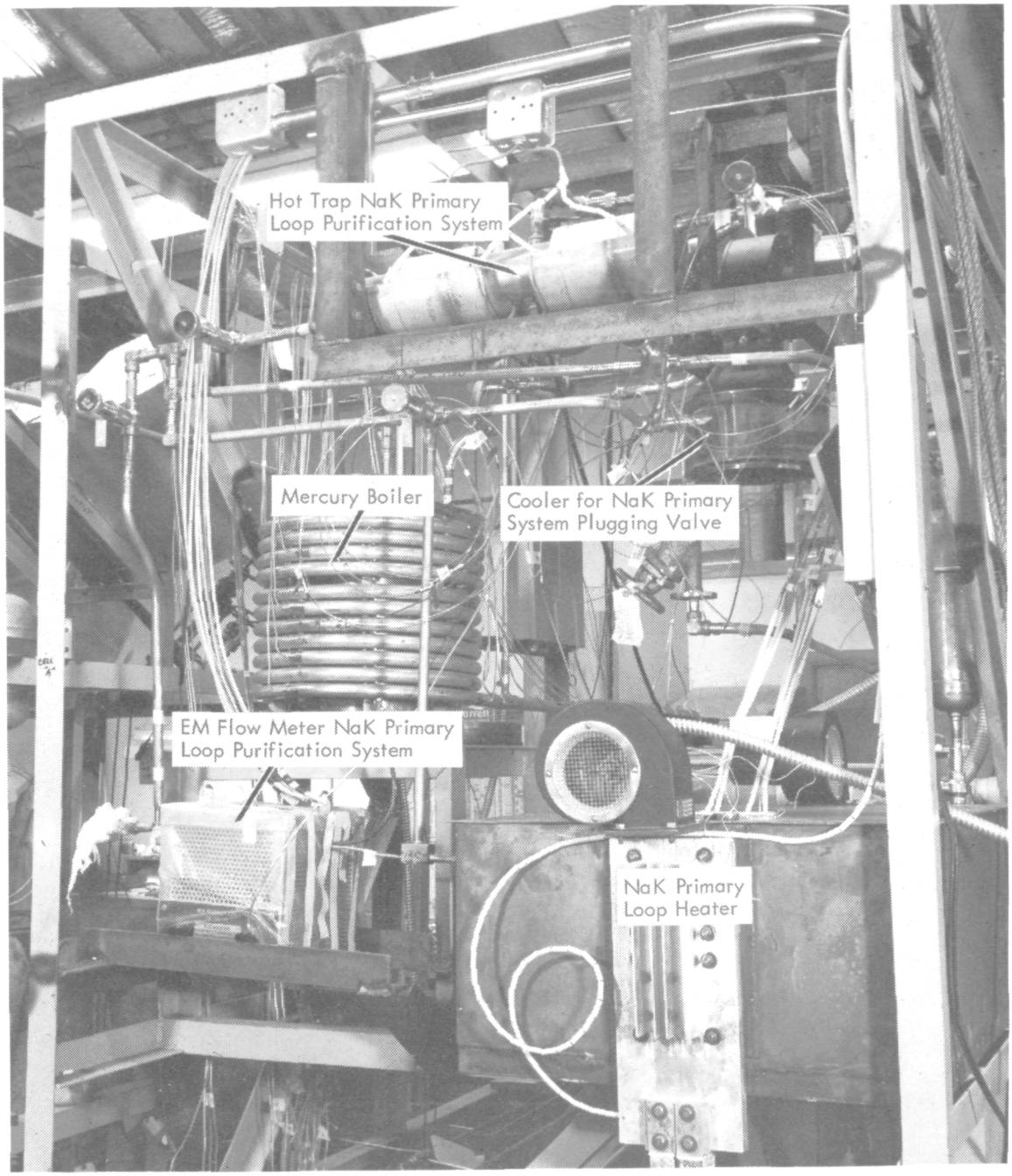

Corrosion Loop Assembly, Cell A, Front View

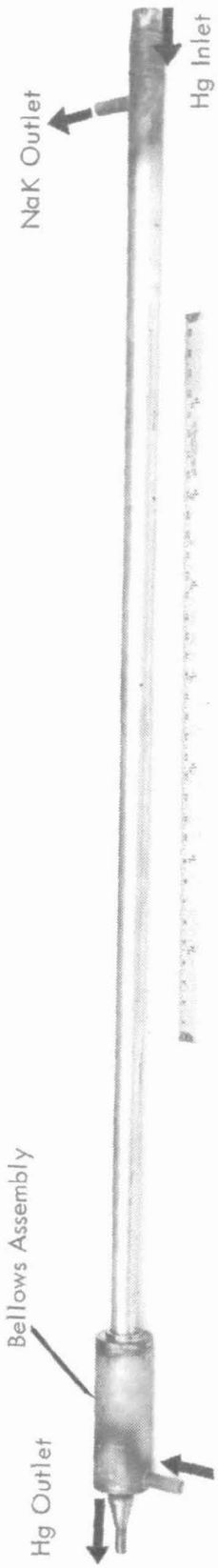

Mercury Condenser

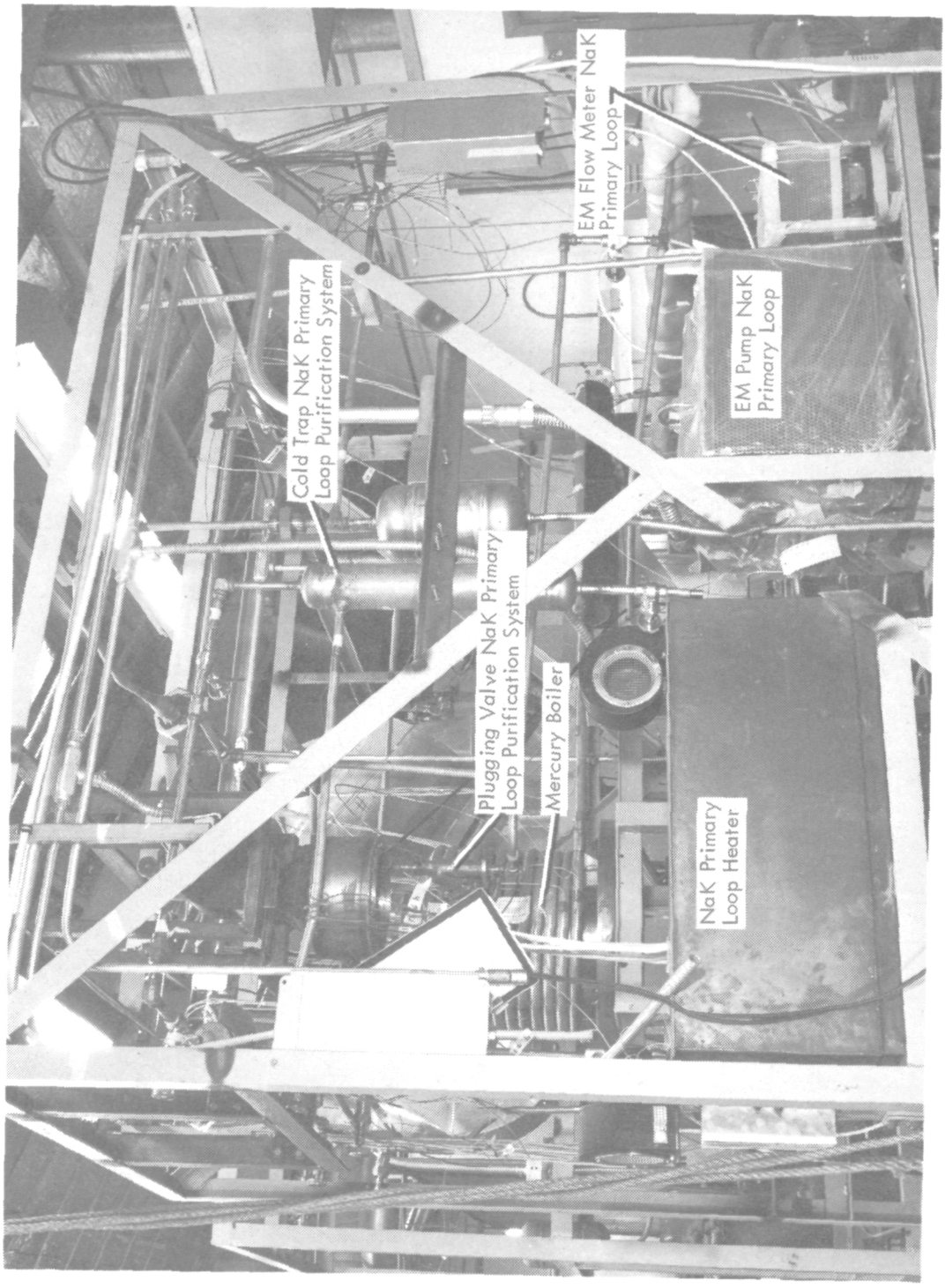

Corrosion Loop Assembly - Cell A (Side View)

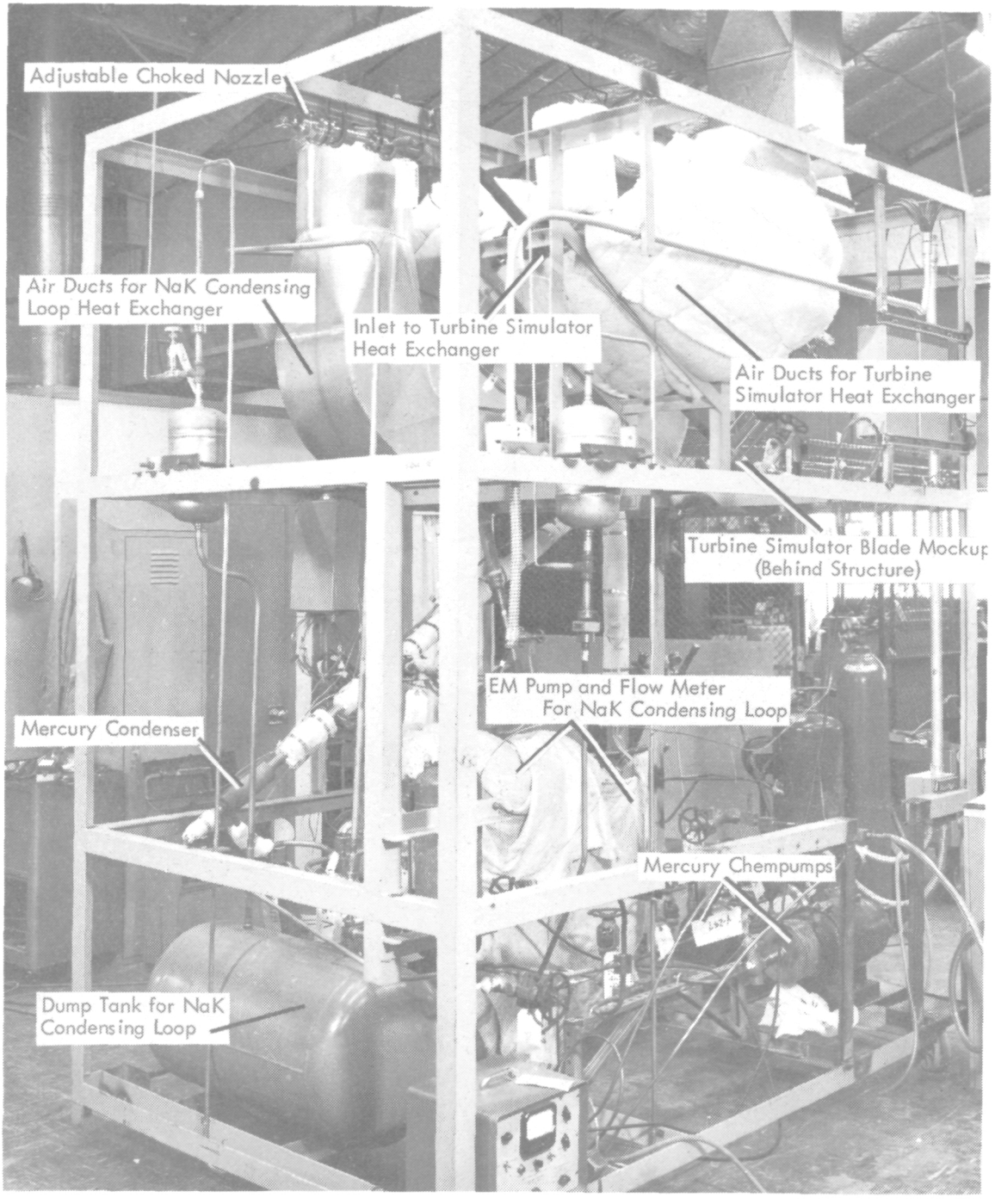

Corrosion Loop Assembly - Cell B

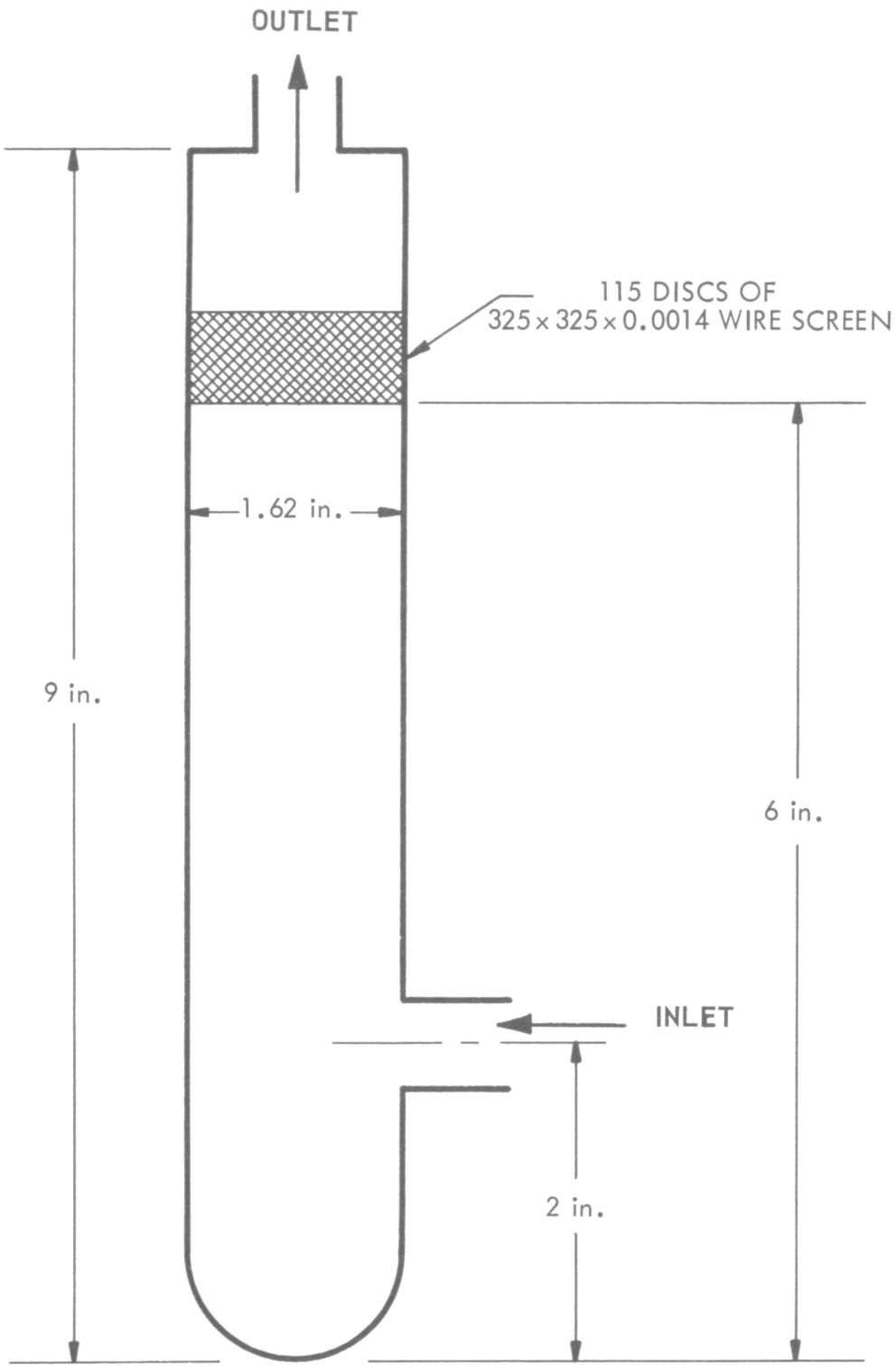

Impingement Separator

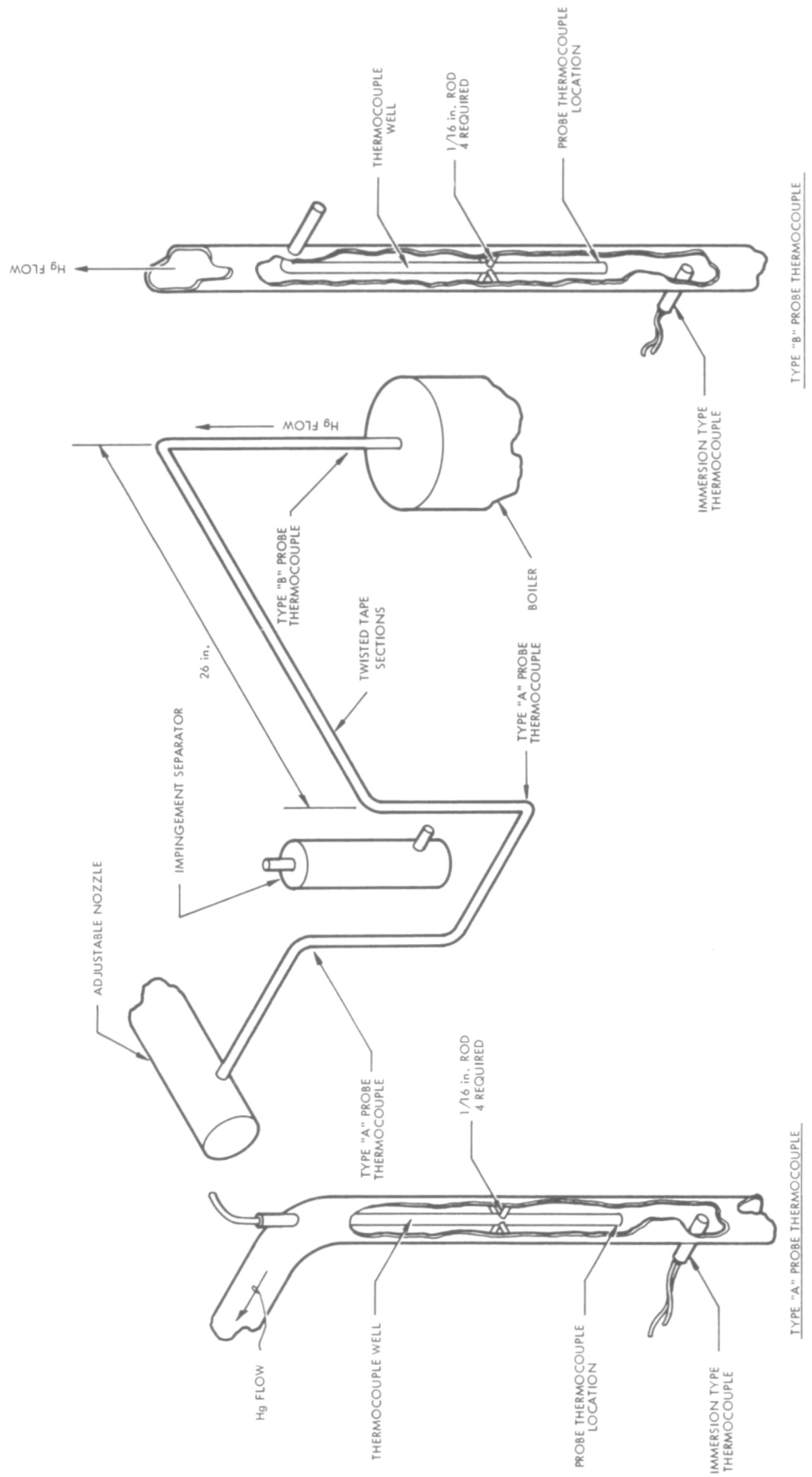

Component Test Loop 2 Modification, Including Details of Thermocouple Assembly

Figure 127

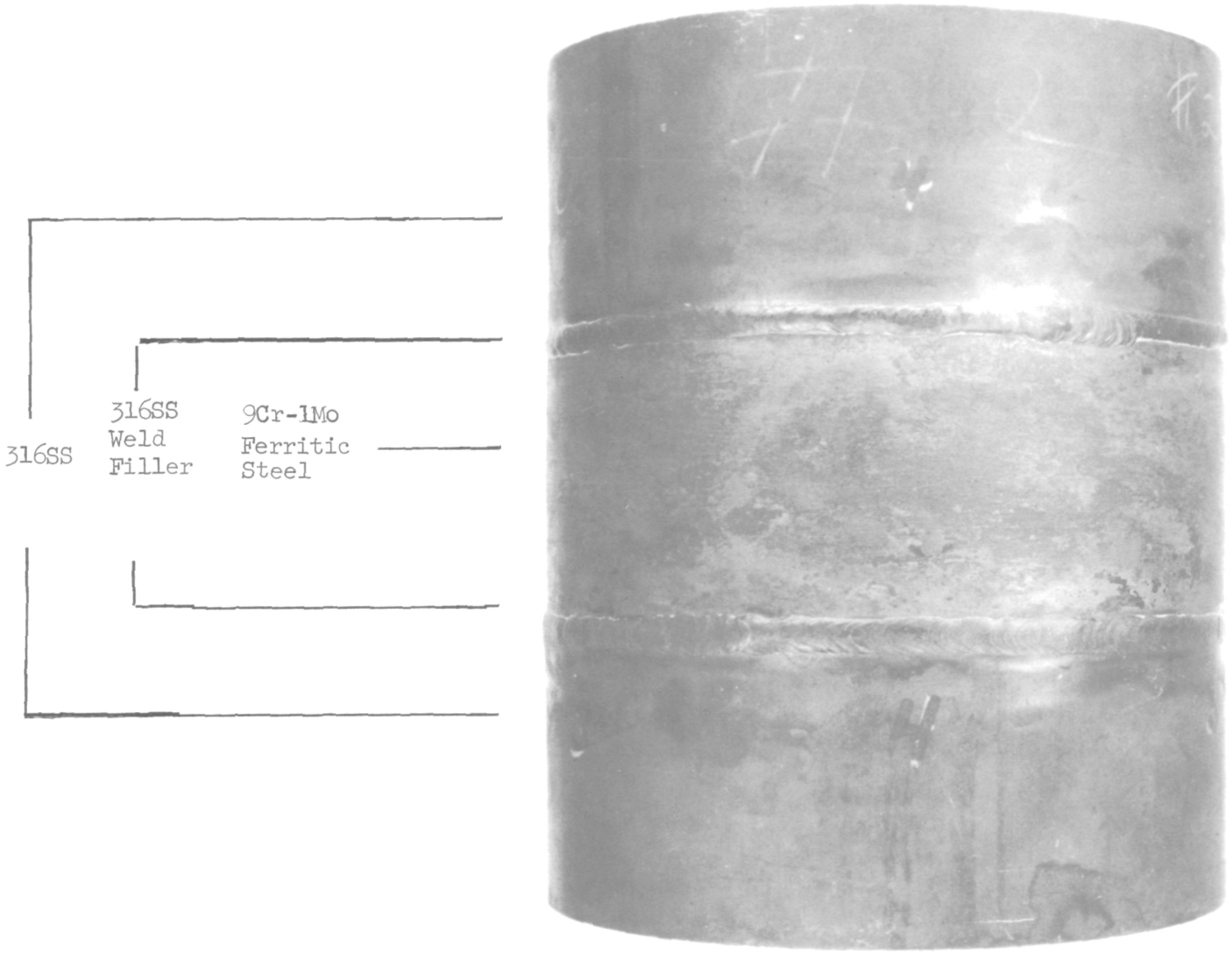

As-Fabricated 9Cr-1Mo/316SS Transition Joint Evaluation

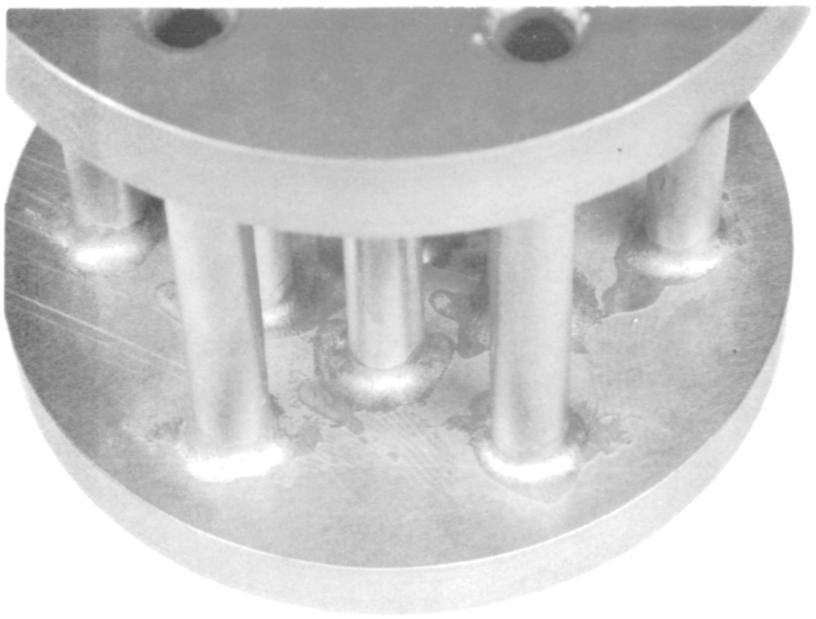

A. Thirteen-Tube 9Cr-1Mo Sample, Welded and Back Brazed with AMS 4778 Alloy, Illustrating Braze Alloy Flow and Filleting.

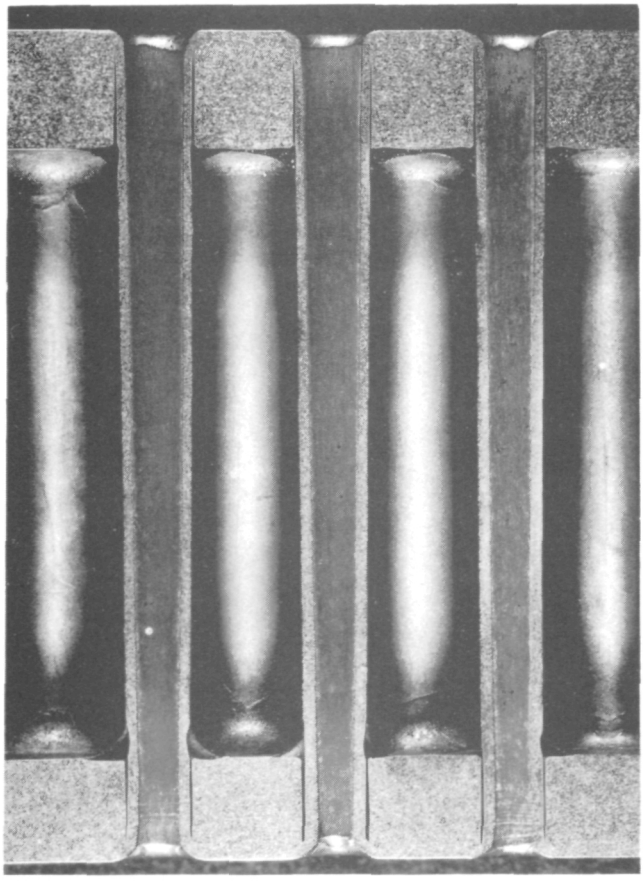

B. Section Through Welded and Back-Brazed Joints of Sample Shown in A. Illustrating Alloy Flow to Root of Welds, Erosion Diffusion of Tube Wall, and Porosity in Fillets.

Thirty-seven-Tube Welded and Back-Brazed Sample Illustrating
Flow and Filleting at the Upper Tube Sheet Joints

Thirty-seven-Tube Welded and Back-Brazed Sample Illustrating Poor Flow and Filleting at Lower Tube Sheet Joints.

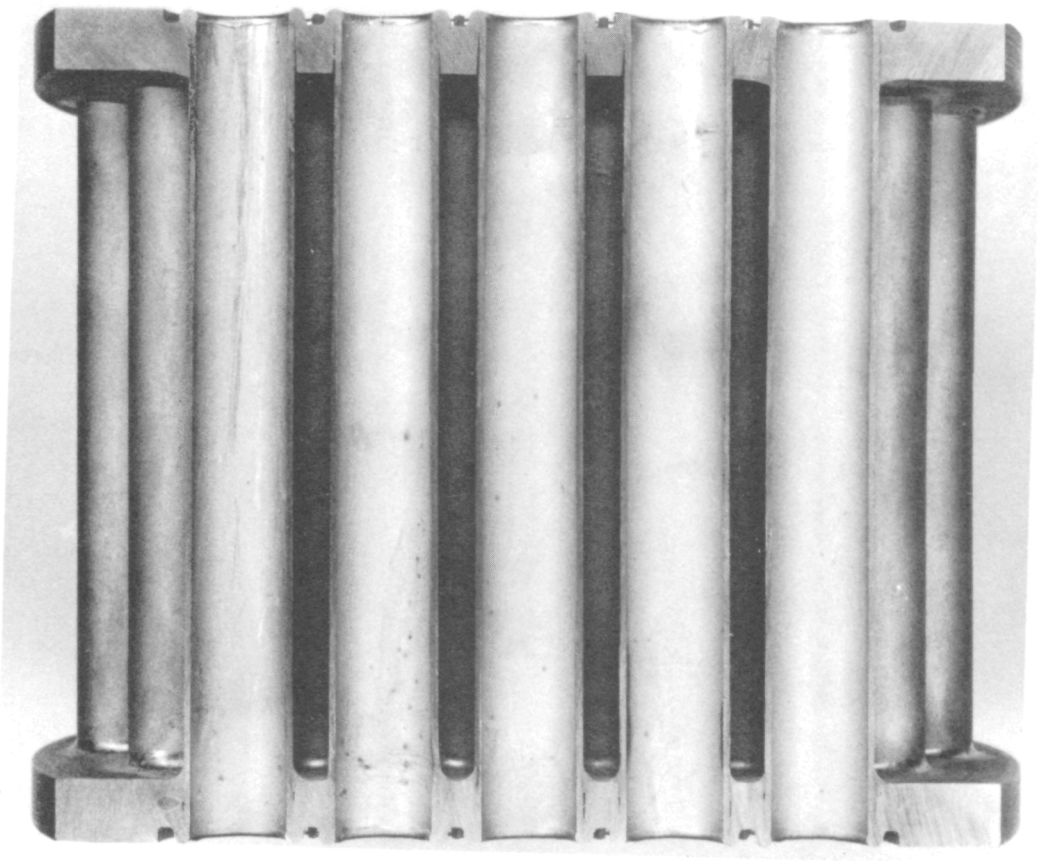

Section Through Welded and Back-Brazed 37-Tube Sample,
Illustrating Gaps in Brazed Joints

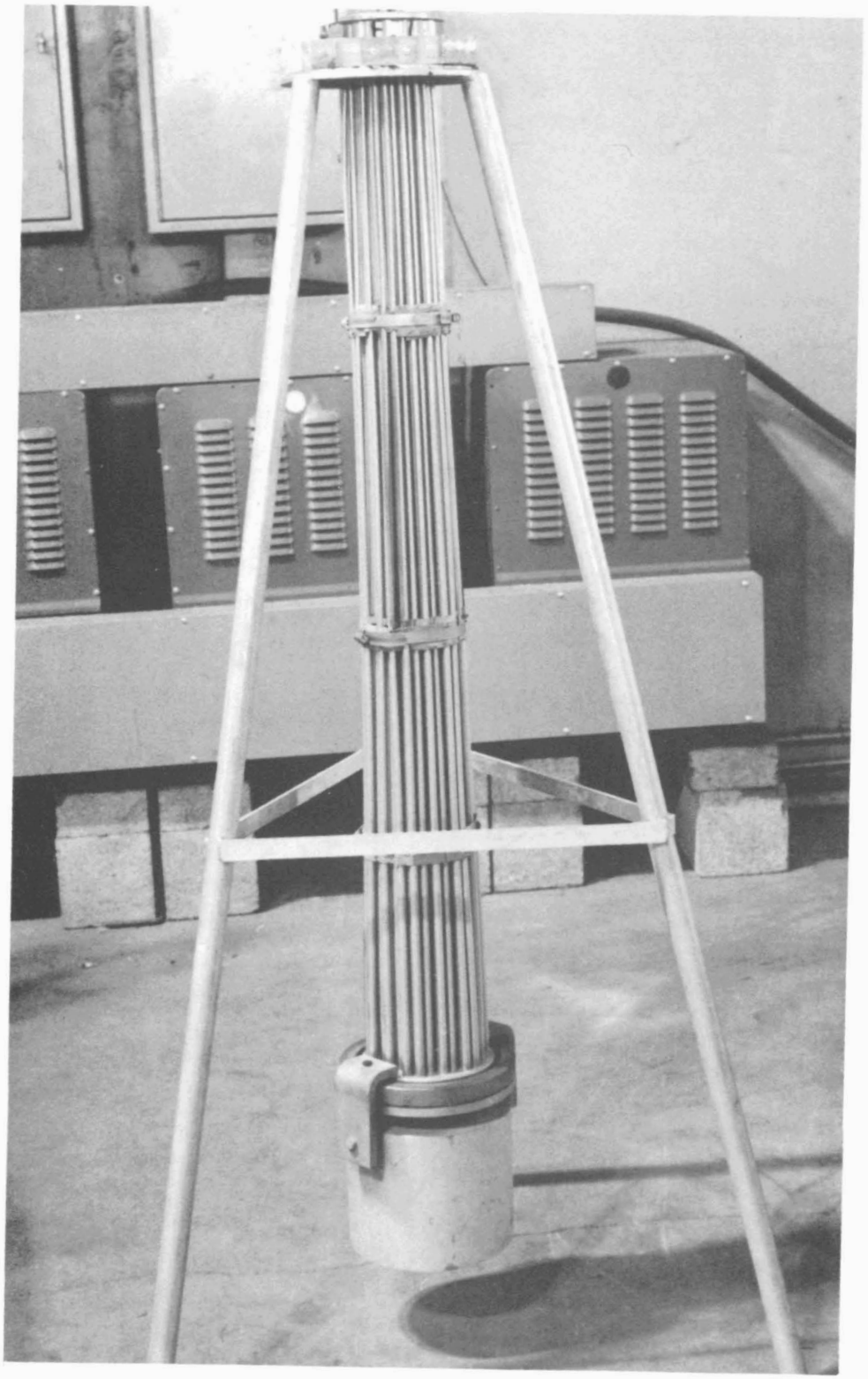

Full-Scale -1 Condenser Suspended from Small Header in Brazing Fixture

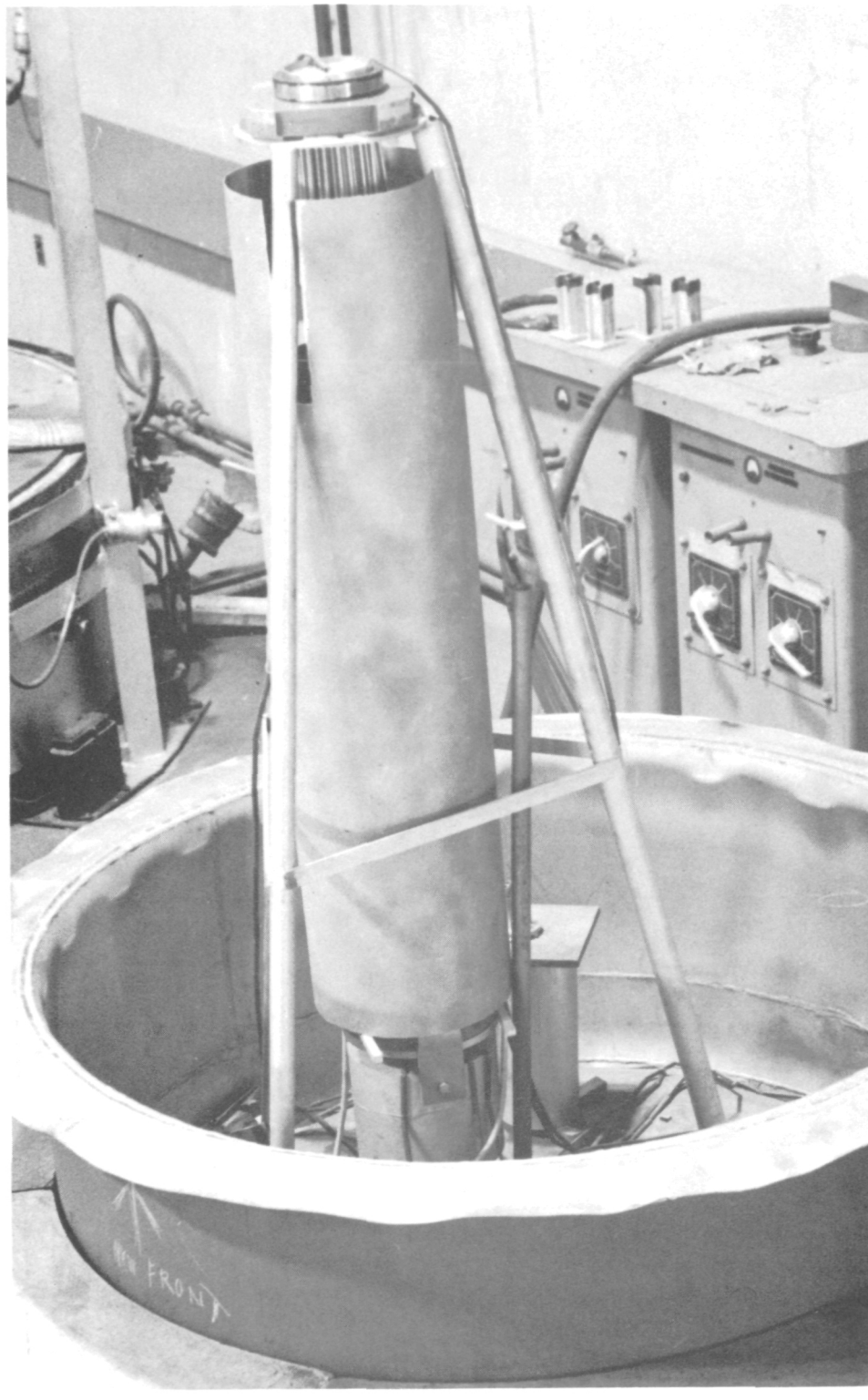

Full-Scale -1 Condenser Suspended in Brazing Fixture, with Radiation Shield in Position

SPECIMEN NUMBER	MATERIAL	MATERIAL HARDNESS	HOURS OF EXPOSURE
1	TZM	28 R_C	5
2	Mo-1/2Ti	29 R_C	5
3	Mo-1/2Ti	29 R_C	5
4	752 Cb	84 R_B	3.5
5	17-4PH, H900	44 R_C	5
6	Lapelloy	34 R_C	5
7	Lapelloy	34 R_C	5
8	Lapelloy	34 R_C	4
9	347	71 R_B	5
10	410	95 R_B	5
11	PH 15-7 Mo, RH 950	48 R_C	5
12	18-4-1	55 R_C	5
13	Dynacut	54 R_C	5
14	Dynacut	62 R_C	5
15	Dynacut	66 R_C	14
16	Dynacut	66 R_C	5
17	Stellite 6B	39 R_C	15
18	Stellite 6B	39 R_C	15
19	Stellite 6B	39 R_C	5
20	Stellite 6B	39 R_C	5
21	Stellite 6B	39 R_C	5

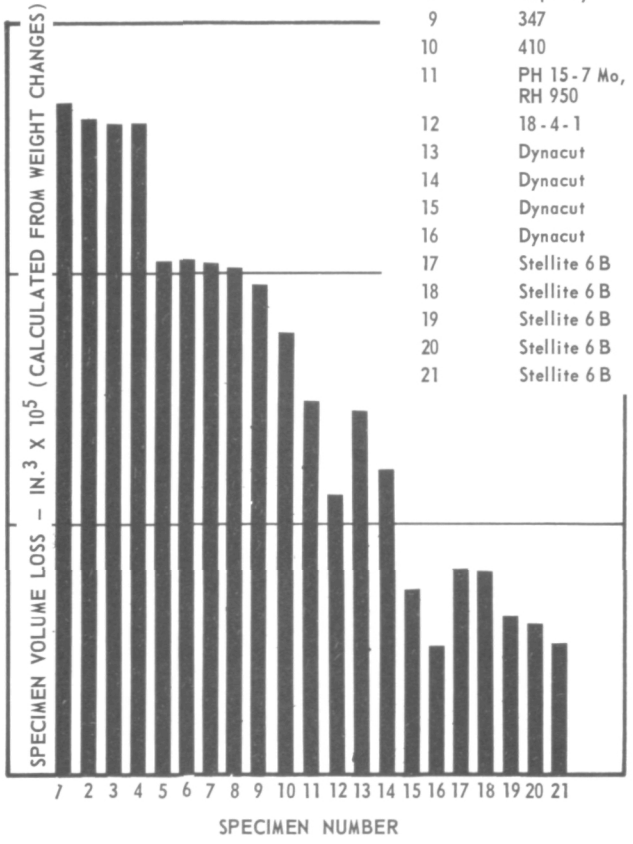

Volume Loss of Specimens - Accelerated Mercury Erosion Test

Figure 135

APPENDIX

CALCULATIONS FOR SNAP-8 EXPANSION RESERVOIRS

SECTION I

CALCULATIONS – LUBRICANT-COOLANT EXPANSION RESERVOIR

SUBJECT EXP. RESERVOIR - L/C

SYSTEM VOLUME -

PUMP - #094246 /COLKER (1-29-64)	50. IN³	2.13 LBS.
RADIATOR - .55 I.D. x 474 FT = /W. TINGLE 1-28-64	1352 IN³	57.5 LBS
MANIFOLD - DATA 3-5-63 - L. KURZWEIL	109 IN³	4.64 LBS
PIPING - DATA 3-5-63 - L.K.	179 IN³	7.62 LBS
	1690	
COLD TRAPS - DATA 3-5-63 - L.K 10%/TRAP (TEST 1-29-63 SYSTEM - L.GLER)	—	—
		71.89 LBS

PUMP-ET-378 INVENTORY - L. KURZWEIL / B. BARCLAY → M. WALDEN 1-29-64

PRIMARY LOOP	10. IN³ → 25. IN³	1.064
HEAT REJ. LOOP	36. IN³ → 25. IN³	1.064
Hg	36. IN³	1.53
TAA (TURBINE ALT. ASSY)	124. IN³	5.28
	206. IN³	8.84 LBS.
	1896 IN³	80.73 LBS

SYSTEM LOSSES -

START-UP (1)	60 IN³
EVAPORATION (10,000 HRS)	60 IN³

SYSTEM TEMPERATURE - FLIGHT (SIM. TO PHASE III) 210°-246°F

210° FOR 50% RADIATOR	676 IN³
MANIFOLD	109 IN³
50% LOOP PUMPS	103 IN³
	888 IN³

SUBJECT EXPAN. RESERVOIR L/C

SYSTEM TEMPERATURE - (CONT'D)

246°F FOR 50% LOOP PUMPS —— 103 IN³
PIPING —— 179 IN³
L/C PUMP —— 50 IN³
50% RADIATOR —— 676 IN³
1008 IN³

DESIGN TEMPERATURE —

$$T_D = \frac{T_1V_1 + T_2V_2}{V_T} = \frac{210 \times 888 + 246 \times 1008}{1896} = 229.\ ^\circ F.$$

RESERVOIR VOLUME -

THERMAL EXPANSION - 60°F TO 229°F
73.5°/FT³ - 69.6°/FT³

$$\left[(1896 + 60) \times \frac{73.5}{69.6}\right] - 1956 = 109.6\ IN^3$$

START-UP LOSS —— 60. IN³
169.6 IN³

S.M. - 10% 17.
186.6 IN³

MAXIMUM DISPLACEMENT —— USE - 190. IN³

SUBJECT EXPAN. RESERVOIR h/e

BELLOWS — 13.00 INSIDE DIA. — .800 SPAN — .20 PITCH - 2 PLY .010 WALL
.030 RADIUS — 13.8 EFF. DIA. & 149.6 IN² AREA

STROKE — $\frac{V_D}{A_E} = \frac{190}{149} = 1.275$

CONVOLUTIONS — $\frac{1.275}{.120} : 10.6$ — USE 20.5

LENGTH — 20.5 x .20 = 4.10

SPRING RATE —

$$R_{70} = \frac{2.30\ E P t^3 (OD+ID)}{K L (OD-ID)^2} = \frac{6.9}{1.6384} \times \frac{(OD+ID)}{L}$$

$$= 4.216 \times \frac{27.6}{4.10} = 28.4\#/IN \text{ OR } .19 \text{ PSI}$$

LOAD @ 1.30 STROKE = 36.9# OR .247 PSI

RESERVOIR - GAS VOLUME

$P_2 = 3.5 - .247 = 3.253$

$V_1 P_1 = (V_1 - V_D) P_2$

$P_1 = 3.0$

$(P_2 - P_1) V_1 = P_2 V_D$

$.253 V_1 = 3.253 \times 190 \times \frac{T_2}{T_1}$ (AT T_2 TEMP.) 244°

$V_1 = 2490 \times \frac{T_2}{T_1} \frac{(709°)}{(520)} = 3310\ IN^3$

LENGTH OF 15. DIA CYL = $\frac{3,310}{176.7} = 18.7$ INCHES APPROX.

BALLPARK-OK

SUBJECT EXPAN. RESERVOIR L/E

RESERVOIR LENGTH - WITH BELLOWS 13 00 INSIDE DIA.
x .80 SPAN - 14.75 TANK O.D.

BELLOWS CORE - 4.10 x 149 IN^2 = 611. IN^3

ELLIPTICAL ENDS - 14.75 DIA x 3.69
VOLUME (2 ENDS) = 4.189 x 7.375^3 x 3.69 = 841. IN^3
1452. IN^3

TANK LENGTH

CYL. - $\frac{3310 - 1452}{A\ (14.70\ DIA)\ 169.7\ IN^2}$ = 10.95 + 4.10 + 7.375 = 22.425 INCH

TANK DESIGN - .014 MINIMUM $\pm .004\ .000$
WALL = $\frac{14.75 \times 3.5 \times 1.5}{2 \times 39,000}$ = .0010 - USE .016 $\pm .002$

MAX. PRESS. OUTSIDE = .807 $\frac{E t^2}{L R} \sqrt[4]{\left(\frac{1}{1-\gamma^2}\right)^3 \frac{t^3}{R^3}}$

$t = .014$
$L = 15.0$
$R = 7.375$

= 19 PSI (OK)

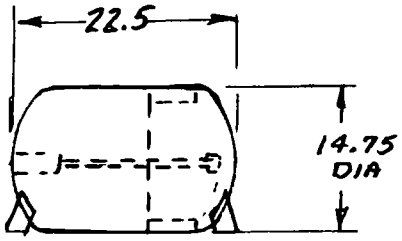

WEIGHT

14.75 x 3.14 x 15.05 x .018	= 12.6 IN^3	
HD 2 x 3.14 x 12.4 x 2.4 x .018	: 3.36	
14.75 x 3.14 x (2.31 x 1.05) x .018	= 2.02	5.38
2ND HEAD + FLOATING HEAD	—	10.76
POS. IND. MTG & SEAL	—	.2
BRACKETS - 4 x 2. x 3. x 2. x .034	= 1.6	30.54 IN^3 = 8.85
BELLOWS - 13.8 x 3.14 x .720 x 41 x .010	= 12 80	
13.8 x 3.14 x (.07 x 3.19) x 41 x .010	= 3.9	
13.0 + 14.75 x 3.14 x .5 x .010	= .44	16.14 IN^3 = 4.7
		46.68 IN^3 x .29 = 13.6 LBS
TRANSDUCER - 2.0 STROKE		.2
	TOTAL	13.8 LBS

SUBJECT EXPAN. RESERVOIR L/C

RESERVOIR VOLUME - LIQUID

14.75 DIA (21.3) - 13.8 DIA × 4.10 = 88.5 IN³

13.9 × 3.14 × .88 × 1.0 = 38.4

126.9 IN³ × 73.5/1728 = 5.4 *

% OF SYSTEM = 126.9/1896 = 6.7%

RESERVOIR WEIGHT -

RESERVOIR — 13.8 LBS

GAS - 3310/1728 × 3.0/19.7 × .11135 = .044

FLUID IN RESERVOIR — 5.4

19.25 LBS

AT LAUNCH - (60 + 20 IN³)

80 IN³ × 73.5/1728 = 3.40

3.4

22.65 LBS

OPERATION TEMP. FLUID.

190 IN³ × 69.6/1725 = 7.65

19.25

7.65

26.90 LBS

RESERVOIR VOLUMES

INSTALLATION @ 60°F — 80. IN³ USABLE

START-UP (.60. IN³ MAX. LOSS) — 20. IN³ "

THERMAL EXPANSION (110.) — 130. IN³ "

LEAKAGE (60. IN³ MAX. LOSS) — 70. IN³ "

RESTART (60. IN³ MAX. LOSS) — 10. IN³ "

SECTION II

CALCULATIONS - HEAT REJECTION LOOP EXPANSION RESERVOIR

SUBJECT EXPANSION RESERVOIR - IHRL

RESERVOIR LENGTH - WITH BELLOWS 13.00 INSIDE DIA.

BELLOWS CORE - $5.90 \times 139\ IN^2 = 820\ IN^3$

" O.D. - $.5 \times 133\ IN^2 = 66\ IN^3$

ELLIPTICAL ENDS - 14.0 DIA x 3.5

VOL. (2-ENDS) - $4.189 \times 7.0^2 \times 3.5 = 717\ IN^3$

$1603\ IN^2$

TANK LENGTH -

$$\frac{3020 - 1603\ IN^2}{153\ IN^2} + 3.5 + 5.90 + .5 + 3.5 = 22.66 \quad (1417)$$

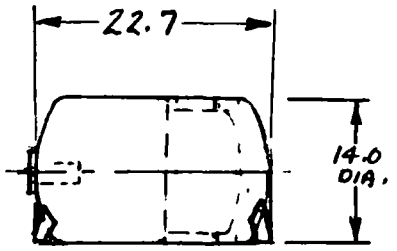

DESIGN FOR PROOF PRESS

WALL = $\frac{14 \times 49 \times 1.5}{2 \times 23,000} = .020$ - USE .022 ± 002

WEIGHT -

$14 \times 3.14 \times 15.7 \times .024 =$	$16.7\ IN^2$	
HD. $2 \times 3.14 \times 11.8(R) \times 2.28 \times .024 = 4.05$		
$14 \times 3.14 \times (2.19 \times 1.05) \times .024 = 2.42$	6.5	
2-END HEADS	13.0	
BKTS - $4 \times 2. \times 3 \times 2 \times .034 =$	1.6	
POSITRAL - $4. \times 3.14 \times .25 \times .040 =$	.2	
TRANSDUCER - 4" STROKE	.2	.2#
BELLOWS - $13.3 \times 3.14 \times .250 \times 59 \times .010 = 5.66$		
$13.3 \times 3.14 \times (.07 \times 3.14) \times 59 \times .010 = 5.39$		
$13.0 \times 3.14 \times .5 \times .016 = .21$		
$14.0 \times 3.14 \times .5 \times .010 = .22$	11.5	

$49.7\ IN^3 \times .29 = 14.5$ LBS.

SUBJECT EXPANSION RESERVOIR-HRL

RESERVOIR VOLUME - LIQUID

(14.137)
13.96 DIA - 13.30 DIA × 5.90 = 83.41 IN³
13.63 × 3.14 × .95 = 40.6
124. IN³ × 54.47/1728 = 3.9 #

% OF SYSTEM = 124/4833 = 2.6 %

RESERVOIR WEIGHT —

RESERVOIR —	14.5 LBS	14.5
GAS - 3020/1728 × 25./19.7 × .11135 =	.57	.6
FLUID @ INSTALLATION	3.9	3.9
	18.97 LBS	

19. + 1.5 = 20.5 × 7G = 143.5 #

OPERATION TEMP. FLUID — 14.5

460 IN³ × 54.47/1728 = 14.5

33.5 LBS

SPRING FORCE LOADED — 4 × 5.0 DIA. OR 14 × 2.5 DIA.

PRELOAD @ 25 PSIA × 139 IN² = 3475 #

OPERATING @ 37.3 PSIA × 139 IN² = 5180 #

OPERATING @ 44 PSIA × 139 IN² = 6110 # (LESS BELLOWS)

OPERATING STROKE — 3.31

SPRING SYSTEMS	PRE-LOAD	WORKING LOAD	Δ L
4-LOCATIONS	870 #	1295 #	425 #
14-LOCATIONS	248	370	122 #

SUBJECT EXP. RESERVOIR - HRL

SPRING FORCE LOADED - 4 @ 5.00 MAX. DIA. - 14 @ 2.50 MAX.

MAX. SPRING LOAD	1300 #	370 #
Δ-LOAD	425 #	122 #
RATE - TOTAL	128 #/INCH	36.8 #/INCH
OUTER SPRINGS	5.00 DIA	2.50 DIA
LOAD	650 #	190. #
RATE	50. #/IN	15. #/IN
WIRE DIA - d	.4375	.2437
K/COIL $\left(\frac{\pi 125. \times d^4 \times 10^9}{(OD-d)^3}\right)$	479. #/IN/COIL	384 #/IN
TOTAL COILS = $\frac{K}{RATE}$ + 2	11.6	27.6
WEIGHT = $(N-1)(OD-d) \times 3.14 \times d^2 \times .78 \times .19$ =	6.75 LBS	2.55 LBS
LENGTH - WORKING	5.58 INCH	7.12 INCH
INNER SPRINGS	4.00 DIA	2.06 DIA
LOAD	650. #	180. #
RATE	78. #/IN	22. #/IN
WIRE DIA - d	.4063	.2188
K/COIL	920. #/IN/COIL	511. #/IN/COIL
TOTAL COILS	13.8	23.3
WEIGHT	5.91 LBS	1.3 LBS
LENGTH - WORKING	6.17 INCH	5.61 INCH
WEIGHT SPRINGS		
SET (OUTER #/INNER)	12.16 LBS	3.85 LBS
TOTAL	48.64 LBS	53.8 LBS.

WEIGHT COMPARISON

FORCE SPRINGS - 48.6 LBS

PRESSURANT GAS - .6 LBS

BELLOWS & STRUCTURE - 14.5 LBS (SIMILAR FOR BOTH)

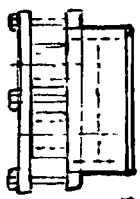

SUBJECT EXP. RESERVOIR - HRL

USING - NaK INVENTORY DATA / C.F. CAMMACK - 10-16-63

SYSTEM UNIT — VOLUMES FOR 324 KW & 392 KW

CONDENSER	690 IN^3 x $\frac{2957}{2033}$ =	834 IN^3
RADIATOR INLET	567 IN^3 —	567 IN^3
RADIATOR	2033 IN^3	2957 IN^3
RADIATOR OUTLET - 1.902 I.D. x 27.05' =	920 IN^3	920 IN^3
PUMP - SAME AS PRIMARY LOOP -	54 IN^3	54 IN^3
	4264	4832 IN^3

EXPANSION RESERVOIR - HRL $\frac{4832}{1728} \times 50.56 \# = 153.4 \text{ LBS}$

CONDITION	@ TEMP -	DENSITY -	VOLUME INCREASE
INSTALLATION-MIN.	50°F	54.56	1.0000
PRE-START - MAX.	140°F	53.81	1.01394
STEADY - STATE	580°F	50.14	1.08815
OPERATION DESIGN	665°F	49.43	1.10378

SYSTEM EXPANSION - 4832 IN^3 FROM 50°F TO 665°F

$4832 \times .10378 = 501.4 \text{ IN}^3$

LESS CHAMBER EXPANSION - SS. 316 - 9.5×10^{-6} / °F EXPANSION

$(665° - 50°) \times 9.5 \times 10^{-6} = .00584 / \text{INCH}$

$(4832 \times 1.00584^3) - 4832 = 85 \text{ IN}^3$

EXPANSION RESERVOIR VOLUME - 501.9 - 85. = 416.4 IN^3

SUBJECT EXP. RESERVOIR - HRL

EXPANSION RESERVOIR VOLUME -

SYSTEM VOLUME INCREASE	—	501.4 IN^3
CHAMBER EXPANSION	—	85.
		416.4 IN^3
DESIGN S.M. (10%)		41.6
		458. IN^3

SYSTEM PRESSURES

INSTALLATION	—	17 PSIA — REVISE SPEC.
OPERATION	—	44 PSIA

SYSTEM LOSSES - 5% x 416.4 = 20.8 IN^3 ALLOWED

5% S.M. ALLOWED FOR EXCESS TEMP.

USING BELLOWS —

13.00 I.D. - .400 SPAN - .20 PITCH - .030 RAD - 2x.005 WALL

13.40 EFF. DIA. - 141.0 IN^2 AREA

STROKE — $\frac{458}{141.} = 3.25$

CONVOLUTIONS — $\frac{3.25}{.120} = 27.1$ — USE 27.5

LENGTH — 27.5 x .200 = 5.5

SPRING RATE -

$$R_{70} = \frac{2.30\ E\ p\ t^3\ (OD+ID)}{K\ L\ (OD+ID)^3} = \frac{6.9 \times 26.8}{.24 \times 5.5} = 140\#/\text{INCH} \text{ @ } 1.0\ \text{PSI/INCH}.$$

SUBJECT EXP. RESERVOIR - HRL

BELLOWS SPRING LOAD @ 3.25 STROKE = 455 # @ 3.25 PSI

RESERVOIR - GAS VOLUME

$P_2 = 44 - 3.25 = 40.75$ PSIA

$P_1 = 17$ PSIA

$$(P_2 - P_1) V_1 = P_2 V_D \times \frac{T_2}{T_1}$$

$$23.75 V_1 = 40.75 \times 458 \times \frac{1125^{\circ} R}{510^{\circ}}$$

$$V_1 = 786 \times 2.203 = 1750 \text{ IN}^3$$

BELLOWS CORE - $5.5 \times 132.7 = 730. \text{ IN}^2$

ELLIPTICAL ENDS - 13.9 DIA. x 3.5

(2 ENDS) = $4.189 \times 6.95^2 \times 3.5 = 709. \text{ IN}^3$

$1439. \text{ IN}^3$

TANK LENGTH -

$\frac{1750 - 1439}{151. \text{ IN}^2 (13.86 \text{ DIA})} = 2.06 \text{ IN} + 5.5 + 7.0 = 14.56$ INCH

TANK DESIGN -

WALL = $\frac{14 \times 44 \times 1.5}{2 \times 23,000} = .020$ - USE .022 ± .002

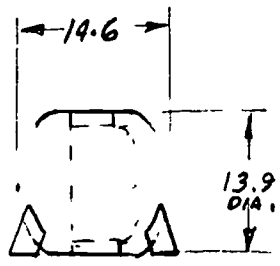

WEIGHT

$13.9 \times 3.14 \times 7.56 \times .024$	=	7.91 IN^3	
HD. $2 \times 3.14 \times 11.8(R) \times 2.26 \times .024$	=	4.01	
$13.9 \times 3.14 \times (2.18 \times 1.05) \times .024$	=	2.90	6.41
2-END HEADS			12.82
BKTS - $4 \times 2. \times 3 \times 2 \times .034$		1.63 IN^3	$28.77 \text{ IN}^3 \times .29 = 8.4$ LBS
BELLOWS - $13.4 \times 3.14 \times .32 \times 55 \times .010$	=	7.40	
$13.4 \times 3.14 \times (.07 \times 3.14) \times 55 \times .010$	=	5.09	
$13.5 \times 3.14 \times 1. \times .010$	=	$.42 \text{ IN}^3$	$12.91 \text{ IN}^3 \times .29 = 3.74$ LBS
TRANSDUCER & MTG			.3
			12.44 LBS

SECTION III

CALCULATIONS - PRIMARY LOOP EXPANSION RESERVOIR

SUBJECT EXP. RESERVOIR - PRI.

SYSTEM PERFORMANCE - RESERVOIR TEMP. -1100°F - 1375°F
SYSTEM PRESSURE - 35 PSIA - 50 PSIA

INVENTORY — 6.042 IN^3 (197.4 #)

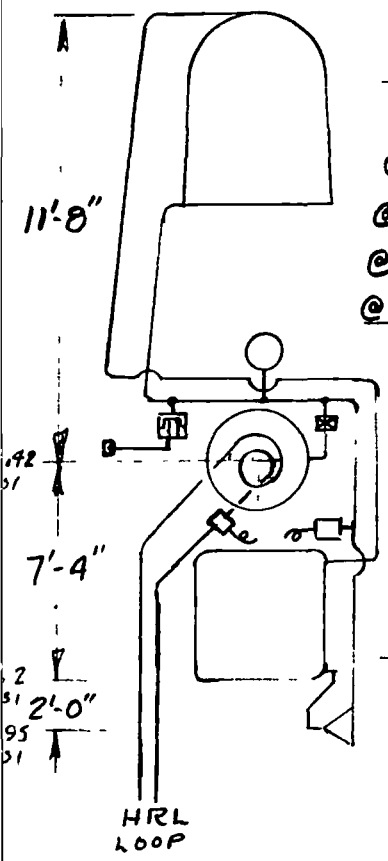

	SYSTEM PRESSURES (PSIA)									
	NON-OPERATION				START			OPERATION		
FORCE	+1G	+7G	-3G	0-G	0-G	0-G	0-G	0-G	+3.5G	0-G
@ 50°F	(11.0)	(0.5)	44.7	15.9	15.4					
@ 140°F	11.0	0.6	44.6	15.4	15.4					
@ 800°F						17.1+ 42.3-				
@ 1375°F							35.0+ 50.0-			
@ 1200°F								47.7	(35.0)	47.7
S.R.		31.4	31.4			17.1+	35.0+		47.7	
E.R.	15.4			15.4	15.4	42.3-	50.0-	47.7		47.7
BOILER		50.9		15.4	15.4				55.7	
PUMP		56.1		15.4	15.4				57.9	
						11.7'		19.0'	21'	

FORCE - @ 50°F = $\frac{54.56}{144}$ = .379 PSI/FT/"G" — 4.42 PSI — 7.2 PSI — 7.96 PSI
7G = 30.9 PSI — 50.7 PSI — 55.92 PSI

@ 140°F - $\frac{53.81}{144}$ = .377 PSI/FT/"G" — 4.90 PSI — 7.16 PSI — 7.91 PSI
7G = 30.8 PSI

AVERAGE @ 1200°F - $\frac{49.96}{144}$ = .312 PSI/FT/"G" — 3.64 PSI — 5.92 PSI — 6.55 PSI
3.5G = 12.7 PSI — 20.7 PSI — 22.9 PSI

UBJECT EXP. RESERVOIR - PRI

OPERATION - RESERVOIR GAS TEMP. - CONTROLLED BY PRESSURE REGULATED COOLING -

FLIGHT SYSTEM - DWG - 09122 / J. BARGER 2-12-64

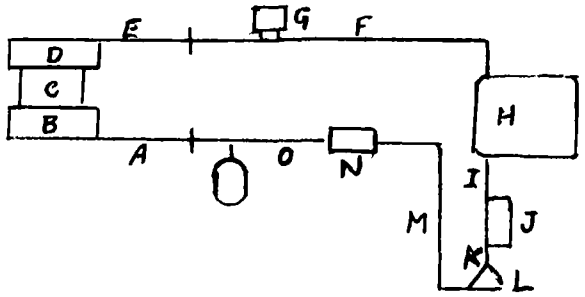

VOLUMES / R. WOODWORTH - 2-19-64

NUCLEAR SYSTEM

A - INLET (FEED) LINE	-	162. IN³
B - INLET PLENUM	-	197.
C - CORE	-	167.
D - OUTLET PLENUM	-	120.
E - DISCHARGE LINE	-	262. IN³ - 908. IN³

PCS - SYSTEM

F - BOILER (FEED) LINE	-	68.5 IN³
G - HOT TRAP	-	
H - BOILER	-	4994.
I - BOIL. DISCHARGE LINE	-	314.
J - AUX. HEAT EXCHANGER	-	76.3
K - PUMP INLET LINE	-	248. ← 30.0 IN³ @ 1100°F @ 3.0°
L - NaK PUMP	-	84.67 1725.1 IN³ MPA / WALOREN 2-17-64
M - PUMP DISCHARGE LINE	-	314.
N - PARASITIC LOAD	-	650
O - SYSTEM DISCHARGE	-	68.5 - 6817.97 IN³
		7725.97 IN³ - 244#
- EXPANSION RES. RESIDUAL	-	186.
		7912. IN³ @ 50°F - 250.#

SYSTEM EXPANSION - 1679 IN³

TEMP.	DENSITY	DISPLACE.	PRESSURE @ 50°F	50/P_G	@ TEMP.	T_2/T_1	GAS TEMP.
50°F	54.56 #/FT³	(186.0 IN³)	15.4 PSI		15.4 PSI	1.0	50.°F
140°	53 81	114.	15.6		18.4	1.18	140°
800°	48.91	918	17.1		42.3	2.47	800°
1160°	45.31	1407	18.1	2.76	50.0	3.17	950°
1200°	44.96	1457	18.2	2.74	"	3.25	940° MAX.
1240°	44.64	1508	18.4	2.72	"	3.33	930°
1375°F	43.51	1679	18.8	2.66	"	3.59	897° MAX,
1200°		1457	18.2	1.92	35.0		520° MIN.

SUBJECT EXP. RESERVOIR - PRI

SYSTEM EXPANSION - (CONT'D)

VOL. DISPL. @ 1375 - $(7726 \times \frac{54.56}{43.51}) - 7726 = 1962.\ IN^3$

LESS METAL EXPANSION - $1325^\circ \times 9.7 \times 10^{-6} = .01285/IN$

$7726 \times (1.01285)^3 - 7726 = 283.$ —— $283.\ IN^3$

$1679.\ IN^3$

BELLOWS DATA - 19.00 I.D. — .400 SPAN - .20 PITCH - .030 R&D,
WALL - 2x.005 - 19.4 EFF. DIA - 295.6 IN^3 AREA

STROKE - $\frac{1679}{295.6} = 5.68 + .03 \text{ (S.M.)} = 5.71$ $8.9\ IN^3$ (S.M.-1)

CONVOLUTIONS - $\frac{5.71}{.120} = 47.6$ - USE 47.5

LENGTH - $47.5 \times .20 = 9.50$

SPRING RATE

$$K_B = \frac{0.575 \times R_E \times t^3 \times E \times P/4}{(5/2)^3 \times L \times K}$$

$R_E = \frac{19.4}{2} = 9.7$
$t = 2 \times .005$
$E = 29 \times 10^6$
$R/4 = .20/4 = .050$
$(5/2)^3 = (.4/2)^3 = .008$
$L = 9.50$
$K = .495$

$$K_B = \frac{0.575 \times 9.7 \times (2 \times .005^3) \times 29 \times 10^6 \times .050}{.008 \times 9.5 \times .495}$$

$= \frac{2.02}{.0377} = 53.6\ \#/\text{INCH}$ & $.182\ PSI/IN.$

FORCE @ 5.71 STROKE - 303 # & 1.04 PSI -

RESERVOIR DATA - 34 LONG (10. + 9.5 + 14.5 CYL)

GAS VOLUME -

BELLOWS CORE - $9.5 \times 295.6 = 2806\ IN^3$

EL. ENDS - 19.9 DIA. x 5.0

2 ENDS = $4.189 \times 9.95^2 \times 5.0 = 2070$

CYL. — $14.5 \times 311.$ (19.9 DIA) = 4510

$9380\ IN^3$

Report No. 0390-04-15

DISTRIBUTION

Incorporating: NASA Amendment 1 (27 November 1963)
NASA Amendment 2 (16 January 1964)
NASA Amendment 3 (5 May 1964)
NASA Amendment 4 (8 May 1964)

	No. of Copies
National Aeronautics and Space Administration Lewis Research Center - SNAP-8 Project Office 21000 Brookpark Road Cleveland, Ohio, 44135	
Attn: H. O. Slone, Manager (Mail Stop 86-5)	2
Attn: D. G. Beremand	1
Attn: R. E. English	2
Attn: S. Lieblein	1
Attn: Dr. B. Lubarsky	1
Attn S. Perrone (Quality and Reliability) (Mail Stop 86-5)	1
Attn: L. Rosenblum	1
Attn: Librarian	1
Attn: Space Power Systems Procurement Section	1
Headquarters National Aeronautics and Space Administration Washington, D.C., 20546	
Attn: Dr. F. Schulman (Code RNP) Program Director	1
Attn: G. C. Deutsch (Code RRM)	1
Attn: T. B. Kerr (Code RNS)	1
Attn: J. Lazar (Code RNR)	1
Attn: P. R. Miller (Code RNP)	1
Attn: W. H. Woodward (Code RN)	1

DISTRIBUTION (cont.)

	No. of Copies
National Aeronautics and Space Administration Western Operations Office 150 Pico Blvd. Santa Monica, California, 90406	
Attn: J. S. Keeler	1
Attn: Patent Counsel	1
NASA – Azusa Field Office Room 152, Building 160 Aerojet-General Corporation Azusa, California	
Attn: J. G. Kennard	1
Attn: E. F. Morris	1
NASA – Scientific and Technical Information Facility Box 5700 Bethesda 14, Maryland	
Attn: NASA Representative	2
National Aeronautics and Space Administration Marshall Space Flight Center Huntsville, Alabama, 35812	
Attn: Dr. E. Stuhlinger	1
National Aeronautics and Space Administration Manned Spacecraft Center Houston 1, Texas	
Attn: Technical Information Division	2
Graham Hagey (ESDE)	1
BuWeps Rep/Azusa - Attn: H.E. Griffin, Bldg. 119	1
Aerospace Corporation P.O. Box 95085 Los Angeles, California, 90045	
Attn: E. R. Berry	1

DISTRIBUTION (cont.)

	No. of Copies
AiResearch Manufacturing Company of Arizona P.O. Box 1947 Phoenix, Arizona	
Attn: H. H. Currey Security Officer	1
Allison Division General Motors Corporation Indianapolis 6, Indiana	
Attn: T. F. Nagey	1
ASRMF-P-1 Aeronautical Systems Division Wright-Patterson AFB, Ohio	
Attn: C. H. Armbruster	1
Atomics International P.O. Box 309 Canoga Park, California	
Attn: Carl E. Johnson	5
AVCO Research & Advanced Development Division 201 Lowell Street Wilmington, Massachusetts	
Attn: Michael I. Yarymovych	1
The Bendix Corporation Red Bank Division Eatontown, New Jersey	1
Brookhaven National Laboratory Associated Universities, Inc. Upton, Long Island, New York	
Attn: Classified Documents Group	1
Director, USAF Project RAND The RAND Corporation 1700 Main Street Santa Monica, California	
Attn: Library VIA: Air Force Liaison Office	1

DISTRIBUTION (cont.)

	No. of Copies
Electro-Optical Systems 300 N. Halstead Street Pasadena, California	
Attn: Mr. Joseph Neustein	1
Flight Propulsion Laboratory Department General Electric Company Cincinnati 15, Ohio	
Attn: Morris A. Zipkin	1
General Dynamics Astronautics Division San Diego, California	
Attn: Paul Slysh	1
General Electric Company Direct Current Motor and Generator Dept. 3001 East Lake Road Erie 1, Pennsylvania	
Attn: C. M. Mathias	1
General Electric Company Missiles & Space Division P.O. Box 8555 Philadelphia 1, Pennsylvania	
Attn: Edward Ray	1
Institute for Defense Analysis Universal Building 1825 Connecticut Avenue Washington 9, D.C.	
Attn: Dr. N. W. Snyder	1
Jet Propulsion Laboratories California Institute of Technology 4800 Oak Grove Drive Pasadena, California	
Attn: John Paulson	3
Attn: Librarian	1

DISTRIBUTION (cont.)

	No. of Copies
Lockheed Missiles and Space Division Lockheed Aircraft Corporation Sunnyvale, California	
Attn: H. H. Greenfield	1
The Martin Company Nuclear Division Baltimore 3, Maryland	1
McDonnell Aircraft Corporation Advanced Engineering Missiles & Space Systems Division St. Louis 66, Missouri	
Attn: R. A. Pepping	1
Northrop Space Laboratories 3401 W. Broadway Hawthorne, California, 90250	
Attn: E. Naumann Orgn. 600, Zone 65	1
Pratt & Whitney Aircraft East Hartford, Connecticut	
Attn: Wm. H. Podolny	1
Rocketdyne 6633 Canoga Avenue Canoga Park, California	
Attn: R. B. Dillaway	1
Thompson Ramo Wooldridge, Inc. 23555 Euclid Avenue Cleveland, Ohio, 44117	
Attn: E. Vargo	1
Attn: J. Picking	1
U.S. Atomic Energy Commission SNAP-8 Reactors Branch Division of Reactors Development Washington 25, D.C.	
Attn: K. Anderson	1

DISTRIBUTION (cont.)

	No. of Copies
U.S. Atomic Energy Commission Canoga Park, California	
Attn: Mr. Carl Malmstrom	1
U.S. Atomic Energy Commission Division of Technical Information Extension P.O. Box 62 Oak Ridge, Tennessee	1
U.S. Atomic Energy Commission Oak Ridge, Tennessee	
Attn: A. Taboada	1
U.S. Atomic Energy Commission Germantown, Maryland	
Attn: Dr. J.D. Lafleur	1
USA Commander Engineer Research & Development Laboratories Support Equipment Branch Diesel and Turbine Section Fort Belvoir, Virginia	
Attn J.E. Montgomery	1
Westinghouse Electric Corporation Astronuclear Laboratory Route 51 P.O. Box 10864 Large, Pennsylvania	
Attn: Richard C. Cunningham	1
Westinghouse Electric Corporation Box 989 Lima, Ohio	
Attn: R. W. Briggs	1
Internal Distribution	44

CONFIDENTIAL

AEROJET
GENERAL TIRE
GENERAL

AEROJET-GENERAL CORPORATION

CONFIDENTIAL